ONTOGENY AND MECHANISMS OF AMMONIA EXCRETION IN RAINBOW TROUT

THE ONTOGENY AND MECHANISMS OF BRANCHIAL AND CUTANEOUS AMMONIA EXCRETION IN FRESHWATER RAINBOW TROUT, *Onchorhynchus mykiss*

By

ALEX M. ZIMMER, B.Sc.

A Thesis

Submitted to the School of Graduate Studies

in Partial Fulfillment of the Requirements

for the Degree

Doctor of Philosophy

McMaster University

DOCTOR OF PHILOSOPHY (2015) McMaster University

(Biology) Hamilton, Ontario

TITLE:	The ontogeny and mechanisms of branchial and cutaneous ammonia excretion in freshwater rainbow trout, *Oncorhynchus mykiss*
AUTHOR:	Alex M. Zimmer, B.Sc. (McMaster University, Hamilton, Ontario)
SUPERVISOR:	Dr. C.M. Wood
NUMBER OF PAGES:	xxii, 238

ABSTRACT

The mechanism by which freshwater fish excrete ammonia, the primary nitrogenous waste, has been a focus of comparative physiologists for nearly a century. The majority of ammonia in typical adult fish is excreted across the gill and is loosely coupled Na^+/NH_4^+ exchange. However, few studies have addressed the mechanisms by which larval fish, lacking a functional gill, excrete ammonia. In the work presented in this thesis, cutaneous surfaces of post-hatch larval rainbow trout accounted for the majority of ammonia excretion (J_{amm}) and Na^+ uptake (J^{Na}_{in}), and both processes shifted to the gills at the exact same time over development (15 days post-hatch; dph), prior to the skin-to-gill shift in oxygen uptake (26 dph). Moreover, branchial J_{amm} and J^{Na}_{in} were tightly correlated over development (R^2=0.95), while no such relationship existed at the skin. Moreover, experimental manipulation of J_{amm} and J^{Na}_{in} demonstrated a lack of coupling of these processes by the yolk sac and body skin while branchial J_{amm} and J^{Na}_{in} were functionally coupled to one another. Thus, J_{amm} by the gill of trout is a Na^+-coupled process, while J_{amm} by the skin of larval trout is Na^+-independent. Perhaps the most important finding of this thesis was that ammonia may play a role in driving the ontogeny of branchial ionoregulation. A new "ammonia hypothesis" was proposed, which is a refinement upon the current theory of gill development (the "ionoregulatory hypothesis") and posits that J_{amm}, coordinated by Na^+/NH_4^+ exchange, is the earliest function of the developing gill. Moreover, the demand for ammonia excretion may represent the primary driving force for the transition from

cutaneous to branchial ionoregulation. Overall, this thesis extends the current knowledge of several aspects of ammonia excretion by freshwater fish, some of which had previously never been explored, and presents a number of new and exciting avenues for future research.

ACKNOWLEDGEMENTS

This thesis, in a general sense, represents the past 10 years of my life spent at McMaster. There is obviously an incredible list of people that I need to acknowledge and thank for not only what they have taught me, but for the support and friendship that I was lucky enough to receive.

First and foremost, I have to thank Chris. Though I have had few bosses in my life, none have been as hard working as Chris. Working for him was always made extremely easy knowing that he was working as hard for me as I was for him. Being in his lab has taught me everything I know about science, has taught me to step out of my comfort zone (e.g., Brazil, 2011), and has taught me the importance of stepping back and having a drink to mull over both science and life. Chris, I cannot thank you enough for the opportunities you have given me and for an amazing 7 years spent in your lab.

I also need to thank my parents, of course! Without their unwavering, though albeit at-times-confused, support, these past 10 years would have been impossible. Mom and Dad, you have always been there for me (and I don't just mean at the airport to pick me up!) and I love you both. I also have to thank you for bestowing upon me the gift of storytelling. Zimmers have always enjoyed telling a good story (some of us stretching the truth of stories more than others…) and I feel that this is something that has helped me incredibly in the world of science. I love you both and hope that if you actually made it past my abstract and are reading this, you know how much both of you mean to me.

Marina, I thank you for all of your love and support over the last nearly 4 years. I know that putting up with my thesis-induced mood swings has not been easy and your patience is amazing! You have changed me (for the better!) in too many ways to count and for that I love you dearly. This thing is over – I will stop complaining about having to sit at my desk for hours on end writing! Te amo muito!

Of everyone I have had the amazing pleasure to have met in the past 7 years, three people have meant so much to me that they need to be acknowledged here. Ryan, Si, and Tamzin (in alphabetical order, no favourites!) you three made my graduate experience what it was. Ryan, you were there from the get-go, from the first Rice Lake which would later become the venue for our romantic moonlit beers on a frozen lake. You have been a constant drinking buddy, a running coach, my "boss", proof-reader of several papers, and, above all, a best friend. So many of the things I have accomplished out of the lab (ATB 2014, my first beer!) would have been impossible without you – thank you. Si, even though you left us (for greener pastures) too soon, you are still one of the people who

made my time here what it was. You made 203, 208, pretty much anywhere you went, a fun place to be. Plus, your shambly life (e.g., the fungus v. bacteria apartment experiment; the Metamucil-multivitamin-Kraft dinner diet) made me feel better about mine! If you ever read this, I hope you know that your presence in the Wood lab brightened all of our lives and you are deeply missed. Last, and you have to know, not least, Tamz. What can I, or anyone, say about Tamzin Blewett? You have been a best friend for the last 6 years of my life – 6 years! Together, you and I have braved the Wood lab world and have stuck it out to the bitterest end! Your friendship has meant so much to me and I can't imagine having stuck out 6 years in the Wood lab with anyone else – we did it! I love all three of you.

There are also a crazy amount of other members of the Wood lab that need to be thanked. I have to thank Michele for being an amazing teacher and getting me started down the path of science. Erin, you were the glue that brought the Wood lab together for so long and were the first person to really make me feel at home in the lab. Sunita and Linda, both of you were absolutely amazing and obviously none of this would have been possible without you. I need to thank Amanda, Julian, and Michael for being amazing undergraduate students. To every other Wood lab friend and colleague, thank you so much!

I'd also like to thank all of the UBC party animals I've been lucky enough to have as friends – you guys made my short Vanouver life amazing. Ryan and Nicole, you guys and RBT were my saving grace from my home life! I thank also all of my Brazilian friends and colleagues. Camila, Mari, Mari, Lygia, Roberta, Josi, and everyone else – you are all phenomenal people and amazing friends. Adalto, you have been a great mentor to me and are one of the kindest, warmest people I have ever met. Muito obrigado para todos – amo voces demais! To all of the newcomers to the physiology group (Brittney, Catie, Cayleih, Neal, Sasha), you guys made the last year(s) of my PhD a lot of fun and I wish you all the best for the rest of your time at McMaster! I also thank all of the editors of this thesis (Catie, Cayleih, Mike, Neal, Ryan, Sasha, Tamz) for putting their time and effort into going through this beast – beers on me!

Finally, I need to thank the members of my committee, Grant, Mike, and Pat, whose incredible feedback at our meetings has helped shape this thesis to be something of which I am very proud. I also acknowledge all of my collaborators, Michele, Indianara, Adalto, Colin, and Pat – working with all of you has been a great pleasure.

The above people have all changed my life in immeasurable ways and I am immensely grateful. Now, if you have made it this far, it's only another 253 pages until the end – you can do it!

PREFACE

This thesis is organized in the "sandwich thesis" format approved by McMaster University. Chapter 1 is a general introduction which provides background information relevant to chapters 2-5. Chapters 2, 5, and 6 represent articles which have been published prior to the completion of this thesis (may be referred to in some chapters as Zimmer et al., 2014b,a,c, respectively), chapter 3 represents work that was done towards a yet unfinished study, and chapter 4 represents a paper which has been submitted for publication. Chapter 7 is a general summary which ties together and discusses the 5 major hypotheses addressed in this thesis.

Thesis organization and format

CHAPTER 1: INTRODUCTION

CHAPTER 2:	**WHAT IS THE PRIMARY FUNCTION OF THE EARLY TELEOST GILL? EVIDENCE FOR Na^+/NH_4^+ EXCHANGE IN DEVELOPING RAINBOW TROUT (*ONCORHYNCHUS MYKISS*)**
Authors:	Zimmer, A.M., Wright, P.A. and Wood, C.M.
Journal:	Proceedings of the Royal Society B 281, 1795 (2014b)
Contributions:	AMZ performed all experiments, analyzed all data, and drafted the initial manuscript under the supervision of CMW. PAW provided critical insights and contributed to editing of the manuscript.
CHAPTER 3:	**MECHANISMS OF AMMONIA EXCRETION AND Na^+ UPTAKE BY THREE DIFFERENT EPITHELIA IN RAINBOW TROUT (*ONCORHYNCHUS MYKISS*): EVIDENCE FOR Na^+/NH_4^+ EXCHANGE AT THE GILL BUT NOT THE SKIN**
Authors:	Zimmer, A.M. and Wood, C.M.

Journal:	To be submitted to American Journal of Physiology – Regulatory, Integrative and Comparative Physiology
Contributions:	AMZ performed all experiments, analyzed all data, and drafted the chapter under the supervision of CMW. Note that several authors will be added to this study after completion of subsequent analyses. P.A. Wright and J.M. Wilson are aiding in the ongoing immunohistochemical (IHC) analyses, and J. Hiroi has provided antibodies for Western blot analysis and IHC.
CHAPTER 4:	**AMMONIA FIRST? THE TRANSITION FROM CUTANEOUS TO BRANCHIAL AMMONIA EXCRETION IN DEVELOPING RAINBOW TROUT (*ONCORHYNCHUS MYKISS*) IS NOT ALTERED BY EXPOSURE TO CHRONICALLY HIGH NaCl**
Authors:	Zimmer, A.M. and Wood, C.M.
Journal:	Journal of Experimental Biology, in revision
Contributions:	AMZ executed the experiments, analyzed and processed samples, and drafted the manuscript under the supervision of CMW. CMW contributed to experimental design and interpretation of results, and edited the manuscript.
CHAPTER 5:	**EXPOSURE TO WATERBORNE Cu INHIBITS CUTANEOUS Na^+ UPTAKE IN POST-HATCH LARVAL RAINBOW TROUT (*ONCORHYNCHUS MYKISS*)**
Authors:	Zimmer, A.M., Brauner, C.J. and Wood, C.M.
Journal:	Aquatic Toxicology 150, 151-158 (2014c)
Contributions:	AMZ executed all experiments, performed all analyses, and drafted the initial manuscript under the supervision of CMW. CJB provided constructive

	insight and facilities for the work, and contributed to the editing of the manuscript.
CHAPTER 6:	**AMMONIA TRANSPORT ACROSS THE SKIN OF ADULT RAINBOW TROUT (*ONCORHYNCHUS MYKISS*) EXPOSED TO HIGH ENVIRONMENTAL AMMONIA (HEA)**
Authors:	Zimmer, A.M., Brauner, C.J. and Wood, C.M.
Journal:	Journal of Comparative Physiology B 184, 77-90 (2014a)
Contributions:	AMZ and CMW jointly executed the experiments and analyses. AMZ drafted the initial manuscript under the supervision of CMW. CJB provided constructive insight and facilities for the work, and contributed to the editing of the manuscript.

CHAPTER 7: SUMMARY

Contributions not appearing in thesis

The following is a list of published articles that I completed, acting as primary author or secondary author to a mentored undergraduate or M.Sc. student student, during my PhD but which were not included in the thesis itself. Some of these papers are referred to in the chapters of this thesis.

Lim, M. Y.-T., Zimmer, A.M. and Wood, C.M. (2015) Acute exposure to waterborne copper inhibits both the excretion and uptake of ammonia in freshwater rainbow trout (*Oncorhynchus mykiss*). *Comparative Biochemistry and Physiology C* 168, 48-54.

Rubino, J.G., Zimmer, A.M. and Wood, C.M. (2014) An in vitro analysis of intestinal ammonia handling in fasted and fed freshwater rainbow trout (*Oncorhynchus mykiss*). *Journal of Comparative Physiology B* 184, 91-105.

Rubino, J.G., Zimmer, A.M. and Wood, C.M. (2015) Intestinal ammonia transport in freshwater and seawater acclimated rainbow trout (*Oncorhynchus mykiss*): Evidence for a Na^+ coupled uptake mechanism. *Comparative Biochemistry and Physiology A* 183, 45-56.

Smith, A.A., Zimmer, A.M. and Wood, C.M. (2012) Branchial and extrabranchial ammonia excretion in goldfish (*Carassius auratus*) following thermally induced gill remodelling. *Comparative Biochemistry and Physiology A* 162, 185-192.

Zimmer, A.M and Wood, C.M. (2014) Exposure to acute severe hypoxia leads to increased urea loss and disruptions in acid-base and ionoregulatory balance in dogfish sharks (*Squalus acanthias*). *Physiological and Biochemical Zoology* 87, 623-639.

Zimmer, A.M., Barcarolli, I.F., Wood, C.M. and Bianchini, A. (2012) Waterborne copper exposure inhibits ammonia excretion and branchial carbonic anhydrase activity in euryhaline guppies acclimated to both fresh water and sea water. *Aquatic Toxicology* 122-123, 172–80.

Zimmer, A.M., Nawata, C.M. and Wood, C.M. (2010) Physiological and molecular analysis of the interactive effects of feeding and high environmental ammonia on branchial ammonia excretion and Na^+ uptake in freshwater rainbow trout. *Journal of Comparative Physiology B* 180, 1191-1204.

TABLE OF CONTENTS

LIST OF TABLES

CHAPTER 2

CHAPTER 3

CHAPTER 4

CHAPTER 5

CHAPTER 6

LIST OF FIGURES

CHAPTER 1

CHAPTER 2

CHAPTER 3

CHAPTER 6

CHAPTER 7

LIST OF ABBREVIATIONS

Amt	ammonium transporter of plants and bacteria
ASIC	acid-sensing ion channel
ATU	accumulated thermal unit
BLM	biotic ligand model
CA	carbonic anhydrase
CPS	carbamoyl phosphate synthetase
CYA	complete yolk sac absorption
DAPI	(4',6-diamidino-2-phenylindole)
DMSO	dimethyl sulfoxide
DOC	dissolved organic carbon
Dpf	days post-fertilization
Dph	days post-hatch
ECF	extracellular fluid
EF	elongation factor
EIPA	5-(N-ethyl-N-isopropyl)amiloride
ENaC	epithelial Na channel
HAT	H^+-ATPase
HEA	high environmental ammonia
J_{amm}	ammonia excretion rate
J^{Na}_{in}	Na^+ uptake rate
MA	methylamine
MEP	methylammonium/ammonium permease
MO_2	oxygen uptake/consumption

MRC	mitochondria rich cell
MS-222	tricaine methanesulfonate
NHE	Na^+/H^+-exchanger
NKA	Na^+/K^+-ATPase
OUC	ornithine-urea cycle
PH	post-hatch
PNH_3	partial pressure of NH_3
PO_2	partial pressure of O_2
qPCR	quantitative polymerase chain reaction
Rh	Rhesus
SA	specific activity or surface area
SIET	scanning ion-selective electrode technique
T_{amm}	total ammonia levels
USEPA	United States Environmental Protection Agency

CHAPTER 1

INTRODUCTION

1.1 PREFACE

The excretion of ammonia by fish has been a focus of comparative physiologists for over eight decades (Smith, 1929). Physiologically, ammonia is of great interest as it serves several vital functions. Aside from acting as the primary form of nitrogenous waste excreted by most fish species, ammonia is also considered to be the "third" respiratory gas (Randall and Ip, 2006), it also acts to eliminate metabolic acid (as NH_4^+ or NH_3/H^+ excretion), it can drive ionoregulatory exchanges (e.g., Na^+/NH_4^+ exchange), and it also serves as the building block for urea, the primary osmolyte of marine elasmobranchs. Ammonia is also a neurotoxin at sufficiently elevated levels (Randall and Tsui, 2002) and, therefore, its concentrations within the plasma and tissues must be regulated. This latter property of ammonia has led to a great deal of research to uncover the toxic mechanisms of ammonia, defense mechanisms against toxicity, and thresholds for ambient ammonia concentrations (see Ip and Chew, 2010; Randall and Tsui, 2002 for review). Indeed, the USEPA guidelines for threshold ammonia levels have been revised as recently as 2013 (USEPA, 2013). With this in mind, it is clear that an understanding of the mechanisms by which fish handle ammonia has warranted the nearly century's worth of research that it has received. In this thesis, my goal was to address a number of current knowledge gaps, highlighted in the present chapter, regarding the mechanisms of ammonia excretion by fish.

1.2 MECHANISMS OF AMMONIA EXCRETION BY FRESHWATER FISH

In the past decade, the discovery of Rhesus (Rh) glycoproteins as transporters which translocate ammonia across biological membranes has greatly advanced our understanding of ammonia excretion (J_{amm}) in a number of fish species. Another important aspect of ammonia excretion by freshwater fish is the involvement of Na^+ uptake (J^{Na}_{in}). The mechanism(s) by which J_{amm} and J^{Na}_{in} are coupled to one another has been studied over many decades and the predominating view of the relationship between J_{amm} and J^{Na}_{in} has changed markedly over this period.

1.2.1 Rh proteins

Rh proteins belong to the ammonia transporter (Amt)/ methylammonium permease (MEP)/Rhesus protein family which incorporates a number of ammonia transporting proteins from extremely diverse taxonomic groups (see Wright and Wood, 2009 for review). These proteins function as bidirectional channels, facilitating the flux of ammonia in either direction according to prevailing gradients (Khademi et al., 2004; Nawata et al., 2010b). The first evidence supporting a role for Rh proteins in J_{amm} by fish came in 2007 from two research groups studying four different fish species (mangrove killifish (*Rivulus marmoratus*) - Hung et al., 2007; zebrafish (*Danio rerio*) - Nakada et al., 2007a; pufferfish (*Takifugu rubripes*) - Nakada et al., 2007b; and rainbow trout (*Oncorhynchus mykiss*) - Nawata et al., 2007). Nakada et al. (2007b) demonstrated that *Xenopus* oocytes injected with *Takifugu* Rh cRNA displayed significant uptake of ^{14}C-methylamine (a commonly used ammonia analog) compared to H_2O-injected controls, providing the first evidence that Rh proteins isolated from a fish species may facilitate ammonia transport. Similar results were later found using oocytes injected with trout Rh

cRNA (Nawata et al., 2010b) and, moreover, this group provided convincing evidence, using the scanning ion-selective electrode technique (SIET), that Rh proteins bind NH_4^+ but transport NH_3. This latter observation, a property of Rh proteins which had been widely debated earlier (see Wright and Wood, 2009), was significant in supporting the "acid-trapping" model for ammonia excretion. This model postulates that ammonia is transported as NH_3 and not as NH_4^+ or by NH_4^+/H^+ exchange. The role of Rh proteins in ammonia transport by fish has also been demonstrated by *in vivo* studies which have shown that Rh gene expression increases upon exposure to ammonia-loading conditions (e.g., Hung et al., 2007; Nawata and Wood, 2008; 2009; Nawata et al., 2007; Zimmer et al., 2010). In addition to being an integral part of the ammonia excretion mechanism in fish, Rh proteins, along with a number of other key transporters, have recently been found to also facilitate Na^+ uptake (J^{Na}_{in}) in freshwater fish, coordinating a functional exchange of Na^+ against NH_4^+. It is noteworthy here that the nomenclature for Rh isoforms in zebrafish, a popular model species whose genome has been fully sequenced, has recently been changed (see http://zfin.org/search?q=rhcg). However, this updated nomenclature applies only to closely related cyprinid fish species (e.g., goldfish, carp), while salmonid nomenclature remains unchanged.

1.2.2 Na^+/NH_4^+ exchange

August Krogh, the "father" of the field of comparative physiology, was the first to suggest that, to achieve ion balance, freshwater fish might absorb Na^+ from the environment in exchange for NH_4^+ (Krogh, 1937; 1938). The first group to address this hypothesis, Maetz and Garcia-Romeu (1964), demonstrated that in goldfish (*Carassius*

auratus), the addition of ammonia to the external environment inhibited both J_{amm} and J^{Na}_{in}, while intraperitoneal injections of ammonia had the opposite effect. These researchers concluded that J_{amm} by freshwater fish occurs via direct Na^+/NH_4^+ exchange (Maetz and Garcia-Romeu, 1964). Later, similar results were also obtained using *in vitro* techniques with perfused gill and perfused head preparations (Kerstetter and Keeler, 1976; Payan, 1978), further supporting the notion that J_{amm} in freshwater fish occurs via direct Na^+/NH_4^+ exchange which remained the predominant view for decades (e.g., Wright and Wood, 1985). However, later studies eventually challenged this view. Wilson et al. (1994), for example, demonstrated that the addition of amiloride, a blocker of Na^+ channels, led to a nearly 100% reduction in J^{Na}_{in} while J_{amm} was inhibited by only ~25%, suggesting an uncoupling of the two processes. Later studies (e.g., Salama et al., 1999; Zimmer et al., 2010) also confirmed that these processes could be uncoupled from one another under experimental conditions. Moreover, the observation that fish have the ability to actively excrete ammonia against a concentration gradient (high external ammonia (HEA); Nawata et al., 2007; Wilson et al., 1994; Zimmer et al., 2010; Sinha et al., 2013), suggests that direct Na^+/NH_4^+ exchange cannot be the only mechanism by which ammonia is excreted. The early observations that once were interpreted as direct Na^+/NH_4^+ exchange are now viewed as evidence of an indirect coupling of J_{amm} to J^{Na}_{in} due to direct Na^+/H^+ exchange or indirect Na^+/H^+ exchange (proton pump –sodium channel model of Avella and Bornancin, 1989), both of which would facilitate the acid-trapping of NH_3 (Weihrauch et al., 2009; Wilkie, 2002; Wright and Wood, 2009).

After the addition of Rh proteins to the model of ammonia excretion in freshwater fish (see Weihrauch et al., 2009; Wright and Wood, 2009), the overall picture of the mechanism of Na^+/NH_4^+ exchange became more clear. The "Na^+/NH_4^+-exchange complex" (Wright and Wood, 2009), in addition to Rh proteins, consists of a number of components which coordinate a loosely coupled Na^+/NH_4^+ exchange. J^{Na}_{in} across the apical gill membrane of freshwater fish may occur by either or both an electrogenic coupling of v-type H^+-ATPase to putative Na^+ uptake channels and/or via an electroneutral Na^+/H^+-exchange (NHE) transporter. The former mechanism, first proposed by Avella and Bornancin (1989), coordinates a "functional" Na^+/NH_4^+ exchange. This occurs because the extrusion of H^+ ions by the H^+-ATPase facilitates J_{amm} via apical gill boundary layer acidification, promoting a cell-to-water PNH_3 gradient, and also powers J^{Na}_{in} by creating an electrical gradient for electrogenic uptake via a Na^+ channel. Part of the problem with this model, however, is that the available genomes for any fish (e.g., zebrafish, pufferfish, medaka), do not contain any orthologs or paralogs of an epithelial Na^+ channel (ENaC). Recently, however, acid-sensing ion channels (ASICs) have been implicated in this model (Dymowska et al., 2014), potentially representing the putative channel by which Na^+ is absorbed electrogenically. The latter mechanism, J^{Na}_{in} via NHE, has also been met with criticism. Parks et al. (2008) questioned the validity of this mechanism based on thermodynamic constraints, concluding that intracellular [Na] could never be low enough to support J^{Na}_{in} from a dilute freshwater environment. However, other researchers have demonstrated that J^{Na}_{in} is inhibited by EIPA, a potent pharmacological blocker of NHEs (Kumai and Perry, 2011; Shih et al., 2012; Wu et al.,

2010) and have concluded that J^{Na}_{in} via NHE may be driven by pH gradients, rather than $[Na^+]$ gradients. Two important factors in the establishment of these micro-gradients are cytosolic carbonic anhydrase (CA), also a part of the Na^+/NH_4^+-exchange complex, and Rh proteins. As discussed above, Rh proteins are believed to be NH_3 gas channels which initially bind NH_4^+. The H^+ stripped off of NH_4^+ in this process is believed to establish a pH micro-gradient which facilitates J^{Na}_{in} via NHE. Indeed, Ito et al. (2013) demonstrated a close association between NHE, Rh, and CA in zebrafish yolk sac ionocytes, and other researchers have shown that morpholino knockdown of apical Rhcg leads to a reduction in J^{Na}_{in} in zebrafish (Kumai and Perry, 2011; Shih et al., 2012). This mechanism, as a whole, has been named the Rh-NHE metabolon and is believed to play an integral role in both J_{amm} and J^{Na}_{in}. Thus, the present view of J_{amm} in freshwater fish is that it occurs via a loose coupling to J^{Na}_{in} which can be uncoupled under experimental conditions and which is coordinated by a number of enzymes and transporters (Fig. 1.1.; see Weihrauch et al., 2009; Wright and Wood, 2009, 2012 for review).

1.3 FACTORS INFLUENCING AMMONIA EXCRETION

There are a number of factors which can alter the excretion of ammonia by fish. These include the manipulation of external or internal pH, buffering of external media, alterations in external or internal $[Na^+]$, feeding (which increases internal ammonia levels), exposure to HEA, and exposure to waterborne Cu, among a number of other factors. For the purposes of the present thesis, however, this section will focus solely on providing an overview of the effects of HEA and Cu exposure on J_{amm} and J^{Na}_{in} in freshwater fish.

1.3.1 High external ammonia (HEA) exposure

Exposure to HEA has been used extensively to understand the mechanisms of J_{amm} by a variety of fish species (Braun et al., 2009b; Kumai and Perry, 2011; Liew et al., 2013; Maetz and Garcia-Romeu, 1964; Nawata et al., 2007; 2010a; Wilson et al., 1994; Wood and Nawata, 2011; Zimmer et al., 2010; Sinha et al., 2013). In these studies, the typical response to HEA is an inhibition or reversal of J_{amm} due to changes in PNH_3 gradients, an increase in plasma total ammonia (T_{amm}), and an inhibition of J^{Na}_{in}, usually attributed to competition at Na^+ uptake sites by NH_4^+ (e.g., Wilson et al., 1994; Liew et al., 2013; Zimmer et al., 2010). The initial inhibition or reversal of J_{amm} caused by HEA is generally followed by an increase in active ammonia excretion against the inwardly directed gradient such that control levels of J_{amm} are eventually restored (e.g., Nawata et al., 2007; Wilson et al., 1994; Wood and Nawata, 2011; Zimmer et al., 2010; Sinha et al., 2013). This upregulation of J_{amm} capacity has also been associated with increases in gene expression and/or activity of Rh proteins, H^+-ATPase, and NHE (Nawata et al., 2007; Sinha et al., 2013; Wood and Nawata, 2011; Zimmer et al., 2010). These studies confirm the importance of Rh proteins to overall J_{amm} in fish, as their upregulation is believed to facilitate the active excretion of ammonia against a concentration gradient. Furthermore, they suggest that active J_{amm} is dependent upon other components of the Na^+/NH_4^+ exchange complex.

1.3.2 Waterborne copper (Cu) exposure

Cu, although found naturally in water bodies of even pristine environments, is a potent ionoregulatory toxicant at sufficiently elevated levels such as those found in regions impacted by anthropogenic activities. The most common responses to sub-lethal waterborne Cu exposure in freshwater fish are the inhibition of ammonia excretion (observed as either an increase in plasma T_{amm} or a decrease in J_{amm}) and/or an inhibition of sodium uptake (observed as either a decrease in plasma [Na^+] or a decrease in J^{Na}_{in}) (see Grosell, 2012 for review). The fact that this toxicant targets both J_{amm} and J^{Na}_{in} lends further support to the notion that J_{amm} is coupled to J^{Na}_{in}. For instance, Wilson and Taylor (1993) demonstrated that exposure to approximately 300 µg/l Cu led to a significant increase in plasma T_{amm} and a significant decrease in plasma [Na^+]. Moreover, Lim et al. (2015) also demonstrated a concomitant inhibition of J_{amm} and J^{Na}_{in} in rainbow trout fry exposed to 50 µg/l Cu. However, these studies are conflicted by those which demonstrate that in freshwater fish, Cu exposure can inhibit one process but not the other (e.g., Blanchard and Grosell, 2006). Indeed, rainbow trout fry exposed to waterborne Cu demonstrated a transient inhibition of J^{Na}_{in} but a sustained inhibition of J_{amm} (Lim et al., 2015). Thus, Cu appears to have the capacity to uncouple the Na^+/NH_4^+ exchange in some instances. In terms of the mechanism(s) of Cu inhibition, there is a fairly clear understanding of J^{Na}_{in} inhibition, while J_{amm} inhibition is not as well understood.

In general, waterborne Cu is believed to inhibit J^{Na}_{in} via two mechanisms: the inhibition of apical Na^+ entry by competing for Na^+ uptake sites at the gill and the inhibition of basolateral Na^+ absorption from the cytosol via the inhibition of Na^+/K^+-ATPase (see Grosell, 2012 for review). Evidence for the former mechanism stems from

studies in rainbow trout which demonstrate that, in addition to J^{Na}_{in} being inhibited by Cu, Cu uptake is also reciprocally inhibited by Na^+ (Grosell and Wood, 2002). Furthermore, these authors also demonstrated that the addition of bafilomycin (an inhibitor of H^+-ATPase) or phenamil (an inhibitor of Na^+ channels) inhibited both J^{Na}_{in} and Cu uptake, clearly showing that Cu and Na^+ share similar uptake routes (Grosell and Wood, 2002). Cu can also inhibit the basolateral transfer of Na^+ from the cytosol to the plasma by inhibiting Na^+/K^+-ATPase, blocking the Mg^{2+} binding site of the ATPase (see Grosell, 2012 for review). Interestingly, however, many studies have demonstrated that Na^+/K^+-ATPase activity in gill homogenates from Cu-exposed fish does not differ from that of control fish (Blanchard and Grosell, 2006; Grosell et al., 2003; Lim et al., 2015; Zimmer et al., 2012), though this may be attributed to the large dilution of samples required by the assay (Grosell, 2012). Grosell et al. (2002) have also suggested CA as a primary target of Cu toxicity. However, similar to the case of Na^+/K^+-ATPase, CA is often unaffected by Cu exposure (Blanchard and Grosell, 2006; Grosell et al., 2003; Lim et al., 2015), again potentially due to dilution effects of the assay. Cu is known to inhibit CA in *in vitro* tests (Ceyhun et al., 2011; Christensen and Tucker, 1976; Soyut et al., 2008), but to date, only two studies (Vitale et al., 1999; Zimmer et al., 2012) have demonstrated *in vivo* inhibition of CA by Cu exposure, with one of these studies (Zimmer et al., 2012) representing the only evidence of *in vivo* CA inhibition in a fish species. Inhibition of CA by Cu could potentially explain the inhibition of J^{Na}_{in} by reducing the amount of cytosolic H^+ available to drive either electrogenic J^{Na}_{in} via H^+-ATPase or to drive electroneutral Na^+/H^+-exchange via NHE. In addition, the inhibition of CA has also been identified as a

potential mechanism for J_{amm} inhibition (Grosell, 2012). Only one study to date has provided evidence for this. In the euryhaline guppy (*Poecilia vivipara*), Zimmer et al. (2012) demonstrated that the inhibition and restoration of J_{amm} in response to Cu exposure was associated with an initial inhibition and later recovery of gill CA activity. However, in other studies, J_{amm} was inhibited by Cu while CA was unaffected (Blanchard and Grosell, 2006; Lim et al., 2015). Interestingly, Grosell (2012) also suggested that Cu might potentially act directly on Rh proteins to inhibit J_{amm} (which would also inhibit J^{Na}_{in} according to the Rh-NHE metabolon model of Na^+/NH_4^+ exchange) and this notion has been supported in a recent study (Lim et al., 2015). This latter investigation provided the first evidence that Cu can inhibit the bi-directional transport of ammonia, implicating Rh proteins in the mechanism of Cu-induced inhibition of J_{amm} (Lim et al., 2015), though more work is needed to truly understand the role of Rh in this mechanism. Regardless, it is clear that Cu has the ability to act upon one or more components of the Na^+/NH_4^+-exchange complex, leading to disruptions in J_{amm} and/or J^{Na}_{in}.

Note that for all of the aforementioned mechanisms, the site of action of Cu toxicity has generally been assumed to be the gill. Indeed, the current model used to predict toxicity in fish species, the biotic ligand model (BLM; Paquin et al., 2002) is based on gill binding coefficients. The model uses known water chemistry parameters to predict the amount of free metal ion (e.g., Cu^{2+}) available for uptake at the gill surface. Interestingly, however, this model does not consider extra-branchial sites of Cu binding. The effects of waterborne Cu on larval fish, which utilize cutaneous surfaces for

physiological exchange (e.g., MO_2, J^{Na}_{in}) have yet to be determined. Does the skin of these fish represent an additional biotic ligand for Cu binding and toxicity?

1.4 PHYSIOLOGY OF EARLY LIFE STAGE FISH

In terms of ammonia excretion, post-hatch freshwater larval fish provide a very interesting research model for a number of reasons. Firstly, fish at this stage are in the process of transitioning from urea production to ammonia excretion as the primary mode of dealing with metabolic ammonia. Secondly, fish at this stage obtain energy from the catabolism of yolk proteins and also grow at a high rate, necessitating an effective mechanism for handling relatively large metabolic loads of nitrogenous waste. Lastly, the site of both ionoregulation and gas exchange shifts from the skin to the gills over larval development, raising questions regarding both the site and mechanism of J_{amm} by larval fish. Below I summarize the current understanding of nitrogen metabolism by larval fish and provide an overview of the oxygen and ionoregulatory hypotheses, two theories aimed at explaining the physiological pressures driving branchial development in larval fish.

1.4.1 Nitrogen metabolism

Wright et al. (1995) were the first researchers to determine that the enzymes of the ornithine urea cycle (OUC), which convert ammonia to urea and are negligibly active in adult fish, are active in the whole bodies of embryonic and larval rainbow trout. Since their discovery, many other researchers have also determined that embryonic fish have the capacity for ureagenesis via the OUC (e.g. LeMoine and Walsh, 2013; Korte et al.,

1997; Steele et al., 2001). This ureagenic capacity is believed to prevent the over-accumulation of ammonia, which is potentially toxic (Randall and Tsui, 2002), throughout embryogenesis. This capacity is critical as production of metabolic ammonia at this stage is generally high for several reasons. Firstly, embryos are fueled primarily by amino acid catabolism of yolk proteins, leading to the generation of a metabolic ammonia load. Secondly, clearance of this ammonia load by the embryo is limited by the presence of the acellular chorion (Dhiyebi et al., 2013). Finally, the naturally crowded environment of embryonic fish results in water stagnation and unfavourable gradients for J_{amm} (Dhiyebi et al., 2013). Indeed, prior to hatch, whole-body T_{amm} and [urea] increase in embryonic rainbow trout and following hatch, there is a sharp increase in J_{amm} by larval fish compared to the embryonic stage, leading to a general stabilization of whole-body T_{amm} levels and a subsequent decrease in [urea] levels (Essex-Fraser et al., 2005; Wright et al., 1995). Thus, it appears that embryonic fish initially use ureagenesis as the primary mechanism of handling metabolic ammonia, whereas later in development, fish rely on J_{amm} as the primary mechanism. The exact timing of the loss of ureagenic capacity in larval fish has yet to be determined empirically, although some evidence of the timing of this transition does exist. In rainbow trout, mRNAs of carbamoyl phosphate synthetase II and III (CPS, key enzymes in the OUC) are highly expressed from 10-21 days post-fertilization (dpf), but by 60-70 dpf, the transcripts are barely detectable (Korte et al., 1997), in agreement with previous reports demonstrating a fall in CPS enzyme activity at approximately the same time (Wright et al., 1995). LeMoine and Walsh (2013) hypothesized that the silencing of CPSIII, a key enzyme in the OUC, is a function of

changes in the methylation status of the promoter region of the gene. However, there were no consistent changes in the overall methylation of the gene over development and, therefore, some other mechanism regulating the changes in CPSIII expression and activity is involved (LeMoine and Walsh, 2013). More research is needed to understand when and how fish switch completely from ureagenesis to J_{amm} to prevent ammonia accumulation and potential toxicity. Important to note, however, is that although most adult teleost fish are considered ammoniotelic, roughly 5-20% of total nitrogen excretion occurs via urea-N (see Wood, 1993 for review), despite these fish lacking a functional OUC. This urea, unlike the urea produced via the OUC in embryonic/larval fish, is generally believed to arise from uricolysis or the catabolism of dietary arginine (see Anderson, 2001 for review).

Regardless of the timing of the complete transition from ureotelism to ammoniotelism, it is clear that following hatch larval fish rapidly increase J_{amm}. In rainbow trout, three Rh transcripts (Rhbg, Rhcg1, and Rhcg2) are expressed as early as 14 dpf in the whole body and at least one of the transcripts, Rhcg1, appears to increase over development in conjunction with an increase in J_{amm} (Hung et al., 2008). Similar developmental increases in Rh expression were also observed in the whole body of zebrafish and were also consistent with increases in J_{amm} over development (Braun et al., 2009a; Nakada et al., 2007a). It is clear that the yolk sac skin of larval fish, in addition to having the capacity for J^{Na}_{in}, also excretes ammonia (e.g., Wu et al., 2010; Shih et al., 2012), and also expresses Rh proteins (Nakada et al., 2007a) but it is currently unknown

at which point over development the gills become the dominant site of J_{amm} and whether this can be attributed to changes in Rh gene expression in the gill and/or skin.

1.4.2 The oxygen and ionoregulatory hypotheses

Following hatch, fish possess only a rudimentary gill, consisting of small filamental buds protruding from the gill arch and, as such, total gill surface area at this stage is lower than cutaneous surface area (Gonzalez et al., 1996; Rombough, 1999). This general observation led to the initial hypothesis for gill development – the "oxygen hypothesis". August Krogh (1941) first hypothesized that oxygen uptake (MO_2), a surface area-dependent phenomenon, represents the earliest function of the developing gill and the need for increased MO_2 as development proceeds would represent the ontogenetic driving force behind branchial development. This theory, however, was initially based anecdotally on the fact that in adult fish, MO_2 is considered to be the most critical gill function (in an acute sense) as exposure to anoxia in most fish quickly leads to death. Furthermore, it was found that skin surface area-to-volume ratio increases at a slower rate over development than metabolic rate, leading to a problematic limitation in O_2 acquisition in developing larvae (Rombough, 2007), necessitating branchial MO_2. The thickening of skin surfaces and the development of scales were also assumed to increase diffusional distance for O_2 transport and further limit cutaneous MO_2. For four decades, the oxygen hypothesis was accepted as the prevailing theory of the ontogeny and evolution of the fish gill. More recently, however, this view has been challenged.

The first group to present evidence contrary to the oxygen hypothesis demonstrated that the ionoregulatory structures of the gill, the chloride cells (termed synonymously as mitochondria-rich cells (MRCs) or ionocytes), appear on the surface of the developing gill of tilapia (*Oreochromis mossambicus*) prior to the development of the respiratory structures of the gill, the lamellae (Li et al., 1995). Since this discovery, many researchers have also drawn the same conclusion in other fish species (see Brauner and Rombough, 2012; Rombough, 2007 for review), though no study has yet to address the specific MRC type(s) (see Dymowska et al., 2012 for review) present in the developing gill. These observations led to the development of a novel theory for gill development in fish, the "ionoregulatory hypothesis", which posits that the earliest gill function, potentially driving gill ontogeny, is ionoregulation. It was not until 2010, however, that a group of researchers provided direct evidence in support of the ionoregulatory hypothesis. Using a divided chamber approach, Fu et al. (2010) determined that the skin-to-gill shifting point (the time in development at which the gills first account for 50% of a given physiological exchange) for J^{Na}_{in} occurred at approximately 15-16 days post-hatch (dph) while the shift for MO_2 occurred significantly later at 23-28 dph, depending on rearing conditions. This evidence thus provided concrete support for the ionoregulatory hypothesis such that it is now considered the favoured theory of branchial development (Brauner and Rombough, 2012). The ionoregulatory hypothesis is also supported by less direct evidence. Rombough (2002) found that in gill-ablated zebrafish (achieved by embedding the gills in agar or by blocking ventilation using a high concentration of anaesthetic), the mean survival time (in hours) in 7 dpf larvae in freshwater was increased

by placing fish in a 50% saline solution while increasing O_2 tension had no effect. Overall, these observations demonstrate that oxygen uptake at this stage is not limited by a non-functional gill, while the opposite is true of ionoregulation, suggesting that the gill becomes a critical site for ionoregulation prior to MO_2. Moreover, the early fish gill actually acts as a sink for O_2, consuming more O_2 than it extracts from the environment (Rombough, 1992), likely in order to support growth and ionoregulation. Therefore, it is now clear that the earliest function of the developing gill is ionoregulation, not O_2 transfer, in accord with the ionoregulatory hypothesis.

What exactly, however, is implied by the term ionoregulation? Brauner and Rombough (2012) suggest that it is unlikely that ionoregulatory processes shift from the skin to the gills early in development for the sole purpose of acquiring mineral nutrients. Rather, the shift to branchial ion uptake likely occurs as coupled exchanges which participate in acid-base and nitrogenous waste excretion (e.g., Na^+/NH_4^+, Na^+/H^+, and Cl^-/HCO_3^- exchanges). This therefore raises an interesting question regarding the mechanism of J_{amm} in developing larvae. Does J_{amm} at this stage occur as coupled Na^+/NH_4^+ exchange as is the case in adult trout (see Section 1.2.2) or is the excretion of NH_3, considered the "third" respiratory gas (Randall and Ip, 2006), follow a pattern closer to that of MO_2? While our understanding of overall nitrogen handling in larval fish is substantial, these questions represent substantial knowledge gaps which have yet to be addressed.

1.5 SITES OF AMMONIA EXCRETION IN FISH

Prior to the pioneering work of Smith (1929), the general consensus regarding J_{amm} by fish was that, similar to mammalian models, the kidney played the dominant role. However, using the classic divided chamber approach, Smith (1929) determined that the gill accounted for over 80% of total J_{amm} in goldfish. Since his discovery, an abundance of work has been conducted to better understand the mechanisms of J_{amm} primarily across the gill and kidney (see Wood, 1993 for review). In addition, both the yolk sac skin of larval fish and the general body skin of specialized fish species have also been demonstrated to contribute to overall J_{amm}.

1.5.1 The gill

As described above, the gill in most adult fish typically accounts for more than 80% of total J_{amm} (Smith, 1929; Smith et al., 2012) while the remainder is believed to occur via renal, gastrointestinal, and/or cutaneous routes. The overall mechanisms of J_{amm} by the gill of freshwater fish were covered in detail above in Section 1.2 and will therefore not be reviewed in this section. To summarize, J_{amm} by the gill is considered to be loosely coupled to J^{Na}_{in} in a Na^+/NH_4^+ exchange complex or metabolon via the actions of a number of enzymes and transporters, and Rh proteins facilitate the transport of NH_3 down its partial pressure gradient (see Wright and Wood, 2009, 2012; Weihrauch et al., 2009). In the past 5 years, however, a number of studies have focused specifically on elucidating the mechanisms of J_{amm} and J^{Na}_{in} by the yolk sac epithelium.

1.5.2 The yolk sac skin

The yolk sac skin of fish has long been known to contain ionocytes and, therefore, is believed to be an important site for ion uptake (e.g., Li et al., 1995). Recently, several studies utilizing SIET paired with pharmacological, molecular, and experimental approaches have concluded that the overall mechanism of J_{amm} by the yolk sac skin of zebrafish and medaka is similar to that of the gill (Shih et al., 2008; 2012; 2013; Wu et al., 2010). Overall, J_{amm} occurs as a Na^+-coupled process though the transporters involved in this coupling can vary from one species to another and can vary depending on acclimation conditions. Interesting to note, however, is that to date no study has attempted to uncover the mechanisms of J_{amm} or J^{Na}_{in} by the yolk sac of larval rainbow trout specifically, despite the fact that these fish are dependent upon ion transport across this epithelium (at least in terms of J^{Na}_{in}) for the first 45 dpf (e.g., Fu et al., 2010). Once again, this represents a knowledge gap in our understanding of overall J_{amm} by larval rainbow trout.

1.5.3 The body skin

Recently, the skin of fish has been reviewed in terms of its importance to a number of different physiological processes, including J_{amm} (Glover et al., 2013). The body skin is considered to be an important site for J_{amm} in specialized fish such as amphibious teleosts (Frick and Wright, 2002; Souza-Bastos et al., 2014) and in some flatfish which have relatively large body skin surface areas (Sayer and Davenport, 1987). In typical fish, however, the body skin has historically been considered to be a negligible site for overall J_{amm} (Smith, 1929). This notion is contested by observations that the skin of adult rainbow trout expresses Rh genes and that these genes are responsive to a number

of ammonia-loading challenges (Nawata et al., 2007; Nawata and Wood, 2008; 2009). The same is true of amphibious species where the exposure to HEA (high external ammonia), air, or altered salinity leads to an increase in Rh gene expression in the skin (Hung et al., 2007; Souza-Bastos et al., 2014). Currently, the role of Rh proteins in the skin of trout has yet to be addressed, nor has any recent study revisited the role of the body skin in overall J_{amm} in these fish. Do Rh proteins expressed in the skin facilitate ammonia transport and does their increased expression aid in clearing ammonia from the plasma in response to experimental loading?

1.6 HYPOTHESES AND OBJECTIVES

In the preceding sections I have outlined the current understanding of ammonia excretion mechanisms in adult and larval trout across different epithelia as well as in terms of the response to experimental manipulation. In these sections, I alluded to a number of knowledge gaps which I have addressed in this thesis through the following five major hypotheses:

1) Following hatch, the skin of larval rainbow trout accounts for the majority of J_{amm}, J^{Na}_{in}, and MO_2 and J_{amm} will shift to the gills in synchrony with J^{Na}_{in}, in accord with the Na^+/NH_4^+ exchange model of J_{amm} in freshwater. This shift will be associated with increases in the gene expression and/or enzyme activity of the components of the exchange model.
2) Similar to the models developed for J_{amm} and J^{Na}_{in} by the yolk sac of zebrafish and medaka, the yolk sac skin of larval rainbow trout will possess a functional

exchange of NH_4^+ for Na^+ as the mechanism of J_{amm} which will shift to the gill over development.

3) If the ontogeny of both branchial J_{amm} and J^{Na}_{in} occurs as this functional Na^+/NH_4^+ exchange mechanism, J_{amm} will represent the driving force for branchial ontogeny given the high demand for clearing metabolic ammonia at the larval stage.
4) Exposure to waterborne Cu will act on both cutaneous and branchial routes of J_{amm} and/or J^{Na}_{in}, implicating, for the first time, the skin of larval fish as a potential biotic ligand for Cu toxicity.
5) The skin of adult trout will retain the capacity for J_{amm} observed in larval trout and this capacity will be upregulated under ammonia-loaded conditions in accordance with previous observations demonstrating the responsiveness of skin Rh genes to ammonia challenges.

1.7 CHAPTER SUMMARY

1.7.1 Chapter 2

In this chapter, hypothesis 1 was tested while some circumstantial evidence addressing hypotheses 2 and 3 was also collected. Using the same divided chamber approach as Fu et al. (2010), I determined that J_{amm} and J^{Na}_{in} by larval rainbow trout shift from the skin to the gills in synchrony at 15 dph, significantly earlier than the shift for MO_2 which occurred at 27 dph. These results add a new element to the ionoregulatory hypothesis, demonstrating that the earliest gill function may be Na^+/NH_4^+ exchange. Moreover, the gene expression of Rhcg1, Rhcg2, NHE-2, and Na^+/K^+-ATPase as well as

the enzymatic activity of Na^+/K^+-ATPase and H^+-ATPase all increased in the gills over larval development, suggesting an overall upregulation of the Na^+/NH_4^+-exchange complex. Evidence supporting the rejection of hypothesis 2 was also found in this study. A very tight, highly significant linear relationship was observed between branchial J_{amm} and J^{Na}_{in} over larval development, while no such relationship existed across the skin, suggesting that the mechanisms of J_{amm} and J^{Na}_{in} by these two epithelia may differ. Moreover, ammonia turnover time, the time needed to completely clear the body of ammonia, increased steadily up to approximately 15 dph (the shifting point) where, thereafter, it decreased linearly. This lends preliminary support to hypothesis 3 in that the ontogeny of branchial ionoregulation (as Na^+/NH_4^+ exchange) may be driven by the need to effectively clear the body of metabolic ammonia.

1.7.2 Chapter 3

Hypothesis 2 was tested in this chapter. Here, in addition to the "traditional" divided chamber used in Chapter 2, I also developed a new divided chamber system which isolated the yolk sac of larval trout. This represents the first experimental approach designed to measure ammonia and Na^+ fluxes across the yolk sac of this species. The overall aim of the chapter was to uncover the mechanism(s) of J_{amm} and J^{Na}_{in} across the gill, body skin, and yolk sac skin. Post-hatch (PH) larvae and trout fry with completely absorbed yolk sacs (CYA) were exposed to HEA for 12 h, in order to experimentally manipulate J_{amm} and J^{Na}_{in}. After transfer to clean water and mounting into divided chambers, the larvae exhibited significantly increased J_{amm} across all three epithelia (gill and body skin of CYA fish, yolk sac skin of PH larvae). However, only at the CYA gill

was this increase coupled to a concomitant increase in J^{Na}_{in}. Moreover, the J^{Na}_{in} blockers EIPA (targeting NHE) and DAPI (targeting ASIC) significantly reduced J^{Na}_{in} across both the gill of CYA fish and the PH yolk sac skin. However, only at the gill did this inhibition occur in conjunction with an inhibition of J_{amm}; none of the blockers altered J_{amm} across the yolk sac skin. These observations from both the HEA and blocker experiments further support the rejection of hypothesis 2 and suggest that J_{amm} by the gill is Na^+-coupled while the yolk sac skin does not possess a Na^+/NH_4^+ exchange mechanism. Interestingly, I found that H^+-ATPase did not contribute significantly to J^{Na}_{in} or J_{amm} by either the gill or the yolk sac skin, in contrast to some of the current models for J_{amm} and J^{Na}_{in} by these tissues. This chapter concludes with the presentation of mechanistic models of J_{amm} and/or J^{Na}_{in} by all three epithelia. Notably, this is the only experimental chapter of the thesis not yet published or submitted for publication. My plan is to first extend this work by measuring the gene expression and protein expression (where antibodies are available) of the various components of the Na^+/NH_4^+-exchange complex (Wright and Wood, 2009; Fig. 1.1) in all three epithelia under control conditions and in response to ammonia loading. Moreover, where antibodies are available, I will utilize immunohistochemical techniques in attempt to uncover the specific localization of components of the complex. For instance, it will be interesting to determine whether the localization of Rh and NHE differs between the CYA gill and PH yolk sac skin.

1.7.3 Chapter 4

In chapter 4, I tested hypothesis 3. As described above in Chapter 2, I found that the ontogeny of J_{amm} and J^{Na}_{in} occurs as Na^+/NH_4^+ exchange. With this in mind, I aimed

to determine which process, J_{amm} or J^{Na}_{in}, was the ontogenetic driving force for the transition from Na^+-independent J_{amm} across the skin to coordinated Na^+/NH_4^+ exchange by the gill. Larval trout were reared from hatch up to 18 dph under control conditions ($[Na^+]$=0.6 mmol/l) or under high NaCl ($[Na^+]$=60 mmol/l), which would greatly reduce ionoregulatory demand of the larvae. Under these conditions, I predicted that if J^{Na}_{in} were the driving force for the shift to branchial Na^+/NH_4^+ exchange, there would be a delay in the skin-to-gill shift in J_{amm}, as measured using divided chambers. On the other hand, if J_{amm} were the driving force, I would predict that the transition to branchial J_{amm} would be unaffected by high NaCl. Indeed, the skin-to-gill shift for J_{amm} occurred at the same time (13 dph) in both control and high NaCl groups and, moreover, this occurred in conjunction with a significantly elevated whole-body $[Na^+]$ in the high NaCl group. Overall, these results suggest that J_{amm} might represent the true earliest function of the gill, with the Na^+/NH_4^+ mechanism shifting to the gills at 13 dph (note the consistency with results from chapter 2) even at the expense of Na^+ balance in the high NaCl group. In accordance, the high NaCl group displayed gill Na^+/K^+-ATPase activities which were not significantly different from those of the control group at 6, 12, or 18 dph, perhaps to maintain overall Na^+/NH_4^+ exchange in order to support J_{amm}. This again occurred at the expense of Na^+ balance which I interpreted as an indication that the need to clear metabolic ammonia during larval development is a stronger ontogenetic pressure than the need to regulate Na^+ balance. I conclude this chapter by proposing the “ammonia hypothesis” which posits that J_{amm} demand drives branchial ontogeny in developing larval fish.

1.7.4 Chapter 5

In this chapter, an applied approach utilizing the information gained in chapter 2 was used with the overall goal of testing hypothesis 4. Larval fish represent an interesting model for performing toxicological studies as they are generally considered to be one of the most sensitive life stages of fish in terms of Cu exposure, primarily due to their large surface area-to-volume ratios and high ion turnover rates. Interestingly, despite the fact that the skin of larval fish represents the major site of J^{Na}_{in} (e.g., Fu et al., 2010) and can participate in J_{amm} (e.g., Shih et al., 2012; Wu et al., 2010), no previous study has examined whether Cu, in addition to acting on the gills, can also inhibit transport processes at the skin. By pre-exposing rainbow trout larvae to 50 µg/l Cu for 3 h at early (3 dph), mid (17 dph), and late (25 dph) developmental time points, then loading them into divided chambers to measure J_{amm} and J^{Na}_{in} across the anterior (gill) and posterior (skin) chambers, I was able to assess the effects of Cu at both epithelia. In early larvae, the skin accounted for the majority of both J_{amm} and J^{Na}_{in} and exposure to Cu significantly inhibited J^{Na}_{in}, but not J_{amm}, by the skin; Cu had no effect on J_{amm} or J^{Na}_{in} by the gill. This represents the first evidence that Cu can target transport across a cutaneous surface in larval fish. At the late developmental stage, when the gill accounted for the majority of both processes, exposure to Cu significantly inhibited both branchial J_{amm} and J^{Na}_{in}, as would be predicted based on the current understanding of the toxic mechanism of action of Cu. Moreover, these results support those of chapters 2 and 3, where I found evidence demonstrating that J_{amm} by the gill is Na^+-coupled while J_{amm} by the skin is Na^+-independent, as Cu inhibited only J^{Na}_{in} at the skin in early larvae but inhibited both J_{amm}

and J^{Na}_{in} in the gills of late larvae. Overall, these results demonstrate that predicting toxicity in larval fish will require an approach where one must consider two biotic ligands (the skin and gill) for Cu binding, which change over development. It is also possible that the BLM, the current regulatory tool used for predicting metal toxicity in fish and, in some instances, used for setting environmental guidelines, might have to be modified to incorporate cutaneous binding constants to ensure the protection of larval fish.

1.7.5 Chapter 6

This final chapter examines the role of the skin in J_{amm} by adult rainbow trout, setting out to test hypothesis 5. *In vivo* and *in vitro* approaches were used to evaluate the capacity of the body skin of adult rainbow trout to transport ammonia. A divided chamber approach was utilized for the *in vivo* experiments wherein cutaneous J_{amm} was isolated by removing the contribution of both renal (via urinary bladder catheterization) and gastrointestinal routes (via anal suturing). Under control conditions, the skin accounted for approximately 5% of total J_{amm}, while renal routes accounted for less than 1%. This observation in itself was interesting because the kidney has historically been assumed to be the second-most important site for J_{amm} in fish (after the gill). Following 12 h exposure to HEA, J_{amm} by the skin increased significantly, however, so did J_{amm} by the gill, such that the skin still accounted for <5% of total J_{amm}. Urinary J_{amm} also increased as a function of increased urine T_{amm} rather than increased urinary output. Using an *in vitro* approach, I found that both J_{amm} and ^{14}C-methylamine (a widely used ammonia analog) permeability increased in skin isolated from HEA-exposed trout, relative to control trout. Moreover, this increased methylamine permeability in HEA-exposed trout was blocked

by the addition of 1 mM NH_4HCO_3, suggesting competition for methylamine uptake sites by ammonia, potentially via Rh proteins which transport both compounds. However, this was not supported by gene expression data where there were no changes in Rh expression in HEA-exposed fish, though the transcripts were detected. Interestingly, I also found that amiloride treatment in the *in vitro* preparation inhibited methylamine permeability, indicating a potential role for Na^+-coupled ammonia transport by the general body skin, which was surprising given the very limited role of the skin in overall J^{Na}_{in} and the apparent lack of coupling in the yolk sac skin of larval trout. Overall, the skin of adult trout appears to have the capacity for J_{amm} which is upregulated in response to ammonia loading and the role of Rh in this process was partially supported by *in vitro* results, though not by gene expression data.

1.8 SUMMARY

Overall, the results presented in this thesis can be summarized as four major findings. Firstly, the skin of both larval and adult trout has the capacity for J_{amm}, with the skin playing a dominant role in overall J_{amm} in the post-hatch larval stage. Secondly, J_{amm} by the gill is Na^+-coupled, while J_{amm} by the yolk sac skin of larval trout is Na^+-independent. This point is particularly important given that a number of transport models are currently based upon cutaneous data (e.g., SIET studies on zebrafish and medaka yolk sac surfaces) serving as surrogates for branchial data – this approach cannot be used in trout as there is a fundamental difference between the transport mechanisms at these epithelia. Thirdly, a refinement to the current theory of branchial ontogeny in fish, the ionoregulatory hypothesis is proposed, named the “ammonia hypothesis”. This amended

hypothesis posits that J_{amm} as Na^+/NH_4^+ exchange is the earliest function of the developing gill and may represent the driving force for the ontogeny and, perhaps, the evolution of the vertebrate gill. Lastly, larval fish represent a complex system in which to predict the toxicity of Cu (and potentially other toxicants) as both the site (skin or gill) and mechanism of action (inhibition of J_{amm} and/or J^{Na}_{in}) changes over development. As a whole, these four findings contribute significantly to our overall understanding of ammonia handling by fish and open the door to a number of novel research avenues to be explored in future work.

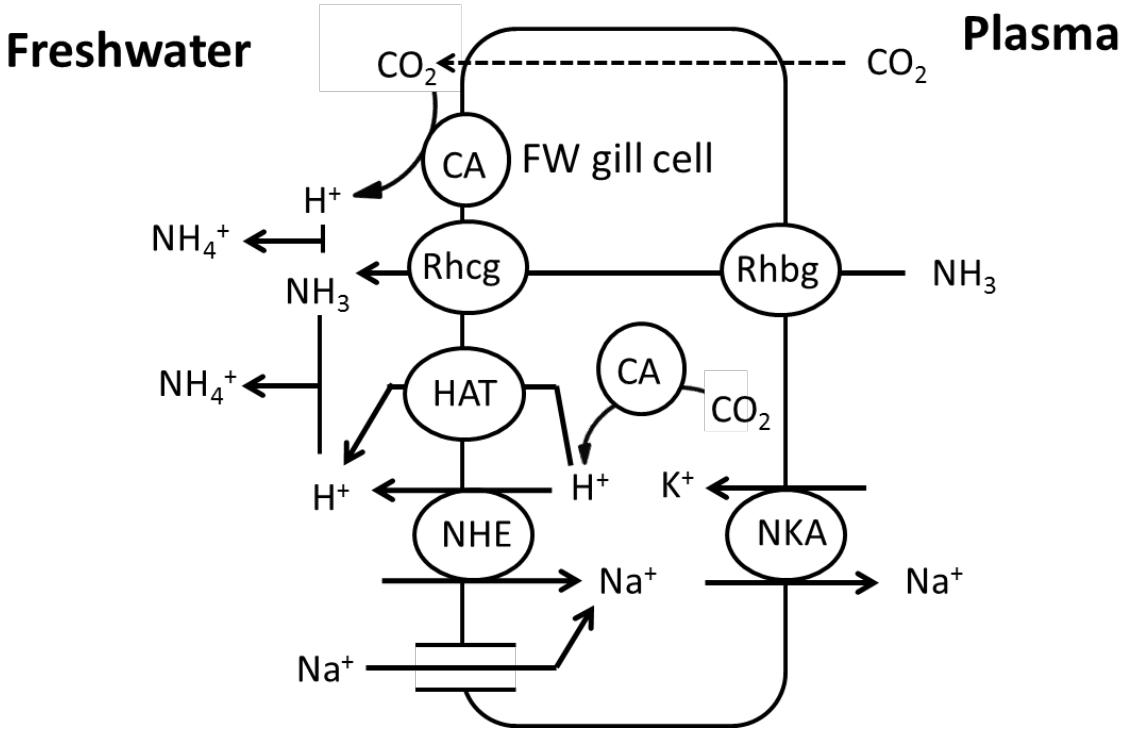
Freshwater
Plasma
CO2
CO2
CA
FW gill cell
H+
NH4+
Rhcg
Rhbg
NH3
NH3
NH4+
HAT
CA
CO2
H+
H+
K+
NHE
NKA
Na+
Na+
Na+

Fig. 1.1. The "Na^+/NH_4^+-exchange complex" model for ammonia excretion by the gill of freshwater fish. CA (carbonic anhydrase); HAT (H^+-ATPase); NHE (Na^+/H^+-exchanger); NKA (Na^+/K^+-ATPase); Rhcg (apical Rhesus protein); Rhbg (basolateral Rhesus protein). Model is adapted from Wright and Wood (2009) and modified from Zimmer et al. (2012).

CHAPTER 2

WHAT IS THE PRIMARY FUNCTION OF THE EARLY TELEOST GILL? EVIDENCE FOR Na^+/NH_4^+ EXCHANGE IN DEVELOPING RAINBOW TROUT (*ONCORHYNCHUS MYKISS*)

2.1 ABSTRACT

Post-hatch fish lack a functional gill and utilize cutaneous surfaces for exchange with the surrounding environment. The ionoregulatory hypothesis posits that ionoregulation is the first physiological process to be limited by cutaneous exchange, necessitating its shift to the gills. We hypothesized that the ontogeny of branchial ammonia excretion (J_{amm}) is coupled to Na^+ uptake (J^{Na}_{in}) in accordance with the current model for Na^+/NH_4^+ exchange in freshwater. Using divided chambers, branchial and cutaneous J_{amm}, J^{Na}_{in}, and oxygen consumption (MO_2) by larval rainbow trout were assessed. Following hatch, the skin accounted for 97 and 86% of total J_{amm} and J^{Na}_{in}, respectively. J_{amm} and J^{Na}_{in} shifted to the gills simultaneously at 15 days post-hatch (dph) and were highly correlated (R^2=0.951) at the gills, but not the skin, over development. In contrast, MO_2 shifted significantly later at 27 dph, in agreement with the ionoregulatory hypothesis. Moreover, the mRNA expression and/or enzymatic activity of Rhesus proteins, Na^+/H^+-exchanger, H^+-ATPase, Na^+/K^+-ATPase, and carbonic anhydrase, all key components of the Na^+/NH_4^+-exchange system, increased in the gills over larval development. We propose that the ontogeny of branchial J^{Na}_{in} occurs as Na^+/NH_4^+ exchange and provide evidence for a novel element to the ionoregulatory hypothesis, the excretion of potentially lethal metabolic ammonia.

2.2 INTRODUCTION

The gill in most teleost fish is the major site for physiological exchanges with the surrounding environment, participating in gas exchange, ion acquisition, acid-base regulation, and nitrogenous waste excretion (reviewed in Evans et al., 2005). In larval fish, however, the gill is undeveloped following hatch and contributes little to physiological exchange (e.g. Wells and Pinder, 1996; Fu et al., 2010). Initially, the skin is the dominant site, and as the gills develop, these exchanges eventually shift to become primarily branchial (Wells and Pinder, 1996; Fu et al., 2010). The selective pressures underlying gill ontogeny in both a developmental and evolutionary context have been debated over several decades.

In larval fish, metabolic rate increases more rapidly over development than skin surface area, leading to a problematic limitation in cutaneous transport, necessitating the development of the gills (reviewed in Rombough, 2007). August Krogh (1941) first suggested that the earliest function of the developing gill is O_2 uptake and this hypothesis, termed the oxygen hypothesis, was the accepted view of gill development for half a century. More recently, however, this view has been challenged. In many fish species, the appearance of branchial ionocytes, the primary site of ionoregulatory exchange, precedes the formation of gill respiratory structures (i.e., filaments or lamellae) (Li et al., 1995; Gonzalez et al., 1996; Rombough, 1999). These observations led to the ionoregulatory hypothesis, which posits that ionoregulation is the earliest gill function (reviewed in Rombough, 2007; Brauner and Rombough, 2012). Most recently, Fu et al. (2010), using divided chambers, directly demonstrated that in rainbow trout larvae reared in soft or hard

water, Na^+ uptake shifts from the skin to the gills prior to O_2 uptake, strongly supporting the ionoregulatory hypothesis.

The goal of the present study was to determine the relationship between the ontogeny of Na^+ uptake and the ontogeny of the excretion of ammonia, the third respiratory gas (Randall and Ip, 2006) at this early life stage in an ammoniotelic teleost fish. As recently suggested (Brauner and Rombough, 2012), the ontogeny of branchial ion uptake may occur as a function of homeostatic processes which are coupled to ion uptake such as acid-base balance and/or ammonia excretion, rather than being solely for the acquisition of mineral nutrients. We hypothesized that branchial ammonia excretion in larval trout would occur as a function of Na^+/NH_4^+ exchange and that this coupling of Na^+ uptake (J^{Na}_{in}) and ammonia excretion (J_{amm}) might represent the earliest function of the developing gill. Moreover, J_{amm} in larval fish is particularly important given that the catabolism of yolk sac proteins, which fuels metabolism at this stage, generates a metabolic ammonia load (Wright and Fyhn, 2001) which can be potentially lethal at elevated levels (Randall and Tsui, 2002).

In adult rainbow trout, J_{amm} is believed to be coupled to J^{Na}_{in} via a Na^+/NH_4^+-exchange complex in which Rhesus (Rh) glycoproteins play a critical role (reviewed in Wright and Wood, 2009). However, it is not clear if this would be the case in larval trout where J^{Na}_{in} shifts from the skin to the gills over development (Fu et al., 2010). We used the same divided chamber approach as employed by Fu et al. (2010) to examine these processes. We predicted that, similar to J^{Na}_{in} and oxygen consumption (MO_2) (Wells and Pinder, 1996; Fu et al., 2010), J_{amm} would initially occur via cutaneous routes, but would

shift to the gills in synchrony with J^{Na}_{in} and not with MO_2. Such a result would indicate that the ontogeny of branchial Na^+ uptake occurs as part of Na^+/NH_4^+ coupled exchange, adding a critical new element to the ionoregulatory hypothesis. Alternatively, if J_{amm} at this stage is not coupled to J^{Na}_{in}, we might expect its shift to be closer to that of another respiratory gas, oxygen. An additional related hypothesis was that J_{amm} and J^{Na}_{in} in larval trout would occur via the components of the Na^+/NH_4^+-exchange complex. We predicted that the increase in branchial J_{amm} and J^{Na}_{in} over development would occur in conjunction with an increase in gene expression and/or enzymatic activity of the key components of the complex (Rh proteins, Na^+/H^+-exchanger (NHE), Na^+/K^+-ATPase, H^+-ATPase, and carbonic anhydrase (CA) (reviewed in Wright and Wood, 2009) in the gills, while a decreased mRNA expression and/or activity of these proteins was expected in skin tissues.

2.3 MATERIALS AND METHODS

2.3.1 Fish husbandry

Rainbow trout (*Oncorhynchus mykiss*) embryos were purchased in the eyed-up stage from Rainbow Springs Hatchery (Thamesford, ON, Canada) and held at 12°C in hatching trays with flow-through Hamilton dechlorinated tapwater (moderately hard: $[Na^+]$= 0.6 mequiv/l, $[Cl^-]$ = 0.8 mequiv/l, $[Ca^{2+}]$= 0.8 equiv/l, $[Mg^{2+}]$= 0.3 mequiv/l, $[K^+]$ =0.05 mequiv/l; titration alkalinity 2.1 mequiv/l; pH ~8.0; hardness ~140 mg/l as $CaCO_3$ equivalents). All larvae used in flux experiments and measurements of whole-body ammonia content were from the same batch of embryos which hatched at the same time.

Hatching took place approximately 1 week after purchase and this marked the beginning of the experimental period. Complete yolk sac absorption (CYA) occurred approximately 30 days post-hatch (dph) at which point exogenous feeding began, with daily meals of approximately 5% fish body mass. All experiments performed after CYA were conducted on 48-h fasted fish; experimental temperature was 12^{o}C. All experimental procedures were approved by the animal care committee of McMaster University.

2.3.2 Experimental design for flux measurements

At 0,3,6,9,12,15,18, 21 dph, and following CYA, experiments were conducted to estimate branchial and cutaneous contributions to ammonia excretion (J_{amm}), Na^+ uptake (J^{Na}_{in}), and oxygen consumption (MO_2) using a divided chamber protocol. Prior to experimentation, fish were anaesthetized in 50-100 ppm clove oil, similar to that used in a previous divided chamber study (Fu et al., 2010). After anaesthesia to stage 3 (McFarland, 1959), each fish was loaded into a small hole in a latex dental dam, such that its head, operculae, and pectoral fins were separated spatially from the rest of its body. The fish and dam were then mounted between two 5-ml half-chambers containing dechlorinated tapwater with 10-15 ppm clove oil. Fresh aerated, clove oil-spiked tapwater was then circulated through both chambers using a peristaltic pump at a rate of 0.2 ml/min for a 1-h acclimation period. An additional control series of experiments was conducted on non-anaesthetized, unrestrained larvae at 3 dph, which revealed that the anaesthetic and divided chamber setup had no significant effect on J_{amm}, J^{Na}_{in}, or MO_2 (data not shown). All experimental procedures, measurements, and analyses used for

control experiments were identical to those used in the divided chamber experiments described below.

2.3.3 J_{amm} and J^{Na}_{in}

Following the 1-h acclimation period, water re-circulation was stopped and 0.5 μCi ^{22}Na (Amersham Pharmacia Biotech Inc.) was added to either the anterior or posterior chamber; it was not possible to measure anterior and posterior Na^+ fluxes on the same fish. Following 5 min of mixing by aeration, initial 1.25-ml samples were taken from both chambers to measure water total ammonia (T_{amm}), Na radioactivity (as counts per minute; cpm), and total [Na^+]. Following a 1.5-h flux period, identical final samples were taken, and the remaining water volume was measured in both chambers. Larvae were removed from the divided chambers and were rinsed 3 times with 5 mM NaCl and once with double-distilled water to remove any surface-bound isotope. Larvae were then euthanized using 0.2 g/l MS-222, weighed, and counted for ^{22}Na radioactivity. Samples for water T_{amm} were stored at -20°C until later analysis while samples for ^{22}Na radioactivity were counted immediately and stored at 4ºC until later [Na^+] analysis. For each flux, a maximum of 10% isotope leak to the unloaded chamber was accepted as a successful dam and all fish recovered completely from anaesthetic treatment within 5 min, prior to euthanasia.

All flux values are presented as flux per g of whole fish including the yolk sac. Total ammonia concentrations (T_{amm}) of water samples were assayed using the protocol

described by (Verdouw et al., 1978). Anterior and posterior ammonia flux rates (J_{amm}; µmol/g/h) were determined using the following equation:

$$(1) \qquad J_{amm} = (T_{amm}f - T_{amm}i)*V/(t \times M)$$

where $T_{amm}f$ and $T_{amm}i$ are the final and initial concentrations of ammonia (µmol/l) in the water samples within the anterior or posterior chambers, V is volume (l) of the given chamber, t is flux duration (h), and M is mass (g) of the fish, yolk sac included. Total J_{amm} was determined by adding anterior and posterior flux rates from the same fish. Radioactivity of ^{22}Na in counts per minute (cpm) of water samples and whole larvae was measured via gamma counting (Perkin Elmer Wizard 1480 3" Auto Gamma Counter), and $[Na^+]$ of water samples was measured using atomic absorption spectrophotometry (SpectrAA 220FS Atomic Absorption Spectrophotometer). Anterior and posterior sodium influx rates (J^{Na}_{in}; µmol/g/h) were calculated as:

$$(2) \qquad J^{Na}_{in} = R_{fish}/(SA_{average} \times t \times M)$$

where R_{fish} is the gamma-radiaoactivity of the fish (cpm) at the end of the flux period and $SA_{average}$ is the mean of the initial and final specific activities (cpm/µmol) of the water from the ^{22}Na-loaded chamber. Total J^{Na}_{in} (anterior + posterior) was calculated by sorting replicate fish by mass and pairing corresponding anterior and posterior replicates together.

2.3.4 MO_2

O_2 consumption rates were measured on separate fish at the same time periods. Following the 1-h acclimation period described above, air lines were removed and anterior and posterior chambers were filled completely with clove oil-spiked tapwater. Initial 600-µl samples were taken from both chambers and replaced with an equal volume of water of known PO_2. The PO_2 of each initial sample was read immediately using a Clarke-type oxygen electrode (Cameron Instruments) connected to a Model 1900 Polarographic Amplifier (AM Systems) kept at 12 ºC. Following 0.5-1 h, a second 600-µl sample was taken from each chamber to assess final PO_2. This procedure was done simultaneously for both anterior and posterior chambers for each replicate fish. Larvae were then removed from the divided chambers, euthanized, and weighed. As in the previous series, 0.5 µCi ^{22}Na was added to one side for the assessment of dam integrity. Anterior and posterior oxygen consumption rates (MO_2; µmol/g/h) were calculated as:

$$(3) \qquad M_{O_2} = [(PO_2i - PO_2f) \times \alpha O_2 \times V]/(t \times M)$$

where PO_2i (mmHg) is the initial PO_2 of the chamber which was corrected for the replacement water of a known PO_2 (see above), PO_2f (mmHg) is the final PO_2 of the chamber, and αO_2 (µmol/l/mmHg) is the solubility constant for O_2 in water at 12°C (Boutilier et al., 1984).

2.3.5 Skin surface area measurements and calculation of branchial and cutaneous flux rates

In a separate batch of larvae, lateral images of larvae at each developmental time point (n=3-6) were taken using a digital camera attached to a Leica EZ4D dissecting microscope. Images were then traced using ImageJ software (Wayne Rasband, National Institutes of Health, USA) and the two-dimensional anterior (head, operculum, pectoral fin) and posterior (body, yolk sac, and dorsal and pelvic fins) surface area (SA) of the lateral aspect of the fish was determined. The resulting proportions of posterior SA relative to total SA over development (% posterior; Table 2.1) were similar to those reported previously using a different method (Fu et al., 2010). Branchial flux rates (μmol/g/h) were then determined as:

(4) Branchial flux rate = anterior flux rate –

[anterior SA x (average posterior flux rate/posterior SA)]

where anterior flux rate (μmol/g/h) is the flux measured in the anterior chamber, anterior SA (cm^2) is average anterior cutaneous surface area, average posterior flux rate (μmol/g/h) is the average flux measured in the posterior chamber, and posterior SA (cm^2) is the average posterior cutaneous surface area. Cutaneous flux rates (μmol/g/h) were calculated as:

(5) Cutaneous flux rate = total flux rate – branchial flux rate

where total flux rate (μmol/g/h) is the sum of anterior and posterior flux rates. As in Fu et al. (2010), these calculations assume that cutaneous flux per unit skin area is the

same in the head region (i.e., anterior chamber) as in the rest of the body (i.e., posterior chamber).

2.3.6 Estimation of cutaneous-to-branchial shifting point

In order to estimate the cutaneous-to-branchial shifting point for a given process (where 50% occurs via branchial or cutaneous routes), % of total branchial and cutaneous values were plotted as x-values against time (dph; y-values). x=0 was then set to 50%, such that the y-intercept (in dph) occurred at x=50% and would correspond to the shifting point for any given process. Y-intercept values and corresponding standard errors of estimate were obtained using SigmaPlot version 10.0 (Systat Software, Inc.).

2.3.7 Whole-body tissue T_{amm} and turnover time

At 0,3,6,9,12,15,18, 21 dph, and following CYA, a random set of larvae were removed from hatching trays, euthanized in neutralized 0.1 g/l MS-222, and immediately flash frozen and stored at -80°C. Larvae (1-4 per replicate) were then ground into a fine powder using a liquid N_2-cooled mortar and pestle. The powder was deproteinized with 8% $HClO_3$ and subsequently neutralized using 2M KOH. Whole-body T_{amm} was measured in neutralized, deproteinized samples using a commercial kit (Cliniqa Corporation, San Diego, CA) described in previous studies (e.g. Zimmer et al., 2014a). Ammonia turnover time was calculated as:

(6) Turnover time = Whole-body T_{amm}/average total J_{amm}

2.3.8 Branchial and cutaneous enzyme activity and gene expression

At 3, 12, 21 dph, and following CYA, a random set of larvae were removed from hatching trays, euthanized using an overdose of neutralized MS-222; whole gill baskets, yolk sac epithelium, and body epithelium samples were taken for gene expression or enzymatic analyses. Tissue samples for gene expression were placed individually directly into 600 µl of ice-cold commercial lysis buffer (PureLink RNA mini kit, Ambion) and homogenized using a small plastic pestle and lysed by passing the homogenate through a 23-gauge needle 3 times. RNA was extracted from tissue samples using the PureLink RNA mini kit according to the manufacturer's protocol. DNAase treatment was performed using an on-column treatment (PureLink DNAse set, Ambion) also according to the manufacturer's protocol. RNA concentration and purity were determined spectrophotometrically (Nanodrop ND-1000, Nanodrop Technologies) and RNA quality was assessed by running samples through a 1% agarose gel stained with RedSafe (FroggaBio). cDNA was synthesized from 200 ng total RNA using an oligo(dT_{17}) primer and Superscript II reverse transcriptase (Invitrogen). mRNA expression of reference and target genes was determined by quantitative polymerase chain reaction (qPCR). Total reactions (10µl) consisted of 4 µl of diluted cDNA template, 5 µl of 2X SsoFast EvaGreen Supermix (Bio-Rad), 0.4 µl each of 100 µmol/l forward and reverse primers of the genes of interest (Table 2.2), and 0.2 µl nuclease-free water, and were performed using a CFX Connect Real-Time PCR Detection System (Bio-Rad). The reaction mix was first heated to 98°C for 2 min to activate polymerase, followed by 40 amplification cycles of 2 s at 98°C and 5 s at the annealing temperature specific to the given primer pair (Table

2.2) which had been optimized beforehand. No template controls were conducted with every run and non-reverse transcribed controls were performed for every primer pair. Melt curve analyses confirmed the presence of a single PCR product for every gene of interest and the efficiency of amplification for every primer pair in each tissue type was between 95 and 110%. Relative expression of target genes was determined via the ΔΔCq method using both EF1α and β-actin as reference genes. Expression was normalized to that of the gill at 3 dph using the CFX Manager 3.0 software.

For enzymatic analyses, each tissue was placed directly into 250 µl of ice-cold EGTA-Na deoxycholate homogenization buffer, flash frozen, and stored at -80°C for later analysis. Pooling of samples (up to 5) was necessary to detect enzyme activity in small tissues. Pooled samples were later homogenized in the EGTA-Na deoxycholate buffer in which they were stored. Na^+/K^+-ATPase, H^+-ATPase and carbonic anhydrase (CA) activities in homogenates were assayed using methods described previously (Nawata et al., 2007; Zimmer et al., 2012). Protein concentration of homogenates was measured with the Bradford reagent (Sigma) using a bovine serum albumen (Sigma) standard curve.

2.3.9 Statistical analyses

All data are represented as means ± 1 SEM (n=sample size) and statistical significance was accepted at the $P<0.05$ level. All statistical and regression analyses were performed using SigmaPlot version 10.0 with SigmaStat 3.5 integration (Systat Software, Inc.). In general, analyses comparing two means were performed using a two-tailed t-test while analyses comparing three or more means were performed using a one-way analysis

of variance (ANOVA) with a Holm-Sidak post-hoc test. In the case of a failed normality test, data were square root or log transformed. Specific tests and normalization procedures used are described further in corresponding Figure captions.

2.4 RESULTS AND DISCUSSION

The ontogeny of J_{amm} and J^{Na}_{in} in larval rainbow trout appears to occur via a Na^+/NH_4^+ exchange complex as seen in the gills of adult trout (Wright and Wood, 2009). Both J_{amm} and J^{Na}_{in} shifted from the skin to the gills at the same time (15 dph) and were highly correlated over development at the gill (R^2=0.951). Moreover, this shift occurred significantly earlier than that of MO_2 (27 dph), confirming previous work (Fu et al., 2010) and providing strong support for the ionoregulatory hypothesis. The mRNA expression and/or enzyme activity of several of the key components of Na^+/NH_4^+ exchange system also increased in the gills, including Rh and NHE, in accordance with the configuration observed in larval zebrafish (Kumai and Perry, 2011). The evolution of such exchange systems and metabolons may have occurred as an effective single solution to limitations in a number of cutaneous exchange processes (ions, acid equivalents, nitrogen wastes) over larval development.

2.4.1 The ontogeny of branchial Na^+/NH_4^+ exchange

Immediately following hatch, the skin represented the dominant site for both J_{amm} and J^{Na}_{in}, accounting for 96.7 ± 2.0 and 86.5 ± 6.5% of total, respectively (Figs. 2.1 and 2.2). Over development, however, both absolute J_{amm} and absolute J^{Na}_{in} by the gills increased while those by the skin remained relatively constant (Fig. 2.1). The cutaneous-

to-branchial shift, at which 50% of a given process occurs via the gills, for J_{amm} occurred at 15.0 ± 0.7 dph remarkably at exactly the same time as J^{Na}_{in} (14.9 ± 1.2 dph), suggesting a coordinated ontogeny of both processes, potentially as Na^+/NH_4^+ exchange. Indeed, both processes were observed to be highly correlated at the gills over development in rainbow trout (R^2=0.951; Fig. 2.3) while, interestingly, such a relationship was not observed at the skin (data not shown). In adult fish, this coupled exchange is coordinated by a complex consisting of a number of different components (reviewed in Wright and Wood, 2009). Perhaps the most integral part of the Na^+/NH_4^+ exchange complex is the Rh-NHE metabolon; recent evidence demonstrates that this metabolon is key to both J_{amm} and J^{Na}_{in} in larval fish (Kumai and Perry, 2011; Shih et al., 2008; Wu et al., 2010; Shih et al., 2012). In larval rainbow trout, gene expression of Rhcg2 in the gill, relative to 3 dph, increased significantly by 21 dph, whereas expression of Rhcg1 and NHE-2 increased significantly by CYA (Figs. 2.4A,B,D); Rhbg mRNA expression was unchanged in the gills over development (Fig. 2.4C). The branchial gene expression of three additional components, Na^+/K^+-ATPase, H^+-ATPase, and carbonic anhydrase, increased significantly over larval development only in the case of Na^+/K^+-ATPase (Fig. 2.4E,F,G). However, the enzymatic activity of these components increased 6.2, 4.8, and 4.2-fold from 3-21 dph (Fig. 2.5) for Na^+/K^+-ATPase, H^+-ATPase, and carbonic anhydrase, respectively, potentially indicating the induction of at least part of the Na^+/NH_4^+ exchange system. Some discrepancies between gene expression and enzymatic activity may not be surprising given that H^+-ATPase, for example, has many regulatory inputs at the post-transcriptional level (reviewed in Beyenbach and Wieczorek, 2006).

These observations suggest that the ontogeny of branchial Na^+/NH_4^+ exchange is coordinated by the same exchange complex as seen in the gill of adult freshwater fish (Wright and Wood, 2009) and zebrafish larvae (Kumai and Perry, 2011) and that this arrangement is present at the onset of branchial J_{amm} and J^{Na}_{in}. In the present larval trout, such a configuration does not appear to exist at the skin. Contrary to our initial hypothesis, cutaneous J_{amm} and J^{Na}_{in} (Fig. 2.1) and the gene expression and enzyme activity of several of the key components of Na^+/NH_4^+ exchange in cutaneous epithelia (yolk sac and body; Figs. 2.4, 2.5) remained relatively constant over larval development. This may suggest alternate mechanisms of transport, consistent with differentiation of distinct gill and skin epithelial surfaces. Moreover, the decrease in relative importance of cutaneous routes over development appears to be a function of increasing branchial exchange, rather than decreasing cutaneous exchange.

2.4.2 Evidence supporting a novel element of the ionoregulatory hypothesis

The coordinated cutaneous-to-branchial shifts for J_{amm} and J^{Na}_{in} at 15 dph occurred significantly earlier in development than the shift for MO_2 at 26.6 ± 2.0 dph (by extrapolation, Fig. 2.2). These results are in agreement with and nearly identical to those of Fu et al. (2010), which provided support for the ionoregulatory hypothesis using a direct physiological approach. The independent replication of these results (Fu et al., 2010) and the wealth of indirect histological evidence that exists (reviewed in Rombough, 2007; Brauner and Rombough, 2012) provide concrete support for the ionoregulatory hypothesis. Moreover, these findings provide evidence for an additional critical element

of the ionoregulatory hypothesis, demonstrating that the ontogeny of branchial Na^+ uptake occurs as Na^+/NH_4^+ exchange.

2.4.3 What is the earliest gill function?

An effective mechanism for excretion of ammonia, the third respiratory gas (Randall and Ip, 2006), may be critically important in developing fish. During larval development, metabolism is fueled by the catabolism of amino acids obtained from yolk proteins, leading to the release of potentially toxic ammonia. Embryonic fish, surrounded by the chorion, accumulate a substantial load of metabolic ammonia prior to hatch (Wright et al., 1995; Essex-Fraser et al., 2005). Whole-body T_{amm} buildup, which continued even after hatch (Fig. 2.6), could potentially be attenuated by gill development. Prior to the cutaneous-to-branchial shift for J_{amm}, whole body T_{amm} accumulated at a rate of 0.18 µmol/g/day over the first 15 dph while from 15-21 dph, T_{amm} accumulation slowed to a rate of 0.06 µmol/g/day (Fig. 2.6). Similarly, ammonia turnover time increased over development until reaching a peak at 12-15 dph (Fig. 2.6), again coinciding with the cutaneous-to-branchial shift for J_{amm} (Fig. 2.2). Thereafter, ammonia turnover time decreased steadily, suggesting that the ontogeny of branchial J_{amm} might allow for a more effective clearance of metabolic ammonia. This may be a particularly critical event in early development given the eventual loss of ureagenic capacity which is utilized in embryonic stages to limit the accumulation of metabolic ammonia (Wright et al., 1995; Korte et al., 1997).

The acquisition of mineral ions required by larval growth, however, is also critical to larval development (reviewed in Rombough, 2007). The simultaneous ontogeny of branchial J_{amm} and J^{Na}_{in} may function to coordinate the elimination of nitrogenous waste, the acquisition of Na^+, and the removal of metabolic acid. At present, it is unclear which of these processes would be the first to be truly limited by cutaneous exchange, necessitating its branchial shift. Gill ablation studies have demonstrated clearly that branchial Na^+ uptake is vital to larval survival earlier in development than branchial O_2 uptake (Rombough, 2002) and similar studies may be useful in determining at which point in development branchial ammonia excretion and acid-base exchange become critical.

2.4.4 Future Perspectives

The present study, in addition to further affirming and adding a novel element to the ionoregulatory hypothesis, provides evidence that the Na^+/NH_4^+-exchange complex develops at the onset of branchial ontogeny. An interesting avenue for future research is the examination of the selective pressures which led to the evolution of such coupled exchanges. Interestingly, in hagfish, extant relatives of the most ancestral jawless fishes, all of the components of the Na^+/NH_4^+-exchange complex are expressed in the gills (Braun and Perry, 2010; Tresguerres et al., 2006) yet these fish display only Na^+/H^+ exchange and not Na^+/NH_4^+-exchange (Evans, 1984), despite ammonia being the dominant form of nitrogenous waste excreted and the gills accounting for the majority of its excretion (Braun and Perry, 2010; Clifford et al., 2014). The question of why and when different branchial exchange metabolons evolved in fish is an interesting one and

may lead to a better overall understanding of the arrangement of branchial ionoregulatory, acid-base, and nitrogen excretion mechanisms in modern fishes.

2.5 TABLES AND FIGURES

Table 2.1. Average wet weight (g) and % of total cutaneous surface area in the posterior chamber at 0, 3, 6, 9, 12, 15, 18, and 21 days post-hatch (dph) and following complete yolk sac absorption (CYA). n=3-6

Larval Age (dph)	Wet Weight (g)	% Cutaneous Surface Area in Posterior Chamber
0	0.0158 ± 0.0007	90.6 ± 0.5
3	0.0222 ± 0.0011	86.9 ± 0.1
6	0.0347 ± 0.0014	78.0 ± 0.6
9	0.0456 ± 0.0014	75.9 ± 0.9
12	0.0617 ± 0.0016	73.1 ± 0.9
15	0.0714 ± 0.0012	74.4 ± 0.3
18	0.0865 ± 0.0021	73.4 ± 0.8
21	0.1075 ± 0.0036	71.4 ± 1.1
CYA	0.1442 ± 0.0070	70.3 ± 4.7

Table 2.2. Accession numbers, forward and reverse primers, and annealing temperatures (ºC) for all primer pairs used in qRT-PCR.

Gene	Accession No.	Forward Primer	Reverse Primer	Annealing Temp. (ºC)
EF1α	AF498320	GGAAAGTCAAC CACCACAG	GATACCACGCT CCCTCTCAG	60
β-Actin	AJ438158	ACTGGGACGAC ATGGAGAAG	AGGCGTATAGG GACAACACG	60
Rhcg1	DQ431244	CATCCTCAGCC TCATACATGC	TGAATGACAGA CGGAGCCAATC	60
Rhcg2	AY619986	CCTCTTCGGAG TCTTCATC	CTATGTCGCTG G TGATGTTG	60
Rhbg	EF051113	CGACAACGACT TTTACTACCGC	GACGAAGCCCT G CATGAGAG	65
NHE2	EF446605	TATGGCCATTG TGACCTGTG	CAGGCCTCTCC A CACTAAGG	60
Na^+/K^+-ATPase1a	AY319391	TTGACCTGGAT GACCACAAG	GGATCTCCTTA GCCCGAAC	57
H^+-ATPase	AF140002	TCAGCCTTGGTT GTGAGATG	CAACATTGGTG GGAAACAGG	60
Carbonic anhydrase 2	AY514870	GCCAGTCTCCC ATTGACATC	CCTGTACGTCC CTGAAATGG	60

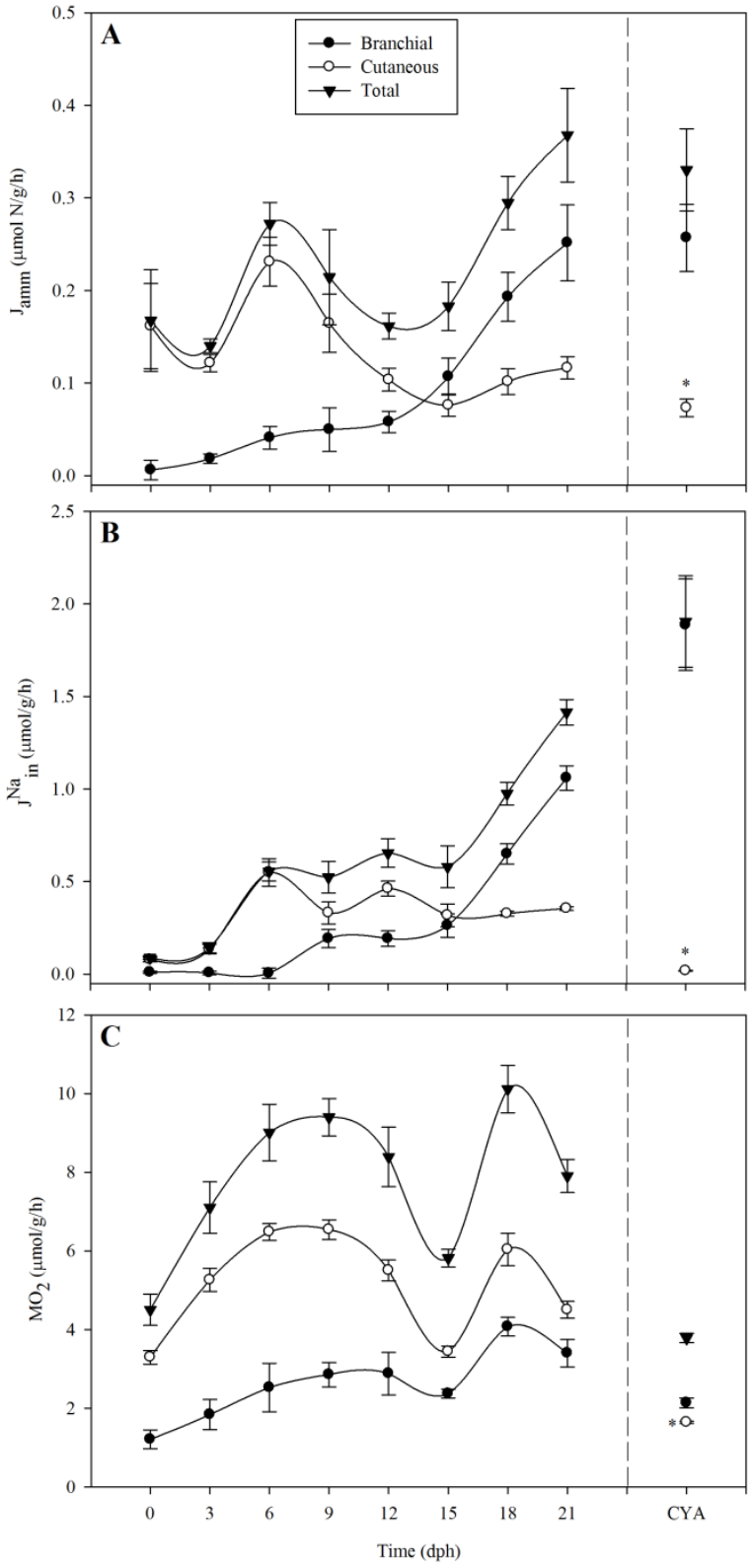
A
Branchial
Cutaneous
Total
J_{amm} (µmol N/g/h)
0.5
0.4
0.3
0.2
0.1
0.0
*
B
J^{Na}_{in} (µmol/g/h)
2.5
2.0
1.5
1.0
0.5
0.0
*
C
MO_2 (µmol/g/h)
12
10
8
6
4
2
0
*
0
3
6
9
12
15
18
21
CYA
Time (dph)

Fig. 2.1. Branchial (filled circles), cutaneous (open circles), and total (filled triangles) ammonia excretion (A; J_{amm}), Na^+ uptake (B; J^{Na}_{in}), and oxygen consumption (C; MO_2) rates over development following hatching in rainbow trout. Asterisks represent cutaneous flux rates which differed significantly from corresponding branchial flux rates following CYA. A one-way ANOVA with a multi-comparison Holm-Sidak post-hoc test (Dunn's method in the case of failed normality or equal variance tests) revealed that there was a significant difference in J_{amm}, J^{Na}_{in}, and MO_2 between 0 and 21 days post-hatch. (n=6-12) CYA = complete yolk sac absorption

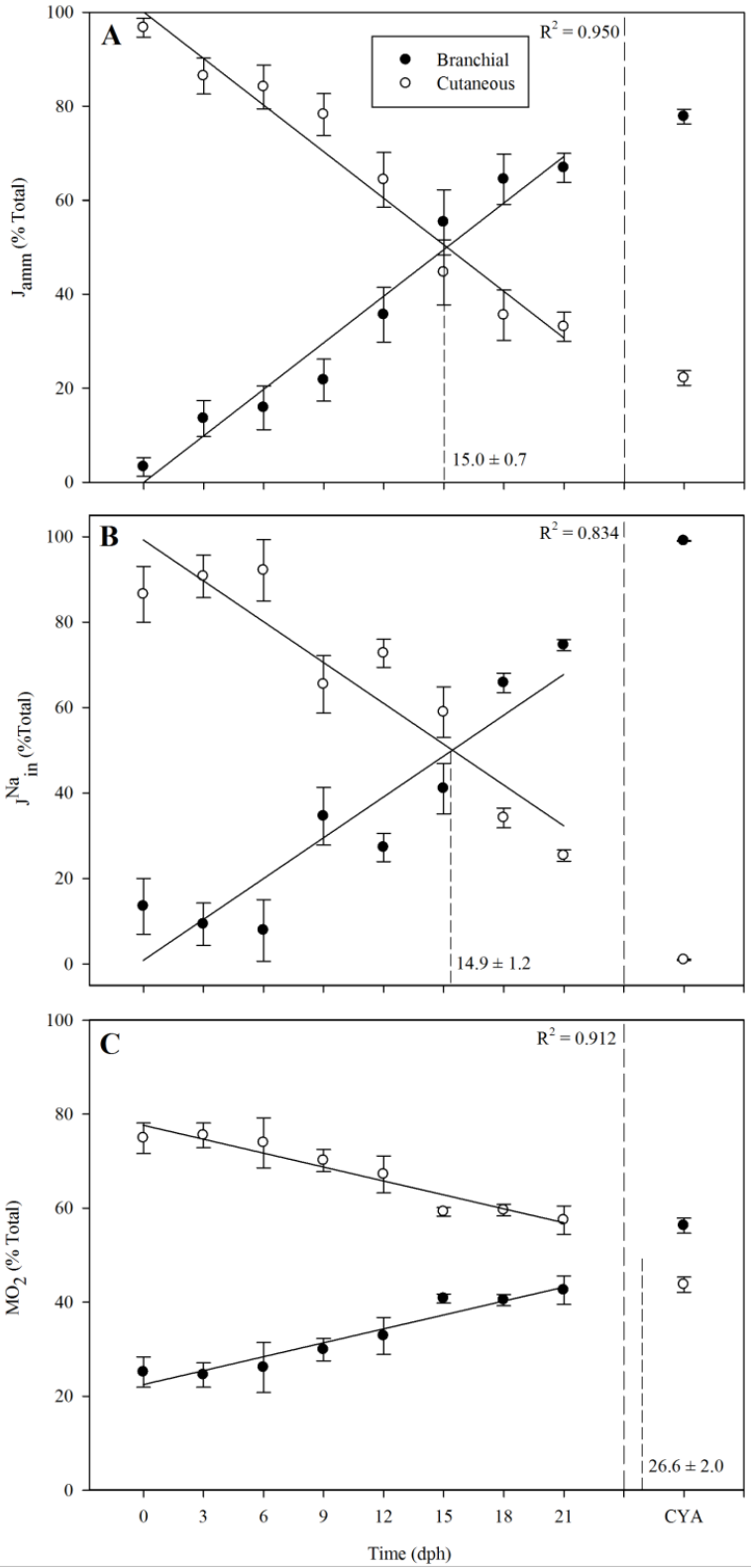
A
B
C
Branchial
Cutaneous
R² = 0.950
R² = 0.834
R² = 0.912
15.0 ± 0.7
14.9 ± 1.2
26.6 ± 2.0
J amm (% Total)
J Na in (%Total)
MO2 (% Total)
Time (dph)
0
3
6
9
12
15
18
21
CYA
20
40
60
80
100

Fig. 2.2. % branchial (filled circles) and cutaneous (open circles) ammonia excretion (A; J_{amm}), Na^+ uptake (B; J^{Na}_{in}), and oxygen consumption (C; MO_2) rates over development following hatching in rainbow trout larve. Regression analyses were performed using SigmaPlot version 10.0 with SigmaStat 3.5 integration (Systat Software, Inc.). $P \leq 0.0001$ for all regressions. (n=6-12) CYA = complete yolk sac absorption

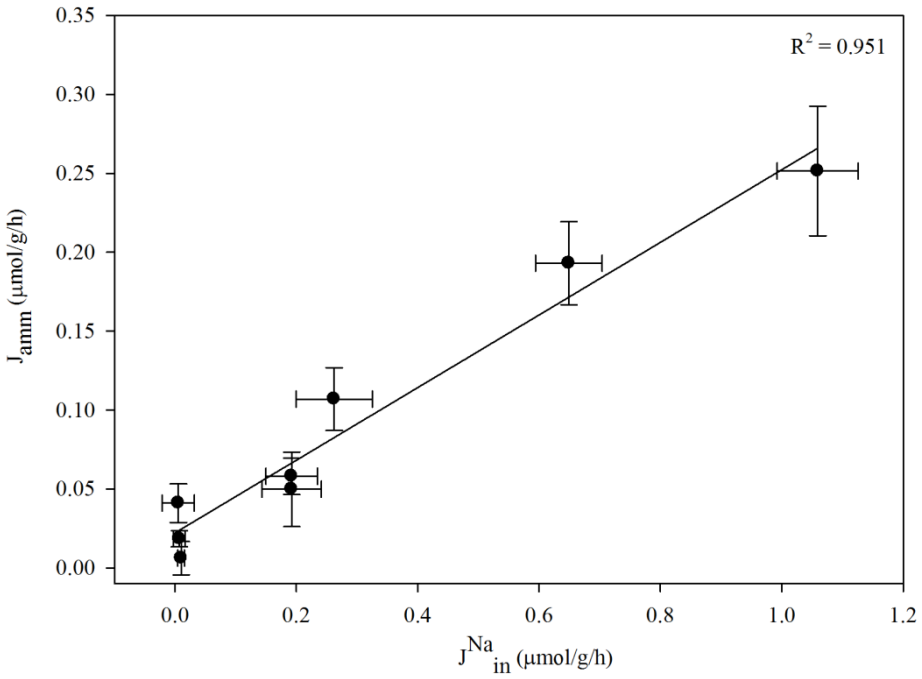
R² = 0.951
0.35
0.30
0.25
0.20
0.15
0.10
0.05
0.00
Jamm (µmol/g/h)
0.0
0.2
0.4
0.6
0.8
1.0
1.2
JNa in (µmol/g/h)

Fig. 2.3. The relationship between branchial ammonia excretion (J_{amm}) and Na^+ uptake (J^{Na}_{in}) over development following hatching in rainbow trout larvae. Regression analyses were performed using SigmaPlot version 10.0 with SigmaStat 3.5 integration (Systat Software, Inc.). R^2=0.951; P<0.0001. (n=6-12)

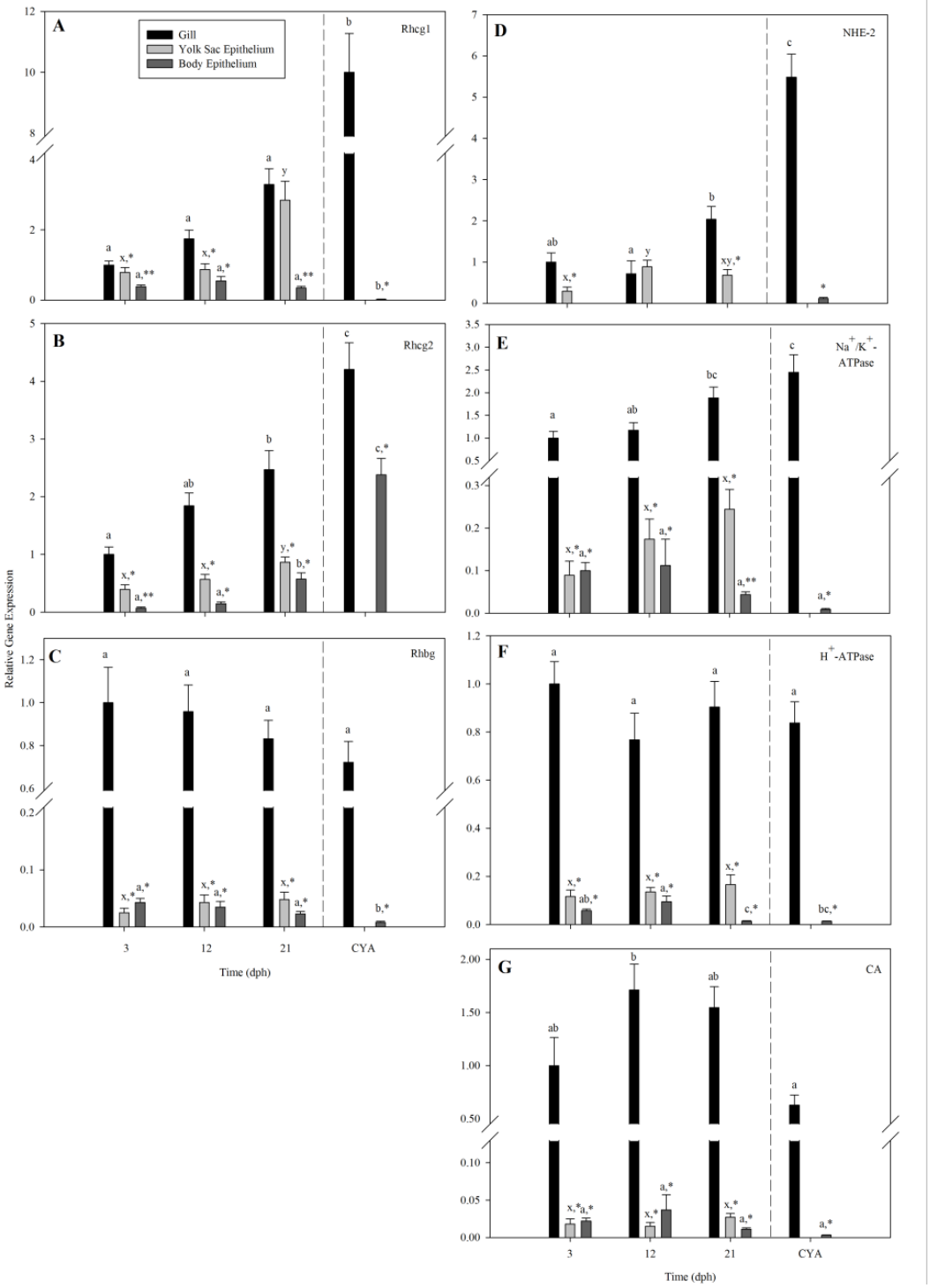
A
Rhcg1
Gill
Yolk Sac Epithelium
Body Epithelium
B
Rhcg2
C
Rhbg
D
NHE-2
E
Na+/K+-ATPase
F
H+-ATPase
G
CA
Relative Gene Expression
Time (dph)
3
12
21
CYA

Fig. 2.4. Relative gene expression of Rhcg1 (A), Rhcg2 (B), Rhbg (C), Na^+/H^+-exchanger-2 (NHE-2; D), Na^+/K^+-ATPase (E) , H^+-ATPase (F), carbonic anhydrase (CA; G) at 3, 12, and 21 days post-hatch (dph) and after CYA in the gills (black bars), yolk sac epithelium (grey bars), and body epithelium (dark grey bars) of developing rainbow trout larvae. Gene expression is relative to the expression of both EF1-α and β-actin and is normalized to the expression seen in the gill at 3 dph. Means within a given tissue across time points which do not share the same letter are significantly different from one another. Asterisks represent yolk sac epithelium means which differ significantly from gill means within a given time point and double asterisks represent body epithelium means which differ significantly from both gill and yolk sac epithelium means within a given time point. (n=4-6) CYA = complete yolk sac absorption

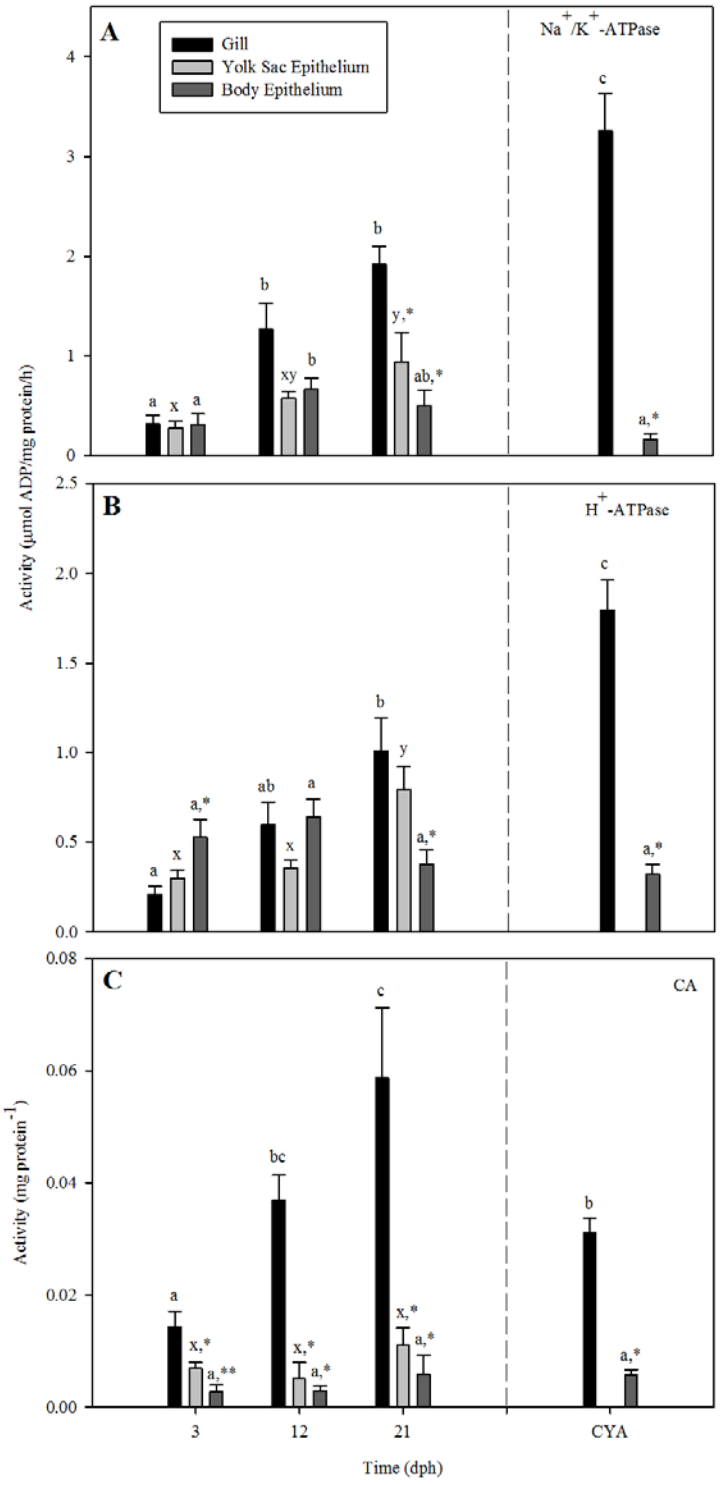
A
Gill
Yolk Sac Epithelium
Body Epithelium
Na+/K+-ATPase
B
H+-ATPase
C
CA
Activity (µmol ADP/mg protein/h)
Activity (mg protein-1)
Time (dph)
3
12
21
CYA

Fig. 2.5. Enzymatic activities of Na^+/K^+-ATPase (A), H^+-ATPase (B), carbonic anhydrase (CA; C) at 3, 12, and 21 days post-hatch (dph) and after CYA in the gills (black bars), yolk sac epithelium (grey bars), and body epithelium (dark grey bars) of developing rainbow trout larvae. Means within a given tissue across time points which do not share the same letter are significantly different from one another. Asterisks represent yolk sac epithelium means which differ significantly from gill means within a given time point and double asterisks represent body epithelium means which differ significantly from both gill and yolk sac epithelium means within a given time point. (n=6-12) CYA = complete yolk sac absorption

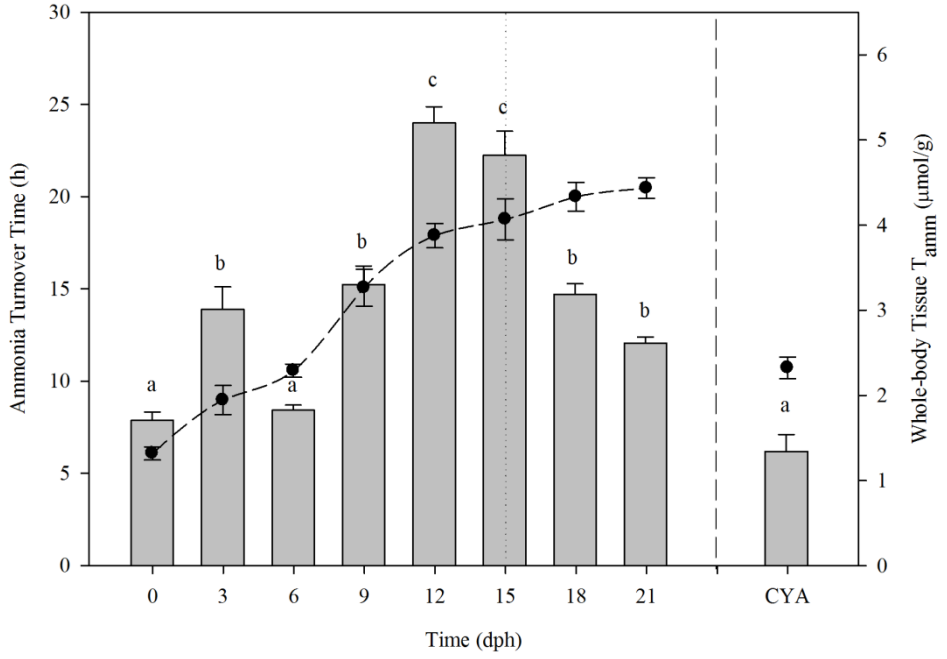
Ammonia Turnover Time (h)
Whole-body Tissue T amm (µmol/g)
Time (dph)
0
3
6
9
12
15
18
21
CYA
a
b
a
b
c
c
b
b
a

Fig. 2.6. Ammonia turnover times (bars) and whole-body T_{amm} (circles) over development following hatching in rainbow trout larvae. Ammonia turnover time means not sharing the same letter are significantly different from one another as determined by a one-way ANOVA followed by a Holm-Sidak post-hoc test following normalization by square root and log transformation, respectively. The dotted line signifies the cutaneous-to-branchial shift for ammonia excretion (15 dph). (n=6) CYA = complete yolk sac absorption

2.6 REFERENCES

Beyenbach, K.W. and Wieczorek, H. (2006) The V-type H^+ ATPase: molecular structure and function, physiological roles and regulation. *J. Exp. Biol.* 209, 577-589.

Boutilier, R.G., Heming, T.A. and Iwama, G.K. (1984) Physiochemical parameters for use in fish respiratory physiology. In *Fish Physiology* 10 (ed. Hoar WS, Randall DJ), pp 403–30. New York, NY: Academic Press.

Braun, M.H. and Perry, S.F. (2010) Ammonia and urea excretion in the Pacific hagfish *Eptatretus stoutii*: Evidence for the involvement of Rh and UT proteins. *Comp. Biochem. Physiol. A* 157, 405-415.

Brauner, C.J. and Rombough, P.J. (2012) Ontogeny and paleophysiology of the gill: new insights from larval and air-breathing fish. *Respir. Physiol. Neurobiol.* 184, 293–300.

Clifford, A.M., Guffey, S.C. and Goss, G.G. (2014) Extrabranchial mechanisms of system pH recovery in hagfish (*Eptatretus stoutii*). *Comp. Biochem. Physiol. A* 168, 82-89.

Essex-Fraser, P.A., Steele, S.L., Bernier, N.J., Murray, B.W., Stevens, E.D. and Wright, P.A. (2005) Expression of four glutamine synthetase genes in the early stages of development of rainbow trout (*Oncorhynchus mykiss*) in relationship to nitrogen excretion. *J. Biol. Chem.* 280, 20268–73.

Evans, D.H. (1984) Gill Na^+/H^+ and Cl^-/HCO_3^- exchange systems evolved before the vertebrates entered fresh water. *J. Exp. Biol.* 113, 465-469.

Evans, D., Piermarini, P. and Choe, K. (2005) The multifunctional fish gill: dominant site of gas exchange, osmoregulation, acid-base regulation, and excretion of nitrogenous waste. *Physiol. Rev.* 85, 97–177.

Fu, C., Wilson, J.M., Rombough, P.J. and Brauner, C.J. (2010) Ions first: Na^+ uptake shifts from the skin to the gills before O_2 uptake in developing rainbow trout, *Oncorhynchus mykiss*. *Proc. R. Soc. B* 277, 1553–60.

Gonzalez, M.E., Blanquez, M.J. and Rojo, C. (1996) Early gill development in the rainbow trout, *Oncorhynchus mykiss*. *J. Morphol.* 229, 201–217.

Korte, J.J., Salo, W.L., Cabrera, V.M., Wright, P.A., Felski, A.K. and Anderson, P.M. (1997) Expression of carbamoyl-phosphate synthetase III mRNA during the early stages of development and in muscle of adult rainbow trout (*Oncorhynchus mykiss*). *J. Biol. Chem.* 272, 6270-6277.

Krogh, A. (1941) *The comparative physiology of respiratory mechanisms*. Philadelphia, PA: University of Pennsylvania Press.

Kumai, Y. and Perry, S.F. (2011) Ammonia excretion via Rhcg1 facilitates Na^+ uptake in larval zebrafish, *Danio rerio*, in acidic water. *Am. J. Physiol. Regul. Integr. Comp. Physiol.* 301, R1517–28.

Li, J., Eygensteyn, J., Lock, R.A.C., Verbost, P.M., Van Der Heijden, A.J.H., Wendellar Bonga, S.E. and Flik G. (1995) Branchial chloride cells in larvae and juveniles of freshwater tilapia *Oreochromis mossambicus*. *J. Exp. Biol.* 198, 2177-2184.

McFarland, W.N. (1959) A study of the effects of anesthetics on the behaviour and physiology of fishes. *Publ. Inst. Mar. Sci. Univ. Tex.* 6, 23-55.

Nawata, C.M., Hung, C.C.Y., Tsui, T.K.N., Wilson, J.M., Wright, P.A. and Wood, C.M. (2007) Ammonia excretion in rainbow trout (*Oncorhynchus mykiss*): evidence for Rh glycoprotein and H^+-ATPase involvement. *Physiol. Genomics* 31, 463–74.

Randall, D.J. and Ip, Y.K. (2006). Ammonia as a respiratory gas in water and air-breathing fishes. *Respir. Physiol. Neurobiol.* 154, 216-225.

Randall, D.J. and Tsui, T.K.N. (2002) Ammonia toxicity in fish. *Mar. Pollut. Bull.* 45, 17–23.

Rombough, P.J. (1999) The gill of fish larvae. Is it primarily a respiratory or an ionoregulatory structure? *J. Fish Biol.* 55, 186–204.

Rombough, P.J. (2002) Gills are needed for ionoregulation before they are needed for O_2 uptake in developing zebrafish, *Danio rerio*. *J. Exp. Biol.* 205, 1787–94.

Rombough, P.J. (2007) The functional ontogeny of the teleost gill: which comes first, gas or ion exchange? *Comp. Biochem. Physiol. A. Mol. Integr. Physiol.* 148, 732–42.

Shih, T.-H., Horng, J.-L., Hwang, P.-P. and Lin, L.-Y. (2008) Ammonia excretion by the skin of zebrafish (*Danio rerio*) larvae. *Am. J. Physiol. Cell Physiol.* 295, 1625-1632.

Shih, T.-H., Horng, J.-L., Liu, S.-T., Hwang, P.-P. and Lin, L.-Y. (2012) Rhcg1 and NHE3b are involved in ammonium-dependent sodium uptake by zebrafish larvae acclimated to low-sodium water. *Am. J. Physiol. Regul. Integr. Comp. Physiol.* 302, R84–93.

Tresguerres, M., Parks, S.K. and Goss, G.G. (2006) V-H^+-ATPase, Na^+/K^+-ATPase and NHE2 immunoreactivity in the gill epithelium of the Pacific hagfish (*Eptatretus stoutii*). *Comp. Biochem. Physiol. A* 145, 312-321.

Verdouw, H., van Echteld, C.J.A. and Dekkers, E.M.J. (1978) Ammonia determination based on indophenols formation with sodium salicylate. *Water Res.* 12, 399-402.

Wells, P. and Pinder, A. (1996) The respiratory development of Atlantic salmon. II. Partitioning of oxygen uptake among gills, yolk sac and body surfaces. *J. Exp. Biol.* 199, 2737–44.

Wright, P.A., Felskie, A. and Anderson, P. (1995) Induction of ornithine-urea cycle enzymes and nitrogen metabolism and excretion in rainbow trout (*Oncorhynchus mykiss*) during early life stages. *J. Exp. Biol.* 198, 127–35.

Wright, P.A. and Fyhn, J.H. (2001) Ontogeny of nitrogen metabolism and excretion. In *Fish physiology* 20 (ed. Wright PA, Anderson PM), pp. 149-186. San Diego, CA: Academic Press.

Wright, P.A. and Wood, C.M. (2009) A new paradigm for ammonia excretion in aquatic animals: role of Rhesus (Rh) glycoproteins. *J. Exp. Biol.* 212, 2303–12.

Wu, S.-C., Horng, J.-L., Liu, S.-T., Hwang, P.-P., Wen, Z.-H., Lin, C.-S. and Lin, L.-Y. (2010) Ammonium-dependent sodium uptake in mitochondrion-rich cells of medaka (*Oryzias latipes*) larvae. *Am. J. Physiol. Cell Physiol.* 298, 237-250.

Zimmer, A.M., Barcarolli, I.F., Wood, C.M. and Bianchini, A. (2012) Waterborne copper exposure inhibits ammonia excretion and branchial carbonic anhydrase activity in euryhaline guppies acclimated to both fresh water and sea water. *Aquat. Toxicol.* 122-123, 172–80.

Zimmer, A.M., Brauner, C.J. and Wood, C.M. (2014a) Ammonia transport across the skin of adult rainbow trout (*Oncorhynchus mykiss*) exposed to high environmental ammonia (HEA). *J. Comp. Physiol. B.* 184, 77-90.

CHAPTER 3

MECHANISMS OF AMMONIA EXCRETION AND Na^+ UPTAKE BY THREE DIFFERENT EPITHELIA IN RAINBOW TROUT (*ONCORHYNCHYS MYKISS*): EVIDENCE FOR Na^+/NH_4^+ EXCHANGE AT THE GILL BUT NOT THE SKIN

3.1 ABSTRACT

In typical teleost fish, the majority of nitrogenous waste is excreted as ammonia. Depending on life stage, however, the site and, potentially, the mechanisms by which ammonia is excreted may be quite different. The aim of the present study was to determine the mechanism(s) of ammonia excretion (J_{amm}) in relation to Na^+ uptake (J^{Na}_{in}) across three epithelia in early life stages of the rainbow trout (*Oncorhynchus mykiss*): the gill and body skin of fish which have completed yolk sac absorption (CYA; approximately 45 days post-hatch; dph), and the yolk sac skin of post-hatch (PH) larvae (5-7 dph). In order to measure fluxes across these epithelia, two different divided chamber systems were used. For CYA fish, the chamber spatially separated the head and gills from the rest of the body. For PH larvae, the chamber spatially separated the yolk sac from the rest of head and body. In the first experimental series, CYA fish and PH larvae were exposed to high external ammonia (HEA; 0.5 mmol/l NH_4HCO_3) for 12 h in order to experimentally elevate J_{amm}. Following 12 h, fish were transferred into ammonia-free water and loaded into divided chambers. HEA pre-exposure resulted in a significant increase in J_{amm} across all three epithelia, however, only at the CYA gill was this associated with a concomitant increase in J^{Na}_{in}. In a second experimental series, a number of blockers targeting transporters for J^{Na}_{in} (EIPA for Na^+/H^+-exchanger (NHE); bafilomycin for H^+-ATPase; DAPI for acid-sensing ion channel (ASIC); and phenamil for Na^+ channel) were employed. In this series, only the CYA gill and PH yolk sac were tested as the CYA body skin contributed little to overall J^{Na}_{in} and was not coupled to J_{amm}. In both the CYA gill and PH yolk sac, J^{Na}_{in} was significantly inhibited by both EIPA and

DAPI, suggesting a role for NHE and ASIC in J^{Na}_{in} by these epithelia; bafilomycin and phenamil had no significant effect on J^{Na}_{in}. J_{amm} by the CYA gill was also significantly inhibited by EIPA and DAPI, while bafilomycin and phenamil had no effects. In contrast, J_{amm} by the yolk sac skin was not altered by any of the applied blockers. Overall, these results demonstrate that J_{amm} by the CYA gill occurs via a Na^+-coupled mechanism, potentially co-ordinated by NHE and/or ASIC, while J_{amm} by the PH yolk sac is Na^+-independent. Moreover, the overall mechanism of J^{Na}_{in}, mediated by NHE and ASIC and independent of H^+-ATPase, appears to be similar between the CYA gill and PH yolk sac. The body skin of CYA trout is capable of clearing an ammonia load, though this is likely independent of J^{Na}_{in} as this epithelium displayed negligible J^{Na}_{in}. These results are summarized in 3 transport models, one for each epithelium. One of these represents the first model ever proposed for J_{amm} and J^{Na}_{in} by the yolk sac epithelium of rainbow trout, a widely used preparation for a number of physiological investigations in other species.

3.2 INTRODUCTION

The relationship between ammonia excretion (J_{amm}) and Na^+ uptake (J^{Na}_{in}) by freshwater fish has been a focus of research by comparative physiologists for over fifty years (e.g., Maetz and Garcia-Romeu, 1964) and has been reviewed extensively (Weihrauch et al., 2009; Wilkie, 1997; 2002; Wright and Wood, 2009; 2012). In most freshwater fish, ammonia is excreted primarily by the gills (> 80% of total J_{amm}; Smith, 1929; Smith et al., 2012; Zimmer et al., 2014a), while the skin, kidney, and gastrointestinal system play minor roles. J^{Na}_{in}, on the other hand, appears to be limited strictly to the gills in almost all developed fish (e.g., Zimmer et al., 2014b).

At the gill, J_{amm} and J^{Na}_{in} are believed to occur as a loosely coupled exchange. This exchange is coordinated by a number of different transporters which together have been named the "Na^+/NH_4^+-exchange complex" (Wright and Wood, 2009). To summarize, ammonia travels across the basolateral and apical membranes of cells as NH_3 via Rhesus (Rh) channel proteins which strip H^+ from NH_4^+ at the channel opening (Nawata et al., 2010b). At the apical surface, there are a number of components of the exchange complex which acidify the apical boundary layer, including cytosolic carbonic anhydrase (CA), Na^+/H^+-exchanger (NHE) and H^+-ATPase. The latter two mechanisms occur in conjunction with the uptake of Na^+, directly via NHE, and electrogenically via a putative epithelial Na channel or acid-sensing ion channel (ASIC; Dymowska et al., 2014) powered by the actions of H^+-ATPase. This acidification maintains a favourable PNH_3 gradient for the excretion of ammonia via acid-trapping of NH_3 at the apical boundary layer. Thus, gill boundary layer acidification by NHE and H^+-ATPase is

responsible for the functional coupling of J_{amm} and J^{Na}_{in} (see Weihrauch et al., 2009; Wright and Wood, 2009; 2012 for reviews).

Following hatch, however, larval fish lack a functional gill and it is the skin which performs the majority of exchange with the surrounding environment. In the period immediately after hatch, the skin accounts for more than 80% of both total oxygen uptake (MO_2), J^{Na}_{in} (Fu et al., 2010; Zimmer et al., 2014b), and J_{amm} (Zimmer et al., 2014b). Virtually all of our present knowledge about the mechanism(s) of J_{amm} and J^{Na}_{in} in the skin of larval fish stems from studies examining zebrafish (*Danio rerio*) and medaka (*Oryzias latipes*) with the scanning ion-selective electrode technique (SIET) (Shih et al., 2008; 2012; 2013; Wu et al., 2010). These studies indicate that J_{amm} and J^{Na}_{in} by the yolk sac skin also occur as Na^+/NH_4^+-exchange, driven primarily by the "Rh-NHE metabolon" in which NHE operates via micro pH gradients established by the H^+-stripping of Rh proteins. These results have also been supported by whole-animal experiments using a wide variety of approaches including pharmacological blockade and morpholino knockdown (Kumai and Perry, 2011). However, there is essentially no information with respect to the mechanism of J_{amm} and J^{Na}_{in} transport across the skin of larval rainbow trout (*Oncorhynchus mykiss*). The yolk sac skin of larval trout expresses Rh, NHE, and H^+-ATPase mRNAs (Zimmer et al., 2014b), but their mechanistic function(s) are presently unknown. Moreover, while in zebrafish, cutaneous J_{amm} is coupled to J^{Na}_{in}, there appears to be no relationship between cutaneous J_{amm} and J^{Na}_{in} in larval rainbow trout over post-hatch development (Zimmer et al., 2014b). Thus, it is possible that there are some

functional differences between the functional models for transport across the skin of larval rainbow trout versus larval zebrafish.

While the yolk sac skin is of primary importance in larval rainbow trout, the general body skin of adult trout also appears to play a minor role in overall J_{amm}. Zimmer at al. (2014a) reported that under control conditions, the skin of adult trout accounts for approximately 5% of total J_{amm} (Zimmer et al., 2014a), a relatively small contribution but greater than that of the kidney. This was somewhat surprising, because historically the kidney has been generally been assumed to be the second-most important site of J_{amm} (e.g., Smith, 1929). The origin and mechanism of ammonia transport by the adult body skin are poorly understood. It is not clear if J_{amm} by the skin represents transcutaneous transport of ammonia from the plasma to the surrounding water, or if the skin produces and excretes its own metabolic ammonia. Indeed, in *in vitro* studies, isolated skin patches produce ammonia (Zimmer et al., 2014a) and have a relatively high MO_2 (Nonnotte, 1981; Nonnotte and Kirsch, 1978). Some evidence has pointed towards the involvement of Rh proteins (Nawata et al., 2007; Nawata and Wood, 2008; 2009) but the role of Na^+/NH_4^+ exchange is likely limited at best given that the skin contributes very little to Na^+ uptake.

Our overall hypothesis was that the mechanisms potentially linking J_{amm} and J^{Na}_{in} would differ among the three different epithelial surfaces of larval rainbow trout, the gill, yolk sac skin, and body skin. Therefore our goal was to establish mechanistic models for J_{amm} and J^{Na}_{in} at the three sites. Two different divided chambers were used. The first or "traditional" divided chamber, based on the design of Fu et al. (2010), spatially separated

flux across the gills from flux across the rest of the body epithelium of rainbow trout fry which had completed yolk sac absorption (CYA). A second type of chamber spatially separated flux across the yolk sac epithelium from flux across the rest of the fish in post-hatch larvae (PH). In one series, the functional coupling between J_{amm} and J^{Na}_{in} was examined by experimentally increasing J_{amm} via pre-exposing the fish to high external ammonia (HEA), and then measuring flux across all three surfaces thereafter. We hypothesized that at the gills, there would be significant Na^+/NH_4^+ exchange (Zimmer et al., 2014b) as in adults (Zimmer et al., 2010; Sinha et al. 2013) while at the yolk sac skin and the body skin, J_{amm} and J^{Na}_{in} would be independent (Zimmer et al., 2014b). In another series, a number of pharmacological blockers (EIPA for NHE; bafilomycin for H^+-ATPase; DAPI for ASIC; phenamil for epithelial Na channels) were used to determine the mechanisms of J_{amm} and J^{Na}_{in} across two of the epithelia. The overall findings of this study are summarized in three mechanistic models describing flux across the three epithelia.

3.3 MATERIALS AND METHODS

3.3.1 Larvae

Rainbow trout embryos (*Oncorhynchus mykiss*) were purchased from Rainbow Springs Hatchery (Thamesford, Ontario) in the eyed stage and were reared at 12ºC in flow-through dechlorinated Hamilton, Ontario tap water (moderately hard: $[Na^+]$= 0.6 mequiv/l, $[Cl^-]$ = 0.8 mequiv/l, $[Ca^{2+}]$= 1.8 mequiv/l, $[Mg^{2+}]$= 0.3 mequiv/l, $[K^+]$ =0.05 mequiv/l; titration alkalinity 2.1 mequiv/l; pH ~8.0; hardness ~140 mg/l as $CaCO_3$

equivalents, 12ºC). Embryos hatched approximately 1 week after purchase and complete yolk sac absorption (CYA) occurred 30 days thereafter. Following CYA, fish were fed a daily ration of commercial trout pellets of approximately 5% body mass. In all experiments, CYA larvae were fasted for at least 24 h prior to experimentation.

3.3.2 Divided chamber design

The designs of both divided chambers used in the present study are illustrated in Fig. 3.1. The first or "traditional" divided chamber (Fig. 3.1A) was designed to separate the head and gills from the rest of the body in CYA fish (Fu et al., 2010) and the protocol was almost identical to those described in previous studies (Zimmer et al., 2014b). The only difference was that in the present experiments, only CYA fish were used. These fish were initially anaesthetized to stage 3 (McFarland, 1959) using 0.1 mg/l neutralized MS-222 while in the chambers, 0.05 mg/l neutralized MS-222 was used to maintain anaesthesia. Flux across the gill epithelium was assessed in the anterior chamber, while flux across the body epithelium was assessed in the posterior chamber.

The second type of divided chamber (Fig. 3.1B) was designed to isolate the yolk sac of post-hatch (PH) larvae from the rest of the body. At 5-7 dph, the stage at which PH larvae were easier to handle and where the oblong shape of the yolk sac was easier to work with, randomly selected larvae were anaesthetized using 0.2 mg/l neutralized MS-222. As reported previously (Zimmer et al., 2014b), rainbow trout larvae require a higher concentration of anaesthetic to reach stage 3 anaesthesia than CYA fish. Once anaesthetized, larvae were loaded into a divided chamber containing 0.05 mg/l

neutralized MS-222. The chamber consisted of a thin latex dam which had a small hole (approximately 3-4 mm) in its center. The yolk sac of the larva was pushed through this hole such that it was spatially separated from the rest of the body. A second latex sheet was placed over the dorsal side of the fish which helped secure the larva in place, keeping it from falling out of the dam. This second latex sheet was perforated to allow exchange between the larva and the surrounding water. The larva, secured within the latex dams, was then loaded between two 5-ml half-chambers such that the fish was positioned laterally with its dorsal side (body and head) contained within one chamber and its ventral side (yolk sac) contained within the other. Flux across the yolk sac epithelium was assessed in the ventral chamber.

3.3.3 Experimental series

Series 1. The first experimental series evaluated, in all three epithelia, the presence or absence of Na^+-coupled J_{amm} in response to ammonia loading. The experimental approach used to assess coupling across each epithelia was identical between CYA and PH fish except for the type of divided chamber used (see above). Fish at either the PH stage (5-7 dph) or following CYA were exposed to either control conditions or to high external ammonia (HEA; 0.5 mmol/l NH_4HCO_3) for 12 h overnight in a 3-l static exposure containing approximately 15 fish per 3 l. Following 12 h, fish were mounted individually into the appropriate divided chamber system containing ammonia-free water, airlines were placed in both chambers, and larvae were allowed to adjust to this setup for 30 min. 0.1 µCi/ml ^{22}Na (Perkin Elmer, Waltham, MA, USA) was added to one chamber. In the divided chambers for CYA fish, radioisotope was added to the anterior chamber for gill

fluxes and the posterior chamber for body epithelium fluxes, while in the divided chambers for PH larvae, radioisotope was added to the ventral chamber (containing the yolk sac). Following 5 min of mixing, an initial 1.25-ml sample was taken from the isotope-loaded chamber. Fluxes lasted 1 h thereafter which a final 1.25-ml sample was taken from the same chamber and, in addition, a 0.25-ml sample was also taken from the unloaded chamber to check for leaks across the dam in order to assess viability. The fish was then removed from the chamber and rinsed in radioisotope-free water for 5 min, during which time they were monitored to assess recovery from anaesthesia. Final chamber volume was recorded and, following euthanasia via neutralized MS-222 overdose, rinsing with 5 mM NaCl twice, and distilled water once, larvae were weighed and stored for later determination of ^{22}Na gamma-radioactivity. Aliquots (0.25 ml) of all samples were stored at 4ºC for later determination of ^{22}Na gamma-radioactivity and total [Na^+]. The remaining 1 ml water sample was stored at -20ºC for later analysis of total ammonia concentration (T_{amm}). In all experiments, radioisotope leak to the unloaded chamber was less than 10% and fish fully recovered from anaesthesia within 5 min.

Series 2. The second experimental series was designed to determine the effects of various pharmacological blockers on J_{amm} and J^{Na}_{in} across the gill, yolk sac, and body epithelia. The protocol for this series followed that described for Series 1 except for some minor changes. For CYA fish, in Series 2, only flux across the gills was assessed as the Series 1 experiments demonstrated that the body skin contributed minimally to overall J^{Na}_{in}, and there was no evidence of linkage to J_{amm} (see Results).

Immediately after loading the fish into the appropriate divided chamber, 50 µl of a given blocker, diluted in DMSO, was added to the same chamber which would later receive the addition of ^{22}Na, such that the final concentration of DMSO was 0.1%. The blockers (and final concentrations) used were 5-(N-ethyl-N-isopropyl)amiloride (EIPA, Sigma, St. Louis, MO, USA; $1x10^{-4}$ mol/l), bafilomycin (Cayman Chemical, Ann Arbor, MI, USA; $1 \times 10^{-7} – 5 \times 10^{-6}$ mol/l), DAPI (Cayman Chemical, Ann Arbor, MI, USA; 1×10^{-5} mol/l), and phenamil (Cayman Chemical, Ann Arbor, MI, USA; 1×10^{-4} mol/l) which targeted NHE, H^+-ATPase, ASIC, and Na channels, respectively. Following the addition of these blockers (or of DMSO alone as a control), fish were left for 30 min to allow blocker effects to develop and to adjust to the divided chamber. The remainder of the experiment followed the same protocol described above for Series 1.

3.3.4 Analytical procedures

T_{amm} in water samples was measured using the protocol outlined by Verdouw et al. (1978). Note that in Series 2, samples were compared against T_{amm} standards prepared in the same DMSO concentration and/or blocker concentration present in the given unknown. This was necessary as each of the DMSO and the blocker/DMSO combinations differentially decreased the sensitivity, but not the linearity, of the assay. Ammonia excretion rates (J_{amm}; µmol/g/h) were calculated using the following equation:

$$J_{smm} = [(T_{amm}f - T_{amm}i)x \ V]/(wt \times t) \quad (1)$$

where $T_{amm}f$ and $T_{amm}i$ are the final and initial total ammonia concentrations (µmol/l), V is chamber volume (l; corrected for sample removal), wt is larval weight (g), and t is flux duration (h).

^{22}Na gamma radioactivities (counts per minute; cpm) in water samples and whole larvae were measured via gamma counting (Perkin Elmer Wizard 1480 3" Auto Gamma Counter, Waltham, MA, USA), and $[Na^+]$ of water samples was determined via atomic absorption spectrophotometry (Varian SpectrAA 220FS Atomic Absorption Spectrophotometer, Palo Alto, CA, USA). Unidirectional Na^+ influx rates (J^{Na}_{in}; µmol/g/h) were calculated using the following equation:

$$J^{Na}_{in} = R_{fish}/(SA_{avg} \times wt \times t) \quad (2)$$

where R_{fish} is the radioactivity of the whole larva (cpm) and SA_{avg} is the average specific activity (cpm/µmol) of the initial and final water samples which is the amount of isotope per µmol of Na. SA_{avg} is calculated by dividing the concentration of isotope (cpm/l) by the total concentration of Na (µmol/l) in the collected water samples.

3.3.5 Statistical analyses

All data have been presented as means ± s.e.m (n=sample size). All statistical analyses were performed using SigmaStat v. 3.5 (Systat Software, Inc.). Significance was accepted at the $P<0.05$ level and, in general, differences are denoted by asterisks. Specific tests used for each data set are explained in detail in corresponding Figure captions.

3.4 RESULTS

3.4.1 Series 1 – Effects of HEA pre-exposure

In CYA trout under control conditions, J^{Na}_{in} through the gills (anterior chamber) was approximately 50-fold higher than through the body epithelium (posterior chamber) (Fig. 3.2A), whereas J_{amm} through the gills was only about 2.4-fold higher than J_{amm} through the body (Fig. 3.2B). Pre-exposing CYA trout to 12 h of HEA (0.5 mmol/l NH_4HCO_3) led to a significant 3-fold increase in J_{amm} by the gill in ammonia-free water (Fig. 3.2B), which was coupled to a nearly 2-fold increase in J^{Na}_{in} (Fig. 3.2A). Notably, HEA pre-exposure also increased J_{amm} by approximately 2-fold across the body epithelium in these CYA fish (Fig. 3.2B), yet J^{Na}_{in} across the body was unchanged (Fig. 3.2A). In the yolk sac epithelium (ventral compartment) of PH fish, a similar pattern to the latter was seen. HEA pre-exposure caused an almost 2-fold increase in J_{amm} (Fig. 3.2B) with no change in J^{Na}_{in} (Fig. 3.2A).

3.4.2 Series 2 – Effects of pharmacological blockers

In this series, a concentration of 0.1% DMSO was necessary to dissolve the blockers in water. As such, a vehicle control (DMSO) was performed to observe the effects of 0.1% DMSO alone on J_{amm} and J^{Na}_{in}; all comparisons examining the effects of the different blockers were performed against the DMSO control. DMSO led to a marked increase in J_{amm} across the gills while J_{amm} by the yolk sac was not affected (Table 3.1; Figs. 3.2,3.3,3.4). J^{Na}_{in} was not noticeably affected by DMSO (Table 3.1; Figs. 3.2,3.3,3.4).

In CYA fish, branchial J^{Na}_{in} was significantly inhibited (85-90% relative to DMSO control) by EIPA and DAPI only, while bafilomycin and phenamil had no significant effects (Fig. 3.3A). Branchial J_{amm} in these CYA fish was also inhibited by EIPA and DAPI (Fig. 3.3B), though these effects (~40% inhibition relative to DMSO control) were much less than the effects on J^{Na}_{in}. Bafilomycin and phenamil also had no significant effects on J_{amm} in these fish (Fig. 3.3B).

In PH fish, J^{Na}_{in},across the yolk sac epithelium (ventral chamber) was inhibited by approximately 50% and 70% by EIPA and DAPI, respectively, relative to DMSO alone (Fig. 3.4A). These effects were similar to those seen at the gill, albeit to a slightly lesser degree. Again bafilomycin and phenamil had no significant effects on J^{Na}_{in}. Notably, none of the blockers used in the present study had any significant effects on J_{amm} across the yolk sac epithelium (Fig. 3.4B).

3.5 DISCUSSION

3.5.1 Overview

The overall goal of the present study was to build mechanistic models for ammonia and Na^+ transport by 3 different epithelial tissues: the gills, yolk sac epithelium, and body epithelium. In a broad sense, we found that the gill of CYA fish, unlike the body or yolk sac epithelia of CYA and PH fish, respectively, displayed Na^+-coupled J_{amm}. This is evidenced by the concomitant increase in both J_{amm} and J^{Na}_{in} in response to HEA loading, which was not observed by the yolk sac or body skin (Fig. 3.2), and by the inhibition of both J_{amm} and J^{Na}_{in} by the Na^+ uptake blockers EIPA and DAPI (Fig. 3.3),

again not observed in the PH yolk sac epithelium (Fig. 3.4). Moreover, we found that, in terms of Na^+ uptake, the gill of CYA fish and yolk sac epithelium of PH larvae possess similar mechanisms, both being sensitive to EIPA and DAPI, while bafilomycin and phenamil had no significant effects (Figs. 3.3 and 3.4). The body epithelium, while having a significant capacity for J_{amm} (Fig. 3.2A), contributed little to Na^+ uptake (Fig. 3.2B). In summary, these results confirm that J_{amm} by the gill of early life stage rainbow trout is a Na^+-coupled process and, for the first time, demonstrate that the same is not true of the yolk sac skin, a critical site for both J_{amm} and J^{Na}_{in} in post-hatch larval trout. The reason for this difference is, at present, not clear. Both qPCR and immunohistochemical approaches will be useful in further discerning the specific transporters, and their localization, which are involved in J_{amm} and J^{Na}_{in} by the yolk sac skin. The results are summarized into mechanistic models presented in Fig. 3.5.

3.5.2 J_{amm} and J^{Na}_{in} by the gill of CYA fish

J_{amm} was experimentally elevated by exposure to high external ammonia (HEA; 0.5 mmol/l NH_4HCO_3) to assess the presence of Na^+/NH_4^+ exchange in the CYA gill. HEA exposure has classically been used in numerous studies as a means for understanding the mechanism of J_{amm} by a wide variety of fish species (Braun et al., 2009b; Kumai and Perry, 2011; Liew et al., 2013; Maetz and Garcia-Romeu, 1964; Nawata et al., 2007; 2010a; Sinha et al., 2013; Wilson et al., 1994; Wood and Nawata; 2011; Zimmer et al., 2010), with many studies focusing on the relationship between J_{amm} and J^{Na}_{in} during HEA exposure (Maetz and Garcia-Romeu, 1964; Kumai and Perry, 2011; Wilson et al., 1994; Zimmer et al., 2010). In CYA fish, pre-exposure to HEA led to a

significant increase in both J_{amm} and J^{Na}_{in} (Fig. 3.2), demonstrating the presence of some type of Na^+/NH_4^+ exchange mechanism. The increase in J_{amm} may have been coordinated by an increase in Rh protein expression, similar to previous reports in various fish species (Hung et al., 2007; Nawata et al., 2007; 2010a; Sinha et al., 2013; Wood and Nawata, 2011; Zimmer et al., 2010). The concomitant increase in J^{Na}_{in} is generally considered to be a function of NHE or H^+-ATPase (e.g., Wood and Nawata, 2011; Zimmer et al., 2010). Recently, NHE has been implicated as a critical component to Na^+/NH_4^+ exchange, being part of a functional metabolon with Rh, facilitating Na^+ absorption against a concentration gradient by utilizing micro-pH gradients established by Rh proteins (Kumai and Perry, 2011; Shih et al., 2012; Wu et al., 2010). Interestingly, recent evidence using the *in vitro* expression of zebrafish NHE3 (zNHE3) in *Xenopus* oocytes also demonstrates that zNHE3 expressed in the oocyte membrane has the capacity for direct Na^+/NH_4^+ exchange (Ito et al., 2014), independent of Rh proteins.

In the CYA gill, EIPA inhibited both J^{Na}_{in} and J_{amm}, which could potentially represent the presence of direct Na^+/NH_4^+ exchange by NHE in the trout gill, as has been suggested for the zNHE3 (Ito et al., 2014). Alternatively, the inhibitory effects of EIPA on J_{amm} may be explained by a decrease in NHE-mediated boundary layer acidification, which would impede J_{amm} via Rh proteins. Wu et al. (2010) also demonstrated an increase in Na^+-coupled J_{amm} by the yolk sac skin of medaka larvae loaded with ammonia via HEA exposure. In their study, they found that the boundary layer at the yolk sac skin of these fish became alkalinized following HEA exposure, suggesting an acid-trapping mechanism for $J_{amm,}$ mediated by a Rh-NHE metabolon, and arguing against direct Na^+/NH_4^+

exchange (Wu et al., 2010). In larval rainbow trout, Na^+/NH_4^+ exchange by the gills increases during the period of post-hatch development in conjunction with increases in the gene expression of apical Rh proteins and NHE-2 (Zimmer et al., 2014b), suggesting the presence of an Rh-NHE metabolon in the gills of these fish (Zimmer et al., 2014b), though this does not necessarily discount the possibility of some Na^+/NH_4^+ exchange occurring as direct exchange via NHE.

Branchial J^{Na}_{in} and J_{amm} in CYA trout were also significantly inhibited by DAPI (Fig. 3.3), which targets acid-sensing ion channels (ASICs) and is a potent inhibitor of J^{Na}_{in} in trout (Dymowska et al., 2014). ASICs have recently been implicated as an integral part of the Na^+ uptake mechanism in freshwater fish, acting as the putative Na^+ channels which function to absorb Na^+ electrogenically via the actions of H^+-ATPase (Dymowska et al., 2014). In the present study, however, we found that bafilomycin had no significant effects on J^{Na}_{in}, while DAPI inhibited J^{Na}_{in} by 90% (Fig. 3.3). Note that the concentration of bafilomycin used was 1×10^{-7} mol/l because at higher concentrations (2.5×10^{-7}, 1×10^{-6}, 5×10^{-6} mol/l) we observed loss of equilibrium and/or mortality in larvae and therefore these concentrations were deemed inappropriate. Thus, it appears that branchial ASIC in these CYA trout functions independently of H^+-ATPase and that H^+-ATPase does not contribute to overall J^{Na}_{in} in rainbow trout raised in Hamilton water (pH 8; see Materials and Methods for composition) unlike larval trout raised in soft water (Bury and Wood, 1999) and zebrafish in neutral or acidic pH (Kumai and Perry, 2011). Interestingly, larval medaka also appear to possess a mechanism for J^{Na}_{in} which is independent of H^+-ATPase (Wu et al., 2010). Dymowska et al. (2014) determined that

apical ASIC expression was co-localized with basolateral Na^+/K^+-ATPase in gill MRCs, indicating that J^{Na}_{in} via ASIC could potentially be powered by basolateral Na^+/K^+-ATPase, however the general function of ASIC at this time is not clear. Indeed, the inhibition of J_{amm} by DAPI is puzzling as it is not clear how ASIC inhibition would alter ammonia transport; perhaps the inhibition of ASIC alters transepithelial potential (TEP) which could affect ammonia transport. It is also possible that DAPI acts non-specifically on NHE to cause these effects, which might also account for the >100% inhibition of J^{Na}_{in} when considering the combined effects of EIPA and DAPI. Though Dymowska et al. (2014) demonstrated that DAPI did not interfere with NHE-mediated changes in pHi measured in isolated cells *in vitro*, their study utilized only one gill cell type (peanut lectin agglutinin-positive; PNA^+) and used a 10-fold lower concentration (1×10^{-6} mol/l) than that used in the present study (1×10^{-5} mol/l). Furthermore, it is likely that under their experimental conditions (external [NaCl]=145 mM), pHi adjustment would be mediated by the "housekeeping", basolateral NHE, as opposed to the apical NHE which functions in dilute environments. In fact, Mrkic et al. (1992) demonstrated that basolateral NHEs are more sensitive to EIPA than the apical NHEs in cultured murine proximal tubule cells. Therefore, more research is needed to better understand the effects of DAPI as a blocker of J^{Na}_{in} and the role of ASICs in branchial Na^+/NH_4^+ exchange in freshwater fish. The overall model for J^{Na}_{in} and J_{amm} across the CYA gill is presented in Fig. 3.5A. Note that in this model, Rh proteins are assumed to be present based on the gene expression of Rhcg1, Rhcg2, and Rhbg in the gill of CYA fish (e.g., Zimmer et al., 2014b).

3.5.3 J_{amm} and J^{Na}_{in} by the yolk sac epithelium

The skin of PH larval rainbow trout, approximately half of which is the yolk sac epithelium (Rombough 1999), accounts for the majority of both J^{Na}_{in} and J_{amm} (Fu et al., 2010; Zimmer et al., 2014b). The present study is the first to directly assess flux across the yolk sac epithelium in rainbow trout. The PH yolk sac does not appear to possess a mechanism for functional Na^+/NH_4^+ exchange, despite the fact that this tissue expresses the genes and displays the activities of several of the key components of the Na^+/NH_4^+ exchange complex (Zimmer et al., 2014b). In contrast to the CYA gill, HEA pre-exposure did not alter J^{Na}_{in} across the PH yolk sac epithelium despite a significant increase in J_{amm} (Fig. 3.2). This is in contrast to larvae of medaka where high ammonia acclimation leads to an increase in both J^{Na}_{in} and J_{amm} across the yolk sac epithelium (Wu et al., 2010). In the present study, J^{Na}_{in} by the yolk sac epithelium of PH trout appears to be mediated at least in part by NHE based on inhibitory action of EIPA (Fig. 3.4A). The presence of NHE-mediated J^{Na}_{in} in the yolk sac epithelium has been reported in at least two other fish species (zebrafish, Shih et al., 2012; medaka, Wu et al., 2010). However, in these species, EIPA treatment leads to the inhibition of both J^{Na}_{in} and J_{amm} (Shih et al., 2012; Wu et al., 2010), whereas J_{amm} across the yolk sac epithelium in PH trout is EIPA-insensitive (Fig. 3.4B). Thus, there appears to be a fundamental difference in the mechanism of J^{Na}_{in} and J_{amm} by the yolk sac among these species and, moreover, between the gill (Fig. 3.3) and yolk sac (Fig. 3.4) of rainbow trout. J^{Na}_{in} by the yolk sac skin of PH larvae was also inhibited by DAPI (Fig. 3.4A), presenting the first evidence that ASICs might also play a role in J^{Na}_{in} across the yolk sac skin of larval fish. Unlike the gill, however, J_{amm} by the

PH yolk sac was not sensitive to DAPI (Fig. 3.4B), further demonstrating a lack of Na^+-coupled J_{amm} by this epithelium. Furthermore, bafilomycin also did not have any effect on J^{Na}_{in} or J_{amm} across the PH yolk sac (Fig. 3.4). This again raises questions regarding the mechanism by which ASIC might operate, as here it appears to be independent of H^+-ATPase, similar to the CYA gill.

The yolk sac skin of trout expresses Rh protein genes as early as 3 dph (Zimmer et al., 2014b) and, therefore, it is possible that J_{amm} across this epithelium is simply a function of NH_3 partial pressure gradients, which may not require boundary layer acidification, at least by NHE or H^+-ATPase. In future studies, it would be interesting to examine the effects of external buffering on J_{amm} across this epithelium. Moreover, it is currently unknown if the yolk sac skin is capable of active excretion against a concentration gradient, as seen in the gill where active J_{amm} occurs in conjunction with increases in the gene expression/enzyme activity of Rh proteins, NHE, and H^+-ATPase (e.g., Nawata et al., 2007; Wood and Nawata, 2011; Zimmer et al., 2010). Given that J_{amm} by the yolk sac skin is independent of H^+-ATPase, does not occur via Na^+/NH_4^+ exchange, and is perhaps independent of acid-trapping, active J_{amm} may not be possible across this epithelium. The transport model for J^{Na}_{in} and J_{amm} across the PH yolk sac epithelium is presented in Fig. 3.5B and in many ways is similar to that presented for the CYA gill except that there is no coupling between the specific routes of J^{Na}_{in} and J_{amm}. Again, Rh proteins are included based on gene expression data (Zimmer et al., 2014b) and the source of external protons for the conversion of NH_3 to NH_4^+ is not known, but could simply be from the surrounding water which has a lower pH (8) than the pK for the

$NH_3 \leftarrow\rightarrow NH_4^+$ reaction (~9.5) or may arise from boundary layer acidification by CO_2 excretion, similar to the case of the gill (Wright et al., 1989). Indeed, Rahaman-Noronha et al. (1996) found that the unstirred layer surrounding rainbow trout embryos is acidified relative to the bulk water, facilitating J_{amm} by maintaining favourable PNH_3 gradients. These authors suggest that CO_2 excretion from the embryo or from the surrounding perivitelline fluid might contribute to acidification (Rahaman-Noronha et al., 1996).

3.5.4 J_{amm} by the body epithelium

The body skin of fish appears to be an important site for J_{amm} in some specialized fish species such as some flatfish with large body surface areas (Sayer and Davenport, 1987) and amphibious fish such as the mangrove killifish (Frick and Wright, 2002) and the blennid *Lipophrys pholis* (Souza-Bastos et al., 2014). At least in the mangrove killifish, cutaneous J_{amm} appears to be coupled to J^{Na}_{in} (Cooper et al., 2013), unlike the body epithelium of rainbow trout (Fig. 3.2). The mechanism of J_{amm} by the skin of trout is likely mediated by Rh, given the expression of Rh genes in this tissue, and their responsiveness to ammonia-loading treatments (Nawata and Wood, 2008; 2009; Nawata et al., 2007; Zimmer et al.. 2014a), with at least one study (on adults, rather than larvae) suggesting linkage to Na^+ transport (Zimmer et al., 2014a). In adult trout, the skin is responsible for approximately 5% of total J_{amm} (Zimmer et al., 2014a) which might represent the skin clearing its own endogenous or exogenous ammonia loads directly to the surrounding water, sparing the fish from further internal ammonia loading, as opposed to transcutaneous clearance of ammonia from the plasma. It is interesting to note, once again, that although the skin plays a relatively small role in overall J_{amm}, at least one study

indicates that this role is greater than that of the kidney (Zimmer et al., 2014a), which has been historically been considered to be the dominant extra-branchial route for J_{amm}. Overall, we hypothesize that the model for J_{amm} by the body skin of early life stage trout (CYA fish) is likely solely a function of Rh proteins (Fig. 3.5C), given the gene expression of these proteins in this tissue of both CYA (Zimmer et al., 2014b) and adult trout (Zimmer et al., 2014a). At present, it is not known if there are morphological differences between the skin of CYA and adult trout (e.g., ionocyte density, vascularization, scale coverage, skin thickness) which might alter the overall function of Rh between these tissues, for example, in terms of transcutaneous ammonia transport.

3.6 TABLES AND FIGURES

Table 3.1. J^{Na}_{in} and J_{amm} by the CYA gill and PH yolk sac under control conditions and in the presence of 0.1% DMSO.

	J^{Na}_{in} (µmol/g/h)		J_{amm} (µmol/g/h)	
	Control	DMSO	Control	DMSO
CYA Gill	0.898 ± 0.044	1.087 ± 0.082	0.402 ± 0.076	1.367 ± 0.116*
PH Yolk Sac	0.124 ± 0.027	0.115 ± 0.012	0.284 ± 0.010	0.257 ± 0.062

Asterisks denote significant differences between control and corresponding DMSO-treated values as determined by a Student's two-tailed t-test.

A

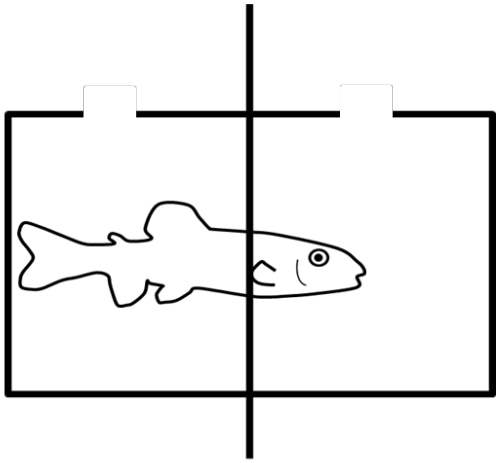

B

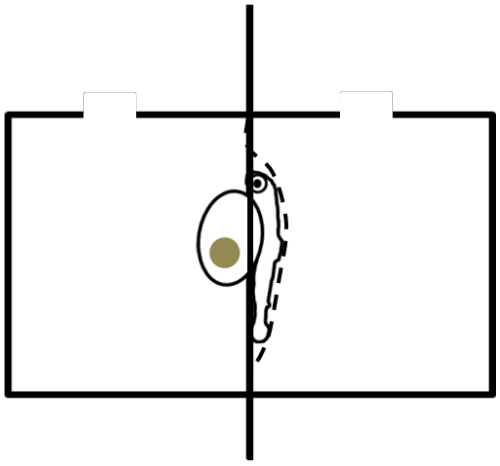

Fig. 3.1. Schematic diagrams of the “traditional” divided chamber (A) used to assess flux across the CYA gill and body and the PH divided chamber (B) used to assess flux across the yolk sac of PH larvae.

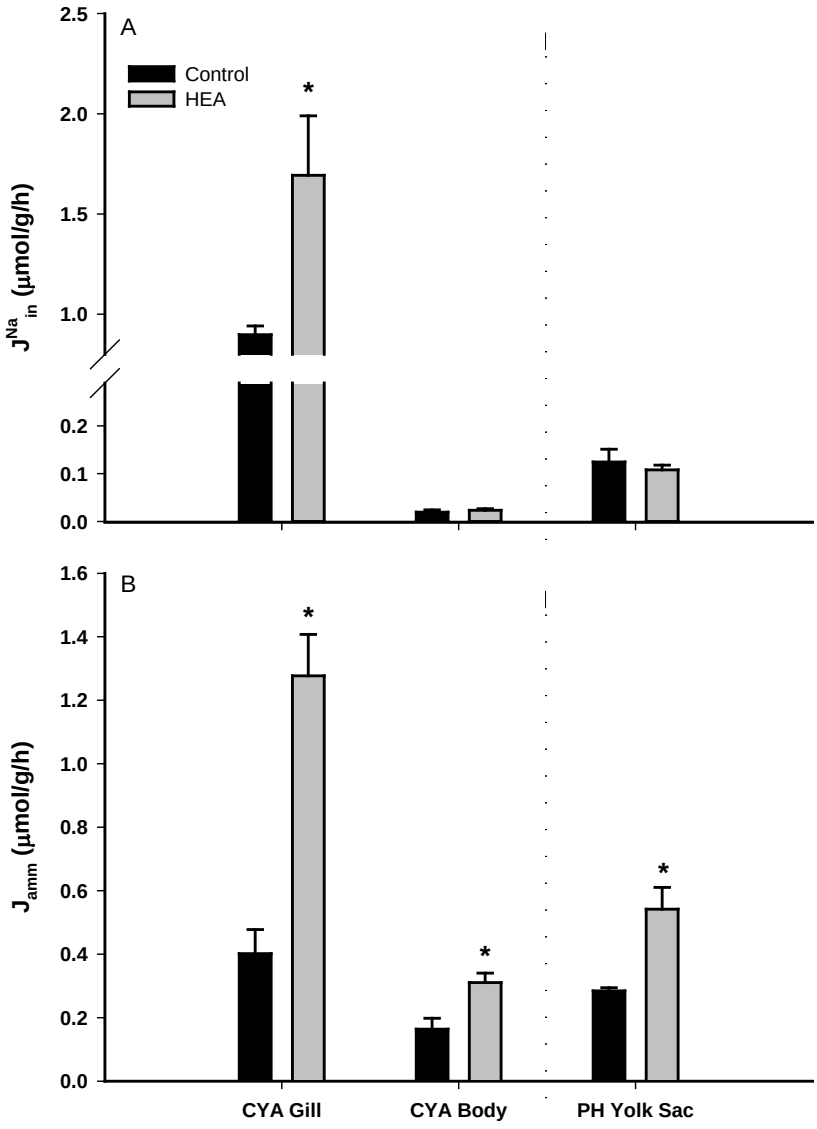
A
Control
HEA
J^{Na}_{in} (µmol/g/h)
2.5
2.0
1.5
1.0
0.2
0.1
0.0
*
B
J_{amm} (µmol/g/h)
1.6
1.4
1.2
1.0
0.8
0.6
0.4
0.2
0.0
*
*
*
CYA Gill
CYA Body
PH Yolk Sac

Fig. 3.2. Na^+ uptake (J^{Na}_{in} ;A) and ammonia excretion (J_{amm}; B) across the CYA gill, CYA body, and PH yolk sac under control conditions (black bars) and following exposure to 0.5 mmol/l NH_4HCO_3 for 12 h (high external ammonia (HEA); grey bars). Asterisks represent statistically significant differences between control and HEA groups across a given epithelium as determined by a Student's two-tailed t-test. (n=6-9; $P<0.05$)

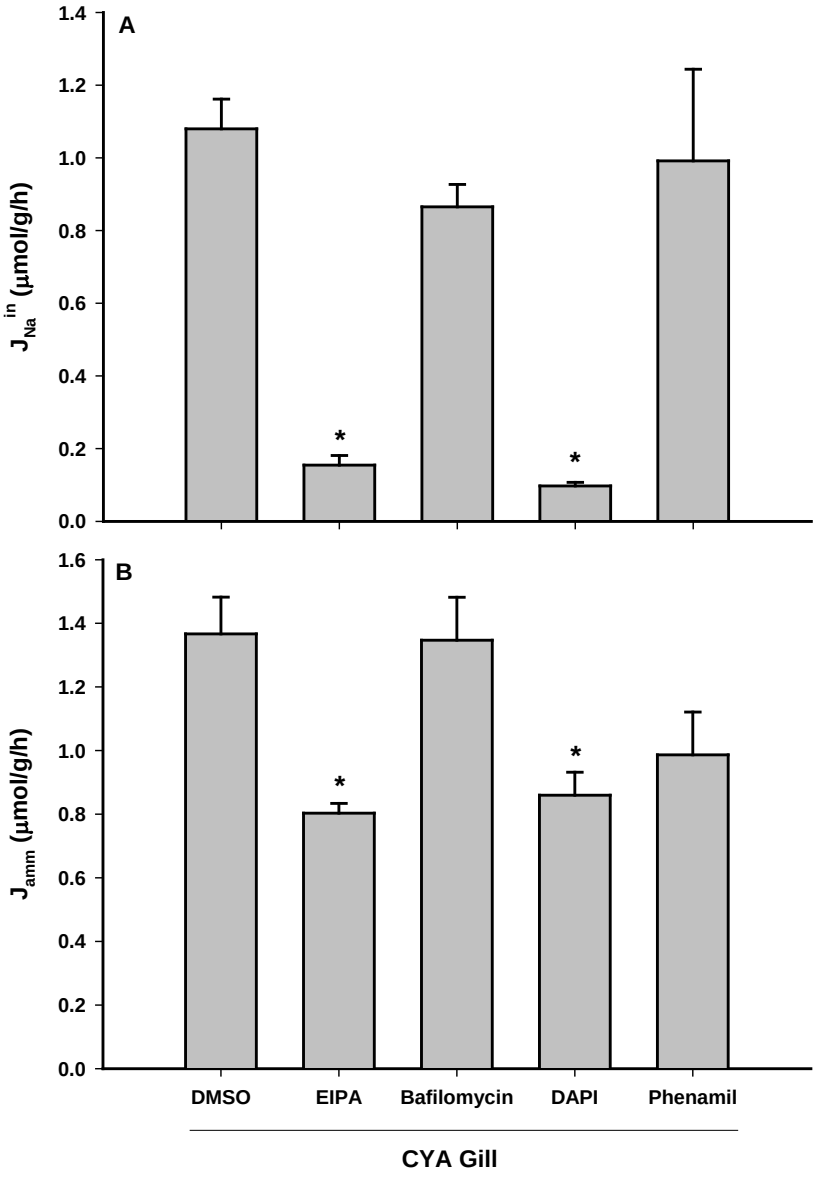
A
B
1.4
1.2
1.0
0.8
0.6
0.4
0.2
0.0
1.6
J_{Na}^{in} (µmol/g/h)
J_{amm} (µmol/g/h)
*
DMSO
EIPA
Bafilomycin
DAPI
Phenamil
CYA Gill

Fig. 3.3. Na^+ uptake (J^{Na}_{in}; A) and ammonia excretion (J_{amm}; B) across the CYA gill in response to DMSO (0.1% vehicle control) and to the pharmacological blockers EIPA ($1x10^{-4}$ mol/l), bafilomycin (1×10^{-7} mol/l), DAPI (1×10^{-5} mol/l), and phenamil (1×10^{-4} mol/l) dissolved in 0.1% DMSO. Asterisks represent statistically significant differences from the DMSO value as determined by a one-way ANOVA followed by a Holm-Sidak post-hoc test. ($n=4-9$; $P<0.05$)

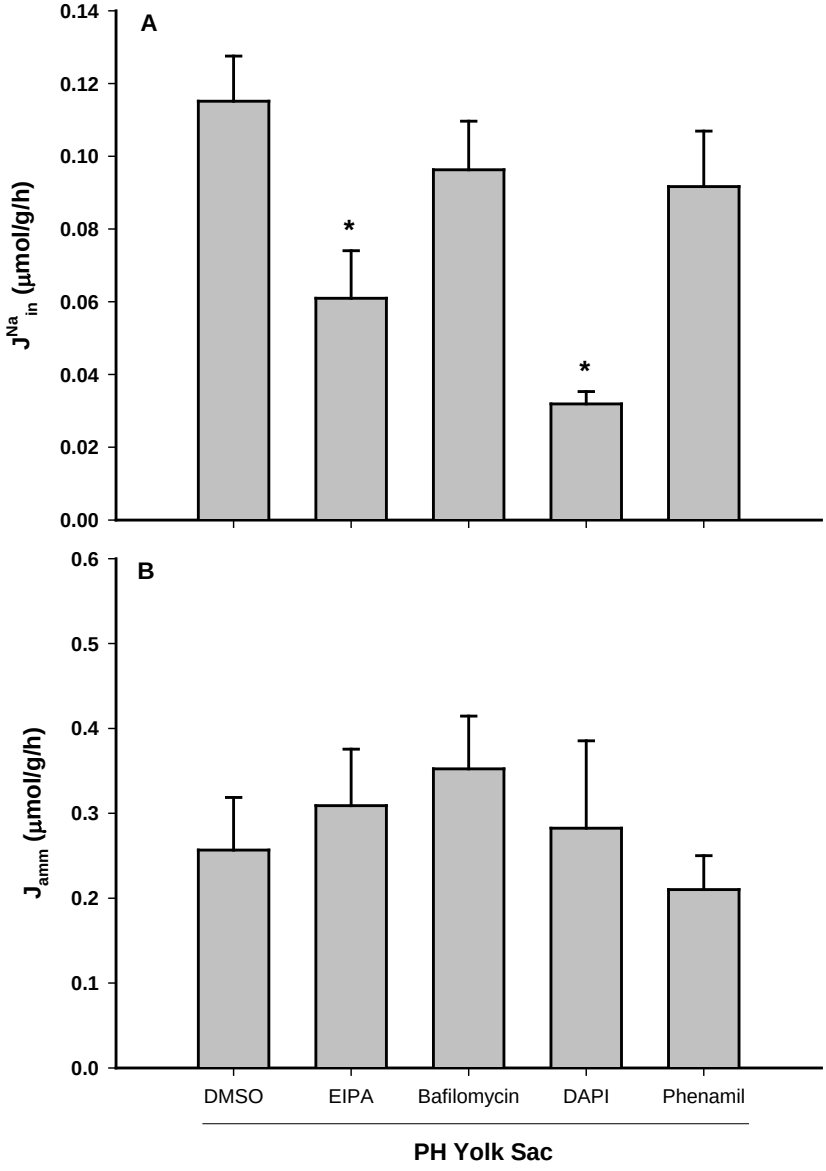
A
B
0.14
0.12
0.10
0.08
0.06
0.04
0.02
0.00
0.6
0.5
0.4
0.3
0.2
0.1
0.0
*
*
J^{Na}_{in} (µmol/g/h)
J_{amm} (µmol/g/h)
DMSO
EIPA
Bafilomycin
DAPI
Phenamil
PH Yolk Sac

Fig. 3.4. Na^+ uptake (J^{Na}_{in}; A) and ammonia excretion (J_{amm}; B) across the PH yolk sac in response to DMSO (0.1% vehicle control) and to the pharmacological blockers EIPA ($1x10^{-4}$ mol/l), bafilomycin (5×10^{-6} mol/l), DAPI (1×10^{-5} mol/l), and phenamil (1×10^{-4} mol/l) dissolved in 0.1% DMSO. Asterisks represent statistically significant differences from the DMSO value as determined by a one-way ANOVA followed by a Holm-Sidak post-hoc test. ($n=4-9$; $P<0.05$)

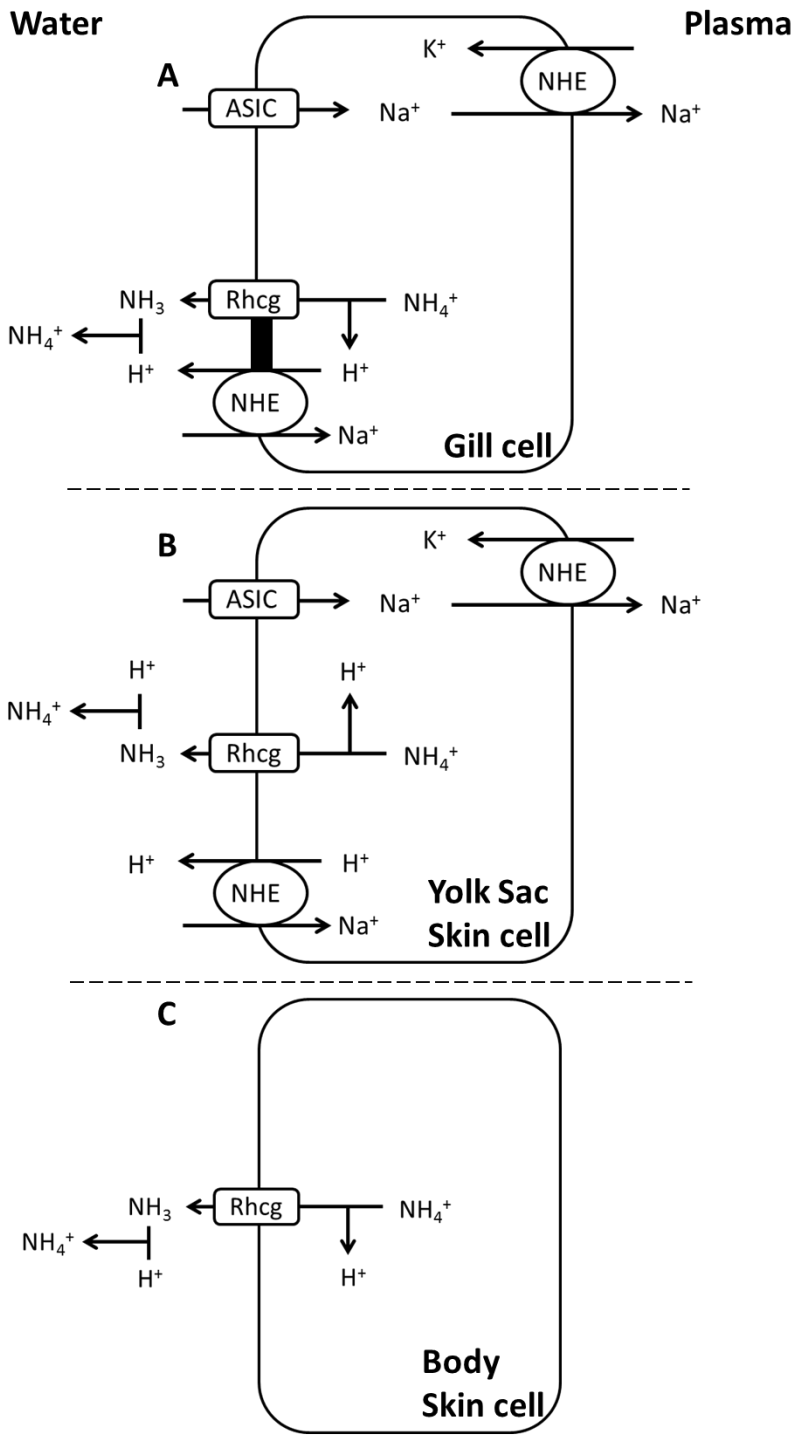
Water
Plasma
A
ASIC
K+
NHE
Na+
Na+
NH3
Rhcg
NH4+
NH4+
H+
H+
NHE
Na+
Gill cell
B
ASIC
K+
NHE
Na+
Na+
H+
H+
NH4+
NH3
Rhcg
NH4+
H+
H+
NHE
Na+
Yolk Sac
Skin cell
C
NH3
Rhcg
NH4+
NH4+
H+
H+
Body
Skin cell

Fig. 3.5. Models illustrating the mechanisms of Na^+ uptake (J^{Na}_{in}) and/or ammonia excretion (J_{amm}) across generalized gill cells (A), yolk sac skin cells (B), and body skin cells (C). Note the coupling of Na^+ transport to ammonia transport in A and the lack thereof in B. Note also that in B and C external protons for the conversion of NH_3 to NH_4^+ do not have a specific source as in A. See text for further details.

3.7 REFERENCES

Braun, M.H., Steele, S.L. and Perry, S.F. (2009b) The responses of zebrafish (*Danio rerio*) to high external ammonia and urea transporter inhibition: nitrogen excretion and expression of rhesus glycoproteins and urea transporter proteins. *J. Exp. Biol.* 212, 3846-3856.

Bury, N.R. and Wood, C.M. (1999) Mechanism of branchial apical silver uptake by rainbow trout is via the proton-coupled Na^+ channel. *Am. J. Physiol. Regul. Integr. Physiol.* 277, 1385-1391.

Cooper, C.A., Wilson, J.M. and Wright, P.A. (2013) Marine, freshwater and aerially acclimated mangrove rivulus (*Kryptolebias marmoratus*) use different strategies for cutaneous ammonia excretion. *Am. J. Physiol. Regul. Integr. Physiol.* 304, R599-R612.

Dymowska, A.K., Schultz, A.G., Blair, S.D., Chamot, D. and Goss, G.G. (2014) Acid-sensing ion channels are involved in epithelial Na^+ uptake in the rainbow trout *Oncorhynchus mykiss*. *Am. J. Physiol. Cell Physiol.* 307, 255-265.

Frick, N.T. and Wright, P.A. (2002) Nitrogen metabolism and excretion in the mangrove killifish *Rivulus marmoratus* II. Significant ammonia volatilization in a teleost during air-exposure. *J. Exp. Biol.* 205, 91-100.

Fu, C., Wilson, J.M., Rombough, P.J. and Brauner, C.J. (2010) Ions first: Na^+ uptake shifts from the skin to the gills before O_2 uptake in developing rainbow trout, *Oncorhynchus mykiss*. *Proc. R. Soc. B* 277, 1553–60.

Hung, C.Y.C., Tsui, K.N.T., Wilson, J.M., Nawata, C.M., Wood, C.M. and Wright, P.A. (2007) Rhesus glycoprotein gene expression in the mangrove killfish *Kryptolebias marmoratus* exposed to elevated environmental ammonia levels and air. *J. Exp. Biol.* 210, 2419-2429.

Ito, Y., Kobayashi, S., Nakamura, N., Miyagi, H., Esaki, M., Hoshijima, K. and Hirose, S. (2013) Close association of carbonic anhydrase (CA2a and CA15a), Na^+/H^+ exchanger (Nhe3b), and ammonia transporter Rhcg1 in zebrafish ionocytes responsible for Na^+ uptake. *Front. Physiol.* 4, 1-17.

Ito, Y., Kato, A., Hirata, T., Hirose, S. and Romero, M.F. (2014) Na^+/H^+ and Na^+/NH_4^+ exchange activities of zebrafish NHE3b expressed in *Xenopus* oocytes. *Am. J. Physiol. Regul. Integr. Comp. Physiol.* 306, R315-327.

Kumai, Y. and Perry, S.F. (2011) Ammonia excretion via Rhcg1 facilitates Na^+ uptake in larval zebrafish, *Danio rerio*, in acidic water. *Am. J. Physiol. Regul. Integr. Comp. Physiol.* 301, R1517–28.

Liew, J.H., Sinha, A.K., Nawata, C.M., Blust, R., Wood, C.M. and De Boeck, G. (2013) Differential responses in ammonia excretion, sodium fluxes, and gill permeability explain different sensitivities to acute high environmental ammonia in three freshwater teleosts. *Aquat. Tox.* 126, 63-76.

Maetz, J. and Garcia-Romeu, F. (1964) The mechanism of sodium and chloride uptake by the gills of a fresh-water fish, *Carassius auratus*: II. Evidence for Na^+/NH_4^+ and HCO_3^-/Cl^- exchanges. *J. Gen. Physiol.* 47, 1209-1227.

McFarland, W.N. (1959) A study of the effects of anesthetics on the behaviour and physiology of fishes. *Publ. Inst. Mar. Sci. Univ. Tex.* 6, 23-55.

Mrkic, B., Forgo, J., Murer, H. and Helmle-Kolb, C. (1992) Apical and basolateral Na/H exchange in cultured murine proximal tubule cells (MCT): effect of parathyroid hormone (PTH). *J. Membrane Biol.* 130, 205-217.

Nawata, C.M. and Wood, C.M. (2008) The effects of CO_2 and external buffering on ammonia excretion and Rhesus glycoprotein mRNA expression in rainbow trout. *J. Exp. Biol.* 211, 3226-3236.

Nawata, C.M. and Wood, C.M. (2009) mRNA expression analysis of the physiological responses to ammonia infusion in rainbow trout. *J. Comp. Physiol. B* 179, 799-810.

Nawata, C.M., Hirose, S., Nakada, T., Wood, C.M. and Kato, A. (2010a) Rh glycoprotein expression is modulated in pufferfish (*Takifugu rubripes*) during high environmental ammonia exposure. *J. Exp. Biol.* 213, 3150-3160.

Nawata, C.M., Hung, C.C.Y., Tsui, T.K.N., Wilson, J.M., Wright, P.A. and Wood, C.M. (2007) Ammonia excretion in rainbow trout (*Oncorhynchus mykiss*): evidence for Rh glycoprotein and H^+-ATPase involvement. *Physiol. Genomics* 31, 463–74.

Nawata, C.M., Wood, C.M. and O'Donnell, M.J. (2010b) Functional characterization of Rhesus glycoproteins from an ammoniotelic teleost, the rainbow trout, using oocyte expression and SIET analysis. *J. Exp. Biol.* 213, 1049-1059.

Nonnotte, G. (1981) Cutaneous respiration in six freshwater teleosts. *Comp. Biochem. Physiol. A* 70, 541-543.

Nonnotte, G. and Kirsch, R. (1978) Cutaneous respiration in seven sea-water teleosts. *Respir. Physiol.* 35, 111-118.

Rahaman-Noronha, E., O'Donnell, M.J., Pilley, C.M. and Wright, P.A. (1996) Excretion and distribution of ammonia and the influence of boundary layer

acidification in embryonic rainbow trout (*Oncorhynchus mykiss*). *J. Exp. Biol.* 199, 2713-2723.

Rombough, P.J. (1999) The gill of fish larvae. Is it primarily a respiratory or an ionoregulatory structure? *J. Fish Biol.* 55, 186–204.

Sayer, M.D.J. and Davenport, J. (1987) The relative importance of the gills to ammonia and urea excretion in five seawater and one freshwater teleost species. *J. Fish. Biol.* 31, 561-570.

Shih, T.-H., Hong, J.-L., Hwang, P.-P. and Lin, L.,-Y. (2008) Ammonia excretion by the skin of zebrafish (*Danio rerio*) larvae. *Am. J. Physiol. Cell Physiol.* 295, 1625-1632.

Shih, T.-H., Horng, J.-L., Lai, Y.-T. and Lin, L.-Y. (2013) Rhcg1 and Rhbg mediate ammonia excretion by ionocytes and keratinocytes in the skin of zebrafish larvae: H^+-ATPase-linked active ammonia excretion by ionocytes. *Am. J. Physiol. Regul. Integr. Comp. Physiol.* 304, R1130–R1138.

Shih, T.-H., Horng, J.-L., Liu, S.-T., Hwang, P.-P. and Lin, L.-Y. (2012) Rhcg1 and NHE3b are involved in ammonium-dependent sodium uptake by zebrafish larvae acclimated to low-sodium water. *Am. J. Physiol. Regul. Integr. Comp. Physiol.* 302, R84–93.

Sinha, A.K., Liew, H.J., Nawata, C.M., Blust, R., Wood, C.M. and De Boeck, G. (2013) Modulation of Rh glycoproteins, ammonia excretion and Na^+ fluxes in three freshwater teleosts when exposed chronically to high environmental ammonia. *J. Exp. Biol.* 216, 2917-2930.

Smith, A.A., Zimmer, A.M. and Wood, C.M. (2012) Branchial and extra-branchial ammonia excretion in goldfish (*Carassius auratus*) following thermally induced gill remodeling. *Comp. Biochem. Physiol. A* 162, 185–192.

Smith, H.W (1929) The excretion of ammonia and urea by the gills of fish. *J. Biol. Chem.* 81, 727-742.

Souza-Bastos, L.R., Pascoa, M.I., Freire, C.A. and Wilson, J.M. (2014) Ammonia excretion and expression of transport proteins in the gills and skin of the intertidal fish *Lipophrys pholis*. *Comp. Biochem. Physiol. A* 167, 15-24.

Verdouw, H., van Echteld, C.J.A. and Dekkers, E.M.J. (1978) Ammonia determination based on indophenols formation with sodium salicylate. *Water Res.* 12, 399-402.

Weihrauch, D., Wilkie, M.P. and Walsh, P.J. (2009) Ammonia and urea transporters in gills of fish and aquatic crustaceans. *J. Exp. Biol.* 212, 1716-1730.

Wilkie, M.P. (1997) Mechanisms of ammonia excretion across fish gills. *Comp. Biochem. Physiol. A* 118, 39-50.

Wilkie, M.P. (2002) Ammonia excretion and urea handling by fish gills: present understanding and future research challenges. *J. Exp. Zool.* 293, 284-301.

Wilson, R.W., Wright, P.M., Munger, S. and Wood, C.M. (1994) Ammonia excretion in freshwater rainbow trout (*Oncorhynchus mykiss*) and the importance of gill boundary layer acidification: lack of evidence for Na^+/NH_4^+ exchange. *J. Exp. Biol.* 191, 37-58.

Wood, C.M. and Nawata, C.M. (2011) Nose-to-nose comparison of physiological and molecular responses of trout to high environmental ammonia in seawater versus freshwater. *J. Exp. Biol.* 214, 3557-3569.

Wright, P.A. and Wood, C.M. (2009) A new paradigm for ammonia excretion in aquatic animals: role of Rhesus (Rh) glycoproteins. *J. Exp. Biol.* 212, 2303–12.

Wright, P.A. and Wood, C.M. (2012) Seven things fish know about ammonia and we don't. *Respir. Physiol. Neurobiol.* 184, 231-240.

Wright, P.A., Felskie, A. and Anderson, P. (1995) Induction of ornithine-urea cycle enzymes and nitrogen metabolism and excretion in rainbow trout (*Oncorhynchus mykiss*) during early life stages. *J. Exp. Biol.* 198, 127–35.

Wright, P.A., Randall, D.J. and Perry, S.F. (1989) Fish gill water boundary layer: a site of linkage between carbon dioxide and ammonia excretion. *J. Comp. Physiol. B* 158. 627-635.

Wu, S.-C., Horng, J.-L., Liu, S.-T., Hwang, P.-P., Wen, Z.-H., Lin, C.-S. and Lin, L.-Y. (2010) Ammonium-dependent sodium uptake in mitochondrion-rich cells of medaka (*Oryzias latipes*) larvae. *Am. J. Physiol. Cell Physiol.* 298, 237-250.

Zimmer, A.M., Brauner, C.J. and Wood, C.M. (2014a) Ammonia transport across the skin of adult rainbow trout (*Oncorhynchus mykiss*) exposed to high environmental ammonia (HEA). *J. Comp. Physiol. B.* 184, 77-90.

Zimmer, A.M., Nawata, C.M. and Wood, C.M. (2010) Physiological and molecular analysis of the interactive effects of feeding and high environmental ammonia on branchial ammonia excretion and Na^+ uptake in freshwater rainbow trout. *J. Comp. Physiol. B* 180, 1191-1204.

Zimmer, A.M., Wright. P.A. and Wood, C.M. (2014b) What is the primary function of the early teleost gill? Evidence for Na^+-coupled ammonia excretion in developing rainbow trout (*Oncorhynchus mykiss*). *Proc. R. Soc. B* 281: 1795.

CHAPTER 4

AMMONIA FIRST? THE TRANSITION FROM CUTANEOUS TO BRANCHIAL AMMONIA EXCRETION IN DEVELOPING RAINBOW TROUT (*ONCORHYNCHUS MYKISS*) IS NOT ALTERED BY EXPOSURE TO CHRONICALLY HIGH NaCl

4.1 ABSTRACT

Larval rainbow trout (*Oncorhynchus mykiss*) were reared from hatch under control ($[Na^+]$=0.60 mmol/l) or high NaCl ($[Na^+]$=60 mmol/l) conditions to elucidate the driving force for the ontogeny of branchial Na^+/NH_4^+ exchange, one of the earliest gill functions. We hypothesized that if Na^+ uptake is the driving force, then in high NaCl there would be a delay in the skin-to-gill shift in ammonia excretion (J_{amm}) and/or an elevation in whole-body total ammonia (T_{amm}). In both groups, however, the skin-to-gill shift for J_{amm}, determined using divided chambers, occurred at the same time (13 days post-hatch; dph) and whole-body T_{amm} was unchanged. Moreover, high NaCl larvae displayed elevated whole-body $[Na^+]$ relative to controls by 18 dph, suggesting that maintaining branchial J_{amm} occurs at the expense of Na^+ balance. Overall, these results support the "ammonia hypothesis" which posits that ammonia excretion, likely as Na^+/NH_4^+ exchange, is the primary function of the early fish gill.

4.2 INTRODUCTION

In most fish species, the gill is the primary site for physiological exchanges of respiratory gases, ions, acid-base equivalents, and nitrogenous wastes with the environment. However, following hatch, larval fish possess only a rudimentary gill, and therefore the skin of these fish performs the majority of physiological functions typical of the gill of adult fish (see Brauner and Rombough, 2012 for review). Several studies have investigated the ontogenetic pressures underlying gill development in larval fish. The original idea of August Krogh (1941) was the "oxygen hypothesis" – i.e. that gill development was driven by the increasing need for O_2 uptake. However, the most recent evidence supports the "ionoregulatory hypothesis" which posits that ionoregulatory demand, in one form or another, is the driving force for branchial ontogeny (see Brauner and Rombough, 2012 for review). To date, two studies have provided direct support for this hypothesis using a divided chamber approach to demonstrate that in developing larval rainbow trout (*Oncorhynchus mykiss*), Na^+ uptake shifts from the skin to the gills prior to oxygen uptake (Fu et al., 2010; Zimmer et al., 2014). However, what remains unclear is the question of which aspect of ionoregulation can be considered the earliest function of the developing gill.

Brauner and Rombough (2012) suggest that it is unlikely that branchial ion uptake in early life stages serves the sole purpose of mineral nutrient acquisition but, rather, that ion uptake likely occurs as coupled exchanges, such as those involved in acid-base regulation and/or N-waste excretion. In typical freshwater fish, branchial Na^+ uptake is believed to occur in part via Na^+/NH_4^+ exchange which is coordinated by an exchange

complex of a number of different transporters (see Wright and Wood, 2009 for review). In larval rainbow trout, the skin-to-gill shift for Na^+ uptake occurs in synchrony with that of ammonia excretion (J_{amm}) and branchial Na^+ uptake is closely correlated with branchial J_{amm} throughout development (Zimmer et al., 2014). However, there is no such relationship between skin Na^+ uptake and skin J_{amm} (Zimmer et al., 2014). Thus, the development of branchial Na^+ uptake occurs as a linked Na^+/NH_4^+ exchange process. In addition, the ontogeny of branchial Na^+/NH_4^+ exchange is coincident with increased branchial gene expression and enzyme activity of the transporters involved in Na^+/NH_4^+ exchange (Zimmer et al., 2014).

But is the driving force for the development of branchial Na^+/NH_4^+ exchange the need for Na^+ uptake or the need for ammonia excretion? To address this question, larval rainbow trout were raised from hatch up to 18 days post-hatch (dph) under control conditions (approximately 0.6 mmol/l NaCl) or in water containing a high concentration of Na^+ (approximately 60 mmol/l NaCl), comparable to the concentration observed in post-hatch larvae (Brauner and Wood, 2002). Over developmental time, whole-body $[Na^+]$ increases (Brauner and Wood, 2002), probably associated with increasing extracellular fluid (ECF) volume. We hypothesized that by providing larvae with greatly increased ambient $[Na^+]$, there would be a reduction in ionoregulatory demand, potentially delaying the skin-to-gill shift for Na^+ uptake. From this hypothesis, we predicted that if Na^+ uptake is driving the development of branchial Na^+/NH_4^+ exchange, there would be a delayed skin-to-gill shift in J_{amm} in the high NaCl group relative to control fish. On the other hand, if ammonia excretion is the driving force, the skin-to-gill

shift in J_{amm} would be unaffected by reduced ionoregulatory demand imposed by high ambient NaCl. We assessed this idea using a divided chamber approach to quantify J_{amm} in the gills versus the skin at 3, 6, 9, 12, and 18 dph. Whole-body [Na^+] and Na^+/K^+-ATPase activity in the gill, yolk sac skin, and body skin were also assessed over the 18-day period as indicators of ionoregulatory status/capacity in both groups of fish. We further predicted that Na^+/K^+-ATPase activity, which increases over larval development at least in the gills (e.g., Fu et al., 2010; Zimmer et al., 2014), likely to support increasing whole-body [Na^+], would be down-regulated in the gill, body skin, and/or yolk sac skin in high ambient NaCl, reflecting a reduction in ionoregulatory demand.

4.3 MATERIALS AND METHODS

4.3.1 Experimental Design

Rainbow trout (*Oncorhynchus mykiss*) were purchased in the eyed-up stage from Rainbow Springs Hatchery (Thamesford, Ontario, Canada) and held in flow-through Hamilton dechlorinated tap water (moderately hard: [Na^+]= 0.6 mequiv/l, [Cl^-] = 0.8 mequiv/l, [Ca^{2+}]= 1.8 mequiv/l, [Mg^{2+}]= 0.3 mequiv/l, [K^+] =0.05 mequiv/l; titration alkalinity 2.1 mequiv/l; pH ~8.0; hardness ~140 mg/l as $CaCO_3$ equivalents, 12ºC). Fish hatched approximately 1 week after purchase and were then randomly separated into two different treatments: control ([Na^+]=0.70 ± 0.00 mmol/l) and high NaCl ([Na^+]=58.29 ± 2.03 mmol/l), the latter made by adding NaCl to dechlorinated tap water. In initial trials, higher levels of ambient [NaCl] (up to 140 mmol/l) were tested, but caused increased mortality after a few days. Therefore, a nominal concentration of 60 mmol/l, the highest level not causing mortality, was selected. Both treatments were conducted at 12ºC using

static, aerated systems in which the water was completely renewed on a daily basis. At 3, 6, 9, 12, and 18 days dph, J_{amm} was measured in a divided chamber system using randomly selected larvae from both groups. Also at the above experimental times, separate larvae from both treatments were randomly selected for the measurement of whole-body tissue total ammonia (T_{amm}) and [Na^+]. At 6, 12, and 18 dph, other randomly selected larvae from each treatment were removed for the determination of Na^+/K^+-ATPase activity in gill, yolk sac epithelium, and body epithelium. Due to the high Na^+ concentration (60 mmol/l), it was not feasible to measure Na^+ uptake as it would require an excessive quantity of radioisotope to obtain the necessary specific activity.

4.3.2 Divided Chamber Ammonia Fluxes

J_{amm} in both groups was measured in a divided chamber system closely following the protocol of Zimmer et al. (2014). The only changes were that fish from respective treatment groups were loaded into divided chambers containing either control water with 0.05 mg/l neutralized MS-222 or high NaCl water with the same concentration of neutralized MS-222. In addition, ^{22}Na (Perkin Elmer, Waltham, MA, USA) was added to one chamber to a final concentration of 0.001 µCi/ml for the sole purpose of ensuring that there were no leaks in the dividing dam. All fluxes were 1 h in duration. Fish recovered from MS-222-induced anaesthesia within 5 min following flux, and isotope leak from the ^{22}[Na]-loaded chamber to the unloaded chamber was less than 10%. Collected water samples from fluxes were stored at -20ºC until subsequent analysis of total ammonia (T_{amm}) using methods described previously (Zimmer et al., 2014). J_{amm} (µmol/g/h) in anterior and posterior chambers was calculated using the following equation:

$$J_{amm} = \frac{[(T_{amm}f - T_{amm}i) \times V]}{(M \times t)} \quad (1)$$

where $T_{amm}f$ and $T_{amm}i$ are final and initial concentrations (µmol/l), respectively, of water samples from anterior or posterior chambers, V is volume of the respective chamber (l), corrected for sample removal, M is larva mass (g), and t is flux duration (h). From these values, branchial and cutaneous J_{amm} was determined by correcting for J_{amm} across the cutaneous surface (skin of the head) in the anterior chamber following calculations and cutaneous surface area estimates used previously (Zimmer et al., 2014).

The skin-to-gill shifting point was then calculated by plotting % total cutaneous and % total branchial J_{amm} means as x-values against time in dph as y-values. X= 0 was then set to 50% by subtracting 50% from all plotted means and a linear regression was used to determine the y-intercept (x=50%) which corresponded to the time in dph at which 50% of total J_{amm} occurred cutaneously or branchially, i.e., the skin-to-gill shifting point.

4.3.3 Tissue T_{amm} and [Na]

At the times outlined above, larvae from each experimental group were removed, anaesthetized with an overdose of neutralized MS-222, rinsed with distilled water, flash-frozen in liquid N_2, and stored at -80ºC. These samples were later ground to a fine powder under liquid N_2 in a chilled mortar and pestle and 150 µl of 8% perchloric acid was added to approximately 50 mg of powdered sample. These samples were kept on ice for 5 min for deproteinization before 5-min centrifugation at 8000 rpm at 4ºC. 10 µl of the resulting supernatant was stored at 4ºC for later [Na^+] analysis. The remainder of the supernatant

was then neutralized using 3 M KOH, flash-frozen, and kept at -80ºC until later T_{amm} analysis.

$[Na^+]$ in tissue homogenates was measured by atomic absorption spectrophotometry (Varian Model 1275, Mulgrave, Victoria, Australia). T_{amm} in deproteinized and neutralized homogenates was measured using a commercial enzymatic assay (Raichem Ammonia Assay, Cliniqa, San Marcos, CA, USA). Ammonia turnover time (h) was calculated using the following equation:

$$Turnover\ time = \frac{Mean\ whole-body\ T_{amm}}{Total\ J_{amm}} \quad (2)$$

4.3.4 Na^+/K^+-ATPase Activity

At 6, 12, and 18 dph, larvae from both treatment groups were euthanized with an overdose of neutralized MS-222. Whole gill baskets, yolk sac skin, and body skin were then dissected from the fish under a stereomicroscope, flash-frozen, and stored at -80ºC. Tissues were later homogenized in an EGTA-deoxycholate buffer and Na^+/K^+-ATPase activity was determined as previously described (Zimmer et al., 2014) based on a protocol modified from McCormick (1993). Activity was normalized to protein content determined with a commercial protein assay (Bio-Rad, Hercules, CA, USA) and a bovine serum albumin standard (Sigma, St. Louis, MO, USA).

4.3.5 Statistics

All data are presented as means ± s.e.m (n=sample size). All statistical analyses were performed using a 2-way ANOVA with treatment and time as factors followed by a Holm-Sidak post-hoc test using SigmaStat v. 3.5 (Systat Software, Inc.). In Fig. 4.1 and Table 4.1, significant differences between treatments ($P<0.05$) are denoted by asterisks.

The skin-to-gill shifting points (together with corresponding s.e.m), represented by dashed lines in Figs 1A,B, were determined using SigmaPlot v.10.0 (Systat Software, Inc.)

4.4 RESULTS AND DISCUSSION

Very clearly, there was no delay in the overall skin-to-gill shift in J_{amm} in the high ambient NaCl treatment relative to the control group (Figs. 4.1A,B). The 50% transition point occurred at 13.0 ± 1.0 days in controls (Fig. 4.1A) and 13.5 ± 0.9 days in the high NaCl group (Fig. 4.1B), values which were not significantly different. In addition, whole-body T_{amm} was unchanged by rearing larvae in high NaCl ($p=0.144$) and embryo mass in the two treatment groups was essentially the same at all time points (Table 4.1A), indicating that developmental rate was also not affected. Overall, this result suggests that the requirement for increased ammonia excretion over development is the key driver in the temporal shift of ionoregulatory function to the gills from the skin. The need for an effective mechanism to excrete metabolic ammonia in developing larvae may be particularly important given the eventual loss of ureagenicity which is critical for ammonia detoxification in the embryonic stage (Wright et al., 1995). Moreover, the transition points reported here were very similar to those reported previously for skin-to-gill shifts for J_{amm} (15.0 ± 0.7 dph; Zimmer et al., 2014) and Na^+ uptake (15-16 dph; Fu et al., 2010, and 14.9 ± 1.2 dph; Zimmer et al., 2014) in a range of different freshwater Na^+ concentrations (0.06 – 2.3 mmol/l) but at similar temperatures (10-12ºC). These observations lend further support to the “ammonia hypothesis” – that ammonia excretion is the primary function of the developing gill. It appears that the timing of the skin-to-gill

transition for J_{amm} is "pre-programmed" into the developmental blueprint so as to ensure adequate excretion of this toxic N-waste, such that it cannot be altered by Na^+ availability.

From 3-18 dph, the overall increase in total J_{amm} in both groups was relatively similar (100% and 82% increases in control and high NaCl groups, respectively), although some temporal differences were observed (Figs. 4.1C,D). At 12 dph, there was a significant 35% depression in total J_{amm} in the high NaCl treatment relative to the controls, and this occurred entirely at the gills (Figs. 4.1C,D). In addition, ammonia turnover time was also significantly increased (Table 4.1A). This relative decrease in branchial J_{amm} by high NaCl larvae occurred just as the gills were starting to come into use, which might suggest that branchial Na^+/NH_4^+ exchange was transiently delayed. Subsequently, at 18 dph, J_{amm} was restored to control levels, occurring entirely via an increase in branchial J_{amm} (Figs. 4.1C,D).

Up to the transition point, the two groups exhibited almost identical temporal profiles of whole-body $[Na^+]$, with approximately 50% increases from day 3 to day 12 (Fig. 4.1E). Clearly, prior to the transition point, whole-body $[Na^+]$ is carefully regulated. Very likely, the rate of active Na^+ uptake was greatly reduced in the high NaCl larvae prior to the skin-to-gill shift at 13 dph, though it is also possible that the rate of Na^+ excretion was greatly increased in these fish. By 18 dph, whole-body $[Na^+]$ increased 20% in the high NaCl group relative to controls (Fig. 4.1E), and this occurred at the same time that branchial J_{amm} was also increased significantly relative to the control group (Figs. 4.1C,D), further supporting the "ammonia hypothesis". Here we are comparing

instantaneous J_{amm} and cumulative whole-body [Na^+], but the same conclusion can be drawn by comparing cumulative whole-body T_{amm} and [Na^+]. Note that whole-body [Na^+] was increased significantly by 18 dph in high NaCl while whole-body T_{amm} was unchanged throughout the exposure, again suggesting that the primary function of the early fish gill is to ensure ammonia excretion, even at the expense of Na^+ balance.

We had initially predicted that in the face of more favourable gradients for Na^+ uptake in high NaCl, there would be an attenuation of the increase in branchial Na^+/K^+-ATPase activity normally seen over development (Fu et al., 2010; Zimmer et al., 2014; Table 4.1B). However, this was not the case, and Na^+/K^+-ATPase activities were not responsive to high NaCl treatment (Table 4.1B). Overall, it appeared that the high NaCl group had the tendency, though not statistically significant ($p=0.075$), to increase branchial Na^+/K^+-ATPase activity, a phenomenon seen in adult trout acclimated to seawater (Richards et al., 2003) or fed a high NaCl diet (Perry et al., 2006).

In summary, our main finding is a lack of plasticity in the ontogeny of branchial ionoregulation in developing rainbow trout larvae, thereby ensuring that requirements for ammonia excretion are met. These results support those of Fu et al. (2010) showing a similar lack of plasticity in the ontogeny of Na^+ uptake. Our new "ammonia hypothesis" refines the "ionoregulatory hypothesis", suggesting that the need to excrete ammonia, likely via Na^+/NH_4^+ exchange, is the primary function of the developing gill and the main ontogenetic pressure for gill development.

4.5 TABLES AND FIGURES

Table 4.1. Larval weight, whole-body T_{amm}, ammonia turnover time, and Na^+/K^+-ATPase activities in the gill, yolk sac epithelium, and body epithelium of larvae raised under control and high NaCl conditions over 18 days post-hatch.

A	**Weight (g)**		**Whole-body T_{amm} (µmol/g)**		**Ammonia Turnover Time (h)**	
Time (dph)	**Control**	**High NaCl**	**Control**	**High NaCl**	**Control**	**High NaCl**
3	0.076 ± 0.002	0.074 ± 0.004	1.70 ± 0.18	1.98 ± 0.26	5.42 ± 0.44	4.63 ± 0.52
6	0.080 ± 0.003	0.080 ± 0.005	2.37 ± 0.44	2.74 ± 0.33	5.68 ± 0.48	4.81 ± 0.38
9	0.085 ± 0.003	0.089 ± 0.005	3.82 ± 0.36	4.30 ± 0.20	4.42 ± 0.20	5.71 ± 0.25
12	0.098 ± 0.003	0.097 ± 0.005	3.16 ± 0.63	3.28 ± 0.22	3.45 ± 0.57	5.72 ± 1.10*
18	0.098 ± 0.005	0.093 ± 0.004	1.99 ± 0.39	2.58 ± 0.56	3.44 ± 0.63	3.15 ± 0.22

B	**Na^+/K^+-ATPase Activity (µmol ADP/mg protein/h)**					
	Gill		**Yolk Sac Epithelium**		**Body Epithelium**	
Time (dph)	**Control**	**High NaCl**	**Control**	**High NaCl**	**Control**	**High NaCl**
6	1.15 ± 0.16	1.07 ± 0.21	0.89 ± 0.14	0.55 ± 0.12	1.38 ± 0.75	1.11 ± 0.24
12	1.70 ± 0.27	2.38 ± 0.32	0.96 ± 0.16	1.27 ± 0.16	1.00 ± 0.28	1.39 ± 0.35
18	2.02 ± 0.36	3.00 ± 0.61	1.64 ± 0.79	1.95 ± 0.67	1.04 ± 0.38	2.04 ± 0.84

Asterisks denote statistically significant differences ($P<0.05$) between control and high NaCl groups as determined by a two-way ANOVA using time and treatment as factors, followed by a Holm-Sidak post-hoc test. (n=4-8)

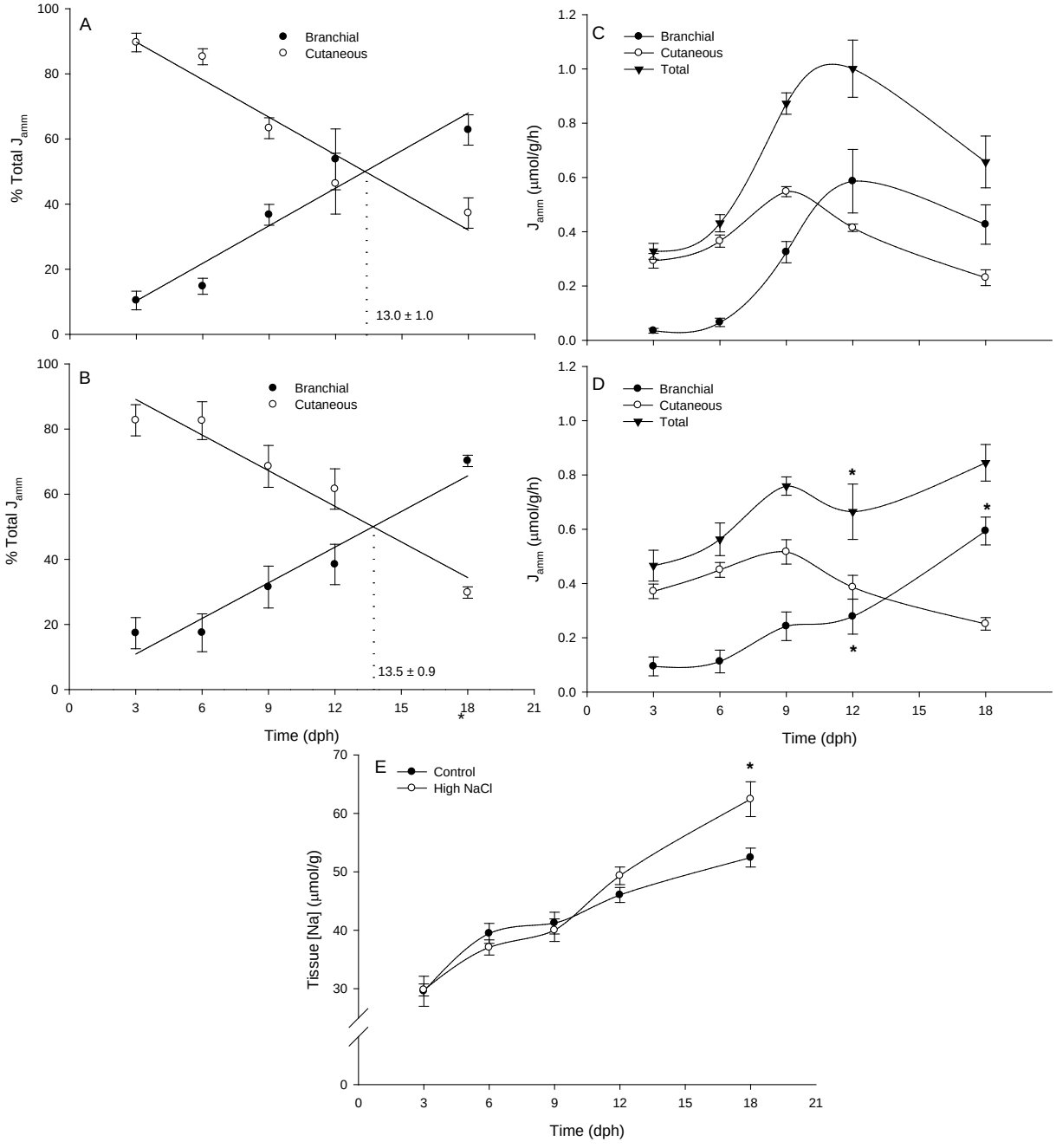
A
Branchial
Cutaneous
% Total J_{amm}
13.0 ± 1.0
B
Branchial
Cutaneous
% Total J_{amm}
13.5 ± 0.9
Time (dph)
C
Branchial
Cutaneous
Total
J_{amm} (µmol/g/h)
D
Branchial
Cutaneous
Total
J_{amm} (µmol/g/h)
Time (dph)
E
Control
High NaCl
Tissue [Na] (µmol/g)
Time (dph)

Fig. 4.1. The percentage of total cutaneous and branchial ammonia excretion (J_{amm}) in (A) control larvae and (B) high NaCl larvae over 18 days post-hatch (dph). Dashed lines in panels A and B represent the skin-to-gill shifting points for J_{amm}. Absolute branchial, cutaneous, and total J_{amm} (µmol/g/h) in (C) control and (D) high NaCl larvae over 18 dph. (E) Tissue [Na^+] in control (filled circles) and high NaCl (open circles) larvae over 18 dph. In panels C and D, asterisks represent statistically significant differences ($P<0.05$) in mean branchial, cutaneous, or total mean J_{amm} between control and high NaCl larvae at a given time point. In panel E, asterisks represent statistically significant differences between mean tissue [Na^+] in control and high NaCl larvae at given time points. All comparisons were made using a two-way ANOVA, with time and treatment as factors, followed by a Holm-Sidak post-hoc test. (n=6-8)

4.6 REFERENCES

Brauner, C.J. and Rombough, P.J. (2012) Ontogeny and paleophysiology of the gill: new insights from larval and air-breathing fish. *Respir. Physiol. Neurobiol.* **184**, 293–300.

Brauner, C.J. and Wood, C.M. (2002) Effect of long-term silver exposure on survival and ionoregulatory development in rainbow trout (*Oncorhynchus mykiss*) embryos and larvae, in the presence and absence of added dissolved organic matter. *Comp. Biochem. Physiol. C* **133**, 161-173.

Fu, C., Wilson, J.M., Rombough, P.J. and Brauner, C.J. (2010) Ions first: Na^+ uptake shifts from the skin to the gills before O_2 uptake in developing rainbow trout, *Oncorhynchus mykiss*. *Proc. R. Soc. B* **277**, 1553–60.

Krogh, A. (1941) *The comparative physiology of respiratory mechanisms*. Philadelphia, PA: University of Pennsylvania Press.

McCormick, S.D. (1993) Method for non-lethal gill biopsy and measurement of Na^+,K^+ ATPase activity. *Can. J. Fish. Aquat. Sci.* **50**, 656-658.

Perry, S.F., Rivero-Lopez, L., McNeil, B. and Wilson, J.M. (2006) Fooling a freshwater fish: how dietary salt transforms the rainbow trout gill into a seawater gill phenotype. *J. Exp. Biol.* **209**, 4591-4596.

Richards, J.G., Semple, J.W., Bystriansky, J.S. and Schulte, P.M. (2003) Na^+/K^+-ATPase α-isoform switching in gills of rainbow trout (*Oncorhynchus mykiss*) during salinity transfer. *J. Exp. Biol.* **206**, 4475-4486.

Wright, P.A., Felskie, A. and Anderson, P. (1995) Induction of ornithine-urea cycle enzymes and nitrogen metabolism and excretion in rainbow trout (*Oncorhynchus mykiss*) during early life stages. *J. Exp. Biol.* **198**, 127–35.

Wright, P.A. and Wood, C.M. (2009) A new paradigm for ammonia excretion in aquatic animals: role of Rhesus (Rh) glycoproteins. *J. Exp. Biol.* **212**, 2303–12.

Zimmer, A.M., Wright. P.A. and Wood, C.M. (2014b) What is the primary function of the early teleost gill? Evidence for Na^+-coupled ammonia excretion in developing rainbow trout (*Oncorhynchus mykiss*). *Proc. R. Soc. B* **281**: 1795.

CHAPTER 5

EXPOSURE TO WATERBORNE Cu INHIBITS CUTANEOUS Na^+ UPTAKE IN POST-HATCH LARVAL RAINBOW TROUT (*ONCHORHYNCHUS MYKISS*)

5.1 ABSTRACT

In freshwater rainbow trout (*Oncorhynchus mykiss*), two common responses to acute waterborne copper (Cu) exposure are reductions in ammonia excretion and Na^+ uptake at the gills, with the latter representing the likely lethal mechanism of action for Cu in adult fish. Larval fish, however, lack a functional gill following hatch and rely predominantly on cutaneous exchange, yet represent the most Cu-sensitive life stage. It is not known if Cu toxicity in larval fish occurs via the skin or gills. The present study utilized divided chambers to assess cutaneous and branchial Cu toxicity over larval development, using disruptions in ammonia excretion (J_{amm}) and Na^+ uptake (J^{Na}_{in}) as toxicological endpoints. Early in development (early; 3 days post-hatch; dph), approximately 95% of J_{amm} and 78% of J^{Na}_{in} occurred cutaneously, while in the late developmental stage (late; 25 dph), the gills were the dominant site of exchange (83 and 87% of J_{amm} and J^{Na}_{in}, respectively). Exposure to 50 µg/l Cu led to a 49% inhibition of J_{amm} in the late developmental stage only, while in the early and middle developmental (mid; 17 dph) stages, Cu had no effect on J_{amm}. J^{Na}_{in}, however, was significantly inhibited by Cu exposure at the early (53% reduction) and late (47% reduction) stages. Inhibition at the early stage of development was mediated by a reduction in cutaneous uptake, representing the first evidence of cutaneous metal toxicity in an intact aquatic organism. The inhibitions of both J_{amm} and J^{Na}_{in} in the late developmental stage occurred via a reduction in branchial exchange only. The differential responses of the skin and gills to Cu exposure suggest that the mechanisms of J_{amm} and J^{Na}_{in} and/or Cu toxicity differ between these tissues. Exposure to 20 µg/l Cu revealed that J_{amm} is the more Cu-sensitive

process. The results presented here have important implications in predicting metal toxicity in larval fish. The Biotic Ligand Model (BLM) is currently used to predict metal toxicity in aquatic organisms. However, for rainbow trout this is based on gill binding constants from juvenile fish. This may not be appropriate for post-hatch larval fish where the skin is the site of toxic action of Cu. Determining Cu binding constants and lethal accumulation concentrations for both skin and gills in larval fish may aid in developing a larval fish-specific BLM. Overall, the changing site of toxic action and physiology of developing larval fish present an interesting and exciting avenue for future research.

5.2 INTRODUCTION

Copper (Cu) is both an essential element and a persistent contaminant in aquatic systems that has toxic effects at elevated levels. Like most metals, Cu elicits toxicity by first binding to a ligand on the surface of aquatic organisms, usually considered to be located on the gills in fish, and acting either directly on the ligand or entering the organism and acting on downstream target organs (reviewed by Grosell, 2012). Cu exposure leads to a wide array of toxic effects including alterations in behaviour, olfaction, ionoregulation, nitrogenous waste excretion, and swimming performance (see Grosell, 2012). However, the key lethal mechanism of action of Cu exposure in freshwater fish is believed to be the reduction of whole-body Na^+ levels, caused by an inhibition of branchial Na^+ uptake (Lauren and McDonald, 1985; 1987a; b; Grosell and Wood, 2002). This understanding has led to the development of a Biotic Ligand Model (BLM) for the prediction of waterborne Cu toxicity (MacRae et al., 1999; Di Toro et al., 2001; Santore et al., 2001; Paquin et al., 2002; Niyogi and Wood, 2004).

Since Cu is potentially bioavailable in the environment to all aquatic organisms, a number of studies have focused on determining the most Cu-sensitive species and life stages (see Grosell, 2012). In general, it appears that aquatic invertebrates represent the most sensitive group of species (e.g., Santore et al., 2001), likely due to the small size of these animals. Indeed, animals with smaller sizes tend to have higher Na^+ turnover rates and, therefore, overall greater sensitivity to Cu (Grosell et al., 2002). In agreement, early life stages of fish, being smaller in size, appear to be overall more sensitive to Cu than fish in later life stages (McKim et al., 1978; Rombough and Garside, 1982).

In larval fish, it is unclear if Cu elicits its toxic effects exclusively at the gills or if the skin is also sensitive to exposure to Cu. Immediately following hatch, the branchial structures are undeveloped, having no lamellae and only small filament buds, leading to an overall small gill surface area (Gonzalez et al., 1996; Rombough, 1999). As such, normal branchial functions, such as ionoregulation, gas transfer, and nitrogenous waste excretion (see Evans et al., 2005) are minimal. Instead, larval fish utilize cutaneous surfaces for the bulk of physiological exchanges with the environment. Indeed, in rainbow trout (*Oncorhynchus mykiss*) the skin is known to be the primary site for oxygen uptake, Na^+ uptake, and ammonia excretion immediately following hatch (Wells and Pinder, 1996; Fu et al., 2010; Zimmer et al., 2014b). As fish develop, the gills become functional and eventually become responsible for the majority of exchanges (Fu et al., 2010; Zimmer et al., 2014b). Given that the primary site for Cu binding is generally considered to be the gill in fish (e.g., MacRae et al., 1999), Cu toxicity might be predicted to be a function of gill surface area. However, in larval topsmelt (*Atherinops affinis*), McNulty et al. (1994) could not attribute Cu sensitivity specifically to changes in gill surface area as both gill and skin surface areas increased over development, similar to previous observations in rainbow trout (Rombough, 1999). Conversely, the increase in sensitivity which occurs over larval development in fish (e.g., Chapman, 1978; McNulty et al., 1994) may be a function of mitochondrial rich cell (MRC) numbers which increase rapidly in the gills following hatch and are also present on skin surfaces of post-hatch fish (Rombough, 1999).

The goal of the present study was to determine the site-dependent responses (gills versus skin) to waterborne Cu exposure in larval rainbow trout over development, using the inhibitions of ammonia excretion (J_{amm}) and Na^+ uptake (J^{Na}_{in}) as toxicological endpoints. These endpoints were chosen because disruptions in both Na^+ and ammonia balance are two of the most commonly observed effects of Cu exposure in freshwater fish (see Grosell, 2012 for review), the two processes are thought to be mechanistically linked, at least in adult trout (Tsui et al., 2009; Wright and Wood, 2009), and both J_{amm} (Zimmer et al., 2014b) and J^{Na}_{in} (Fu et al. 2010, Zimmer et al., 2014b) are known to progress from the skin to the gills during larval development over a similar time frame.

Larval trout were exposed to two sublethal concentrations of waterborne Cu at three stages of development following hatch but prior to complete yolk sac absorption to determine the effects of Cu on whole-body J_{amm} and J^{Na}_{in}. Additional experiments were conducted to determine gill and skin-specific responses to Cu exposure using divided chambers identical to those used in previous studies (Fu et al., 2010; Zimmer et al., 2014b), which allowed for the estimation of cutaneous and branchial fluxes. We hypothesized that if Cu exposure inhibited either J_{amm} or J^{Na}_{in} immediately following hatch, that this would occur via blockade of cutaneous exchanges as the skin accounts for the majority of both processes at this stage (Fu et al., 2010; Zimmer et al., 2014b). Alternatively, Cu may elicit its effects solely via the gills, inhibiting the small proportion of exchange occurring branchially at this stage. If the skin proves to be responsive to waterborne Cu exposure, this may have important implications for the development of a

BLM for the prediction of Cu toxicity (Di Toro et al., 2001) which is specific for larval fish.

5.3 MATERIALS AND METHODS

5.3.1 Fish

Rainbow trout (*Oncorhynchus mykiss*) were obtained by donation from the Vancouver Island Trout Hatchery in Duncan, BC, Canada. Trout were received at three developmental stages, eyed embryos (230 accumulated thermal units (ATUs)), post-hatch larvae (420 ATUs), and larvae near-yolk sac absorption (349 ATUs). All fish were held in soft, dechlorinated Vancouver Metro tap water (in mM: Na^+,0.06; Cl^-, 0.05; Ca^{2+}, 0.03; Mg^{2+}, 0.007; K^+, 0.004; dissolved organic carbon (DOC), 2-3 mg C/l; alkalinity, 3.0 mg/l $CaCO_3$; hardness, 3.3 mg/l $CaCO_3$; pH 7.0) at 10ºC at the University of British Columbia in Vancouver, BC. Approximately 200 trout embryos or larvae of each developmental stage were maintained in 3 separate 3-l containers with aerated, dechlorinated Vancouver tap water exchanged daily. Fish were never fed exogenously and were held in these conditions for at least 5 d prior to experimentation. Experiments were performed on fish at the following developmental stages, referred to subsequently as: early: 3 days post-hatch (dph) (330 ATUs); mid: 17 dph (470 ATUs); and late: 25 dph (550 ATUs).

5.3.2 Experimental design

Series 1: An initial series of experiments was conducted to determine the effects of sublethal Cu exposure (50 µg/l Cu as $CuSO_4$, nominal concentration) on whole-body

ammonia excretion (J_{amm}) and Na^+ uptake (J^{Na}_{in}) at the different stages of larval development. Fish in the early, mid, and late developmental stages were placed individually in small (25 ml) plastic beakers containing 5 ml (early and mid) or 10 ml (late) water containing nominal 0 (control) or 50 µg/l Cu. Fish were pre-exposed to these conditions for a 3-h period to allow for the full inhibitory effects of Cu prior to flux measurements; water was aerated for the duration of this period. Following the pre-exposure period, ^{22}Na (Amersham Pharmacia Biotech Inc.) was added to the water to a concentration of 0.05 µCi/ml and allowed to mix via aeration for 5 min, after which an initial 1-ml sample was taken for the determination of ^{22}Na radioactivity, [Na], and total ammonia levels (T_{amm}) (see below). Following a 1.5-h flux period, a final 1-ml sample was then taken and fish were euthanized with a lethal dose of neutralized MS-222, rinsed 3 times with 5 mM NaCl to removed surface-bound isotope, weighed, and counted for ^{22}Na radioactivity. A 0.25-ml aliquot of each water sample was used for counting ^{22}Na radioactivity and measuring [Na], while the remaining sample was frozen at -20ºC until later T_{amm} analyses. All subsequent experiments followed the same 3-h pre-exposure, 1.5-h flux exposure protocol.

Series 2: A separate set of control experiments was performed to assess the effects of clove oil anaesthesia which was used in Series 3 (see below) to calm larvae in divided chambers. These experiments were performed in the exact same manner as those described for the divided chamber protocol in Series 3 except fish were left in the pre-exposure containers for the 1.5-h flux, not loaded into divided chambers. In these experiments only nominal 0 and 50 µg/l Cu concentrations were tested; all other

experimental protocols followed those described below for the divided chamber experiments in Series 3.

Series 3: A third set of experiments was conducted to assess the effects of exposure to 20 and 50 µg/l Cu on branchial and cutaneous J_{amm} and J^{Na}_{in}. The experimental series utilized a divided chamber system similar to those employed previously (Fu et al., 2010; Zimmer et al., 2014b). These chambers require fish to be lightly anaesthetized in order to prevent struggling and experimental stress. As such, fish from the early, mid, and late developmental stages were initially anaesthetized using a 50-100 mg/l clove oil solution to reach stage 3 anaesthesia (McFarland, 1959). Following this, fish were placed in small plastic beakers (25 ml) containing 5 ml (early and mid) or 10 ml (late) of aerated dechlorinated tap water containing 10 mg/l clove oil to maintain anaesthesia, and nominal 0 (control), 20, or 50 µg/l Cu. Fish were exposed to these media for 3 h and were then loaded into divided chambers, comprising two half-chambers separated by a latex dam. The fish was pushed through a small hole in the dam such that its head, opercula, and pectoral fins were separated spatially from the rest of its body. The latex dam and fish were then loaded between the two 5-ml half-chambers which were secured together using elastic bands. During this process, fish were kept submerged at all times in "loading containers" (plastic wash basins) containing 5-l of water dosed with 10 mg/l clove oil and the same nominal Cu concentrations used in the corresponding pre-exposure. Both half-chambers were filled completely with the corresponding exposure medium and fitted with aeration lines. The fish were allowed to adjust to this setup for 15 min prior to experimentation.

Following this settling period, ^{22}Na was added to either the anterior (for determining anterior J^{Na}_{in}) or posterior (for determining posterior J^{Na}_{in}) half-chamber to a final concentration of 0.05 µCi/ml and, after 5 min of mixing by aeration, initial 1-ml samples were taken from both half-chambers. Note that it was necessary to add the isotope to only one half-chamber per flux (i.e., anterior or posterior, not both) as uptake was calculated as ^{22}Na appearance in the fish, and sampling of the non-labelled chamber was performed to detect leaks (see below). Following a 1.5-h flux period, final anterior and posterior samples were taken and fish were removed from the chambers and allowed to recover in dechlorinated tap water for a maximum of 5 min. This was done in order to verify that fish were able to fully recover from anaesthesia and divided chamber treatments within 5 min, which was a requisite for an acceptable flux. Fish were then euthanized with a lethal dose of neutralized MS-222, rinsed 3 times with 5 mM NaCl to remove surface-bound isotope, weighed, and counted for ^{22}Na radioactivity. Another requisite for acceptable flux was a < 10% isotope leak from the loaded chamber to the unloaded chamber. In cases where fish did not recover from experimentation within 5 min, or there was more than 10% isotope leakage, data were rejected. The success rate of these divided chamber experiments was, on average, 85% across all developmental stages and treatments. Water samples from these experiments were handled in the same manner as the experiments conducted in Series 1.

In all experiments, final water samples were taken for the measurement of dissolved Cu concentrations. 1-ml samples were extracted from the final water volume (in Series 3, samples were taken from the non-isotope loaded side) and were filtered through

0.45 µm membrane filters (Acrodisc syringe filters, Pall Corporation, USA). These samples were then acidified to 1% HNO_3 and stored at 4ºC until further analysis. Water samples for the measurement of dissolved organic carbon concentrations (30 ml; filtered using 0.45 µm membrane) were taken from the water source used throughout the experiments periodically over the entire study period. These samples were stored at 4ºC for a maximum of 2 months prior to analysis.

5.3.3 Analytical techniques and calculations

Water samples were analyzed for water total ammonia concentration (T_{amm}) using the methods described by Verdouw et al. (1978). J_{amm} (µmol/g/h) was calculated using the following equation:

$$J_{amm} = (T_{amm}f - T_{amm}i)*V/(M*t), \quad (1)$$

where $T_{amm}f$ and $T_{amm}i$ (µmol/l) are final and initial water total ammonia concentrations, V is volume (l), M is mass (g), and t is flux time (h).

Water and fish ^{22}Na gamma radioactivity (counts per minute; cpm) was measured using a gamma counter (PerkinElmer, Turku, Finland), while total $[Na^+]$ of initial and final water samples was determined via flame atomic absorption spectrometry (Varian Australia Pty Ltd, Australia). J^{Na}_{in} (µmol/g/h) was calculated using the following equation:

$$J^{Na}_{in} = R_{fish}/(SA_{average}*M*t), \quad (2)$$

where R_{fish} is the gamma radioactivity of the fish (cpm) and $SA_{average}$ is the average of the initial and final specific activities (cpm/µmol Na) of the exposure medium. Dissolved Cu concentrations were measured using graphite furnace atomic absorption spectrometry (SpectroAA220, Varian, Mulgrave, Australia). During determinations a National Research Council of Canada reference standard (TM-15.2; Ottawa, ON, Canada) was used to determine the percentage recovery of Cu, which was 92 ± 2% (n=9) over all determinations. DOC concentration was measured using a Shimadzu TOC-$V_{CPH/CPN}$ total organic carbon analyzer (Shimadzu Corporation, Kyoto, Japan). Measurements were made against a prepared standard solution of potassium phthalate.

5.3.4 Statistical analyses

All data are reported as mean values ± 1 standard error of mean (SEM). Comparisons between control (nominal 0 µg/l Cu exposure) means over development were made using a one-way ANOVA with a Student-Newman-Keuls post-hoc test. Significant differences between means of animals exposed to 0 µg/l Cu *versus* means of Cu-exposed animals under the same conditions were determined using Student's unpaired t-tests. Comparisons among dissolved Cu concentrations were made using a one-way ANOVA with a Holm-Sidak post-hoc test. Significance in all cases was accepted at the $P < 0.05$ level.

5.4 RESULTS

5.4.1 Cu exposure concentrations

Measured dissolved Cu concentrations in Series 1, Series 2, and in the 3-h pre-exposures from Series 3 did not differ significantly from one another and were averaged together (Table 5.1A). Dissolved Cu concentrations in these experiments were all significantly different from one another and were close to nominal values (Table 5.1A). In the divided chamber exposures from Series 3, Cu concentrations were generally lower (~70% of nominal values) than in the exposures described above, however a significant difference between each nominal exposure concentration was still observed (Table 5.1B).

5.4.2 Developmental patterns of J^{Na}_{in} and J_{amm} and effects of divided chambers and clove oil

In Series 1, J_{amm} increased progressively from early to late developmental stages (Fig. 5.1A), whereas J^{Na}_{in} approximately tripled in the mid and late developmental stages (not significantly different from one another) relative to the early stage (Fig. 5.1B). Overall, fish in divided chambers (Series 3) exhibited significantly lower total rates of both J_{amm} and J^{Na}_{in} at all developmental stages compared to those of Series 1 where the larvae were not anaesthetized or restrained (Table 5.2). When averaged over all stages, the divided chamber system reduced J_{amm} by 53% and J^{Na}_{in} by 40%. In most cases, J_{amm} and J^{Na}_{in} were not significantly different between Series 2 (clove oil alone) and Series 3 (Table 5.2), indicating that the depressions of J_{amm} and J^{Na}_{in} in Series 3 were mainly due to anaesthesia rather than to restraint.

In Series 3, fish in the early developmental stage demonstrated posterior J_{amm} and J^{Na}_{in} which were significantly greater than respective anterior values, accounting for 95

and 78% of total exchange, respectively (Fig. 5.2). In contrast, in the late developmental stage, anterior exchange dominated, accounting for 83% and 87% of total J_{amm} and J^{Na}_{in}, respectively (Fig. 5.2). In the mid developmental stage, no significant differences existed between anterior and posterior J_{amm} or J^{Na}_{in} (Fig. 5.2).

5.4.3 Effects of Cu exposure

Exposure to nominal 50 µg/l Cu in Series 1 led to a 24% inhibition of J_{amm} in the late developmental stage only, while J_{amm} in early and mid-developmental stages was not affected by Cu exposure (Fig. 5.1A). J^{Na}_{in}, however, was significantly inhibited by this level of Cu exposure at both the early (38% inhibition) and late (50% inhibition) developmental stages, while a non-significant inhibition was observed at the mid-developmental stage (P=0.096; Fig. 5.1B). Though absolute values varied, these same stage-specific responses were also observed in both Series 2 and Series 3 (Table 5.2).

In Series 3, nominal 50 µg/l Cu led to a 53% inhibition of total J^{Na}_{in} in the early developmental stage, while in the late stage, Cu reduced both total J_{amm} and J^{Na}_{in} by 49% and 47%, respectively (Figs. 5.3C and 5.4C; Table 5.2). The mid developmental stage, again, was not affected by Cu exposure. An additional exposure in Series 3 using nominal 20 µg/l Cu revealed that only total J_{amm} in the late stage was significantly inhibited by this concentration of Cu (Fig. 5.3C). The specific site of the inhibitory action of Cu was always that which dominated exchange (i.e., posterior in early stage; anterior in late stage). When considering J_{amm}, the inhibitory effects of Cu seen at the late stage of development occurred via an inhibition of anterior J_{amm}, while posterior J_{amm} was never

affected by Cu exposure (Figs. 5.3A and 5.3B). Inhibition of J^{Na}_{in} in the late stage also occurred via an inhibition of anterior uptake; however, inhibition in the early stage was driven by a reduction in posterior uptake (Figs. 5.4A and 5.4B).

5.5 DISCUSSION

5.5.1 Overview

The present study demonstrates that larval rainbow, similar to juvenile and adult trout, respond to waterborne Cu exposure with a reduction in both J_{amm} and J^{Na}_{in} (Fig. 5.1). In juvenile and adult trout, this toxicity is believed to be mediated via an inhibition of transport processes at the gill. The same was true of larval trout in the late developmental stage (25 dph) where Cu led to the inhibition of both J_{amm} and J^{Na}_{in} across the gills (Figs. 5.3 and 5.4). While J_{amm} was only affected in the late stage, J^{Na}_{in} was also inhibited by Cu at the early developmental stage (3 dph; Fig. 5.1). This inhibition occurred via a reduction in cutaneous J^{Na}_{in} (Fig. 5.4), demonstrating, to our knowledge, the first evidence of cutaneous metal toxicity in an intact aquatic organism. Interestingly, our results suggest that the mechanisms of J_{amm} and J^{Na}_{in} and/or of Cu toxicity differ between the gill and skin of larval trout. These results have important implications in our current understanding and prediction of metal toxicity in developing larval fish.

5.5.2 Validation of divided chamber tests

The Cu concentrations used in the present study (Table 5.1) were chosen based on preliminary results (data not shown) and a 96-h LC50 of 125 µg/l for rainbow trout in

dechlorinated Vancouver tap water predicted by the Biotic Ligand Model (BLM version 2.2.3, Hydroqual, 2007). This relatively high prediction, given the extremely soft water of Vancouver (~3 mg/l $CaCO_3$), was likely due to the substantial DOC present in the water (2.5 mg/l C). All concentrations reported are dissolved Cu concentrations (Table 5.1) and, for Series 1, Series 2, and the 3-h pre-exposure from Series 3, values were very close to nominal concentrations (Table 5.1A). The measured concentrations in the divided chamber experiments from Series 3, however, were slightly lower than nominal concentrations (Table 5.1B), potentially due to the adsorption to the walls of the 5-l "loading containers" or to the latex dam. Regardless, the same pattern of inhibitory effects of Cu was seen across all exposure conditions (Table 5.2). Overall, clove oil (Series 2) tended to reduce J_{amm} and J^{Na}_{in}, similar to previous reports (Fu et al., 2010; Smith et al., 2012) and the resulting rates, for the most part, were not significantly different than the values measured in divided chambers (Series 3), suggesting that the anaesthetic was the cause of the reductions, but nevertheless was effective in reducing experimental stress. These results suggest that the use of divided chamber experiments in Cu toxicity testing is valid and, moreover, appears to be a useful tool in understanding the mechanisms of Cu toxicity in specific regions (i.e., skin versus gill) in larval fish.

As there is a significant amount of head skin in the anterior half-chamber (see Fu et al, 2010; Zimmer et al., 2014b), potentially some of the fluxes measured in the anterior chamber are cutaneous, whereas in the posterior half-chamber some of the fluxes could be renal. Nevertheless, it seems very likely that the majority of the fluxes in the two sections are predominantly branchial and cutaneous, respectively. In the subsequent discussion,

flux via the anterior half-chamber is considered to be branchial, while flux via the posterior chamber is considered to be cutaneous.

5.5.3 Cu inhibits branchial J_{amm} and J^{Na}_{in}

The disruption of both ammonia and Na^+ balance are two of the most common responses to acute Cu exposure in juvenile and adult freshwater fish (see Grosell, 2012 for review). This also appears to be the case in larval trout, where exposure to 50 µg/l Cu significantly impaired both J_{amm} and J^{Na}_{in}, regardless of experimental condition (e.g., Series 1,2, or 3; Table 5.2). As is believed to be the case in juvenile and adult fish, this response to Cu in the late developmental stage appeared to be mediated entirely by an inhibition of branchial exchange (Figs. 5.3A and 5.4A). The inhibition of ammonia excretion by Cu in fish is observed as either a decrease in J_{amm} (Lauren and McDonald, 1985; Blanchard and Grosell, 2006; Zimmer et al., 2012) or an increase in plasma ammonia levels (Lauren and McDonald, 1985; Wilson and Taylor, 1993a; b; Wang et al., 1998; Grosell et al., 2003; 2004). The mechanism of this inhibition, however, is not clear, but may be associated with inhibition of carbonic anhydrase activity (Vitale et al., 1999; Grosell et al., 2002; Zimmer et al., 2012) , although there is no consensus in the literature (e.g., Blanchard and Grosell, 2006). The mechanism of inhibition of branchial J^{Na}_{in}, however, is usually attributed to competitive blockade of apical Na^+ uptake by Cu via an as yet uncharacterized epithelial Na^+ channel (Grosell and Wood, 2002) and/or by Cu inhibition of basolateral Na^+/K^+-ATPase activity (Lauren and McDonald, 1987b; Pelgrom et al., 1995; Sola et al., 1995). Since there appears to be a functional linkage between J^{Na}_{in} and J_{amm} at the gills of adult trout which is mediated via Rh proteins (“sodium-ammonium

exchange complex or metabolon"; Tsui et al., 2009; Wright and Wood, 2009) and this is also seen in the gills of developing trout larvae (Zimmer et al., 2014b), it is possible that inhibition of these processes by Cu may share a common mechanism which has yet to be elucidated. Two possibilities are i) the inhibition of carbonic anhydrase activity (Zimmer et al., 2012; Grosell, 2012) or ii) inhibition of ammonia-transporting Rhesus (Rh) proteins in the gill given their integral role in both ammonia and Na^+ transport (Wright and Wood, 2009; Kumai and Perry, 2011; Shih et al., 2012; 2013).

5.5.4 Cu inhibits cutaneous J^{Na}_{in} but not cutaneous J_{amm}

In the early stage of development, rainbow trout larvae utilized their skin for the majority of both J_{amm} and J^{Na}_{in} (Fig. 5.2). This has been observed previously (Zimmer et al., 2014b), and it is generally believed that the skin performs the majority of all physiological exchanges immediately following hatch (Wells and Pinder, 1996; Rombough, 2002; Fu et al., 2010; see Brauner and Rombough, 2012 for review). This reliance on cutaneous exchange is due to limited gill surface area and high skin mitochondrial rich cell (MRC) abundance in early stages of larval development (Gonzalez et al., 1996; Rombough, 1999). Thus, the response of the skin to contaminant exposure is crucial to fully understand overall toxic responses at this stage. Moreover, it is known that larvae represent the most Cu-sensitive life stage in most fish (McKim et al., 1978; Rombough and Garside, 1982), likely due to the high Na^+ turnover rates of these animals associated with their small size (Grosell et al., 2002). Indeed, larval trout exposed to Cu experienced an inhibition of J^{Na}_{in} at all 3 developmental stages (though non-significantly in the mid-developmental stage; Fig. 5.1), which occurred via an inhibition

of cutaneous uptake in the early stage, and branchial uptake in the late stage (Fig. 5.4). To our knowledge, this represents the first *in vivo* evidence of the inhibition of cutaneous exchange processes by Cu in fish. Though the skin plays little to no role in Na^+ acquisition by the end of yolk sac absorption (Fig. 5.2B; Zimmer et al., 2014b), these results may have important implications for earlier life stages which, in general, utilize cutaneous surfaces for Na^+ uptake (e.g., Fu et al., 2010; Wu et al., 2010; Shih et al., 2012).

Furthermore, a significant proportion of Ca^{2+} uptake, which is inhibited by exposure to other divalent metals (e.g., Pb; Rogers et al., 2003), is believed to occur across the general body surface of adult rainbow trout (Perry and Wood, 1985), potentially implicating another role for cutaneous metal toxicity. Cutaneous metal toxicity may also be important in specialized epithelia such as the cleithrum skin (e.g., Marshall et al., 1992) and opercular epithelium (see Marshall, 2003) which contribute significantly to whole-body ionoregulation in some fish species. Indeed, Crespo and Karnaky (1983) demonstrated *in vitro* inhibition of Cl^- transport across the isolated opercular epithelium of killifish (*Fundulus heteroclitus*) by Cu, though this inhibition occurred only when Cu was applied to the serosal (blood-facing) side while Cu application to the apical (water-facing) side was without effect. Moreover, the skin of frogs, used extensively to model epithelial Na^+ transport in *in vitro* studies pioneered by Hans Ussing (Ussing and Zerahn, 1950), is also responsive to Cu exposure *in vitro*. Exposure to monovalent Cu^+ has been shown to inhibit Na^+ uptake across isolated frog skin in some studies (Skulskii and Lapin, 1992) and stimulate Na^+ uptake in others (Zadunaisky et al., 1963; Flonta et al., 1998);

see Handy et al. (2002) for review. While it is clear that Cu can alter cutaneous Na^+ transport in post-hatch larval fish (designated here as "early"; Fig. 5.4B), it is unclear why this response is absent in later stages of development (mid and late stages). It may be a result of a reduction in yolk sac skin surface area, which seems to be the major site of cutaneous exchange (e.g., Shih et al., 2008) and MRC expression in larval fish (Rombough, 1999), however, further studies are required to address this.

Interestingly, Cu did not inhibit cutaneous J_{amm} at any developmental stage, despite reducing cutaneous J^{Na}_{in} in early stages (Fig, 4B) and branchial J_{amm} in the late stages of development (Fig. 5.3). Furthermore, Zimmer et al. (2014b) did not find a relationship between J^{Na}_{in} and J_{amm} at the skin in larval trout, while a clear relationship between the two was observed at the gills. Taken together, these data indicate that the mechanism for J_{amm} and J^{Na}_{in} and/or the mode of toxic action of Cu is different between the skin and gills. More work is now needed to elucidate the cutaneous and branchial mechanisms of ammonia and Na^+ exchange in larval fish and the pathways by which Cu inhibits this exchange.

5.5.5 Perspectives and future directions

The depletion of whole-body Na^+ stores by inhibition of Na^+ acquisition is believed to be the lethal mechanism of action of Cu exposure in juvenile and adult freshwater fish (Grosell et al., 2002; Grosell, 2012). Understanding the mechanisms of Cu toxicity and lethality in larval fish is of particular importance due to the high sensitivity to Cu at this life stage (McKim et al., 1978). In general, Cu sensitivity increases following

hatch (e.g., Stouthart et al., 1996), likely due to the shedding of the chorion, the outer egg capsule of embryonic fish, which is capable of binding metals (Guadagnalo et al., 2001; Brix et al., 2004), and continues to increase over larval development (e.g., Chapman, 1978; McNulty et al., 1994). Interestingly, the most sensitive endpoint statistically in the present study was the inhibition of total J_{amm} in the late developmental stage as it was responsive to 20 µg/l Cu, whereas this lower Cu concentration never significantly inhibited J^{Na}_{in} (Fig. 5.4). This may indicate that the lethal mechanism of action for Cu in larval fish is also different. Indeed, the large changes in nitrogen handling and metabolism which occur over this development stage (Wright et al., 1995; Essex-Fraser et al., 2005; Zimmer et al., 2014b) may lead to greater susceptibility to detrimental disruptions in ammonia balance. Overall, the drastic physiological changes which occur over larval development, and the physiological differences between these fish and mature fish, warrant further investigation in understanding the nature of Cu toxicity in larval fish.

The BLM is used for a variety of scientific and regulatory purposes (Di Toro et al., 2001; Santore et al., 2001; Niyogi and Wood, 2004; Paquin et al., 2002; Hydroqual, 2007; USEPA, 2007; Ng et al., 2010). The current Cu BLM model for rainbow trout (version 2.2.3, Hydroqual, 2007) uses only gill lethal accumulation thresholds (LA50s) obtained from trout in later stages (MacRae et al., 1999) to predict toxicity. This may not be appropriate in immediately post-hatch larval fish lacking a functioning gill, where biotic ligands on the skin appear to be key targets of Cu toxicity. The skin is the major site of whole-body Na^+ uptake, and cutaneous J^{Na}_{in} was significantly inhibited by Cu (Fig. 5.4B). Future work should focus on characterising and quantifying skin and gill Cu

binding over larval development to determine how these relate to toxicity. A critical step in this regard will be to measure skin and gill Cu burdens associated with acute lethality (LA50 values; Hydroqual, 2007). Overall, larval fish pose a new and exciting area of research in metal toxicity. Determining the possible toxicological implications of the changes in physiology and biotic ligand sites (i.e., skin to gills) which occur over larval development may lead to a more comprehensive understanding of metal toxicity in fish.

5.6 TABLES AND FIGURES

Table 5.1. Measured dissolved Cu concentrations in Series 1, Series 2, and 3-h pre-exposures from Series 3 (A) and in divided chamber exposures from Series 3 (B). (n=15-40)

A.

Nominal Concentration (µg/l)	Measured Dissolved Concentration (µg/l)
0	$3.43 \pm 0.47_a$
20	$19.88 \pm 0.91_b$
50	$46.95 \pm 1.00_c$

B.

Nominal Concentration (µg/l)	Measured Dissolved Concentration (µg/l)
0	$2.94 \pm 0.44_a$
20	$14.33 \pm 0.91_b$
50	$34.70 \pm 1.57_c$

Means not sharing the same letters indicate statistically significant differences among Cu exposure concentrations by a one-way ANOVA with a Holm-Sidak post-hoc test.

Table 5.2. Ammonia excretion rates (A; J_{amm}; µmol/g/h; n=6-14) and sodium uptake rates (B; J^{Na}_{in}; µmol/g/h; n=4-12) in developing rainbow trout larvae exposed to nominal 0 or 50 µg/l Cu in Series 1 (unrestrained and non-anaesthetized), Series 2 (clove oil alone), and Series 3 (total divided chamber plus clove oil).

A.

Developmental Stage	Exposure (µg/l Cu)	Series 1	Series 2	Series 3
Early	0	$0.47 \pm 0.04_{a}$	$0.29 \pm 0.05_{b}$	$0.15 \pm 0.03_{c}$
	50	$0.38 \pm 0.04_{x}$	$0.27 \pm 0.03_{xy}$	$0.15 \pm 0.03_{y}$
Mid	0	$0.60 \pm 0.10_{a}$	$0.56 \pm 0.09_{a}$	$0.31 \pm 0.04_{b}$
	50	$0.58 \pm 0.09_{x}$	$0.54 \pm 0.10_{x}$	$0.21 \pm 0.04_{y}$
Late	0	$0.81 \pm 0.07_{a}$	$0.63 \pm 0.05_{ab}$	$0.47 \pm 0.05_{b}$
	50	$0.58 \pm 0.06^{*}_{x}$	$0.46 \pm 0.03^{*}_{x}$	$0.24 \pm 0.04^{*}_{y}$

B.

Developmental Stage	Exposure (µg/l Cu)	Series 1	Series 2	Series 3
Early	0	$0.21 \pm 0.03_{a}$	$0.12 \pm 0.02_{b}$	$0.17 \pm 0.01_{ab}$
	50	$0.13 \pm 0.03^{*}_{x}$	$0.07 \pm 0.01^{*}_{x}$	$0.08 \pm 0.01^{*}_{x}$
Mid	0	$0.64 \pm 0.10_{a}$	$0.31 \pm 0.05_{b}$	$0.29 \pm 0.07_{b}$
	50	$0.39 \pm 0.10_{x}$	$0.33 \pm 0.08_{x}$	$0.16 \pm 0.04_{x}$
Late	0	$0.71 \pm 0.09_{a}$	$0.53 \pm 0.09_{ab}$	$0.38 \pm 0.06_{b}$
	50	$0.36 \pm 0.05^{*}_{x}$	$0.27 \pm 0.04^{*}_{x}$	$0.20 \pm 0.04^{*}_{x}$

Means not sharing the same letters represent flux rates that are significantly different during exposure to nominal 0 (a,b,c) or 50 (x,y,z) µg/l Cu in Series 1, 2, and 3 within a given developmental stage of larval trout. Differences were determined using a one-way ANOVA with a Student-Newman-Keuls post-hoc test. Asterisks represent means at 50 µg/l Cu that differ significantly from their respective 0 µg/l Cu means by Student's t-test.

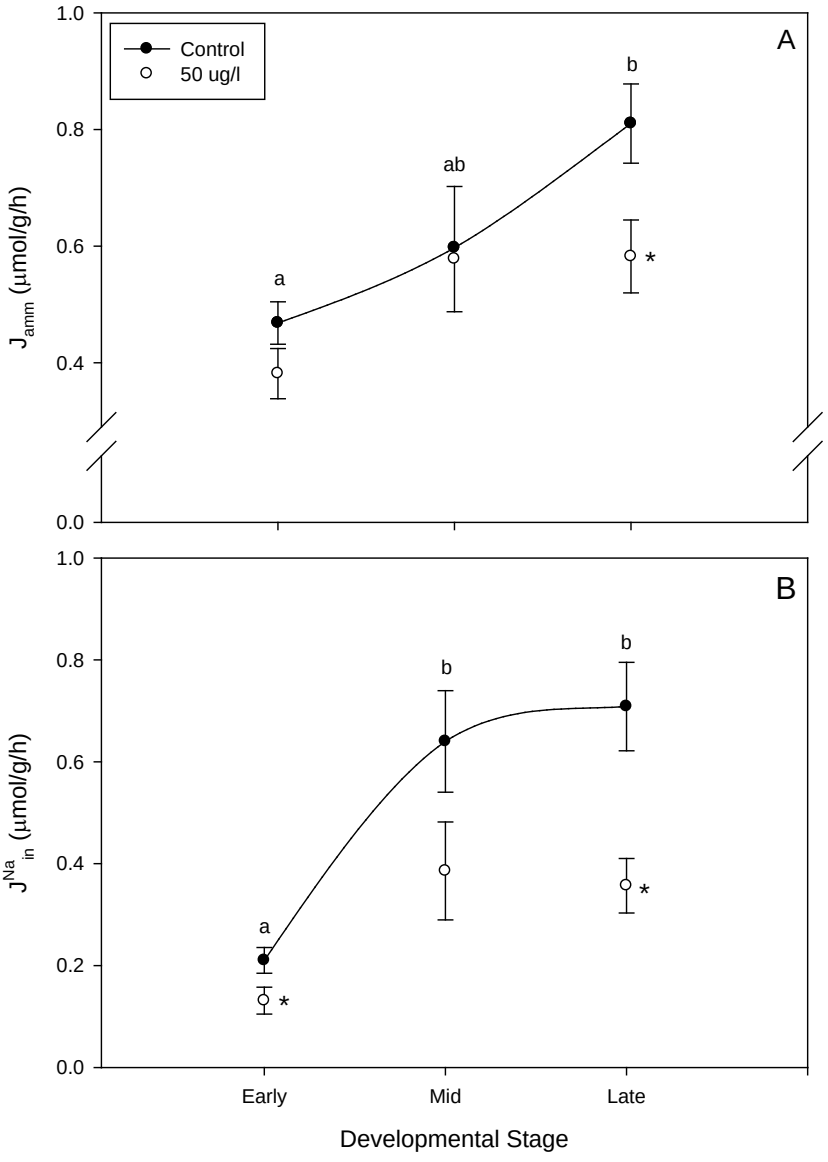
A
B
Control
50 ug/l
J_{amm} (µmol/g/h)
J^{Na}_{in} (µmol/g/h)
1.0
0.8
0.6
0.4
0.2
0.0
a
ab
b
a
b
b
*
*
*
Early
Mid
Late
Developmental Stage

Fig. 5.1. Total ammonia excretion (A; J_{amm}; µmol/g/h; n=6-12) and sodium uptake (B; J^{Na}_{in}; µmol/g/h; n=6-12) in larval trout from Series 1 (unrestrained and non-anaesthetized) exposed to nominal 0 (control) or 50 µg/l Cu in early, mid, and late developmental stages. Means not sharing the same letters indicate statistically significant differences with development. Asterisks represent statistically significant differences between 50 and 0 µg/l Cu exposure at a given developmental stage.

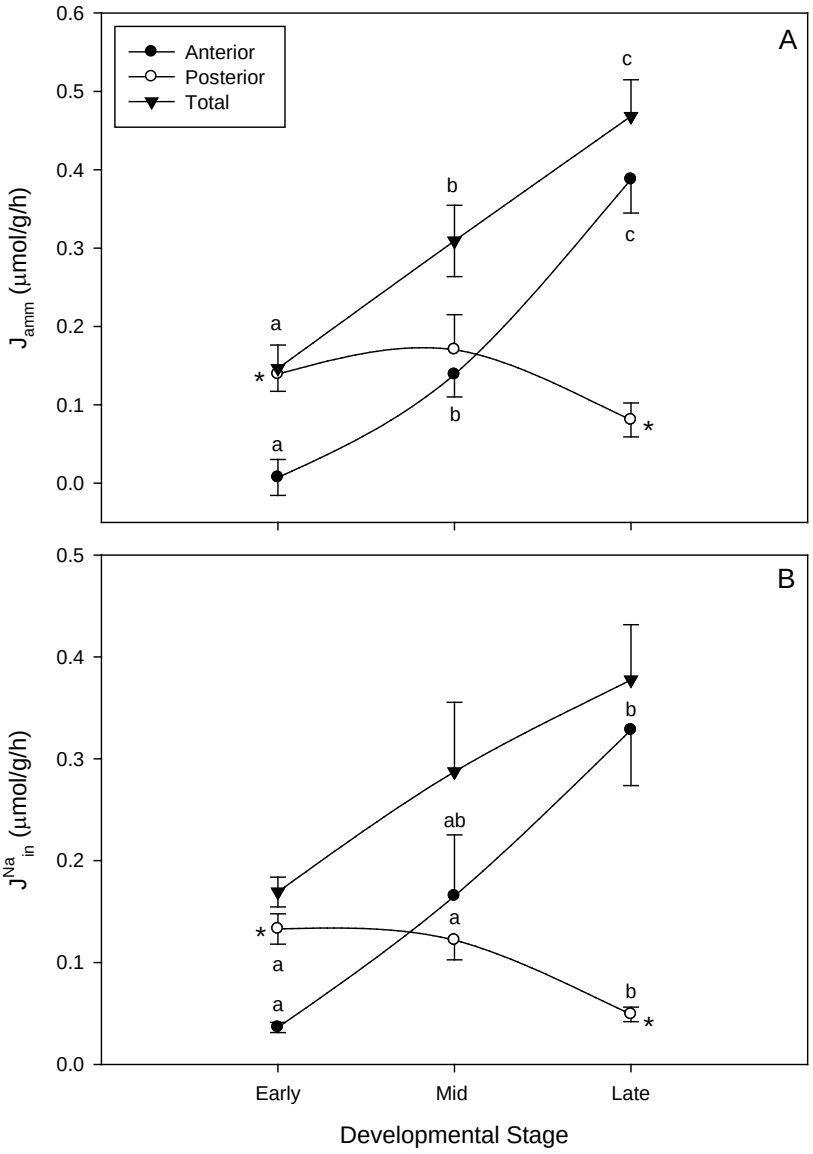
A
Anterior
Posterior
Total
J_{amm} (µmol/g/h)
0.6
0.5
0.4
0.3
0.2
0.1
0.0
a
b
c
a
b
c
*
*
B
J^{Na}_{in} (µmol/g/h)
0.5
0.4
0.3
0.2
0.1
0.0
a
ab
b
a
a
b
*
*
Early
Mid
Late
Developmental Stage

Fig. 5.2. Anterior (filled circles), posterior (open circles) and total (filled triangles) ammonia excretion (A; J_{amm}; µmol/g/h; n=9-13) and sodium uptake (B; J^{Na}_{in}; µmol/g/h; n=4-7) in control larval rainbow trout from Series 3 (divided chamber) at early, mid, and late developmental stages. Means not sharing the same letters indicate statistically significant differences among developmental stage within anterior, posterior, or total data sets. Asterisks represent posterior means which differ significantly from respective anterior means within a given developmental stage.

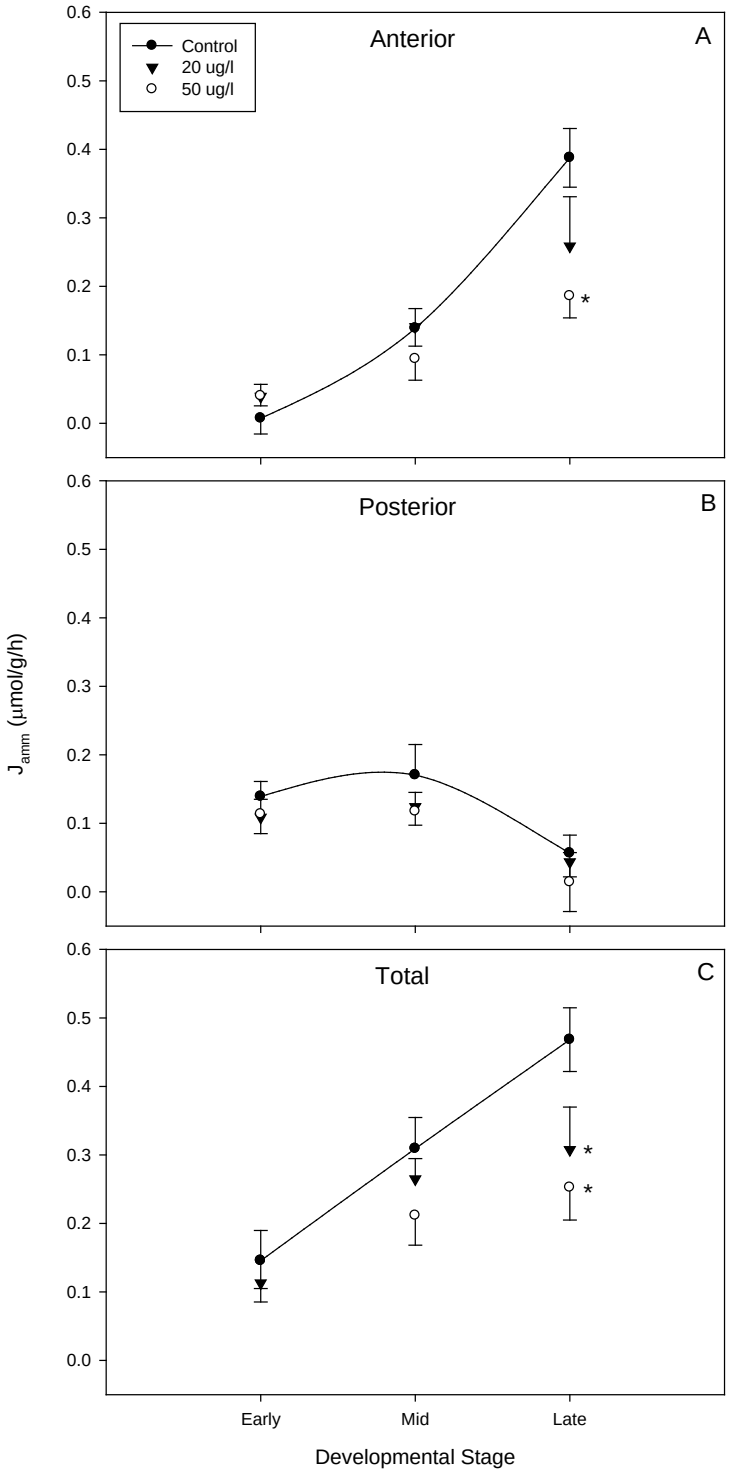
Anterior
A
Control
20 ug/l
50 ug/l
Posterior
B
Total
C
0.6
0.5
0.4
0.3
0.2
0.1
0.0
*
*
*
J_{amm} (µmol/g/h)
Early
Mid
Late
Developmental Stage

Fig. 5.3. Anterior (A), posterior (B), and total (C) ammonia excretion (J_{amm}; µmol/g/h) in larval rainbow trout from Series 3 (divided chambers) exposed to nominal 0 µg/l (control; filled circles), 20 µg/l (filled triangles), and 50 µg/l Cu (open circles) in early, mid, and late developmental stages. Asterisks represent means from Cu-exposed fish (20 or 50 µg/l Cu) which are significantly different from respective 0 µg/l Cu control values at a given developmental stage within anterior, posterior, or total data sets. (n=9-14)

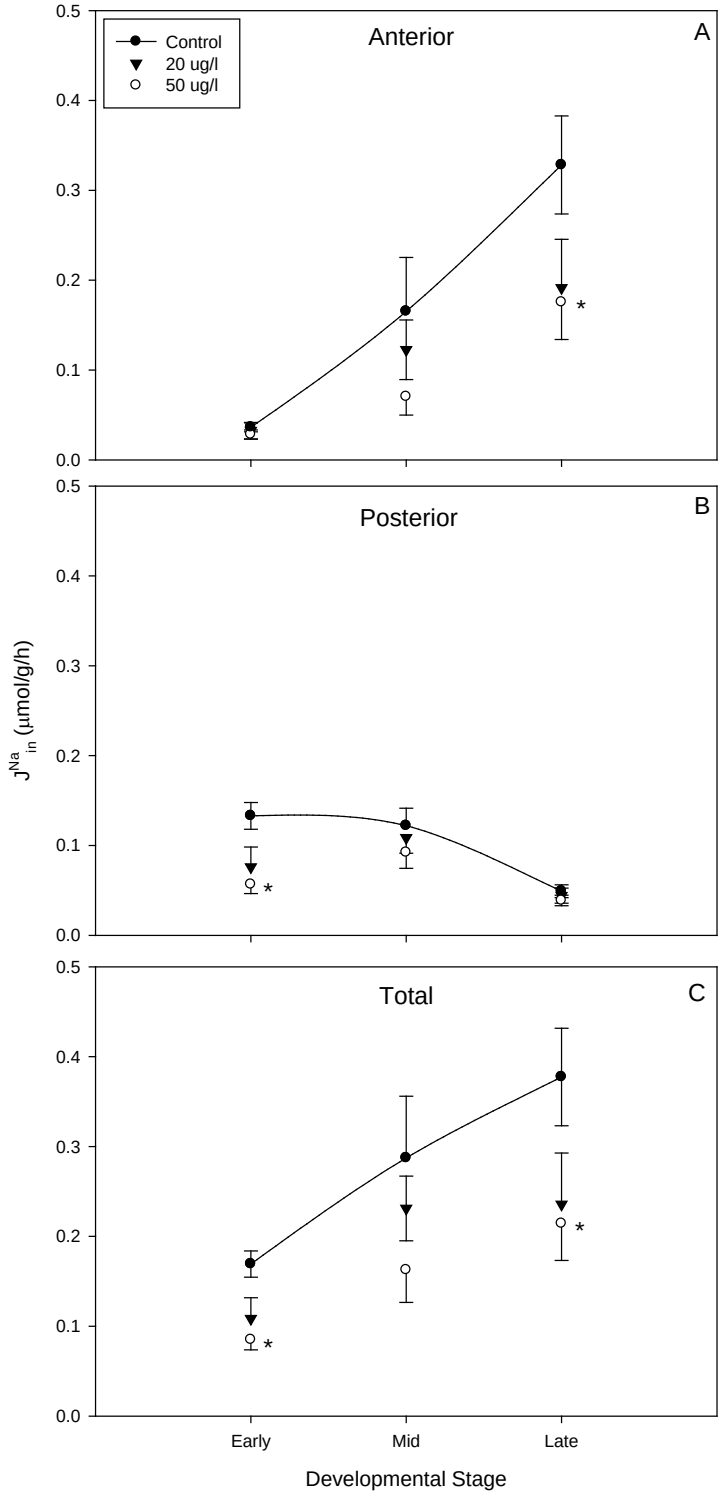
Control
20 ug/l
50 ug/l
Anterior
A
Posterior
B
Total
C
0.5
0.4
0.3
0.2
0.1
0.0
*
J^{Na}_{in} (µmol/g/h)
Early
Mid
Late
Developmental Stage

Fig. 5.4. Anterior (A), posterior (B), and total (C) sodium uptake (J^{Na}_{in}; µmol/g/h) in larval rainbow trout from Series 3 (divided chambers) exposed to nominal 0 µg/l (control; filled circles), 20 µg/l (filled triangles), and 50 µg/l Cu (open circles) in early, mid, and late developmental stages. Asterisks represent means from Cu-exposed fish (20 or 50 µg/l Cu) which are significantly different from respective 0 µg/l Cu control values at a given developmental stage within anterior, posterior, or total data sets. (n=4-8)

5.7 REFERENCES

Blanchard, J. and Grosell, M. (2006) Copper toxicity across salinities from freshwater to seawater in the euryhaline fish *Fundulus heteroclitus*: Is copper an ionoregulatory toxicant in high salinities? *Aquat. Toxicol.* 80, 131–139.

Brauner, C.J. and Rombough, P.J. (2012) Ontogeny and paleophysiology of the gill: new insights from larval and air-breathing fish. *Respir. Physiol. Neurobiol.* 184, 293–300.

Brix, K. V., Keithly, J., DeForest, D.K. and Laughlin, J. (2004) Acute and chronic toxicity of nickel to rainbow trout (*Oncorhynchus mykiss*). *Environ. Toxicol. Chem.* 23, 2221–2228.

Chapman, G.A. (1978) Toxicities of cadmium, copper, and zinc to four juvenile stages of chinook salmon and steelhead. *Trans. Am. Fish. Soc.* 107, 841-847.

Crespo, S. and Karnaky Jr., K.J. (1983) Copper and zinc inhibit chloride transport across the opercular epithelium of seawater-adapted killifish *Fundulus heteroclitus*. *J. Exp. Biol.* 102, 337-341.

Di Toro, D.M., Allen, H.E., Bergman, H.L., Meyer, J.S., Paquin, P.R. and Santore, R.C. (2001) Biotic ligand model of the acute toxicity of metals. 1. Technical basis. *Environ. Toxicol. Chem.* 20, 2383–2396.

Essex-Fraser, P.A, Steele, S.L., Bernier, N.J., Murray, B.W., Stevens, E.D. and Wright, P.A. (2005) Expression of four glutamine synthetase genes in the early stages of development of rainbow trout (*Oncorhynchus mykiss*) in relationship to nitrogen excretion. *J. Biol. Chem.* 280, 20268–20273.

Evans, D., Piermarini, P. and Choe, K. (2005) The multifunctional fish gill: dominant site of gas exchange, osmoregulation, acid-base regulation, and excretion of nitrogenous waste. *Physiol. Rev.* 85, 97–177.

Flonta, M.L., De Beir-Simaels, J., Mesotten, D. and Van Driessche, W. (1998) Cu^{2+} reveals different binding sites of amiloride and CDPC on the apical Na channel of frog skin. *Biochim. Biophys. Acta* 1370, 169–174.

Fu, C., Wilson, J.M., Rombough, P.J. and Brauner, C.J. (2010) Ions first: Na^{+} uptake shifts from the skin to the gills before O_2 uptake in developing rainbow trout, *Oncorhynchus mykiss*. *Proc. R. Soc. B.* 277, 1553–1560.

Gonzalez, M.E., Blanquez, M.J. and Rojo, C. (1996) Early gill development in the rainbow trout, *Oncorhynchus mykiss*. *J. Morph.* 229, 201–217.

Grosell, M. (2012) Copper. *Fish Physiology 31A* (ed. Farrell AP, Wood CM, Brauner CJ), pp. 54–110. San Diego, CA: Academic Press.

Grosell, M., McDonald, M.D., Wood, C.M. and Walsh, P.J. (2004) Effects of prolonged copper exposure in the marine gulf toadfish (*Opsanus beta*). I. Hydromineral balance and plasma nitrogenous waste products. *Aquat. Toxicol.* 68, 249–262.

Grosell, M., Nielsen, C. and Bianchini, A. (2002) Sodium turnover rate determines sensitivity to acute copper and silver exposure in freshwater animals. *Comp. Biochem. Physiol. C* 133, 287–303.

Grosell, M. and Wood, C.M. (2002) Copper uptake across rainbow trout gills: mechanisms of apical entry. *J. Exp. Biol.* 205, 1179–1188.

Grosell, M., Wood, C.M. and Walsh, P.J. (2003) Copper homeostasis and toxicity in the elasmobranch *Raja erinacea* and the teleost *Myoxocephalus octodecemspinosus* during exposure to elevated water-borne copper. *Comp. Biochem. Physiol. C* 135, 179–190.

Guadagnolo, C.M., Brauner, C.J. and Wood, C.M. (2001) Chronic effects of silver exposure on ion levels, survival, and silver distribution within developing rainbow trout (*Oncorhynchus mykiss*) embryos. *Environ. Toxicol. Chem.* 20, 553–560.

Handy, R.D., Eddy, F.B. and Baines, H. (2002) Sodium-dependent copper uptake across epithelia: A review of rationale with experimental evidence from gill and intestine. *Biochim. Biophys. Acta* 1566, 104–115.

HydroQual (2007) The Biotic Ligand Model Windows Interface, Version 2.2.3: User's Guide and Reference Manual, HydroQual, Inc, Mahwah, NJ, April 2005.

Kumai, Y. and Perry, S.F. (2011) Ammonia excretion via Rhcg1 facilitates Na^+ uptake in larval zebrafish, *Danio rerio*, in acidic water. *Am. J. Physiol. Regul. Integr. Comp. Physiol.* 301, R1517–28.

Lauren, D.J. and McDonald, D.G. (1985) Effects of copper on branchial ionoregulation in the rainbow trout, *Salmo gairdneri* Richardson - Modulation by water hardness and pH. *J. Comp. Physiol.B* 155, 635–644.

Lauren, D.J. and McDonald, D.G. (1987a) Acclimation to copper by rainbow trout, *Salmo gairdneri*: Physiology. *Can. J. Fish. Aquat. Sci.* 44, 99-104.

Lauren, D.J. and McDonald, D.G. (1987b) Acclimation to copper by rainbow trout, *Salmo gairdneri*: Biochemistry. *Can. J. Fish. Aquat. Sci.* 44, 105-111.

MacRae, R.K., Smith, D.E., Swoboda-Colberg, N., Meyer, J.S. and Bergman, H.L. (1999) Copper binding affinity of rainbow trout (*Oncorhynchus mykiss*) and brook trout (*Salvelinus fontinalis*) gills: Implications for assessing bioavailable metal. *Envion. Toxicol. Chem.* 18, 1180–1189.

Marshall, W.S., Bryson, S.E. and Wood, C.M. (1992) Calcium transport by isolated skin of rainbow trout. *J. Exp. Biol.* 166, 297–316.

Marshall, W.S. (2003) Rapid regulation of NaCl secretion by estuarine teleost fish: Coping strategies for short-duration freshwater exposures. *Biochim. Biophys. Biomembranes* 1618, 95–105.

McFarland, W.N. (1959) A study of the effects of anesthetics on the behaviour and physiology of fishes. *Publ. Inst. Mar. Sci. Univ. Tex.* 6, 23-55.

McKim, J.M., Eaton, J.G. and Holcombe, G.W. (1978) Metal toxicity to embryos and larvae of eight species of freshwater fish-II: Copper. *Bull. Environ. Contam. Toxicol.* 19, 608–616.

McNulty, H.R., Anderson, B.S., Hunt, J.W., Turpen, S.L. and Singer, M.M. (1994) Age-specific toxicity of copper to larval topsmelt *Atherinops affinis*. *Environ. Toxicol. Chem.* 13, 487–492.

Ng, T.Y.-T., Chowdhury, M.J. and Wood, C.M. (2010) Can the Biotic Ligand Model predict Cu toxicity across a range of pHs in softwater-acclimated rainbow trout? *Environ. Sci. Tech.* 44, 6263-6268.

Niyogi, S. and Wood, C.M. (2004) The Biotic Ligand Model, a flexible tool for developing site-specific water quality guidelines for metals. *Environ. Sci. Tech.* 38, 6177-6192.

Paquin, P.R., Gorsuch, J.W., Apte, S., Batley, G.E., Bowles, K.C., Campbell, P.G.C., Delos, C.G., Di Toro, D.M., Dwyer, R.I., Galvez, F., Gensemer, R.W., Goss, G.G., Hogstrand, C., Janssen, C.R., McGeer, J.C., Naddy, R.B., Playle. R.C., Santore, R.C., Schneider, U., Stubblefield, W.A., Wood, C.M. and Wu, K.B. (2002) The biotic ligand model: a historical overview. *Comp. Biochem. Physiol. C* 133, 3–35.

Pelgrom, S.M.G.J., Lock, R.A.C., Balm, P.H.M. and Bonga, S.E.W. (1995) Integrated physiological response of tilapia, *Oreochromis mossambicus*, to sublethal copper exposure. *Aquat. Toxicol.* 32, 303–320.

Perry, S.F. and Wood, C.M. (1985) Kinetics of branchial calcium uptake in the rainbow trout: Effects of acclimation to various external calcium levels. *J. Exp. Biol.* 433, 411–433.

Rogers, J.T., Richards, J.G. and Wood, C.M. (2003) Ionoregulatory disruption as the acute toxic mechanism for lead in the rainbow trout (*Oncorhynchus mykiss*). *Aquat. Toxicol.* 64, 215–234.

Rombough, P.J. (2002) Gills are needed for ionoregulation before they are needed for O_2 uptake in developing zebrafish, *Danio rerio*. *J. Exp. Biol.* 205, 1787–1794.

Rombough, P.J. (1999) The gill of fish larvae. Is it primarily a respiratory or an ionoregulatory structure? *J. Fish Biol.* 55, 186–204.

Rombough, P.J. and Garside, E.T. (1982) Cadmium toxicity and accumulation in eggs and alevins of Atlantic salmon *Salmo salar*. *Can. J. Zool.* 60, 2006–2014.

Santore, R.C., Di Toro, D.M., Paquin, P.R., Allen, H.E. and Meyer, J.S. (2001) Biotic ligand model of the acute toxicity of metals. 2. Application to acute copper toxicity in freshwater fish and daphnia. *Environ. Toxicol. Chem.* 20, 2397–2402.

Shih, T.-H., Hong, J.-L., Hwang, P.-P. and Lin, L.,-Y. (2008) Ammonia excretion by the skin of zebrafish (*Danio rerio*) larvae. *Am. J. Physiol. Cell Physiol.* 295, 1625-1632.

Shih, T.-H., Horng, J.-L., Lai, Y.-T. and Lin, L.-Y. (2013) Rhcg1 and Rhbg mediate ammonia excretion by ionocytes and keratinocytes in the skin of zebrafish larvae: H^+-ATPase-linked active ammonia excretion by ionocytes. *Am. J. Physiol. Regul. Integr. Comp. Physiol.* 304, R1130–R1138.

Shih, T.-H., Horng, J.-L., Liu, S.-T., Hwang, P.-P. and Lin, L.-Y. (2012) Rhcg1 and NHE3b are involved in ammonium-dependent sodium uptake by zebrafish larvae acclimated to low-sodium water. *Am. J. Physiol. Regul. Integr. Comp. Physiol.* 302, R84–93.

Skulskii, I.A. and Lapin, A. V. (1992) Highly selective blockade of the frog skin sodium channels by monovalent copper cations. *Biochim. Biophys. Acta* 1112, 27–28.

Smith, A.A., Zimmer, A.M. and Wood, C.M. (2012) Branchial and extra-branchial ammonia excretion in goldfish (*Carassius auratus*) following thermally induced gill remodeling. *Comp. Biochem. Physiol. A* 162, 185–192.

Sola, F., Isaia, J. and Masoni, A. (1995) Effects of copper on gill structure and transport function in the rainbow trout, *Oncorhynchus mykiss*. *J. App. Tech.* 15, 391–398.

Stouthart, X.J.H.X., Haans, J.L.M., Lock, R.A.C. and Wendelaar Bonga, S.E. (1996) Effects of water pH on copper toxicity to early life stages of the common carp (*Cyprinus carpio*). *Environ. Toxicol. Chem.* 15, 376–383.

Tsui, T.K.N., Hung, C.Y.C., Nawata, M., Wilson, J.M., Wright, P. A. and Wood, C.M. (2009) Ammonia transport in cultured gill epithelium of freshwater rainbow trout: the importance of Rhesus glycoproteins and the presence of an apical Na^+/NH_4^+ exchange complex. *J. Exp. Biol.* 212, 878-898.

U.S. Environmental Protection Agency (2007) Aquatic Life Ambient Freshwater Quality Criteria-Copper, 2007 Revision. EPA-822-R-07-001. Office of Water, Washington, DC

Ussing, H.H. and Zerahn, K. (1950) Active Transport of Sodium as the Source of Electric Current in the Short-circuited Isolated Frog Skin. *Acta. Physiol. Scand.* 23, 110-127.

Verdouw, H., van Echteld, C.J.A. and Dekkers, E.M.J. (1978) Ammonia determination based on indophenols formation with sodium salicylate. *Water Res.* 12, 399-402.

Vitale, A.M., Monserrat, J.M., Castilho, P. and Rodriguez, E.M. (1999) Inhibitory effects of cadmium on carbonic anhydrase activity and ionic regulation of the estuarine crab *Chasmagnathus granulata* (Decapoda, Grapsidae). *Comp. Biochem. Physiol. C* 122, 121-129.

Wang, T., Knudsen, P.K., Brauner, C.J., Busk, M., Vijayan, M.M. and Jensen, F.B. (1998) Copper exposure impairs intra- and extracellular acid-base regulation during hypercapnia in the fresh water rainbow trout (*Oncorhynchus mykiss*). *J. Comp. Physiol. B* 168, 591-599.

Wells, P.R. and Pinder, A.W. (1996) The respiratory development of Atlantic salmon. II. Partitioning of oxygen uptake among gills, yolk sac and body surfaces. *J. Exp. Biol.* 199, 2737-4274.

Wilson, R.W. and Taylor, E.W. (1993a) The physiological responses of freshwater rainbow trout, *Oncorhynchus mykiss*, during acutely lethal copper exposure. *J. Comp. Physiol. B* 38–47.

Wilson, R.W. and Taylor, E.W. (1993b) Differential responses to copper in rainbow trout (*Oncorhynchus mykiss*) acclimated to sea water and brackish water. *J. Comp. Physiol. B* 239–246.

Wright, P.A., Felskie, A. and Anderson, P. (1995) Induction of ornithine-urea cycle enzymes and nitrogen metabolism and excretion in rainbow trout (*Oncorhynchus mykiss*) during early life stages. *J. Exp. Biol.* 198, 127–35.

Wright, P.A. and Wood, C.M. (2009) A new paradigm for ammonia excretion in aquatic animals: role of Rhesus (Rh) glycoproteins. *J. Exp. Biol.* 212, 2303–12.

Wu, S.-C., Horng, J.-L., Liu, S.-T., Hwang, P.-P., Wen, Z.-H., Lin, C.-S. and Lin, L.-Y. (2010) Ammonium-dependent sodium uptake in mitochondrion-rich cells of medaka (*Oryzias latipes*) larvae. *Am. J. Physiol. Cell Physiol.* 298, 237-250.

Zadunaisky, J.A., Candia, O.A. and Chiarandini, D.J. (1963) The origin of the short-circuit current in the isolated skin of the South American frog *Leptodactylus ocellatus*. *J. Gen. Physiol.* 47, 393-402.

Zimmer, A.M., Barcarolli, I.F., Wood, C.M. and Bianchini, A. (2012) Waterborne copper exposure inhibits ammonia excretion and branchial carbonic anhydrase activity in euryhaline guppies acclimated to both fresh water and sea water. *Aquat. Toxicol.* 122-123, 172–80.

Zimmer, A.M., Wright. P.A. and Wood, C.M. (2014b) What is the primary function of the early teleost gill? Evidence for Na^+-coupled ammonia excretion in developing rainbow trout (*Oncorhynchus mykiss*). *Proc. R. Soc. B* 281: 1795.

CHAPTER 6

AMMONIA TRANSPORT ACROSS THE SKIN OF ADULT RAINBOW TROUT (*ONCORHYNCHUS MYKISS*) EXPOSED TO HIGH ENVIRONMENTAL AMMONIA (HEA)

6.1 ABSTRACT

Recent molecular evidence points towards a capacity for ammonia transport across the skin of adult rainbow trout. A series of *in vivo* and *in vitro* experiments were conducted in order to understand the role of cutaneous ammonia excretion (J_{amm}) under control conditions and after 12-h pre-exposure to high environmental ammonia (HEA; 2 mmol/l NH_4HCO_3). Divided chamber experiments with bladder-catheterized, rectally-ligated fish under light anaesthesia were performed to separate cutaneous J_{amm} from branchial, renal, and intestinal J_{amm}. Under control conditions, cutaneous J_{amm} accounted for 4.5% of total J_{amm} *in vivo*. In fish pre-exposed to HEA, plasma total ammonia concentration increased 20-fold to approximately 1000 µmol/l, branchial J_{amm} increased 1.5 to 2.7-fold, and urinary J_{amm} increased about 7-fold. Urinary J_{amm} still accounted for less than 2% of total J_{amm}. Cutaneous J_{amm} increased 4-fold yet amounted to only 5.7% of total J_{amm} in these fish. Genes (Rhcg1, Rhcg2, Rhbg, NHE-2, v-type H^+-ATPase) known to be involved in ammonia excretion at the gills of trout were all expressed at the mRNA level in the skin, but their expression did not increase with HEA pre-exposure. *In vitro* analyses using [^{14}C] methylamine (MA), an ammonia analogue which is transported by Rh proteins, demonstrated that MA permeability in isolated skin sections was higher in HEA pre-exposed fish than in control fish. The addition of basolateral ammonia (1000 µmol/l) to this system abolished this increase in permeability, suggesting ammonia competition with MA for Rh-mediated transport across the skin of HEA pre-exposed trout; this did not occur in skin sections from control trout. Moreover, *in vitro* J_{amm} by the skin of fish which had been pre-exposed to HEA was also higher than in control fish in

the absence of basolateral ammonia, pointing towards a possible cutaneous ammonia loading in response to HEA. *In vitro* MA permeability was reduced upon the addition of amiloride (10^{-4} mol/l), but not phenamil (10^{-5} mol/l) suggesting a role for a Na/H-exchanger (NHE) in cutaneous ammonia transport, as has been previously described in the skin of larval fish. Overall, it appears that under control conditions and in response to HEA pre-exposure, the skin makes only a very minor contribution to total J_{amm} but the observed increases in cutaneous J_{amm} *in vivo* and in cutaneous J_{amm} and MA permeability *in vitro* demonstrate the capacity for ammonia transport in the skin of adult trout. It remains unclear if this capacity may become significant under certain environmental challenges or if it is merely a remnant of cutaneous transport capacity from early life stages in these fish.

6.2 INTRODUCTION

The majority of freshwater teleost fish excrete ammonia to eliminate the nitrogenous wastes produced by protein metabolism. In an early pinnacle study, Homer Smith (1929) first determined that the majority (80-90%) of ammonia excreted by freshwater fish (goldfish; *Carassius auratus* and carp; *Carassius carassius*) occurred via the gills and that the remaining portion (10-20%) occurred renally. Since this study, a mechanistic model describing ammonia transport across the gills of fish has been developed. The model has incorporated Rhesus (Rh) glycoproteins as the putative ammonia transport channels in gill epithelial cells, with basally and apically expressed Rhbg and Rhcg isoforms (see Weihrauch et al. 2009; Wright and Wood 2009). Furthermore, the branchial excretion model for freshwater fish has been named the "Na^+/NH_4^+-exchange complex" (Tsui et al. 2009; Wright and Wood 2009) as the excretion of ammonia across the gill is coupled to Na^+ uptake, through an as yet unidentified epithelial Na^+ channel coupled to an apical H^+-ATPase and/or a Na^+/H^+-exchanger (NHE). Furthermore, both NHE and H^+-ATPase facilitate ammonia efflux via boundary layer acidification (i.e., acid-trapping) (see Weihrauch et al. 2009; Wright and Wood 2009).

To date, much of our current understanding of the mechanisms underlying ammonia transport in fish has been gained by studying physiological and molecular responses to ammonia challenges. One such challenge, the exposure to high environmental ammonia (HEA), generally leads to an initial reversal of ammonia excretion relative to control values, indicative of ammonia uptake from the environment,

and occurs in conjunction with a subsequent rise in plasma total ammonia (T_{amm}) levels (Wilson et al. 1994; Nawata et al. 2007; Zimmer et al. 2010). The rainbow trout (*Oncorhynchus mykiss*) used in these studies were eventually able to re-establish ammonia efflux against the inwardly directed gradient of HEA and this increase in excretion capacity was coupled to increased branchial mRNA expression of Rh proteins and of those transporters involved in Na^+ uptake (Nawata et al. 2007; Zimmer et al. 2010; Wood and Nawata 2011; Sinha et al. 2013). Interestingly, Nawata et al. (2007) demonstrated that Rh genes in the skin of trout were also responsive to HEA exposure, as observed in pufferfish (Nawata et al., 2010a), though the timing and isoform-specificity of this response were different than that seen in the gills. Regardless, this observation suggests the capacity for ammonia transport across an epithelium which is generally believed to be impermeable to both water and ions (Fromm 1968; Kirsch 1972) and which is not believed to contribute to whole-body ammonia excretion in adult freshwater fish (Smith 1929). To date, *in vivo* cutaneous ammonia excretion in adult fish appears to only occur as a specialized adaptation in a few fish species (e.g., mangrove killifish, *Kryptolebias marmoratus*, Frick and Wright 2002; common dab, *Limanda limanda*, Sayer and Davenport 1987). Cutaneous ammonia transport in a typical teleost fish, however, has yet to be demonstrated despite increasing evidence that the skin of these fish appears capable of physiological exchange with the surrounding environment (Glover et al. 2013).

In post-hatch larval fish, when the gills are still undeveloped and branchial surface area is low, cutaneous surfaces (body and yolk sac skin) comprise the majority of total fish surface area (Rombough 1999). As such, at this stage the skin is considered to be the

major site for ion and gas exchange with the surrounding environment. It has been demonstrated, to date, that both oxygen and Na^+ uptake are predominantly cutaneous following hatch and eventually progress to become primarily branchial as the gills develop (Wells and Pinder 1996; Fu et al. 2010). Furthermore, several studies have demonstrated that the skin of larval zebrafish (*Danio rerio*) and Japanese medaka (*Oryzias latipes*) is also capable of ammonia excretion which appears to be coupled to Na^+ uptake, in accordance with the current model for branchial ammonia transport (Shih et al. 2008; 2012; Wu et al. 2010; Ito et al. 2013). Similarly, in larval rainbow trout, ammonia excretion and Na^+ uptake both occur cutaneously following hatch and, with development, both processes eventually shift simultaneously to become predominantly branchial, suggesting both cutaneous and branchial coupling of these exchange processes at this life stage (Zimmer et al., 2014b). Thus, it is clear that a capacity for ammonia transport by the skin of larval fish exists, but it is unknown to what degree this capacity might be retained in adult fish. Presently, the general view of the skin in adult fish is that it is an impermeable barrier to water and ion movement which does not contribute to physiological exchange, however, this notion is currently being contested (see Glover et al. 2013).

The overall aim of the present study was to assess the potential for cutaneous ammonia excretion (J_{amm}) in adult rainbow trout, a model teleost fish. Based on molecular evidence in adult fish (Nawata et al. 2007), we hypothesized that cutaneous J_{amm} in rainbow trout under control conditions would be low but that it would increase and contribute significantly to whole-body J_{amm} in fish exposed to HEA. Thus, the first

objective of this study was to directly measure *in vivo* cutaneous J_{amm} using a divided chamber setup wherein the contribution of the skin to total J_{amm} could be isolated from branchial, renal, and gastrointestinal routes of excretion. Changes in *in vivo* J_{amm} could then be correlated with possible changes in skin Rh gene expression or Rh protein function. We further hypothesized that the skin of HEA-exposed fish would display an intrinsic increase in ammonia permeability, indicative of increased transport capacity of this tissue. Thus, our second objective was to assess ammonia flux and permeability to [^{14}C]methylamine (MA) in isolated skin sections *in vitro* using a modified Ussing chamber design, similar to that of Glover et al. (2011). MA is an ammonia analog previously demonstrated to travel through trout Rh proteins (Nawata et al., 2010b). We also measured mRNA expression in the skin of genes (Rhcg1, Rhcg2, Rhbg, NHE-2, v-type H^+-ATPase) known to be involved in the linkage of Na^+ uptake to ammonia excretion in the gills of trout (Nawata et al. 2007; Tsui et al. 2009; Zimmer et al. 2010; Wood and Nawata 2011; Sinha et al. 2013). The final objective of the present study was to determine if ammonia transport across the skin of adult rainbow trout is linked to Na^+ uptake, as appears to be the case in larval fish (Wu et al. 2010; Shih et al. 2012; Ito et al. 2013), including larval trout (Zimmer et al., 2014b), and in adult mangrove killifish (Cooper et al. 2013) by assessing the effects of pharmacological blockers of Na^+ uptake pathways (amiloride: general NHE and Na^+ channel blocker, and phenamil: specific Na^+ channel blocker) on *in vitro* MA permeability and J_{amm}. We hypothesized that, similar to the case of larval zebrafish (Shih et al. 2012) and adult mangrove killifish (Cooper et al. 2013), cutaneous ammonia transport would be linked to Rh and NHE function.

6.3 MATERIAL AND METHODS

6.3.1 Fish

Adult rainbow trout obtained from Spring Valley Trout Farm (Langley, British Columbia, Canada), weighing 200-450 g, were held in large outdoor tanks at the University of British Columbia in Vancouver, BC, supplied with flow-through dechlorinated Metro Vancouver tap water (in mM: Na^+,0.06; Cl^-, 0.05; Ca^{2+}, 0.03; Mg^{2+}, 0.007; K^+, 0.004; and in mg/l $CaCO_3$, alkalinity, 3.0; hardness 3.3; pH 7.0) at 10ºC. Fish were fed commercial trout pellets (Skretting, Orient 4-0) at a ration of 1% per day 3 times a week. Prior to experiments, fish were fasted for at least 1 week. All experiments were performed at a constant temperature (10.0 ± 0.5ºC) on a natural photoperiod and were approved by the animal care committees of the University of British Columbia and McMaster University.

6.3.2 Series 1 - Range-finding experiments

To determine the concentration of high environmental ammonia (HEA) to be used in experiments, fish were exposed to control conditions and to HEA of 1, 2, and 3 mmol/l NH_4HCO_3 for 12 h. Fish were exposed in a 150-l static system (maximum of 8 per exposure) where pH for all treatments was kept at 7.0 via the addition of HCl. At the end of the 12 h of exposure, half the fish were euthanized via neutralized MS-222 overdose and blood was sampled via caudal puncture using a heparinized 1-ml syringe. Blood samples were immediately spun down and plasma was collected and stored briefly on ice until further total ammonia (T_{amm}) analysis. The remaining half of the fish were then

removed and placed individually into 4-l flux boxes containing control (i.e., no ammonia added), aerated water. Following a 15-min period to allow fish to settle down, an initial 10-ml water sample was taken from each box and another 10-ml water sample every 2 h for 6 h to determine whole-body ammonia excretion rates (J_{amm}). Following this flux period, fish were lightly anaesthetized with a 0.05 g/l neutralized MS-222 solution and weighed. All water samples were kept at -20ºC until further analysis.

6.3.3 Series 2 - Anaesthetic control experiments

Based on these initial results, the 2 mmol/l HEA pre-exposure was deemed appropriate for subsequent experiments as this was the lowest concentration where both plasma ammonia levels and ammonia excretion rates increased significantly following HEA exposure (see Results). A second experimental series was then designed to determine the effect of light anaesthesia (using MS-222) on whole-body J_{amm} (stage 1; McFarland 1959) which was required to calm fish in the divided chamber system described below in order to avoid both struggling during handling and escape from the dam. Fish were subjected to the same 12-h protocol described above in control or 2 mmol/l HEA and then their whole-body J_{amm} was measured in 4-l flux boxes in the presence and absence of 0.03 g/l of neutralized MS-222 (pH 7). All water samples were stored at -20ºC until further analysis.

6.3.4 Series 3 - Divided chamber experiments

In this series, the aim was to determine the contribution of the skin, separate from those of the gills, kidney, and intestinal tract, to total J_{amm} under control conditions and in

response to pre-exposure to HEA (2 mmol/l NH_4HCO_3, pH 7.0). First, fish were anaesthetized (0.1 g/l neutralized MS-222) and placed onto a V-shaped operating table, with constant anaesthetic irrigation of the gills via a recirculating pump, in order to fit fish with internal urinary bladder catheters (Wood and Patrick 1994). The catheters were made from a length of PE50 tubing with a small flare at one end. The catheter was filled with distilled water and the flared end inserted into the urinary papilla and advanced to the middle of the urinary bladder. The papilla was then tied snugly around the catheter using 2.0 silk thread and the catheter was held in place using a PE160 sheath (flared at both ends) which was glued to the catheter and held in place close to the papilla using two ligatures on the underside of the fish. A pin was used to occlude the other end of the distilled water-filled catheter. Following catheterization, the anus of the fish was sewn shut via a ligation made through the underside of the fish, anterior to the rectum. Fish were then transferred to 4-l flux boxes supplied with re-circulating control water.

After a 2-h settling period, individual 4-l flux boxes were supplied with either re-circulating control or HEA water (2 mmol/l NH_4HCO_3, pH 7.0) (~35 l/fish) for 12 h overnight. During this time, pins were removed from the end of the catheters and urine was collected by siphon (approximately 3 cm H_2O head pressure) into pre-weighed, 25-ml Erlenmeyer flasks. After the 12-h flux period, pins were re-inserted into the end of the catheters, urine vials were weighed, and urine was collected and stored at -20ºC until further analysis. Flow to the flux boxes was then stopped and fish were lightly anaesthetized via the addition of neutralized MS-222 to a concentration of 0.03 g/l. Next, a latex sheet with a hole cut into its center (approximately 2-3 cm in diameter) was fitted

around the anaesthetized fish, immediately posterior to the pectoral fins. The latex sheet was tight enough around the fish such that it was not necessary to physically glue the dam to the body of the fish. The fish, with its latex collar, was then loaded tail first into a length of PVC pipe (7 cm diameter, 30 cm length), sealed at the back end with a latex sheet, through which the urinary catheter was pulled, in order to collect urine during the divided chamber fluxes. The latex collar around the fish was then secured to the front end of the PVC pipe using an elastic band. The PVC pipe, with the head of the fish protruding from the front latex sheet and the urinary catheter exiting through the back latex sheet, was submerged into a 4-l flux box containing 0.03 g/l neutralized MS-222 in control water. The top of each PVC pipe was fitted with a sampling port (a modified 10-ml pipette tip) through which an airline was also inserted for aeration and mixing of the water. A second airline was placed directly into the 4-l box. Fish were allowed to adjust to this setup for 15 minutes prior to water sampling (10-ml) from the 4-l box (anterior chamber) and the PVC pipe (posterior chamber). Anterior and posterior water samples were taken every 2 h thereafter for a total of 6 h and all water samples were frozen and stored at -20ºC until further analysis. Water pH tended to rise slightly over this period but stayed in the range of 7.0 – 7.4. Over this 6-h period, urine flow rate was generally depressed and sometimes zero, likely due to the effects of the anaesthetic (see Results). Following the 6-h flux, a green dye was loaded into the posterior chamber and left to equilibrate for 1 h, after which 1-ml samples were taken from the anterior and posterior chamber s to assess potential leakage in the system, determined colorimetrically (spectrophotometry at 590 nm). The sensitivity of this test was such that a leakage

corresponding to as low as 1% of the volume of the posterior chamber could be reliably detected. Fish were then removed from the chambers, weighed, and anterior and posterior final volumes were recorded.

6.3.5 In vitro experiments

In vitro experiments were performed to measure the cutaneous flux rate of ammonia and the permeability of the skin to the ammonia analogue [^{14}C]methylamine (MA) (NEC-061, specific activity 2.26 Gbq/mmol, NEN-Dupont, Boston, MA, USA), and to assess regional variability of MA permeability. Trout were euthanized (0.5 g/l neutralized MS-222) either under control conditions or after 12-h exposure to HEA water (2 mmol/l NH_4HCO_3, pH 7.0). Fish were thoroughly rinsed in control water and kept on ice during dissection. Strips of skin were cut by making parallel longitudinal incisions: (i) just above the lateral line and just below the dorsal fin (for epaxial skin), and (ii) just below the lateral line and at the point of juncture to the lighter-coloured belly (for hypaxial skin). In addition, samples were excised from (iii) the ventral midline (belly), (iv) the top of the head, and (v) from the caudal peduncle (tail). The samples were taken in the above order. For each strip or sample, the skin was grasped firmly with forceps and peeled off slowly. Bits of adhering muscle tissue were removed, but no attempt was made to scrape the basolateral surface clean so as to avoid damage, so in occasional samples there may have been small remnants of adherent muscle. The scales were left intact for both the *in vitro* flux experiments and the gene expression studies, but for the latter, any underlying muscle and connective tissues were removed by thorough scraping.

The first samples taken were epaxial, and for some fish, a subsection (approximately 5 cm^2) was immediately immersed in 5 volumes of RNA*later*® (Ambion Inc., Austin, TX, U.S.A) and stored overnight at 4ºC, and then frozen at -20ºC for later analysis of gene expression. All other skin samples were used in flux experiments employing modified Ussing chambers similar to the design of Glover et al. (2011). These were manufactured from 7-ml plastic scintillation vials with snap-on lids in which the centre of the lid had been removed, revealing an aperture of 1.13 cm^2. The vial was filled with 2 ml of Cortland salmonid saline containing either no ammonia or 1 mmol/l NH_4HCO_3 to duplicate blood plasma T_{amm} values measured in fish which had been exposed to HEA water (2 mmol/l NH_4HCO_3, referred to as HEA water from this point forward) for 12 h (see Results). The saline was also labeled with [^{14}C]methylamine so as to achieve a radioactivity of approximately 100,000 cpm/ml. The saline had been pre-equilibrated with 99.7% O_2/0.3 % CO_2 to achieve normal *in vivo* PCO_2 levels, and the final pH was set to 7.7-7.8 with NaOH. A sub-section of skin was placed over the mouth of the scintillation vial such that the basolateral side faced the saline, and was sealed in placed with the snap-on lid, revealing an exposed surface area of 1.13 cm^2. The vial was then blotted dry and weighed to 1 mg accuracy. The flux period (2 h) was initiated by inverting the vial into a larger plastic container containing 5 ml of dechlorinated Vancouver tapwater (pH = 7.0, composition as above) that was continually gassed with water-saturated air (to prevent evaporation). Thus, the basolateral surface of the skin was bathed in saline, and the apical surface in water. Drugs were present in the water in some trials, as outlined below. After 2 h, the flux measurement was terminated by removing the

vial from the larger container, blotting dry, and re-weighing. Any preparations that leaked could be detected (and their data rejected) by large weight gains as there was a differential hydrostatic pressure of about 0.3 cm H_2O from the outer water bath to the inner saline bath. Final basolateral saline and apical water samples (1 ml each) were taken and added to 4 ml of Ultima Gold AB fluor (Perkin-Elmer, Waltham, MA, USA) for later scintillation counting. Tests showed that quench was constant so no corrections were made. Additional apical samples were frozen for later analysis of water T_{amm}.

The following experimental series were performed. (i) a survey of regional variation in ammonia flux rates and MA permeability using different skin regions (epaxial, hypaxial, belly, head, tail) from HEA-exposed fish in the presence of 1 mmol/l basolateral NH_4HCO_3 saline; (ii) a comparison of ammonia flux rates and MA permeability among epaxial skin preparations from control and HEA-exposed fish, with basolateral control saline or 1 mmol/l NH_4HCO_3 saline, and *vice versa*; and (iii) an assessment of the responses of ammonia flux rates and MA permeability in the hypaxial skin of HEA-exposed fish (in the presence of 1 mmol/l basolateral NH_4HCO_3) to pharmacological blockers (amiloride, phenamil) present in the apical water. In these experiments, amiloride (amiloride hydrochloride hydrate; Sigma-Aldrich, St. Louis, MO, U.S.A.) was used at 10^{-4}M and phenamil (phenamil methanesulfonate, Sigma-Aldrich, St. Louis, MO, U.S.A.) was used at 10^{-5}M, and both drugs were first dissolved in dimethyl sulfoxide (DMSO), yielding a final DMSO concentration in the water of 0.1%. For these experiments, the non-drug control water also contained 0.1% DMSO. For all series, each

treatment was performed in duplicate or triplicate on one fish, and the results averaged, representing N = 1. Total N numbers were 4-8 for each series.

6.3.6 Determination of skin gene expression

Total RNA was extracted from minced and homogenized epaxial skin samples using Trizol (Invitrogen, Burlington, ON). Total RNA was then quantified spectrophotometrically (Nanodrop ND-1000, Nanodrop Technologies, Wilmington, DE, USA) and RNA integrity was assessed by running samples on a 1% agarose gel stained with Redsafe (Froggabio, Toronto, ON). cDNA was synthesized from 1 µg of DNAse1-treated (Fermentas, Fisher Scientific, Pittsburgh, PA) RNA using an oligo(dT_{17}) primer and Superscript II reverse transcriptase (Invitrogen). This synthesized cDNA was then used to determine the mRNA expression levels of EF1α, Rhcg1, Rhcg2, Rhbg, and NHE2, and v-type H^+-ATPase (GenBank accession numbers: AF498320, DQ431244, AY619986, EF051113, EF446605, AF140002, respectively) using quantitative polymerase chain reaction (qPCR). 20 µl reactions consisted of 4 µl of 5x diluted cDNA, 4 pmol of both forward and reverse primers, previously determined for each gene (Nawata et al. 2007), 0.8 µl of 10x diluted ROX dye, and 10 µl of Platinum SYBR Green qPCR SuperMix-UDG (Invitrogen) and were performed using a Mx3000P qPCR System (Stratagene, Cedar Creek, TX). Reactions were conducted at 50ºC (2 min) and 95 ºC (2 min), followed by 40 cycles of 95 ºC (15 s) then 60 ºC (30 s). No template controls and non-reverse transcribed controls were run in parallel and the formation of a single PCR product was verified by melt curve analysis. Relative gene expression values were obtained from a standard curve, generated by the serial dilution of a randomly selected

sample, and were then normalized to elongation factor 1α (EF1α) expression which was equal in control and HEA pre-exposed samples.

6.3.7 Estimation of skin surface area

To estimate skin surface area of adult rainbow trout, a separate group of fasted fish were sacrificed with a lethal dose of MS-222 and were weighed. Following this, pectoral, pelvic, dorsal, and anal fins were surgically removed from the fish. Photos were then taken of all of the separated fins, and of lateral, dorsal, and ventral aspects of the whole fish. In each photo, a ruler was included for determination of scale. Photos were then analyzed using ImageJ software (Wayne Rasband, National Institutes of Health, USA) to measure fin surface area (SA) and whole-body skin SA (lateral*2 + ventral + dorsal). To estimate posterior SA, the same photos were analyzed though only the portion of the fish posterior to the pectoral fins was included in the SA measurement. By doing this, a skin SA/weight (cm^2/g) value for anterior, posterior, and total skin SA was obtained and could be applied to those fish used in the divided chamber experiments for the determination of *in vivo* cutaneous J_{amm}.

6.3.8 Analytical techniques and calculations

Total ammonia concentrations in water, plasma, and saline samples were measured using the assay described by Verdouw et al. (1978). In the *in vitro* experiments, the presence of 0.1% DMSO in apical water samples markedly reduced the sensitivity of the assay, but did not affect its linearity, so standard curves were made up in 0.1% DMSO for the relevant treatments.

Whole-body ammonia flux rates (J_{amm}; µmol/kg/h) were calculated using the following equation:

$$J_{amm} = (T_{amm}f - T_{amm}i)*V/(wt*t), \quad (1)$$

where $T_{amm}f$ and $T_{amm}i$ are the final and initial concentrations of ammonia (µmol/l), respectively, V is volume (l), wt is weight of the fish (kg), and t is time of the flux (h).

Urine flow rate (UFR; ml/kg/h) was calculated using the following equation:

$$UFR = V/(wt \times t), \quad (2)$$

where V is the urine volume (ml), wt is the weight of the fish, and t is flux time. Urinary J_{amm} (µmol/kg/h) was calculated using the following equation:

$$J_{amm} = T_{amm} \times V/(wt \times t), \quad (3)$$

where T_{amm} is the concentration of ammonia in the urine (µmol/l) V is urine volume (l) collected over the measurement period, wt is the weight of the fish (kg), and t is flux time (h).

For *in vitro* ammonia fluxes in isolated skin preparations, J_{amm} (µmol/cm^2/h) was expressed per unit surface area and calculated as:

$$J_{amm} = T_{amm}f \times V_{ap}/SA/t,$$

(4)

where $T_{amm}f$ is the final concentration of ammonia (µmol/l) in the apical water (tests verified that $T_{amm}i$ was zero), V_{ap} is the volume of the apical water (l), SA is the surface area of the skin (cm^2), and t is time of the flux (h).

In vitro MA permeability (P_{MA}, in cm/sec) of isolated skin preparations was calculated using the standard permeability equation (e.g. Wood et al., 1998) as:

$$P_{MA} = \frac{[MA_{ap}]f * V_{ap}}{0.5([MA_{bl}]i + [MA_{bl}]f) \times t \times 3600 \times SA},$$

(5)

where $[MA_{ap}]_f$ is final [^{14}C]MA radioactivity in the apical water (cpm cm^{-3}), $[MA_{bl}]i$ is initial [^{14}C]MA radioactivity in the basolateral saline (cpm cm^{-3}), and $[MA_{bl}]f$ is final [^{14}C]MA radioactivity in the basolateral saline (cpm cm^{-3}), V_{ap} is the volume of the apical water (cm^3), t is time (h), SA is surface area of the skin (cm^2), and 3600 converts hours to seconds.

Plasma T_{amm} values were measured using the Raichem commercial kit (Cliniqa Corporation, San Marcos, CA) which quantifies the concentration of ammonia in a sample via the disappearance of NADPH (measured at 340 nm) in a reaction catalyzed by glutamate dehydrogenase.

Branchial J_{amm} (µmol/kg/h) was calculated using anterior and posterior J_{amm} values from divided chambers and skin SA values obtained from fasted trout, as:

$$\text{Branchial } J_{amm} = \text{anterior } J_{amm} - [\text{posterior } J_{amm} \text{ per unit SA} \times (\text{anterior SA/wt})], \quad (6)$$

where anterior J_{amm} is ammonia excretion in the anterior chamber (µmol/kg/h), posterior J_{amm} per unit SA is posterior ammonia excretion per estimated posterior SA (µmol/cm^2/h), anterior SA is the skin surface area isolated to the anterior chamber (cm^2), and wt is the weight of the fish (kg). This assumes that the ammonia excretion through anterior skin per unit surface area is the same as through posterior skin per unit surface area. Cutaneous J_{amm} (µmol/kg/h) was then calculated as:

$$\text{Cutaneous } J_{amm} = \text{total } J_{amm} - \text{branchial } J_{amm}, \quad (7)$$

where total J_{amm} is the sum of posterior and anterior J_{amm} (µmol/kg/h).

6.3.9 Statistical analyses

All data are presented as means ± 1 SEM where N represents sample size and significance was accepted at the $P < 0.05$ level. All statistical analyses were conducted using SigmaStat version 3.5 (Systat Software, Inc.) and descriptions of the specific analyses used in individual comparisons are included in Figure captions.

6.4 RESULTS

6.4.1 In vivo experiments

In Series 1, under control conditions, plasma T_{amm} levels were 55.5 ± 19.6 µmol/l (N=4) and increased by approximately 5, 20, and 25-fold in fish exposed to 12 h of 1, 2, and 3 mmol/l HEA, respectively (Fig. 6.1A). Notably, in all three levels of HEA, plasma T_{amm} remained substantially below water T_{amm}. Pre-exposure to HEA also led to increases in J_{amm}, after transfer to clean water, relative to control fish (J_{amm} = 409.5 ± 57.3 µmol/kg/h; N=7), though this was significant only in 2 and 3 mmol/l HEA-exposed fish where J_{amm} was 1.5 and 3.5-fold higher, respectively, than control J_{amm} (Fig. 6.1B). Based on these results, a pre-exposure treatment of 2 mmol/l NH_4HCO_3 was selected for all subsequent tests.

Overnight urinary J_{amm} in Series 3, prior to divided chamber experiments, also responded with a 7-fold increase over 12 h of 2 mmol/l HEA exposure relative to control excretion rates (Fig. 6.2). It is important to note that these differences in urinary J_{amm} were a result of changes in urine T_{amm} as urine flow rate (UFR) was not significantly different between these treatments (Table 6.1). Based on whole-body J_{amm} from control fish and fish pre-exposed to 2 mmol/l HEA (Fig. 6.1A), it can be estimated that 0.4% of total J_{amm} occurred renally under control conditions and that under HEA conditions, this value increased to 1.9%.

In Series 2, MS-222-induced anaesthesia led to a depression of J_{amm} relative to non-anaesthetized fish. This amounted to a 56 % decrease in control fish, and a 44% decrease in fish pre-exposed to HEA and transferred to clean water (Fig. 6.3). Whole-

body J_{amm} of fish in divided chambers was also significantly reduced relative to non-anaesthetized fish but these values did not differ significantly relative to the respective MS-222 anaesthetic controls (Fig. 6.3).

In Series 3, posterior J_{amm} in control fish accounted for 3.6% of total excretion (Fig. 6.4A). In HEA pre-exposed fish, posterior J_{amm} after transfer to clean water was 4-fold higher than that seen in control fish but despite this, posterior J_{amm} still accounted for only 4.9% of total J_{amm} due to a simultaneous 2.4-fold increase in anterior J_{amm} that was seen at this time (Fig. 6.4A). Urinary J_{amm} values at this time have not been reported, as urine flow rate was generally depressed and sometimes ceased altogether when the fish were placed in the divided chambers, despite these fish having normal urine output overnight, prior to experimentation (see Discussion). The post-experimental 1-h dye flux period revealed that the seal between anterior and posterior compartments in our setup was effective as no dye was detected (i.e., absorbance equal to or lesser than background) in the anterior chamber following 1 h of equilibration (data not shown). A leak as small as 1% of the volume of the posterior chamber could have been reliably detected; sensitivity calculations indicate that at most this would have resulted a 1.05-fold overestimation of posterior J_{amm} (because anterior T_{amm} was routinely higher than posterior T_{amm}).

6.4.2 In vitro experiments

Skin samples were taken from different regions of HEA-exposed fish (epaxial, hypaxial, belly, head, and tail) to assess *in vitro* J_{amm}. In the presence of 1 mmol/l basolateral NH_4HCO_3, a concentration chosen to mimic plasma T_{amm} following 12 h of 2

mmol/l HEA exposure (Fig. 6.1A), *in vitro* J_{amm} did not differ between any of the sections and had an overall mean value of 0.36 µmol/cm^2/h (Fig. 6.5A). In the presence of control basolateral saline, epaxial skin from HEA-exposed fish had J_{amm} values which were significantly greater than those seen in the epaxial skin of control fish. The same trend was observed when preparations from control and HEA fish were incubated in the presence of 1 mmol/l NH_4HCO_3 in the basolateral saline, however, it was not statistically significant (P=0.160; Fig. 6.5B). The addition of DMSO, a vehicle needed to dissolve the blockers, to the apical water in hypaxial skin preparations from HEA exposed fish, incubated with 1 mmol/l NH_4HCO_3 in the basolateral saline, resulted in a significant increase in J_{amm} but the further addition of the blockers amiloride (10^{-4} mol/l) or phenamil (10^{-5} mol/l) did not result in a significant difference relative to this value (Fig. 6.5C).

Unlike the case for *in vitro* J_{amm}, MA permeability in skin of HEA-exposed fish in the presence of 1 mmol/l basolateral NH_4HCO_3 was generally higher in tail and head sections relative to epaxial, hypaxial, and belly sections, which were not significantly different from one another (Fig. 6.6A). In the absence of basolateral NH_4HCO_3, MA permeability across epaxial skin taken from HEA-exposed fish was 2.9-fold greater than in epaxial skin from control fish (Fig. 6.6B). However, in the presence of 1 mmol/l basolateral NH_4HCO_3, this difference was abolished and MA permeability was unchanged regardless of pre-exposure condition (Fig. 6.6B). Similar to J_{amm}, 0.1% DMSO significantly increased MA permeability across the hypaxial skin of HEA-exposed fish (Fig. 6.6A). Unlike J_{amm}, the further addition of amiloride significantly reduced

permeability relative to the DMSO only value, whereas phenamil had no such effect, similar to the case for J_{amm} (Fig. 6.6C).

6.4.3 Surface area estimates and excretion rates

Total skin surface area (SA) per unit weight in fasted rainbow trout was determined to be 1.56 ± 0.07 cm^2/g (N=3). Posterior skin SA/weight was approximately 80% of total skin SA/weight with a value of 1.27 ± 0.07 cm^2/g (N=3). From these values, *in vivo* cutaneous J_{amm} was determined by dividing posterior J_{amm} (Fig. 6.4A), by the estimated posterior SA for each fish based on individual weight. *In vivo*, fish pre-exposed to HEA displayed cutaneous J_{amm} approximately 3-fold greater than control fish (Table 6.2). When compared to *in vitro* cutaneous J_{amm} (from epaxial skin; Fig. 6.5B), *in vivo* cutaneous J_{amm} was 91% lower than *in vitro* rates in control fish and approximately 83% lower in HEA-exposed fish (Table 6.2). Using the surface area values obtained from fasted rainbow trout and J_{amm} values from divided chamber experiments, it was determined that, under control conditions, cutaneous J_{amm} was 6.2 ± 1.5 µmol/kg/h (N=4), accounting for 4.5% (Fig. 6.4B) of total J_{amm} measured in the divided chamber experiment. In fish pre-exposed to HEA, this value increased 4-fold to 25.5 ± 3.2 µmol/kg/h (N=7) but still only accounted for 5.7% (Fig. 6.4B), similar to the trends seen in posterior J_{amm}.

6.4.4 Gene expression

Rhcg1, Rhcg2, Rhbg, NHE-2, v-type H^+-ATPase were all expressed in the epaxial skin of adult rainbow trout (Fig. 6.7). In the skin of HEA-exposed fish, relative gene

expression (normalized to the expression of elongation factor 1α; EF1α) of all genes measured did not differ significantly from that of control fish, despite a slight increase ($P = 0.106$) in Rhcg2 gene expression in HEA-exposed fish (Fig. 6.7).

6.5 DISCUSSION

6.5.1 Overview

The overall goal of the present study was to use both *in vivo* and *in vitro* approaches to assess the potential for cutaneous ammonia excretion in adult rainbow trout in light of previous reports of Rh gene expression in the skin of this species (Nawata et al. 2007; Nawata and Wood 2008; 2009). The range-finding experiments determined that 2 mmol/l was an appropriate HEA exposure for *in vivo* experiments as this was the lowest exposure level where significant increases in both plasma T_{amm} and J_{amm} were observed (Fig. 6.1). Notably, the trout were able to keep plasma T_{amm} well below water T_{amm} concentrations, consistent with previous studies where HEA exposure led to increases in ammonia excretion capacity against a prevailing inward ammonia concentration gradient (e.g., Wilson et al. 1994; Nawata et al. 2007; Tsui et al. 2009; Zimmer et al. 2010; Wood and Nawata 2011; Liew et al. 2013; Sinha et al. 2013). Also important to note is the relatively high exposure concentrations used in the present study (up to 3 mM NH_4HCO_3) which were necessary to achieve sufficient ammonia loading and subsequent increases in J_{amm} (Fig. 6.1) in the Vancouver tap water to which the fish were acclimated, which has a relatively low pH (7.0). The low buffer capacity of this very soft water may also have facilitated elimination of ammonia loads following HEA exposure.

In the divided chamber experiments, fish had to be anaesthetized to avoid struggling during handling and to avoid escape from the chamber. As such, a set of controls was designed to assess the effects of anaesthesia alone on J_{amm}. In agreement with a similar study on goldfish (Smith et al. 2012), anaesthesia led to a significant reduction of J_{amm} (Fig. 6.3), presumably the result of a reduction in metabolic rate as MS-222 exposure is known to reduce oxygen consumption in rainbow trout (McKim et al. 1987). This reduced excretion rate, however, was not significantly different than the whole-body J_{amm} (anterior + posterior) of fish in the divided chamber setup. Furthermore, the inhibitory effect was approximately equal on a percentage basis, regardless of pre-exposure condition (Fig. 6.3), suggesting that our anaesthetic treatment was effective in reducing experimental stress. Furthermore, the use of divided chamber experiments requires the assessment of dam integrity by dye leakage, an approach used in previous studies (e.g., Frick and Wright 2002). The seal in our system was effective, as there was no detectable dye leakage, whereas we could have reliably detected a 1% leakage, and sensitivity calculations indicated that such a leakage would have raised posterior J_{amm} by less than 5%, with negligible impact on the estimation of cutaneous J_{amm}.

Increased urinary J_{amm} occurs in response to an acidosis in fish (e.g., McDonald and Wood 1981, Perry et al. 1987; Wood et al. 1999; Lawrence et al. *In Revision*). In the present study, we have demonstrated that trout also utilize renal routes for the clearance of plasma ammonia loads resulting from HEA exposure (Fig. 6.2) and that this occurs solely via an increase in urine T_{amm} as UFR was unchanged by HEA exposure (Table 6.1). Furthermore, the UFR values observed in the present study are quite similar to those

reported previously for rainbow trout (Swift and Lloyd 1974; Wood 1988), demonstrating that the catheters were functioning well overnight prior to divided chamber experiments where UFR was inhibited such that the calculation of urinary J_{amm} was not meaningful. Nawata et al. (2007) demonstrated mRNA expression of Rhbg in the kidney of trout, but it is unclear whether this gene would be responsive to HEA exposure. Despite the HEA-induced increase in urinary J_{amm}, however, this route would appear to account for less than 2% of total J_{amm} in rainbow trout, a much lower contribution than that observed by Smith (1929) in carp and goldfish.

6.5.2 Importance of the skin in ammonia excretion

We hypothesized, based on previous molecular evidence, that the skin of adult trout would become an important site for J_{amm} in response to HEA pre-exposure. In adult trout under control conditions, cutaneous J_{amm} contributed less than 5% to total J_{amm} (Fig. 6.4), suggesting that this route of excretion is of little importance to overall J_{amm}. Following HEA exposure, however, cutaneous J_{amm} increased 4-fold but yet only accounted for less than 6% of total J_{amm} (Fig. 6.4) because there was a simultaneous 2.5-fold increase in branchial J_{amm}, demonstrating that the gills are indeed by far the most important site for ammonia clearance. Thus our hypothesis could not be confirmed, yet it is clear that this tissue is responsive to HEA exposure. It is not clear, however, if the increase in posterior J_{amm} is a result of greater clearance from the plasma or simply the unloading of a cutaneous tissue ammonia burden accumulated during the 12-h HEA pre-exposure.

In many teleost species, the presence of a secondary circulatory system (SCS), which vascularizes the skin, has been observed (e.g.,Chopin et al. 1998; Satchell 1991; Skov and Bennett 2003; Skov and Bennett 2004; Steffensen et al. 1986). The SCS, previously believed to be a lymphatic system due to its lack of red blood cells (Vogel and Claviez 1981), originates from the primary circulation and eventually drains back into the primary circulation via the lateral cutaneous vein (LCV) (see Olson 1996; Satchell 1991 for review). In the longfin eel (*Anguilla reinhardtii*), SCS capillaries periodically emerge from capillary beds, forming hairpin loops in close proximity to mitochondria-rich cells (MRCs) in the epidermis (Skov and Bennett 2004). Indeed, Ishimatsu et al. (1992) observed that plasma [HCO_3^-] and [Cl^-] differed between the primary circulation and the LCV during hypercapnic exposure, suggesting transcutaneous exchange and demonstrating that plasma acid-base corrections during hypercapnic exposure may occur via the skin. Therefore, such a role for the skin may exist in excreting ammonia from plasma following HEA exposure. On the other hand, however, the *in vitro* results, showing greater cutaneous J_{amm} in preparations from HEA-exposed fish compared to control fish regardless of the presence or absence of basolateral (i.e. plasma) NH_4HCO_3 (Fig. 6.5B), may indicate a release of ammonia from the skin tissue itself, rather than the transcutaneous clearance of plasma ammonia.

Recent molecular evidence has pointed towards a role for the skin in whole-body J_{amm} in rainbow trout (Nawata et al. 2007; Nawata and Wood 2008; 2009). Indeed, in the skin of mangrove killifish, which is known to contribute significantly to overall J_{amm} during air exposure (Frick and Wright 2002; Cooper et al. 2013), HEA exposure led to

the induction of Rhcg1 and Rhcg2 (Hung et al. 2007). In the pufferfish, HEA exposure caused an upregulation of Rhbg and Rhcg2 expression (Nawata et al., 2010a). In larval fish, the skin is an important site for J_{amm} (Shih et al. 2008; 2012; Wu et al. 2010; Zimmer AM, Wright PA, Wood CM unpublished results) though it is not known if this capacity is retained into adulthood. Moreover, it is unclear whether the skin of larval trout has an ability to handle HEA challenges in the same way as the gill of adult fish. In rainbow trout embryos, prior to hatch, no significant changes in Rhcg2 gene expression were observed following 4 or 48 h of HEA exposure (Sashaw et al, 2010).

Based on studies with other adult fish, it appears that when gill function is limited, the skin may become an important site for J_{amm} (Glover et al. 2013). For example, the mangrove killifish volatilizes ammonia across the body skin, presumably via Rh proteins, during periods of emersion where gill ventilation may be impeded (Frick and Wright 2002; Hung et al. 2007; Cooper et al. 2013). Similarly, up to 50% of ammonia excretion occurs over the general body surface of the common dab, a flatfish which often lives buried in sand where gill ventilation is limited (Sayer and Davenport 1978). In goldfish, when gill surface area is low due to the presence of an interlamellar cell mass (ILCM), J_{amm} via extra-branchial routes is increased (Smith et al. 2012). Interestingly, in rainbow trout exposed to HEPES buffer, where gill J_{amm} was reduced via an inhibition of branchial acid-trapping mechanisms, Rhcg1 and Rhcg2 mRNA expression increased in the skin while the expression of these genes was unchanged or reduced in the gills (Nawata and Wood 2008). In future studies, it may be interesting to utilize the *in vivo* and *in vitro* systems developed in this study to assess the contribution of the skin to total J_{amm} in adult

trout when HEA exposure is continued during the test period, and also when HEPES buffering limits branchial J_{amm}.

6.5.3 Mechanisms of cutaneous ammonia excretion

To date, the studies which have addressed the mechanisms of cutaneous J_{amm} in fish have focussed mainly on cutaneous excretion in larval fish. In larval zebrafish, Rhcg1 protein is expressed in MRCs on the yolk sac skin and the increase in expression of this protein over developmental time is consistent with an increase in whole-body J_{amm} (Nakada et al. 2007). Furthermore, J_{amm} in larval fish is coupled to Na^+ uptake via a Rhcg1-NHE metabolon (Kumai and Perry 2011; Ito et al. 2013), though it is unclear if this mechanism is purely cutaneous at this life stage. Using the scanning ion-selective electrode technique (SIET), Shih et al. (2012) confirmed the existence of such a metabolon in the yolk sac skin of zebrafish and it is clear that cutaneous J_{amm} in larval fish is dependent upon acid-trapping (Shih et al. 2008; Wu et al. 2010), in concordance with the branchial model for ammonia transport (Wright and Wood 2009). In adult mangrove killifish, *in vitro* J_{amm} across isolated skin of freshwater-acclimated fish was inhibited significantly by amiloride, a blocker of NHEs, and also by phenamil and bafilomycin, suggesting that the H^+-ATPase/Na^+ channel system is also important to cutaneous J_{amm} in these fish (Cooper et al. 2013). Thus, the skin is an important site for J_{amm} in the larval stages of several fish species and in the adult stages of at least two highly specialized fish species (*Kryptolebias marmoratus* and *Limanda limanda*, see Introduction), but it is not known whether the skin might contribute to J_{amm} generally in adult fish or if this capacity is lost completely over development.

In the present study, pre-exposure to HEA, resulting in a significant increase in cutaneous J_{amm} *in vivo* (Fig. 6.4; Table 6.2), also resulted in an increase in J_{amm} and MA permeability across the skin *in vitro* in the absence of basolateral NH_4HCO_3 (Figs. 6.5B, 6.6B). Interestingly, 1 mmol/l basolateral NH_4HCO_3 abolished the observed HEA-dependent increase in MA permeability, consistent with the *Xenopus* oocyte expression study by Nawata et al. (2010b) which demonstrated that MA flux is facilitated by Rh proteins and that increases in [NH_4Cl] reduce MA uptake, suggesting competition for binding sites on the protein channels. Thus, we interpret our *in vitro* results as an increase in cutaneous Rh protein function following HEA, though our gene expression data do not directly support this interpretation (Fig. 6.7). It is possible, however, that non-genomic changes in expression had occurred such as post-translational modification, as indicated by a change in Rh protein molecular size seen in HEA-exposed pufferfish (Nawata et al., 2010a), or increases in protein expression in the absence of changes in mRNA expression or increased plasma membrane insertion, both of which have been demonstrated to occur for Rh proteins (Seshadri et al. 2006a; 2006b). Furthermore, the addition of amiloride (with DMSO as a vehicle) in the present *in vitro* preparations decreased MA permeability relative to DMSO controls, which may indicate a role for NHE in flux via Rh. This is consistent with the model for cutaneous J_{amm} in larval fish (Kumai and Perry 2011; Shih et al. 2012; Ito et al. 2013), though further pharmacological analyses (bafilomycin, EIPA), flux studies (radioisotopic ^{22}Na fluxes), and immunohistochemical analyses would be necessary to better understand the mechanisms of ammonia transport in the skin of adult trout. Also noteworthy was that phenamil, a blocker of epithelial Na^+ channels, had

no effect on MA permeability in trout skin (Fig. 6.6C), in contrast to skin from freshwater-acclimated mangrove killifish (Cooper et al. 2013).

Important to note is that the overall patterns seen for J_{amm} *in vitro* (Fig. 6.5C) do not reflect those for MA permeability (Fig. 6.6C). However, it is not clear in this preparation if observed ammonia fluxes originate from the release of stored ammonia loads, from metabolic ammonia production, or from degradation of tissue proteins over experimental time. Indeed, skin *in vitro* J_{amm} was significantly greater than *in vivo* J_{amm} (Table 6.2), suggesting that some degradation may have occurred *in vitro*. Additionally, it is possible that the skin becomes more permeable to ammonia after handling. Moreover, it is possible that some ammonia originates from the small amount of underlying muscle tissue which could not always be removed in the preparation, or even from the scales. Regardless however, *in vitro* skin J_{amm} did depend on pre-treatment condition (Fig. 6.5B), with HEA-exposed fish demonstrating a greater J_{amm}, arguing that the J_{amm} *in vitro* may originate from the release of skin tissue ammonia stores. Moreover, it is likely that any small changes in transcutaneous ammonia fluxes, as indicated by changes in the permeability of the radiolabelled and easily detected ammonia analogue MA, are masked by the unloading of tissue ammonia from these various sources.

Finally, in adult trout, a spatial pattern for MA permeability along the body of the fish was observed, with the head and tail demonstrating the highest permeabilities (Fig. 6.6A). This may be a reflection of a number of different factors including skin thickness, vascularization, mitochondria-rich cell (MRC) density, or Rh protein expression. In larval

zebrafish, a gradient for J_{amm} was also seen across the body, though curiously, the head and tail of these fish were the sites of lowest flux rates (Shih et al. 2008).

6.5.4 Concluding remarks

Overall, cutaneous J_{amm} plays a negligible role in whole-body J_{amm} in adult rainbow trout under control conditions and, contrary to our initial hypothesis, its role remains minimal following HEA pre-exposure. Nevertheless, the intrinsic ammonia excretion capacity of this tissue appears to increase under these conditions, as evidenced by increases in *in vitro* MA permeability and J_{amm} of isolated skin sections, despite its minimal contribution to total J_{amm}. It is not clear if the apparent responsiveness of the skin to ammonia challenges (e.g., Nawata et al. 2007; Nawata and Wood 2008; 2009) is a vestigial trait retained from larval stages where the skin is the dominant site for ammonia transport (Zimmer AM, Wright PA, Wood CM unpublished results) or if these adult trout may, in fact, rely on this site for ammonia excretion under certain conditions. It is also possible that ammonia excretion by the skin occurs largely as a result of its own metabolic activity which can account for up to 15% of total MO_2 in trout (Kirsch and Nonnotte 1977). If this is the case, this tissue may spare further plasma loading of ammonia during HEA by excreting its waste apically into the surrounding environment as opposed to basally, into the plasma. Overall, it appears that the skin of rainbow trout has some capacity for ammonia transport which warrants further research. In a recent review, it has been suggested that the skin may act as an important surface for physiological exchange in many fish species (Glover et al., 2013). This is a promising area for future research.

6.6 TABLES AND FIGURES

Table 6.1. Urine flow rates (UFR; ml/kg/h) in rainbow trout during 12 h of overnight control or HEA (2 mM NH_4HCO_3) treatments. (N= 5-7)

	Control	**HEA**
UFR	2.3 ± 0.5	2.3 ± 0.3

Table 6.2. *In vivo* and *in vitro* cutaneous ammonia excretion rates (μmol/cm^2/h; N=4-7 for *in vivo* fluxes, N=4-5 for *in vitro* fluxes)

	Control	**HEA**
in vivo	$0.016 \pm 0.004_a$	$0.051 \pm 0.008_b$
in vitro	$0.18 \pm 0.01_x$*	$0.30 \pm 0.04_y$*

Means that possess letters that differ indicate statistically significant difference within *in vivo* or *in vitro* data sets. Asterisks represent *in vitro* means which differed significantly from respective *in vivo* means. Significance was determined using a t-test.

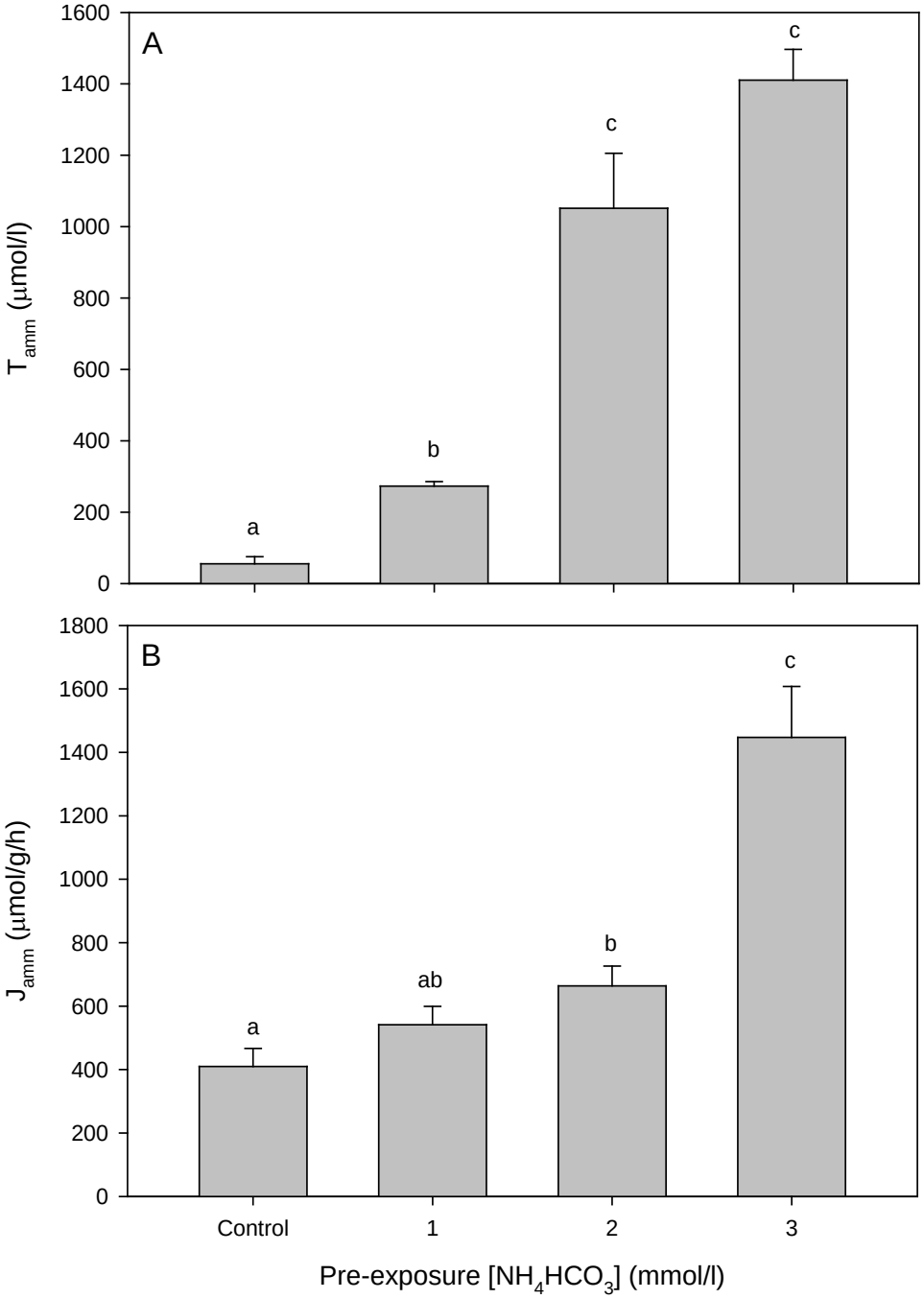
A
B
T_{amm} (µmol/l)
J_{amm} (µmol/g/h)
0
200
400
600
800
1000
1200
1400
1600
1800
a
b
c
c
a
ab
b
c
Control
1
2
3
Pre-exposure [NH_4HCO_3] (mmol/l)

Fig. 6.1. Plasma total ammonia levels (A; T_{amm}) and whole-body ammonia excretion rates (B; J_{amm}) after transfer to control water following 12 h of pre-exposure to control conditions or to 1, 2, and 3 mmol/l high environmental ammonia (HEA) as NH_4HCO_3, in Series 1. Means that possess letters that differ indicate statistically significant difference as determined by a one-way ANOVA with a Holm-Sidak post-hoc test. Plasma T_{amm} values were normalized using a square root transformation. (N=4, 4, 4, and 2 for control and 1, 2, and 3 mmol/l HEA, respectively for T_{amm}; N= 7, 5, 7, and 2 for control and 1, 2, and 3 mmol/l HEA, respectively for J_{amm})

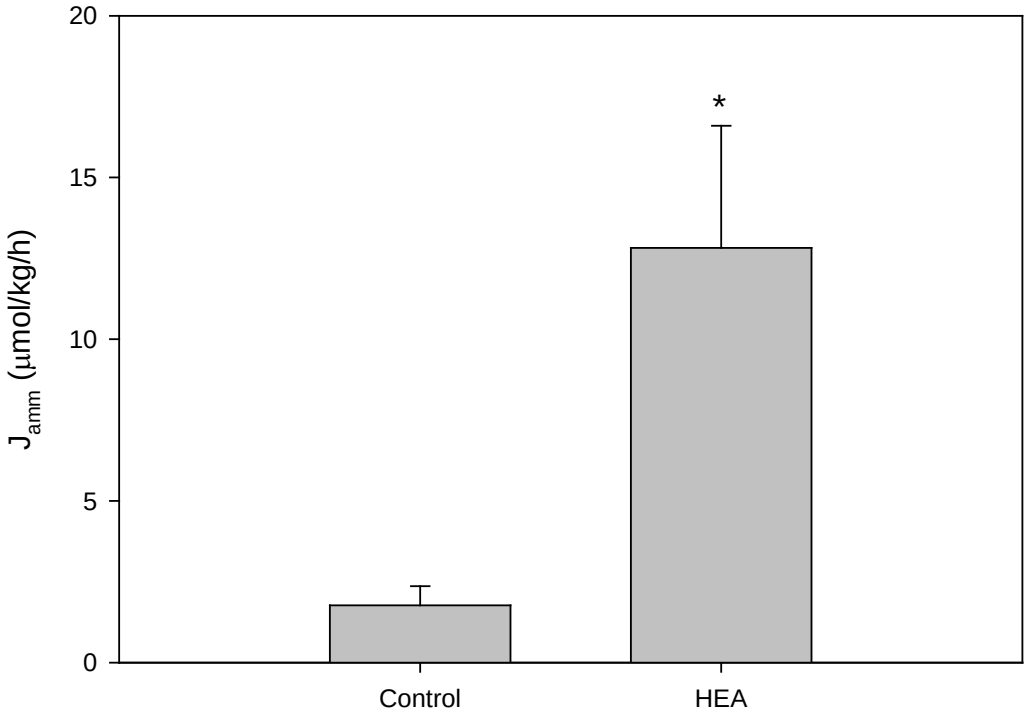
20
15
10
5
0
J_{amm} (µmol/kg/h)
*
Control
HEA

Fig. 6.2. Urinary ammonia flux rates (J_{amm}) during 12 h of control or HEA (2 mmol/l NH_4HCO_3) pre-exposure, in Series 3. Asterisks represent means from HEA-exposed fish which differed significantly from control means as determined by a two-tailed t-test. Means were normalized using a log transformation. (N=5-7)

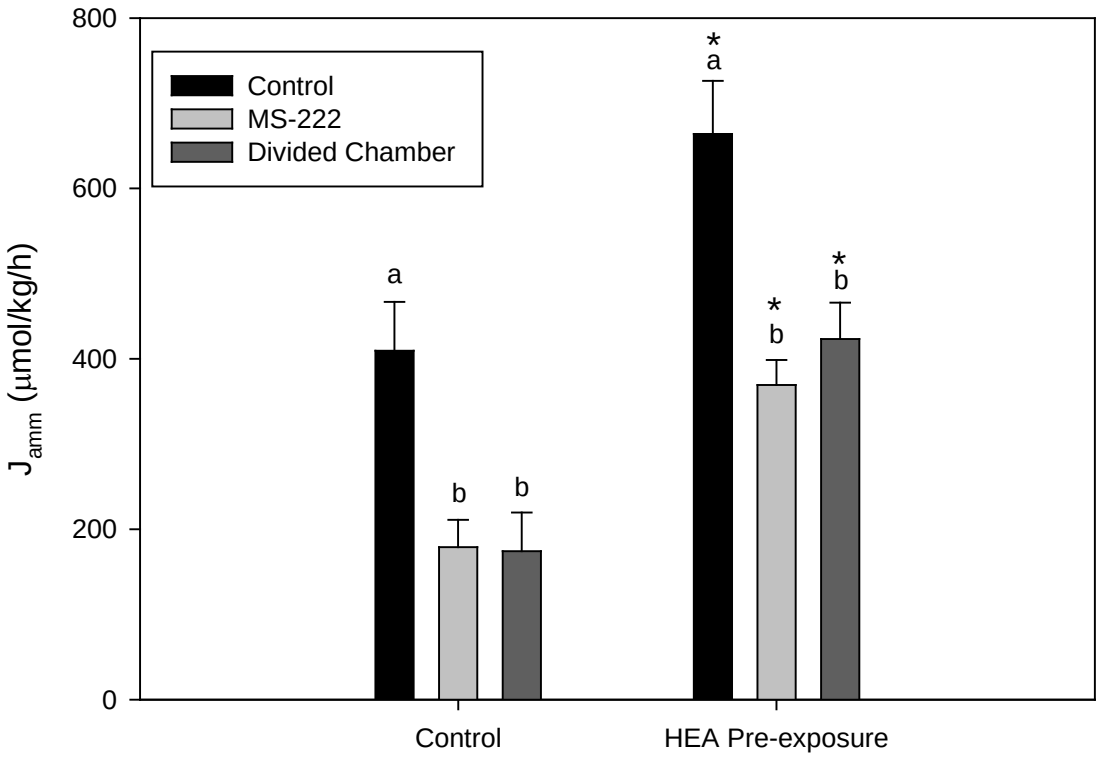
800
600
400
200
0
J_{amm} (µmol/kg/h)
Control
MS-222
Divided Chamber
a
b
b
*
a
*
b
*
b
Control
HEA Pre-exposure

Fig. 6.3. Total ammonia excretion rates (J_{amm}) after transfer to control water following 12 h of control or HEA (2 mmol/l NH_4HCO_3) pre-exposure under control conditions, MS-222 anaesthesia alone, or in divided chambers with MS-222 anaesthesia, in Series 2. Means within control or HEA that possess letters that differ indicate statistically significant difference as determined by a one-way ANOVA with a Holm-Sidak post-hoc test. Asterisks represent means from HEA-exposed fish from control, MS-222 or divided chamber series which differed significantly from respective control means as determined by a two-tailed t-test. (N=4-7)

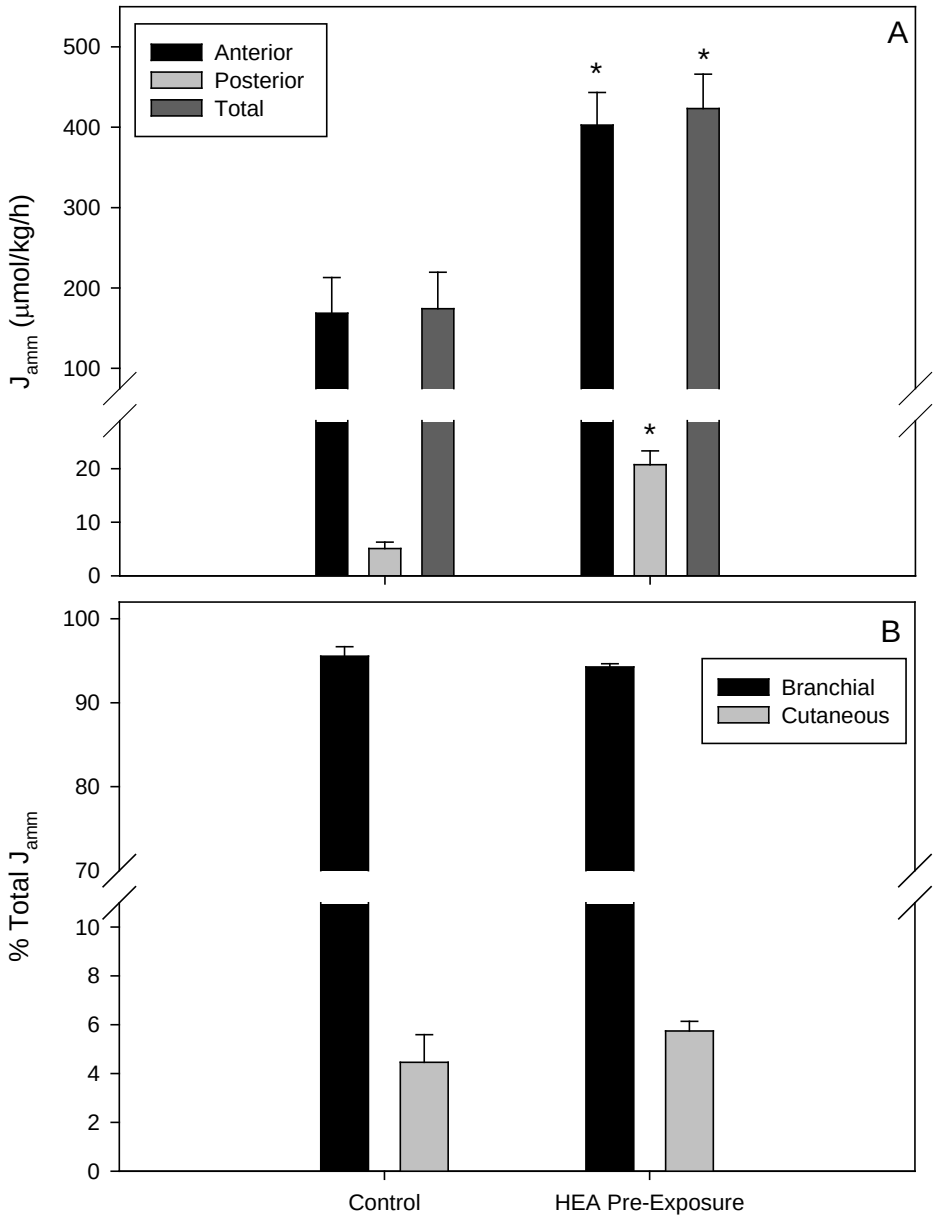
A
Anterior
Posterior
Total
J_{amm} (µmol/kg/h)
500
400
300
200
100
20
10
0
*
*
*
B
Branchial
Cutaneous
% Total J_{amm}
100
90
80
70
10
8
6
4
2
0
Control
HEA Pre-Exposure

Fig. 6.4. Anterior, posterior, and total ammonia excretion rates (A; J_{amm}) and % of total branchial and cutaneous ammonia excretion (B) after transfer to control water following 12 h of control or HEA (2 mmol/l NH_4HCO_3) pre-exposure, in Series 3. Asterisks represent anterior, posterior, or total J_{amm} means from HEA-exposed fish which differed significantly from respective control means as determined by a two-tailed t-test. (N=4-7)

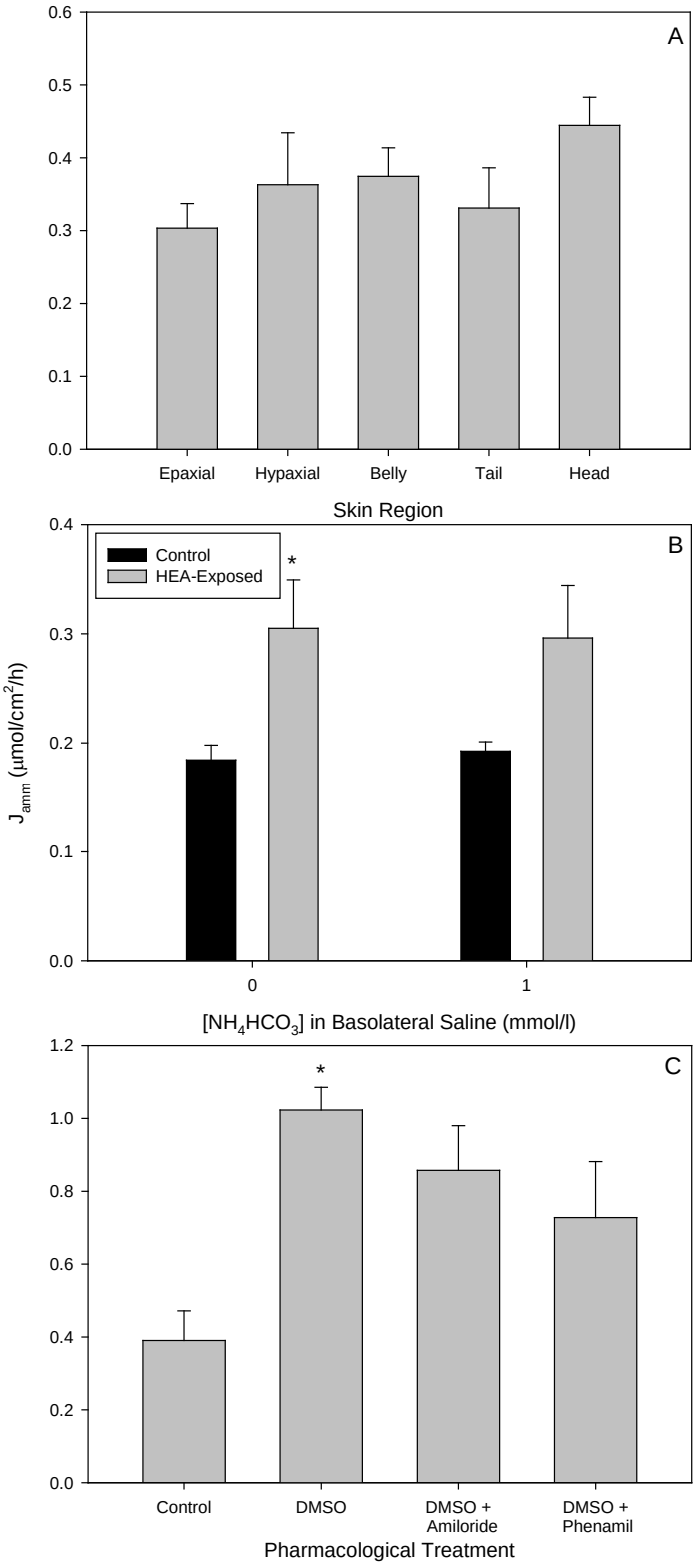
A
0.6
0.5
0.4
0.3
0.2
0.1
0.0
Epaxial
Hypaxial
Belly
Tail
Head
Skin Region
B
Control
HEA-Exposed
*
0.4
0.3
0.2
0.1
0.0
J_{amm} (µmol/cm^2/h)
0
1
[NH_4HCO_3] in Basolateral Saline (mmol/l)
C
*
1.2
1.0
0.8
0.6
0.4
0.2
0.0
Control
DMSO
DMSO + Amiloride
DMSO + Phenamil
Pharmacological Treatment

Fig. 6.5. *In vitro* ammonia flux rates (J_{amm}) in different skin regions from fish pre-exposed to HEA (2 mmol/l NH_4HCO_3) in the presence of 1 mmol/l basolateral NH_4HCO_3 (A), in the epaxial skin of control and HEA-exposed fish treated with either 0 or 1 mmol/l basolateral NH_4HCO_3 (B), and in the hypaxial skin of HEA-exposed fish in response to pharmacological blockers (10^{-4} mol/l amiloride, 10^{-5} mol/l phenamil, all in the presence of 0.1% DMSO) in the presence of 1 mmol/l basolateral NH_4HCO_3 (C). A: No significant differences existed between skin regions. (N=4-7) B: Asterisks represent means from skin of HEA-exposed fish which differed significantly from respective control means as determined by a one-tailed t-test. (N=4-5) C: An asterisk represents means from DMSO treatment which differed significantly from control means as determined by a one-tailed paired t-test. (N=4-5)

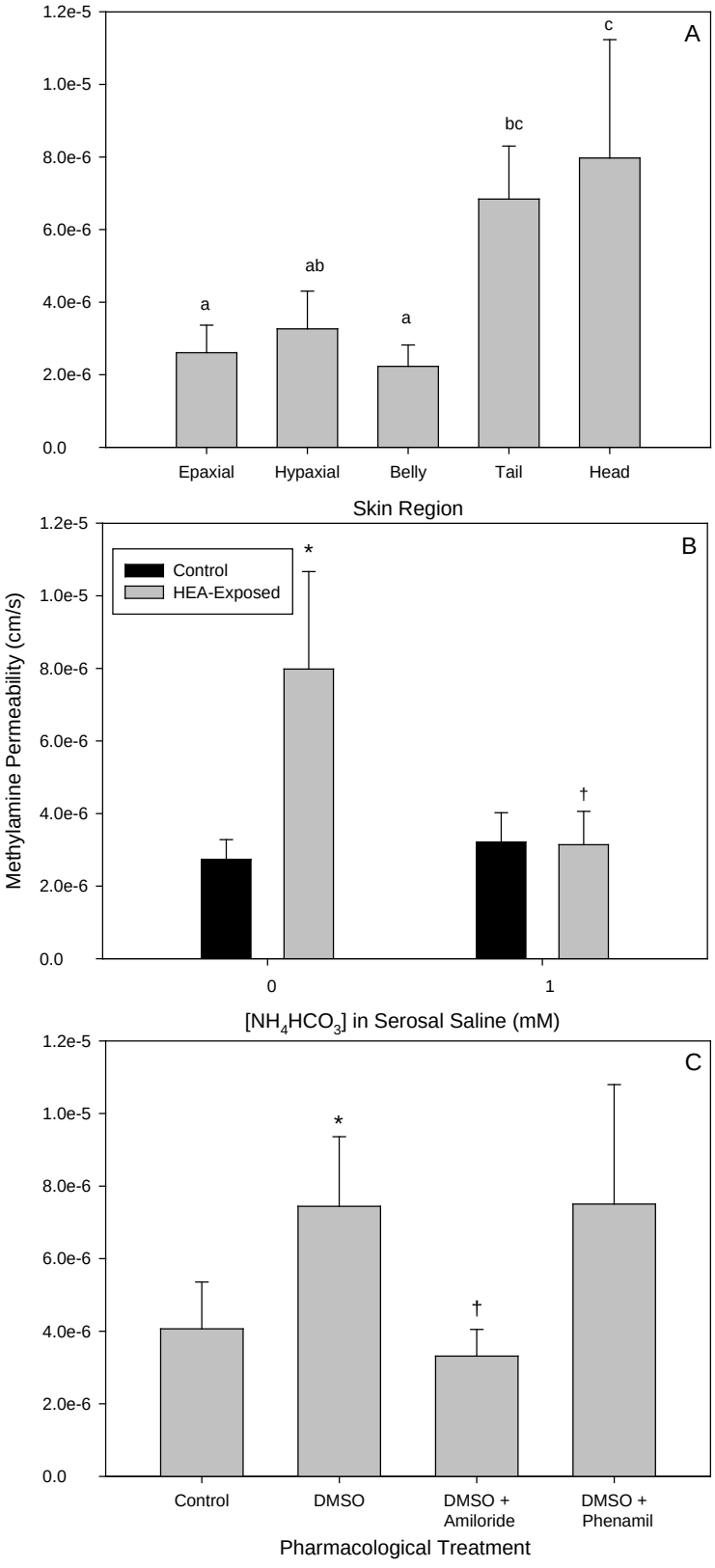
A
1.2e-5
1.0e-5
8.0e-6
6.0e-6
4.0e-6
2.0e-6
0.0
a
ab
a
bc
c
Epaxial
Hypaxial
Belly
Tail
Head
Skin Region
B
Control
HEA-Exposed
*
†
Methylamine Permeability (cm/s)
0
1
[NH4HCO3] in Serosal Saline (mM)
C
*
†
Control
DMSO
DMSO + Amiloride
DMSO + Phenamil
Pharmacological Treatment

Fig. 6.6. *In vitro* methylamine permeability rates (cm/s) in different skin regions from fish pre-exposed to HEA (2 mmol/l NH_4HCO_3) in the presence of 1 mmol/l basolateral NH_4HCO_3 (A), in the epaxial skin of control and HEA-exposed fish treated with either 0 or 1 mmol/l basolateral NH_4HCO_3 (B), and in the hypaxial skin of HEA-exposed fish in response to pharmacological blockers (10^{-4} mol/l amiloride, 10^{-5} mol/l phenamil, all in the presence of 0.1% DMSO) in the presence of 1 mmol/l basolateral NH_4HCO_3 (C). A: Means that possess letters that differ indicate statistically significant difference as determined by a one-way repeated measures ANOVA with a Fisher LSD post-hoc test. Flux rates were normalized using a square root transformation. (N=5-8) B: Asterisks represent means from skin of HEA-exposed fish which differed significantly from respective control means as determined by a one-tailed t-test using log transformation-normalized data. Daggers represent means from 1 mmol/l basolateral NH_4HCO_3 treatments which differed significantly from respective control means as determined by a paired t-test. (N=6) C: An asterisk represents means from DMSO treatment which differed significantly from control means as determined by a one-tailed paired t-test. Daggers represent DMSO + blocker means which differed significantly from DMSO means as determined by a paired t-test. (N=4-5)

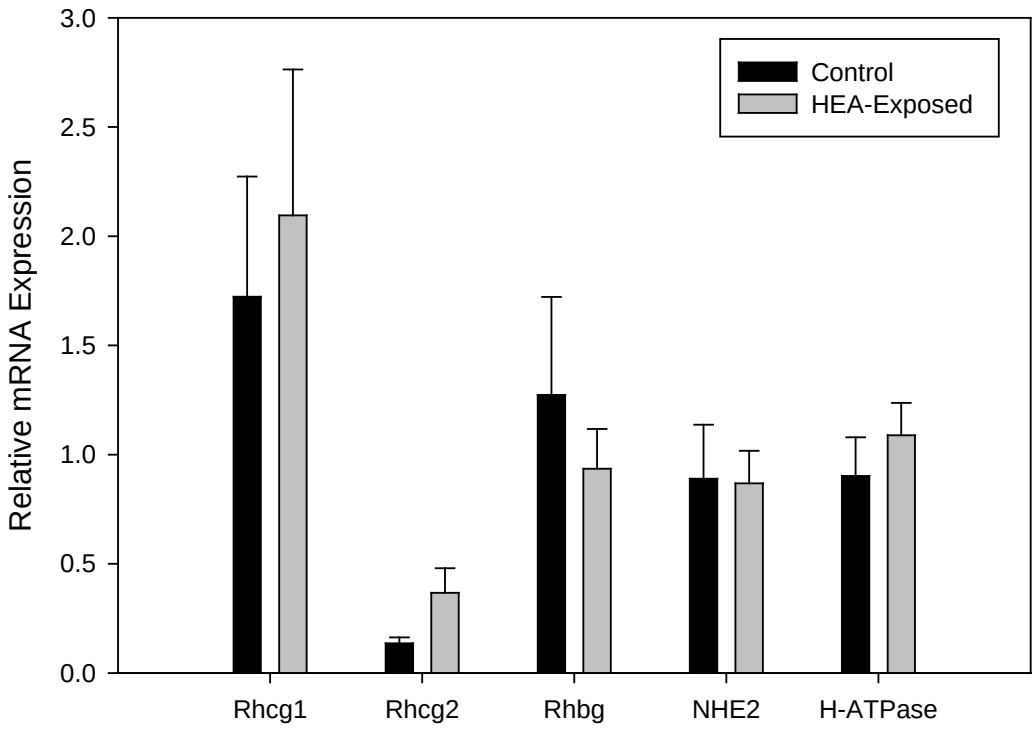
Relative mRNA Expression
3.0
2.5
2.0
1.5
1.0
0.5
0.0
Control
HEA-Exposed
Rhcg1
Rhcg2
Rhbg
NHE2
H-ATPase

Fig. 6.7. Relative gene expression (normalized to EF1α gene expression) of Rhcg1, Rhcg2, Rhbg, NHE2, and H^+-ATPase in epaxial skin samples taken from trout following 12 h of control or HEA pre-exposure. (N=4-5)

6.7 REFERENCES

Chopin L.K., Amey A.P., and Bennett M.B. (1998) A systemic secondary vessel system is present in the teleost fish *Tandanus tandanus* and absent in the elasmobranchs *Carcharhinus melanopterus* and *Rhinobatos typus* and in the dipnoan *Neoceratodus forsteri*. *J. Zool. Lond*. 246, 105-110.

Cooper, C.A., Wilson, J.M., Wright, P.A. (2013) Marine, freshwater and aerially acclimated mangrove rivulus (*Kryptolebias marmoratus*) use different strategies for cutaneous ammonia excretion. *Am. J. Physiol. Regul. Integr. Physiol.* 304, R599-R612.

Frick, N.T. and Wright, P.A. (2002) Nitrogen metabolism and excretion in the mangrove killifish *Rivulus marmoratus* II. Significant ammonia volatilization in a teleost during air-exposure. *J. Exp. Biol.* 205, 91-100.

Fromm, P.O. (1968) Some quantitative aspects of ion regulation in teleosts. *Comp. Biochem. Physiol.* 27, 865-869.

Fu, C., Wilson, J.M., Rombough, P.J. and Brauner, C.J. (2010) Ions first: Na^+ uptake shifts from the skin to the gills before O_2 uptake in developing rainbow trout, *Oncorhynchus mykiss*. *Proc. R. Soc. B* 277, 1553–60.

Glover, C.N., Bucking, C., Wood, C.M. (2013) The skin of fish as a transport epithelium: a review. *J. Comp. Physiol. B* 183, 877-891.

Glover, C.N., Bucking, C., Wood, C.M. (2011) Adaptations to *in situ* feeding: novel nutrient acquisition pathways in an ancient vertebrate. *Proc. R. Soc. B* 278, 3096-3101.

Hung, C.Y.C., Tsui, K.N.T., Wilson, J.M., Nawata, C.M., Wood, C.M. and Wright, P.A. (2007) Rhesus glycoprotein gene expression in the mangrove killfish *Kryptolebias marmoratus* exposed to elevated environmental ammonia levels and air. *J. Exp. Biol.* 210, 2419-2429.

Ishimatsu, A., Iwama, G.K., Bentley, T.B. and Heisler, N. (1992) Contribution of the secondary circulatory system to acid-base regulation during hypercapnia in rainbow trout (*Oncorhynchus mykiss*). *J. Exp. Biol.* 170, 43-56.

Ito, Y., Kobayashi, S., Nakamura, N., Miyagi, H., Esaki, M., Hoshijima, K. and Hirose, S. (2013) Close association of carbonic anhydrase (CA2a and CA15a), Na^+/H^+ exchanger (Nhe3b), and ammonia transporter Rhcg1 in zebrafish ionocytes responsible for Na^+ uptake. *Front. Physiol.* 4, 1-17.

Kirsch, R. (1972) The kinetics of peripheral exchanges of water and electrolytes in the silver eel (*Anguilla anguilla* L.) in fresh water and in sea water. *J. Exp. Biol.* 57, 489-512.

Kirsch, R. and Nonnotte, G. (1977) Cutaneous respiration in three freshwater teleosts. *Respir. Physiol.* 29: 339-354.

Kumai, Y. and Perry, S.F. (2011) Ammonia excretion via Rhcg1 facilitates Na^+ uptake in larval zebrafish, *Danio rerio*, in acidic water. *Am. J. Physiol. Regul. Integr. Comp. Physiol.* 301, R1517–28.

Lawrence, M.J., Wright, P.A. and Wood, C.M. Physiological and molecular responses of the goldfish kidney (*Carassius auratus*) to metabolic acidosis, and potential mechanisms of renal ammonia transport. *J. Exp. Biol. In Revision*

Liew, J.H., Sinha, A.K., Nawata, C.M., Blust, R., Wood, C.M. and De Boeck, G. (2013) Differential responses in ammonia excretion, sodium fluxes, and gill permeability explain different sensitivities to acute high environmental ammonia in three freshwater teleosts. *Aquat. Tox.* 126, 63-76.

McDonald, D.G. and Wood, C.M. (1981) Branchial and renal acid and ion fluxes in the rainbow trout, Salmo gairdneri, at low environmental pH. *J. Exp. Biol.* 93, 101-118

McFarland, W.N. (1959) A study of the effects of anesthetics on the behaviour and physiology of fishes. *Publ. Inst. Mar. Sci. Univ. Tex.* 6, 23-55.

McKim, J.M., Schmieder, P.K., Carlson, R.W. and Hunt, E.P. (1987) Use of respiratory-cardiovascular responses of rainbow trout (*Salmo gairdneri*) in identifying acute toxicity syndromes in fish: Part 1. Pentachlorophenol, 2,4-dinitrophenol, tricaine methanesulfonate and 1-octanol. *Environ. Toxicol. Chem.* 6, 295-312.

Nakada, T., Hoshijima, K., Esaki, M., Nagayoshi, S., Kawakami, K. and Hirose, S. (2007) Localization of ammonia transporter Rhcg1 in mitochondrion-rich cells of yolk sac, gill, and kidney of zebrafish and its ionic strength-dependent expression. *Am. J. Physiol. Regul. Integr. Comp. Physiol.* 293, R1743-R1753.

Nawata, C.M., Hirose, S., Nakada, T., Wood, C.M. and Kato, A. (2010a) Rh glycoprotein expression is modulated in pufferfish (*Takifugu rubripes*) during high environmental ammonia exposure. *J. Exp. Biol.* 213, 3150-3160.

Nawata, C.M., Hung, C.C.Y., Tsui, T.K.N., Wilson, J.M., Wright, P.A. and Wood, C.M. (2007) Ammonia excretion in rainbow trout (*Oncorhynchus mykiss*): evidence for Rh glycoprotein and H^+-ATPase involvement. *Physiol. Genomics* 31, 463–74.

Nawata, C.M. and Wood, C.M. (2008) The effects of CO_2 and external buffering on ammonia excretion and Rhesus glycoprotein mRNA expression in rainbow trout. *J. Exp. Biol.* 211, 3226-3236.

Nawata, C.M. and Wood, C.M. (2009) mRNA expression analysis of the physiological responses to ammonia infusion in rainbow trout. *J. Comp. Physiol. B* 179, 799-810.

Nawata, C.M., Wood, C.M. and O'Donnell, M.J. (2010b) Functional characterization of Rhesus glycoproteins from an ammoniotelic teleost, the rainbow trout, using oocyte expression and SIET analysis. *J. Exp. Biol.* 213, 1049-1059.

Olson, K.R. (1996) Secondary circulation in fish: anatomical organization and physiological significant. *J. Exp. Zool.* 275, 172-185.

Perry, S.F., Malone, S. and Ewing, D. (1987) Hypercapnic acidosis in the rainbow trout (*Salmo gairdneri*). II. Renal ionic fluxes. *Can. J. Zool.* 65, 896-902.

Rombough, P.J. (1999) The gill of fish larvae. Is it primarily a respiratory or an ionoregulatory structure? *J. Fish Biol.* 55, 186–204.

Sashaw, J., Nawata, M., Thompson, S., Wood, C.M. and Wright, P.A. (2010) Rhesus glycoprotein and urea transporter genes in rainbow trout embryos are upregulated in response to alkaline water (pH 9.7) but not elevated water ammonia. *Aquat. Tox.* 96, 308-313.

Satchell, G.H. (1991) Physiology and form of fish circulation. Cambridge University Press, Cambridge.

Sayer, M.D.J. and Davenport, J. (1987) The relative importance of the gills to ammonia and urea excretion in five seawater and one freshwater teleost species. *J. Fish. Biol.* 31, 561-570.

Seshadri, R.M., Klein, J.D., Kozlowski, S., Sands, J.M., Kim, Y.H., Han, K.H., Handlogten, M.E., Verlander, J.W. and Weiner, I.D. (2006a) Renal expression of the ammonia transporters, Rhbg and Rhcg, in response to chronic metabolic acidosis. *Am. J. Physiol. Renal. Physiol.* 290, F397-F408.

Seshadri, R.M., Klein, J.D., Smith, T., Sands, J.M., Handlogten, M.E., Verlander, J.W. and Weiner, I.D. (2006b) Changes in subcellular distribution of the ammonia transporter, Rhcg, in response to chronic metabolic acidosis. *Am. J. Physiol. Renal. Physiol.* 290, F1443-F1452.

Shih, T.-H., Horng, J.-L., Hwang, P.-P. and Lin, L.-Y. (2008) Ammonia excretion by the skin of zebrafish (*Danio rerio*) larvae. *Am. J. Physiol. Cell Physiol.* 295, 1625-1632.

Shih, T.-H., Horng, J.-L., Liu, S.-T., Hwang, P.-P. and Lin, L.-Y. (2012) Rhcg1 and NHE3b are involved in ammonium-dependent sodium uptake by zebrafish larvae acclimated to low-sodium water. *Am. J. Physiol. Regul. Integr. Comp. Physiol.* 302, R84–93.

Sinha, A.K., Liew, H.J., Nawata, C.M., Blust, R., Wood, C.M. and De Boeck, G. (2013) Modulation of Rh glycoproteins, ammonia excretion and Na^+ fluxes in three freshwater teleosts when exposed chronically to high environmental ammonia. *J. Exp. Biol.* 216, 2917-2930.

Skov, P.V. and Bennett, M.B. (2003) The secondary vascular system of Actinopterygii: interspecific variations in origins and investment. *Zoomorph*. 122, 181–190.

Skov, P.V. and Bennett, M.B. (2004) Structural basis for control of secondary vessels in the long-finned eel *Anguilla reinhardtii*. *J. Exp. Biol.* 207, 3339-3348.

Smith, H.W (1929) The excretion of ammonia and urea by the gills of fish. *J. Biol. Chem.* 81, 727-742.

Smith, A.A., Zimmer, A.M. and Wood, C.M. (2012) Branchial and extrabranchial ammonia excretion in goldfish (*Carassius auratus*) following thermally induced gill remodelling. *Comp. Biochem. Physiol. A* 162, 185-192.

Steffensen, J.F., Lomholt, J.P. and Vogel, W.O.P. (1986) *In vivo* observations on a specialized microvasculature, the primary and secondary vessels in fishes. *Acta Zool* . 67, 193-200.

Swift, D.J. and Lloyd, R. (1974) Changes in urine flow rate and haematocrit value of rainbow trout *Salmo gairdneri* (Richardson) exposed to hypoxia. *J. Fish. Biol.* 6, 379-387.

Tsui, T.K.N., Hung, C.Y.C., Nawata, C.M., Wilson, J.M., Wright, P.A. and Wood, C.M. (2009) Ammonia transport in cultured gill epithelium of freshwater rainbow trout: the importance of Rhesus glycoproteins and the presence of an apical Na^+/NH_4^+ exchange complex. *J. Exp. Biol.* 212, 878-892.

Verdouw, H., van Echteld, C.J.A. and Dekkers, E.M.J. (1978) Ammonia determination based on indophenols formation with sodium salicylate. *Water Res.* 12, 399-402.

Vogel, W.O.P. and Claviez, M. (1981) Vascular specialization in fish, but no evidence for lymphatics. *Z. Naturforsch.* 36c, 490-492.

Weihrauch, D., Wilkie, M.P. and Walsh, P.J. (2009) Ammonia and urea transporters in gills of fish and aquatic crustaceans. *J. Exp. Biol.* 212, 1716-1730.

Wells, P. and Pinder, A. (1996) The respiratory development of Atlantic salmon. II. Partitioning of oxygen uptake among gills, yolk sac and body surfaces. *J. Exp. Biol.* 199, 2737–44.

Wilson, R.W., Wright, P.M., Munger, S. and Wood, C.M. (1994) Ammonia excretion in freshwater rainbow trout (*Oncorhynchus mykiss*) and the importance of gill boundary layer acidification: lack of evidence for Na^+/NH_4^+ exchange. *J. Exp. Biol.* 191, 37-58.

Wood, C.M. (1988) Acid-base and ionic exchanges at gills and kidney after exhaustive exercise in the rainbow trout. *J. Exp. Biol.* 136, 461-481.

Wood, C.M., Gilmour, K.M. and Part, P. (1998) Passive and active transport properties of a gill model, the cultured branchial epithelium of the freshwater rainbow trout (*Oncorhynchus mykiss*). *Comp. Biochem. Physiol. A* 119, 87-96.

Wood, C.M. and Nawata, C.M. (2011) Nose-to-nose comparison of physiological and molecular responses of trout to high environmental ammonia in seawater versus freshwater. *J. Exp. Biol.* 214, 3557-3569.

Wood, C.M., Milligan, L.M. and Walsh, P.J. (1999) Renal responses of trout to chronic respiratory and metabolic acidosis and metabolic alkalosis. *Am. J. Physiol.* 277, R482-R492.

Wood, C.M. and Patrick, M.L. (1994) Methods for assessing kidney and urinary bladder function in fish. In: *Biochemistry and Molecular Biology of Fishes* 3 (ed. Hochachka PW, Mommsen TP), pp. 127-143.

Wright, P.A. and Wood, C.M. (2009) A new paradigm for ammonia excretion in aquatic animals: role of Rhesus (Rh) glycoproteins. *J. Exp. Biol.* 212, 2303–12.

Wu, S.C., Horng, J.L., Liu, S.T., Hwang, P.P., Wen, Z.H., Lin, C.S. and Lin, L.Y. (2010) Ammonium-dependent sodium uptake in mitochondrion-rich cells of medaka (*Oryzias latipes*) larvae. *Am. J. Physiol.* 298, C237-C250.

Zimmer, A.M., Nawata, C.M. and Wood, C.M. (2010) Physiological and molecular analysis of the interactive effects of feeding and high environmental ammonia on branchial ammonia excretion and Na^+ uptake in freshwater rainbow trout. *J. Comp. Physiol. B* 180, 1191-1204.

Zimmer, A.M., Wright. P.A. and Wood, C.M. (2014b) What is the primary function of the early teleost gill? Evidence for Na^+-coupled ammonia excretion in developing rainbow trout (*Oncorhynchus mykiss*). *Proc. R. Soc. B* 281: 1795.

CHAPTER 7

SUMMARY

7.1 PREFACE

The body of work presented in this thesis sheds light on a number emerging issues in the field of comparative fish physiology. I found evidence demonstrating the importance of the skin as a site of ammonia excretion (J_{amm}) in larval and, to a lesser degree, adult rainbow trout. Moreover, I found that the mechanisms by which the skin of rainbow trout (yolk sac skin or body skin) excretes ammonia differs fundamentally from that of the gill, leading to the development of 3 transport models for 3 different epithelia (gill, yolk sac skin, body skin). I also found that Cu, a potent inhibitor of J_{amm} and J^{Na}_{in}, can elicit its effects on both the gill and yolk sac skin (a novel observation) and that the mechanism of toxicity differs between these sites. Finally, and perhaps most importantly, I have provided evidence supporting the proposal of a new theory explaining branchial ontogeny in developing fish. The "ammonia hypothesis" posits that the earliest function of the developing gill is J_{amm}, coordinated by Na^+/NH_4^+ exchange, and that the demand for J_{amm} is the primary driving force for the transition from cutaneous to branchial ionoregulation. In this thesis, I addressed 5 hypotheses (see chapter 1 - Introduction) which will be the basis of the discussion for this summary chapter.

7.2 HYPOTHESIS 1 - *Following hatch, the skin accounts for the majority of physiological exchange and J_{amm} shifts to the gills in synchrony with J^{Na}_{in}.*

The earliest function of the developing gill, once believed to be gas transfer (e.g., Krogh, 1941), has now been clearly demonstrated to be ionoregulation (Fu et al., 2010). However, the overall function of ionoregulation by developing fish larvae is not clear. In

this first hypothesis, I tested the prediction, using the same divided chamber system as Fu et al. (2010), that the skin of larval rainbow trout would initially account for the majority of both J_{amm} and J^{Na}_{in}. Moreover, I also hypothesized that both processes would shift from the skin to the gills in synchrony, prior to MO_2, demonstrating that ionoregulation (i.e., J^{Na}_{in}) by the early fish gill occurs as Na^+/NH_4^+ exchange. I found that the skin of larvae accounted for the majority (>80%) of both J_{amm} and J^{Na}_{in} following hatch (Fig. 2.1, 2.2). This observation in itself is significant as, prior to this study, the skin of larval fish was demonstrated to have the capacity for J_{amm} (Shih et al., 2012; Wu et al., 2010), but it was not known if the skin represented the dominant site for J_{amm}, as is the case for J^{Na}_{in} (Fu et al., 2010) and MO_2 (Fu et al., 2010; Wells and Pinder, 1996). Moreover, I found that the skin-to-gill shifting points (where the gill first accounts for 50% of a given exchange) for J_{amm} and J^{Na}_{in} occurred in synchrony at 15 days post-hatch (dph), significantly earlier than the shift for MO_2 at approximately 26 dph (Fig. 2.2). In accord with this observation, branchial J_{amm} and J^{Na}_{in} were very highly correlated over larval development (R^2=0.95; Fig. 2.3). These results clearly demonstrate that the ontogeny of branchial J^{Na}_{in} occurs as Na^+/NH_4^+ exchange, confirming this aspect of my hypothesis. I thus proposed that the ionoregulatory hypothesis be refined to incorporate the excretion of ammonia (as Na^+/NH_4^+ exchange) as one of the earliest gill functions. What remained unclear following this work, however, was whether it is the demand for J_{amm} or J^{Na}_{in} which drives the transition from cutaneous to branchial ionoregulation and, potentially, drives overall gill development.

An additional component of hypothesis 1 was that the transition from cutaneous to branchial J_{amm} and J^{Na}_{in} is coordinated by increases in gene expression and/or activity of the components of the "Na^+/NH_4^+ exchange complex" (Wright and Wood, 2009) in the gill. Prior to this study, it was clear that Rh proteins, integral components of the complex, are expressed in larval fish, increasing over development (Braun et al., 2009a; Hung et al., 2008) and in addition, could be localized specifically to the yolk sac epithelium in post-hatch zebrafish (Nakada et al., 2007a). However, it was unclear how the tissue-specific expression of Rh and the other components of the Na^+/NH_4^+-exchange complex might change over development. I found that in the gill of developing larvae, gene expression of two apical Rh isoforms (Rhcg1 and Rhcg2), NHE-2, and Na^+/K^+-ATPase and the enzymatic activities of both Na^+/K^+-ATPase and H^+-ATPase increased following complete yolk sac absorption (CYA) relative to 3 dph larvae (Figs. 2.4 and 2.5). These results lend support to my hypothesis and, furthermore, suggest the presence of a Rh-NHE metabolon in the gill of developing rainbow trout. This metabolon has been shown to coordinate Na^+/NH_4^+ exchange in whole larval zebrafish (Kumai and Perry, 2011). These results represent the first understanding of tissue-specific ontogenetic changes in the Na^+/NH_4^+ exchange complex in any fish species, and suggest that this complex is responsible for coordinating J_{amm} and J^{Na}_{in} by the gill of trout from the onset of branchial ionoregulation.

7.3 HYPOTHESIS 2 – *The Na^+/NH_4^+ exchange complex is present in the yolk sac skin of larval trout and the complex shifts to the gills over development.*

I further hypothesized that J_{amm} by the yolk sac skin occurs via Na^+/NH_4^+ exchange, based on observations from zebrafish and medaka models (Shih et al., 2012; Wu et al., 2010), and that this exchange complex shifts to the gills over development. In chapter 2, while confirming the latter part of this hypothesis, I garnered preliminary evidence rejecting the initial part of this hypothesis. There was no correlation between cutaneous J_{amm} and J^{Na}_{in} in developing larvae while, in contrast, I found evidence of Na^+/NH_4^+ exchange at the gill from the onset of branchial J_{amm} in these larvae (Fig. 2.3). Hypothesis 2 was explored further in chapter 3. I predicted that any treatment which would alter J_{amm} or J^{Na}_{in} by the gill or skin would result in a similar alteration of J^{Na}_{in} or J_{amm}, respectively. Using 2 different types of divided chambers, I found that that the gill and skin of fish which had completely absorbed their yolk sac (CYA fish) and the yolk sac skin of post-hatch (PH) larvae contributed to the clearance of an ammonia load imposed by a 12-h pre-exposure to HEA following transfer to ammonia-free water (Fig. 2.2B). However only at the CYA gill was there a concomitant increase in J^{Na}_{in} (Fig. 3.2A). In agreement, the J^{Na}_{in} blockers EIPA (acting on NHE) and DAPI (acting on acid-sensing ion channels; ASICs) significantly inhibited J^{Na}_{in} by both epithelia (Figs. 3.3A, 3.4A), but J_{amm} was significantly inhibited only across the CYA gill and not the PH yolk sac (Figs. 3.3B, 3.4B). Interestingly, this represents the first evidence for the involvement of ASICs, recently implicated in the Na^+ transport model for the rainbow trout gill (Dymowska et al., 2014), in the mechanism of J^{Na}_{in} by the yolk sac skin of larval fish. Furthermore, these results overall strongly suggest that J_{amm} by the gill occurs via

Na^+/NH_4^+ exchange, confirming the current model (Wright and Wood, 2009), while J_{amm} by the yolk sac skin is Na^+-independent.

This is an important observation as current ionoregulatory models for zebrafish and medaka are based on combinations of both cutaneous and branchial data (see Dymowska et al., 2012 for review) which might be valid for these species, but the same is certainly not true for rainbow trout. Moreover, these data demonstrate that the models being developed for zebrafish and medaka (Kumai and Perry, 2011; Shih et al., 2008; 2012; 2013; Wu et al., 2010) may not be applicable to rainbow trout, and perhaps to other salmonid species. I further concluded, based on nearly negligible J^{Na}_{in} by the CYA skin (Fig. 3.2A), that the mechanism of J_{amm} by the body skin of CYA trout is likely solely a function of Rh proteins (Nawata and Wood, 2008; 2009; Nawata et al., 2007; Figs. 6.6 and 6.7B), though there is some evidence suggesting Na^+ coupling in the skin of adult trout (Fig. 6.6C). Fig. 3.5 summarizes these findings into transport models.

Interestingly, and quite unexpectedly, the rejection of hypothesis 2 was also supported by results from the Cu exposure study in chapter 5. I found that exposure to 50 µg/l Cu significantly inhibited J^{Na}_{in}, but not J_{amm}, by the skin of 3dph trout larvae (Figs. 5.3A, 5.4A) while the same exposure inhibited both J_{amm} and J^{Na}_{in} by the gill of 25 dph larvae (Figs. 5.3C, 5.4C). Thus, in summary, hypothesis 2 was rejected based on several lines of evidence. Firstly, there was no correlation between cutaneous J_{amm} and J^{Na}_{in} (chapter 2); secondly, experimental manipulation of J_{amm} and J^{Na}_{in} at the PH yolk sac did not result in accompanying changes in J^{Na}_{in} and J_{amm}, respectively (chapter 3); thirdly, Cu exposure inhibited only J^{Na}_{in} at the skin, but inhibited both J_{amm} and J^{Na}_{in} at the gill

(chapter 5). Therefore, Na^+/NH_4^+ exchange in rainbow trout is a phenomenon specific to the gill, arising at the onset of branchial ionoregulation, while the skin possesses a different mechanism which does not couple these processes to one another (Fig. 3.5). The rejection of hypothesis 2 and the support for hypothesis 1, two important findings of this thesis, have been represented in a conceptual summary figure (Fig. 7.1) which illustrates the ontogeny of branchial ionoregulation as Na^+/NH_4^+ exchange, in relation to the ontogeny of MO_2.

7.4 HYPOTHESIS 3 – *J_{amm} represents the driving force for branchial ontogeny.*

The third hypothesis of this thesis was that the transition from cutaneous to branchial ionoregulation can be explained by the "ammonia hypothesis", i.e., that J_{amm}, likely as Na^+/NH_4^+, is the earliest gill function, and that the need to clear metabolic ammonia drives gill development. Preliminary evidence in support of this hypothesis was found in chapter 2. I found that ammonia turnover time (the time it takes to clear the body of ammonia) increased from 0 dph up to 15 dph, the same time as the skin-to-gill shift for J_{amm}, whereas thereafter, turnover time decreased linearly (Fig. 2.6). This suggests that the onset of branchial J_{amm} ensures the effective clearance of metabolic ammonia, which can be toxic if accumulated to elevated levels. As discussed in chapter 1, the transition from ureotelism in embryos to eventual ammoniotelism in juveniles may present a substantial driving force for the development of an effective system for clearing ammonia. To further address this hypothesis, rainbow trout larvae were raised from hatch up to 18 dph in either control ($[Na^+]$=0.6 mmol/l) or high NaCl ($[Na^+]$=60 mmol/l) conditions (chapter 4). I predicted that under high NaCl, ionoregulatory demand would be

reduced and therefore, there would be a delay in the transition from cutaneous to branchial J^{Na}_{in}. If J^{Na}_{in} was the primary driving force for the ontogeny of branchial Na^+/NH_4^+ exchange, the skin-to-gill shift in J_{amm}, measured using the "traditional" divided chamber (Fu et al., 2010), would be delayed. On the other hand, if J_{amm} demand drives the branchial transition, high NaCl would not alter the skin-to-gill shift of J_{amm}. In both the control and high NaCl groups, the skin-to-gill shift for J_{amm} occurred at 13 dph (Fig. 4.1), demonstrating that there was no effect of rearing larvae at high NaCl. Moreover, maintaining this developmental ionoregulatory trajectory in high NaCl appeared to occur at the expense of Na^+ balance as whole-body $[Na^+]$ was significantly elevated in these fish, relative to the control group, by 18 dph (Fig. 4.1D). These observations support my hypothesis, and also suggest the "ammonia hypothesis" to be plausible. This is a significant finding in terms of our current understanding of both the ontogeny and evolution of the fish gill which has changed substantially within the last decade.

It is now clear that ionoregulation, not gas transfer, is the earliest branchial function (Fu et al., 2010; Fig. 2.3), potentially driving gill development, and the ammonia hypothesis posits that it is ionoregulation in the form of Na^+/NH_4^+ exchange which represents the earliest branchial function of developing larvae. Rombough (2007) suggested that understanding the ontogenetic pressures of gill development in larval fish may help understand the driving pressures for the evolution of the vertebrate gill from the branchial basket of protochordates. This is because the pressures believed to drive gill ontogeny in larval fish (e.g., increasing activity, decreasing surface area-to-volume ratios)

are the same pressures faced by early vertebrates. In an evolutionary context, it can be argued that the gill may have evolved in order to support ammonia excretion. One of the early arguments for the oxygen hypothesis of branchial evolution was that as early vertebrates grew larger and became more active, MO_2 by the skin eventually became limiting, necessitating the shift to branchial MO_2 (see Rombough, 2007 for review). These arguments could certainly be applied equally to the ammonia hypothesis. Moreover, Evans (1984) suggested that the gill of early fish species, initially inhabiting a marine environment, served to regulate acid-base balance and that the mechanisms which arose (electroneutral Na^+/H^+ and Cl^-/HCO_3^- exchange) allowed for the eventual colonization of freshwater environments. Once again, the same notion could also apply to the ammonia hypothesis (e.g., Na^+/NH_4^+ exchange, however Evans (1984) did not find significant Na^+/NH_4^+ exchange in hagfish (*Myxine glutinosa*), the most ancient extant vertebrates and the only aquatic vertebrate which has never colonized freshwater. More work is needed to verify the capacity of Na^+/NH_4^+ exchange in hagfish as the gills of these fish account for the majority of J_{amm} (Clifford et al., 2014) and the gill expresses the components of the Na^+/NH_4^+ exchange complex (Braun et al., 2010; Tresguerres et al., 2006). Clearly, more research is needed to understand the role of ammonia in driving gill ontogeny and evolution. Perhaps the evolution of the branchial Na^+/NH_4^+ exchange complex in freshwater fish represented the most effective solution to coordinate three different physiological needs: ion acquisition, nitrogenous waste excretion, and acid excretion. More studies comparable to that conducted in chapter 4 are needed to

understand which of these processes, which for now appears to be J_{amm}, is the first to be limited by cutaneous exchange, representing the first true function of the developing gill.

7.5 HYPOTHESIS 4 – *Exposure to waterborne Cu inhibits both branchial and cutaneous J_{amm}/J^{Na}_{in}, implicating the skin as a potential biotic ligand for Cu toxicity.*

In chapter 5, I addressed the hypothesis that waterborne Cu elicits its toxic effects at the skin of post-hatch larval fish. It is clear that larval fish represent the most sensitive life stage in terms of Cu toxicity, being more sensitive than both the embryonic and adult stages (e.g., Chapman, 1978; McNulty et al., 1994; Stouthart et al., 1996), yet few studies have investigated the underlying mechanism(s) of this increased sensitivity. In addition, no study to date has considered the skin of larval fish, in addition to the gill, as a site of Cu toxicity. Indeed, the skin of post-hatch larval fish accounts for the majority of both J_{amm} and J^{Na}_{in}, two processes commonly inhibited by Cu exposure (see Grosell, 2012 for review). I found that J^{Na}_{in} by the skin of 3 dph larval trout was significantly inhibited by exposure to 50 µg/l Cu (Fig. 5.4B), while J_{amm} by the skin of these fish was unaffected (Fig. 5.3B). As described earlier, this is an agreement with findings from both chapters 2 and 3 where J_{amm} by the skin of larval fish was shown to be independent of J^{Na}_{in}. On the other hand, 25 dph larvae exposed to the same concentration of Cu displayed inhibitions of both J_{amm} and J^{Na}_{in} by the gill (Figs. 5.3A, 5.4A), in accord with branchial J_{amm} occurring as Na^+/NH_4^+ exchange. The mechanism by which Cu elicits these differing effects, however, is unclear at present.

As outlined in chapters 1 and 5, there are a number of proposed mechanisms by which Cu inhibits both J_{amm} and J^{Na}_{in}. Both inhibitions likely occur via a common mechanism because of both their functional coupling at the gill and the fact that they are both commonly inhibited by Cu. In the gill of 25 dph larvae, there does appear to be Na^+/NH_4^+ exchange, while the same is not true of the skin of post-hatch larvae. Interestingly, the J^{Na}_{in} blockers EIPA and DAPI (chapter 3) had a very similar effect to that of Cu exposure, inhibiting only J^{Na}_{in} by the skin and both J_{amm} and J^{Na}_{in} by the gill. This suggests a potential role for both NHE and ASIC in the functional mechanism of Cu toxicity – to date these routes have not been considered. These results also question the role of Rh proteins in the overall mechanism of Cu toxicity (e.g., Lim et al., 2015). If Rh blockade by Cu represented the primary mechanism by which both J_{amm} and J^{Na}_{in} are inhibited (see section 1.3.2), I would predict that J_{amm} would always be inhibited in response to Cu, while J^{Na}_{in} would only be sensitive to Cu when it occurs as functional Na^+/NH_4^+ exchange, such as at the gills. However, results presented here demonstrate that the opposite is true and perhaps Rh in the skin of larvae is not sensitive to Cu exposure. Presently, it is not clear if Cu can in fact bind to Rh proteins, and whether or not this binding would differ in a tissue-dependent manner; perhaps Rh proteins expressed in the skin are less accessible to Cu binding than those expressed in the gill. This represents a large gap in our understanding of the toxic mechanism of action of Cu and requires further attention in future studies.

Overall, these results confirm my hypothesis that the skin is sensitive to Cu exposure and represents an additional biotic ligand to which Cu can bind and elicit toxic

effects, an important conclusion from a regulatory standpoint. The BLM, currently implemented in some parts of North America, Europe and Asia as a tool to set environmental water quality guidelines for ambient Cu levels, is calibrated with gill binding constants (Paquin et al., 2002). In larval fish, both the skin and gill must act as ligands, complicating toxicity prediction. At the very least, more work needs to be done to determine the affinity and capacity of the skin to bind Cu, in addition to understanding how this might alter the sensitivity of fish to Cu over larval development. These types of studies will determine whether the BLM, in its current form, offers sufficient protection to this sensitive early fish life stage.

7.6 HYPOTHESIS 5 – *The skin of adult trout retains the capacity for J_{amm} observed in larval fish and this capacity is upregulated in response to ammonia-loading conditions.*

My final hypothesis, that the skin of adult trout retains the capacity for J_{amm} observed in larval fish (chapters 2-5), was tested by pre-exposing adult rainbow trout to 12 h of HEA and, thereafter, measuring *in vivo* and *in vitro* cutaneous J_{amm} in ammonia-free water. While historically, the skin of adult fish has been considered to contribute negligibly to overall J_{amm} (Smith, 1929), more recent evidence has implicated the skin in J_{amm}. In several studies, Rh genes expressed in the skin of adult rainbow trout have been shown to respond to ammonia-loading conditions such as HEA exposure or ammonia infusion (Nawata and Wood, 2008; 2009; Nawata et al., 2007), implicating the skin as a site for J_{amm}. Indeed, rainbow trout pre-exposed to HEA increased cutaneous J_{amm} *in vivo*, but even under these conditions the skin still accounted for less than 5% of total J_{amm} (Fig. 6.4). Regardless, however, this result still demonstrates that the skin of trout has the

capacity for J_{amm} which can be upregulated in response to ammonia challenges. This was further supported by *in vitro* results demonstrating an increase in both J_{amm} and ^{14}C-methylamine permeability of isolated skin patches taken from HEA-exposed fish, relative to control fish (Figs. 6.5B, 6.6B). Moreover, although not supported by gene expression data, this increased mechanism appears to be mediated by a facilitated carrier, potentially Rh (Fig. 6.6B). Overall, these results support my initial hypothesis that the skin of adult fish has the capacity for J_{amm}, though it contributes only minimally (<5%) to total J_{amm} even when overall capacity is increased following HEA exposure.

Although cutaneous J_{amm} does not contribute a great deal to overall J_{amm} in rainbow trout, this contribution may be significant for other reasons. For instance, the metabolism of the skin is generally high (Nonnotte, 1981; Nonnotte and Kirsch, 1978), producing a substantial ammonia load when isolated *in vitro* (Fig. 6.5). The excretion of this metabolic ammonia directly to the surrounding water, as opposed to the plasma, might function to spare fish from further ammonia loading, especially in response to HEA. At present, it is unclear whether cutaneous J_{amm} can act to clear ammonia directly from the plasma. However the skin has been previously demonstrated to act in other physiological exchanges such as acid-base exchange (Ishimatsu et al., 1992) and calcium uptake (Perry and Wood, 1985). Also of significance is the observation that rainbow trout appear to excrete more ammonia via the skin than via renal routes (chapter 6). Historically, the kidney has generally been assumed to be the second-most important site for J_{amm} in fish, a notion which is challenged by these observations. In fact, the skin has recently been implicated as being a critical site for a number of physiological functions

(Glover et al., 2013), suggesting that cutaneous contributions to J_{amm} (and other fluxes) should not be overlooked in future studies.

7.7 IMPLICATIONS AND FUTURE DIRECTIONS

Perhaps the most fundamental finding of this thesis is the observation that ammonia might play a substantial role in driving the ontogeny of branchial ionoregulation. Though this notion has certainly been suggested in the literature (Brauner and Rombough, 2012; Rombough, 2007), work presented here is the first to provide direct evidence in support of a refined version of the ionoregulatory hypothesis, the "ammonia hypothesis". I hope that these findings open a new avenue of research with respect to understanding the ontogenetic pressures for gill development. This field of research, pioneered by Krogh in 1941, has received a great deal of attention ever since the first suggestion that the gill might serve as an ionoregulatory organ prior to a gas exchange organ (Li et al., 1995).

As described above, the role of ammonia in driving the evolution of the vertebrate gill is of great interest but, in addition, its role in the evolution of a number of different systems is also of interest. For instance, the nervous system of fish, compared to mammals, is generally believed to be relatively simple. As such, fish are less sensitive to the neurotoxic effects of ammonia exposure, being able to withstand much greater internal concentrations than mammals (see Ip and Chew, 2010). On the other hand, ammonia appears to be sensed by neuroepithelial cells in the gills, playing a key role in the control of gill ventilation in fish (Zhang et al., 2011), and a remnant of this

mechanism may persist in higher vertebrates (Zhang et al., 2015). The evolution of ureotelism by land animals, may have allowed for the development of a more complex nervous system, representing another way in which ammonia has shaped the evolutionary trajectory of a physiological system.

More work is also needed to understand the basis of the differing mechanisms of J_{amm} and J^{Na}_{in} utilized by gill and skin epithelia. This difference is particularly interesting when considering the CYA gill and PH yolk sac. The mechanism of J^{Na}_{in} by both epithelia appear to be the same (NHE and ASIC-driven, Cu-sensitive), yet their functional coupling to J_{amm} is completely different. Why does this difference exist? Is this a function of the presence or absence of physical coupling of proteins via metabolons (e.g., Rh-NHE metabolon) or is there an aspect of the mechanism of J_{amm}/J^{Na}_{in} by these tissues which has yet to be explored? Moreover, these results further demonstrate that one single transport model for J_{amm} and J^{Na}_{in} cannot be applied to all freshwater fish species (see Dymowska et al., 2012). In fact, it appears that the same transport model cannot even be applied to one species reared under different conditions (e.g., Kumai and Perry, 2011; Wu et al., 2010). I suggest in this thesis (chapter 2), however, that uncovering the ontogenetic and evolutionary pressures underlying different modes of ionoregulation will be useful towards an overall understanding of ionoregulatory mechanisms in various fish species from various environments.

Another important finding of this thesis was that the skin of fish has the capacity for J_{amm}. Interestingly, it has been known for some time that the skin possesses its own vascular system, the secondary vascular system (SVS), which was originally believed to

be a lymphatic system in fish (e.g.,Chopin et al., 1998; Satchell, 1991; Skov and Bennett, 2003; Skov and Bennett, 2004; Steffensen et al., 1986). In at least one fish species, the flow of blood through this system is under hormonal control (Rummer et al., 2014), raising questions regarding whether or not these changes in local cutaneous blood flow can alter flux rates across the skin. Overall, the role of the skin in physiological exchanges with the surrounding environment, and the role of the SVS in regulating these exchanges, requires further attention in future studies.

In conclusion, this thesis has outlined a number of gaps in our current understanding of ammonia excretion in fish and, in the chapters presented here, has shed light on some of these knowledge gaps. Based on my work, this thesis has opened at least 4 new avenues for future research: the mechanism(s) of J_{amm} by the skin of fish, the role of ammonia in driving branchial ontogeny and evolution, the role of the skin in metal toxicity in larval fish, and the role of the skin of adult trout in the overall ammonia handling mechanism. I hope that my findings can serve as a starting point for future research in these exciting new fields of comparative fish physiology and toxicology.

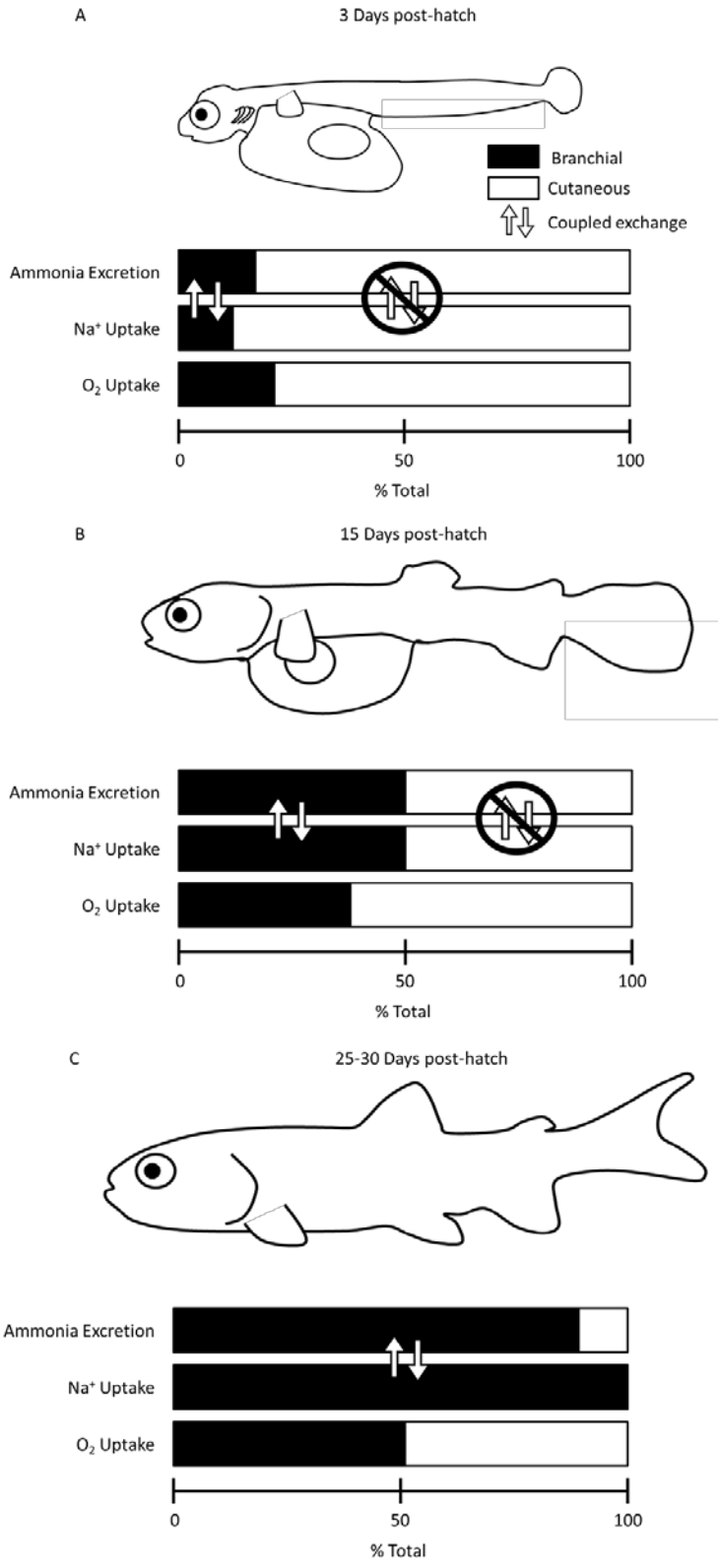
A
3 Days post-hatch
Branchial
Cutaneous
Coupled exchange
Ammonia Excretion
Na+ Uptake
O2 Uptake
0
50
100
% Total
B
15 Days post-hatch
Ammonia Excretion
Na+ Uptake
O2 Uptake
0
50
100
% Total
C
25-30 Days post-hatch
Ammonia Excretion
Na+ Uptake
O2 Uptake
0
50
100
% Total

Fig. 7.1. A summary figure illustrating the ontogeny of branchial ammonia excretion, Na^+ uptake, and oxygen uptake in developing rainbow trout. Horizontal bars represent ammonia excretion, Na^+ uptake, and oxygen uptake, each as a % of total; filled space is the branchial contribution while open space is the cutaneous contribution. Opposing arrows represent the presence of functional exchange between ammonia excretion and Na^+ uptake. Note the presence of exchange by the gill and lack thereof by the skin. This figure is based on data presented in chapters 2,3, and 5.

REFERENCES

(FOR CHAPTERS 1 AND 7)

Anderson, P.M. (2001) Urea and glutamine synthesis: environmental influences on nitrogen excretion. In *Fish physiology* 20 (ed. Wright PA, Anderson PM), pp. 239-270. San Diego, CA: Academic Press.

Avella, M. and Bornancin, M. (1989) A new analysis of ammonia and sodium transport through the gills of the freshwater rainbow trout (*Salmo gairdneri*). *J. Exp. Biol.* 142, 155-175.

Blanchard, J. and Grosell, M. (2006) Copper toxicity across salinities from freshwater to seawater in the euryhaline fish *Fundulus heteroclitus*: Is copper an ionoregulatory toxicant in high salinities? *Aquat. Toxicol.* 80, 131–139.

Boutilier, R.G., Heming, T.A. and Iwama, G.K. (1984) Physiochemical parameters for use in fish respiratory physiology. In *Fish Physiology* 10 (ed. Hoar WS, Randall DJ), pp 403–30. New York, NY: Academic Press.

Braun, M.H. and Perry, S.F. (2010) Ammonia and urea excretion in the Pacific hagfish *Eptatretus stoutii*: Evidence for the involvement of Rh and UT proteins. *Comp. Biochem. Physiol. A* 157, 405-415.

Braun, M.H., Steele, S.L., Ekker, M. and Perry, S.F. (2009a) Nitrogen excretion in developing zebrafish (*Danio rerio*): a role for Rh proteins and urea transporters. *Am. J. Physiol. Renal. Physiol.* 296, 994-1005.

Braun, M.H., Steele, S.L. and Perry, S.F. (2009b) The responses of zebrafish (*Danio rerio*) to high external ammonia and urea transporter inhibition: nitrogen excretion and expression of rhesus glycoproteins and urea transporter proteins. *J. Exp. Biol.* 212, 3846-3856.

Brauner, C.J. and Rombough, P.J. (2012) Ontogeny and paleophysiology of the gill: new insights from larval and air-breathing fish. *Respir. Physiol. Neurobiol.* 184, 293–300.

Ceyhun, S.B., Sentürk, M., Yerlikaya, E., Erdogan, O., Küfrevioglu, O., Ekinci, D. (2011) Purification and characterization of carbonic anhydrase from the teleost fish *Dicentrarchus labrax* (European seabass) liver and toxicological effects of metals on enzyme activity. *Envion. Toxicol. Phar.* 32, 69–74.

Chapman, G.A. (1978) Toxicities of cadmium, copper, and zinc to four juvenile stages of chinook salmon and steelhead. *Trans. Am. Fish. Soc.* 107, 841-847.

Chopin, L.K., Amey, A.P. and Bennett, M.B. (1998) A systemic secondary vessel system is present in the teleost fish *Tandanus tandanus* and absent in the elasmobranchs *Carcharhinus melanopterus* and *Rhinobatos typus* and in the dipnoan *Neoceratodus forsteri*. *J. Zool. Lond.* 246,105-110.

Christensen, G.M. and Tucker, J.H. (1976) Effects of selected water toxicants on the in vitro activity of fish carbonic anhydrase. *Chem-Biol Interact.* 13, 181–192.

Clifford, A.M., Guffey, S.C. and Goss, G.G. (2014) Extrabranchial mechanisms of system pH recovery in hagfish (*Eptatretus stoutii*). *Comp. Biochem. Physiol. A* 168, 82-89.

Dhiyebi, H.A., O'Donnell, M.J. and Wright, P.A. (2013) Water chemistry in the microenvironment of rainbow trout *Oncorhynchus mykiss* embryos is affected by development, the egg capsule and crowding. *J. Fish Biol.* 82, 444-457.

Dymowska, A.K., Schultz, A.G., Blair, S.D., Chamot, D. and Goss, G.G. (2014) Acid-sensing ion channels are involved in epithelial Na^+ uptake in the rainbow trout *Oncorhynchus mykiss*. *Am. J. Physiol. Cell Physiol.* 307, 255-265.

Dymowska, A.K., Hwang, P.-P. and Goss, G.G. (2012) Structure and function of ionocytes in the freshwater fish gill. *Respir. Physiol. Neurobiol.* 184, 282-292.

Essex-Fraser, P.A, Steele, S.L., Bernier, N.J., Murray, B.W., Stevens, E.D. and Wright, P.A. (2005) Expression of four glutamine synthetase genes in the early stages of development of rainbow trout (*Oncorhynchus mykiss*) in relationship to nitrogen excretion. *J. Biol. Chem.* 280, 20268–20273.

Evans, D.H. (1984) Gill Na^+/H^+ and Cl^-/HCO_3^- exchange systems evolved before the vertebrates entered fresh water. *J. Exp. Biol.* 113, 465-469.

Frick, N.T. and Wright, P.A. (2002) Nitrogen metabolism and excretion in the mangrove killifish *Rivulus marmoratus* II. Significant ammonia volatilization in a teleost during air-exposure. *J. Exp. Biol.* 205, 91-100.

Fu, C., Wilson, J.M., Rombough, P.J. and Brauner, C.J. (2010) Ions first: Na^+ uptake shifts from the skin to the gills before O_2 uptake in developing rainbow trout, *Oncorhynchus mykiss*. *Proc. R. Soc. B* 277, 1553–60.

Glover, C.N., Bucking, C., Wood, C.M. (2013) The skin of fish as a transport epithelium: a review. *J. Comp. Physiol. B* 183, 877-891.

Gonzalez, M.E., Blanquez, M.J. and Rojo, C. (1996) Early gill development in the rainbow trout, *Oncorhynchus mykiss*. *J. Morphol.* 229, 201–217.

Grosell, M. (2012) Copper. *Fish Physiology 31A* (ed. Farrell AP, Wood CM, Brauner CJ), pp. 54–110. San Diego, CA: Academic Press.

Grosell, M. and Wood, C.M. (2002) Copper uptake across rainbow trout gills: mechanisms of apical entry. *J. Exp. Biol.* 205, 1179–1188.

Grosell, M., Nielsen, C. and Bianchini, A. (2002) Sodium turnover rate determines sensitivity to acute copper and silver exposure in freshwater animals. *Comp. Biochem. Physiol. C* 133, 287–303.

Grosell, M., Wood, C.M. and Walsh, P.J. (2003) Copper homeostasis and toxicity in the elasmobranch *Raja erinacea* and the teleost *Myoxocephalus octodecemspinosus* during exposure to elevated water-borne copper. *Comp. Biochem. Physiol. C* 135, 179–190.

Hung, C.Y.C., Nawata, C.M., Wood, C.M. and Wright, P.A. (2008) Rhesus glycoprotein and urea transporter genes are expressed in early stages of development of rainbow trout (*Oncorhynchus mykiss*). *J. Exp. Zool. A* 309, 262-268.

Hung, C.Y.C., Tsui, K.N.T., Wilson, J.M., Nawata, C.M., Wood, C.M. and Wright, P.A. (2007) Rhesus glycoprotein gene expression in the mangrove killfish *Kryptolebias marmoratus* exposed to elevated environmental ammonia levels and air. *J. Exp. Biol.* 210, 2419-2429.

Ip, Y.K. and Chew, S.F. (2010) Ammonia production, excretion, toxicity, and defense in fish: a review. *Front. Physiol.* 1, 134.

Ishimatsu, A., Iwama, G.K., Bentley, T.B. and Heisler, N. (1992) Contribution of the secondary circulatory system to acid-base regulation during hypercapnia in rainbow trout (*Oncorhynchus mykiss*). *J. Exp. Biol.* 170, 43-56.

Ito, Y., Kobayashi, S., Nakamura, N., Miyagi, H., Esaki, M., Hoshijima, K. and Hirose, S. (2013) Close association of carbonic anhydrase (CA2a and CA15a), Na^+/H^+ exchanger (Nhe3b), and ammonia transporter Rhcg1 in zebrafish ionocytes responsible for Na^+ uptake. *Front. Physiol.* 4, 1-17.

Kerstetter, T.H. and Keeler, M. (1976) On the interaction of NH_4^+ and Na^+ fluxes in the isolated trout gill. *J. Exp. Biol.* 64, 517-527.

Khademi, S., O'Connell, J. III, Remis, J., Robles-Colmenares, Y., Miercke, L.J. and Stroud, R.M. (2004) Mechanism of ammonia transport by Amt/MEP/Rh: structure of AmtB at 1.35 Å. *Science* 305, 1587.

Korte, J.J., Salo, W.L., Cabrera, V.M., Wright, P.A., Felski, A.K. and Anderson, P.M. (1997) Expression of carbamoyl-phosphate synthetase III mRNA during the

early stages of development and in muscle of adult rainbow trout (*Oncorhynchus mykiss*). *J. Biol. Chem.* 272, 6270-6277.

Krogh, A. (1937) Osmotic regulation in freshwater fishes by active absorption of chloride ions. *Z. Vergl. Physiol.* 24, 656-666.

Krogh, A. (1938) The active absorption of ions in some freshwater animals. *Z. Vergl. Physiol.* 25, 335-250.

Krogh, A. (1941) *The comparative physiology of respiratory mechanisms*. Philadelphia, PA: University of Pennsylvania Press.

Kumai, Y. and Perry, S.F. (2011) Ammonia excretion via Rhcg1 facilitates Na^+ uptake in larval zebrafish, *Danio rerio*, in acidic water. *Am. J. Physiol. Regul. Integr. Comp. Physiol.* 301, R1517–28.

LeMoine, C.M.R. and Walsh, P.J. (2013) Ontogeny of ornithine-urea cycle gene expression in zebrafish (*Danio rerio*). *Am. J. Physiol. Regul. Integr. Comp. Physiol.* 304, 991-1000.

Li, J., Eygensteyn, J., Lock, R.A.C., Verbost, P.M., Van Der Heijden, A.J.H., Wendellar Bonga, S.E. and Flik G. (1995) Branchial chloride cells in larvae and juveniles of freshwater tilapia *Oreochromis mossambicus*. *J. Exp. Biol.* 198, 2177-2184.

Liew, J.H., Sinha, A.K., Nawata, C.M., Blust, R., Wood, C.M. and De Boeck, G. (2013) Differential responses in ammonia excretion, sodium fluxes, and gill permeability explain different sensitivities to acute high environmental ammonia in three freshwater teleosts. *Aquat. Tox.* 126, 63-76.

Lim, M. Y.-T., Zimmer, A.M. and Wood, C.M. (2015) Acute exposure to waterborne copper inhibits both the excretion and uptake of ammonia in freshwater rainbow trout (*Oncorhynchus mykiss*). *Comp. Biochem. Physiol. C* 168, 48-54.

Maetz, J. and Garcia-Romeu, F. (1964) The mechanism of sodium and chloride uptake by the gills of a fresh-water fish, *Carassius auratus*: II. Evidence for Na^+/NH_4^+ and HCO_3^-/Cl^- exchanges. *J. Gen. Physiol.* 47, 1209-1227.

McNulty, H.R., Anderson, B.S., Hunt, J.W., Turpen, S.L. and Singer, M.M. (1994) Age-specific toxicity of copper to larval topsmelt *Atherinops affinis*. *Environ. Toxicol. Chem.* 13, 487–492.

Nakada, T., Hoshijima, K., Esaki, M., Nagayoshi, S., Kawakami, K. and Hirose, S. (2007a) Localization of ammonia transporter Rhcg1 in mitochondrion-rich cells of

yolk sac, gill, and kidney of zebrafish and its ionic strength-dependent expression. *Am. J. Physiol. Regul. Integr. Comp. Physiol.* 293, R1743-R1753.

Nakada, T., Westhoff, C.M., Kato, A. and Hirose, S. (2007b) Ammonia secretion from fish gill depends on a set of Rh glycoproteins. *FASEB J.* 21, 1067-1074.

Nawata, C.M. and Wood, C.M. (2008) The effects of CO_2 and external buffering on ammonia excretion and Rhesus glycoprotein mRNA expression in rainbow trout. *J. Exp. Biol.* 211, 3226-3236.

Nawata, C.M. and Wood, C.M. (2009) mRNA expression analysis of the physiological responses to ammonia infusion in rainbow trout. *J. Comp. Physiol. B* 179, 799-810.

Nawata, C.M., Hirose, S., Nakada, T., Wood, C.M. and Kato, A. (2010a) Rh glycoprotein expression is modulated in pufferfish (*Takifugu rubripes*) during high environmental ammonia exposure. *J. Exp. Biol.* 213, 3150-3160.

Nawata, C.M., Hung, C.C.Y., Tsui, T.K.N., Wilson, J.M., Wright, P.A. and Wood, C.M. (2007) Ammonia excretion in rainbow trout (*Oncorhynchus mykiss*): evidence for Rh glycoprotein and H^+-ATPase involvement. *Physiol. Genomics* 31, 463–74.

Nawata, C.M., Wood, C.M. and O'Donnell, M.J. (2010b) Functional characterization of Rhesus glycoproteins from an ammoniotelic teleost, the rainbow trout, using oocyte expression and SIET analysis. *J. Exp. Biol.* 213, 1049-1059.

Nonnotte, G. (1981) Cutaneous respiration in six freshwater teleosts. *Comp. Biochem. Physiol. A* 70, 541-543.

Nonnotte, G. and Kirsch, R. (1978) Cutaneous respiration in seven sea-water teleosts. *Respir. Physiol.* 35, 111-118.

Paquin, P.R., Gorsuch, J.W., Apte, S., Batley, G.E., Bowles, K.C., Campbell, P.G.C., Delos, C.G., Di Toro, D.M., Dwyer, R.I., Galvez, F., Gensemer, R.W., Goss, G.G., Hogstrand, C., Janssen, C.R., McGeer, J.C., Naddy, R.B., Playle. R.C., Santore, R.C., Schneider, U., Stubblefield, W.A., Wood, C.M. and Wu, K.B. (2002) The biotic ligand model: a historical overview. *Comp. Biochem. Physiol. C* 133, 3–35.

Parks, S.K., Tresguerres, M. and Goss, G.G. (2008) Theoretical considerations underlying Na^+ uptake mechsnisms in freshwater fishes. *Comp. Biochem. Physiol. C* 148, 411-418.

Payan, P. (1978) A study of the Na^+/NH_4^+ exchange across the gill of the perfused head of the trout (*Salmo gairdneri*). *J. Comp. Physiol.* 124, 181-188.

Perry, S.F. and Wood, C.M. (1985) Kinetics of branchial calcium uptake in the rainbow trout: Effects of acclimation to various external calcium levels. *J. Exp. Biol.* 433, 411–433.

Randall, D.J. and Ip, Y.K. (2006). Ammonia as a respiratory gas in water and air-breathing fishes. *Respir. Physiol. Neurobiol.* 154, 216-225.

Randall, D.J. and Tsui, T.K.N. (2002) Ammonia toxicity in fish. *Mar. Pollut. Bull.* 45, 17–23.

Rombough, P.J. (1992) Intravascular oxygen tensions in cutaneously respiring rainbow trout (*Oncorhynchus mykiss*) larvae. *Comp. Biochem. Physiol. A* 101, 23-27.

Rombough, P.J. (1999) The gill of fish larvae. Is it primarily a respiratory or an ionoregulatory structure? *J. Fish Biol.* 55, 186-204.

Rombough, P.J. (2002) Gills are needed for ionoregulation before they are needed for O_2 uptake in developing zebrafish, *Danio rerio*. *J. Exp. Biol.* 205, 1787–94.

Rombough, P.J. (2007) The functional ontogeny of the teleost gill: which comes first, gas or ion exchange? *Comp. Biochem. Physiol. A. Mol. Integr. Physiol.* 148, 732–42.

Rummer, J.L., Wang, S., Steffensen, J.F. and Randall, D.J. (2014) Function and control of the fish secondary vascular system, a contrast to mammalian lymphatic systems. *J.Exp. Biol.* 217, 751-757.

Salama, A., Morgan, I.J. and Wood, C.M. (1999) The linkage between Na^+ uptake and ammonia excretion in rainbow trout: kinetic analysis, the effects of $(NH_4)_2SO_4$ and NH_4HCO_3 infusion and the influence of gill boundary layer pH. *J. Exp. Biol.* 202, 697-709.

Satchell, G.H. (1991) Physiology and form of fish circulation. Cambridge, England: Cambridge University Press.

Sayer, M.D.J. and Davenport, J. (1987) The relative importance of the gills to ammonia and urea excretion in five seawater and one freshwater teleost species. *J. Fish. Biol.* 31, 561-570.

Shih, T.-H., Hong, J.-L., Hwang, P.-P. and Lin, L.,-Y. (2008) Ammonia excretion by the skin of zebrafish (*Danio rerio*) larvae. *Am. J. Physiol. Cell Physiol.* 295, 1625-1632.

Shih, T.-H., Horng, J.-L., Lai, Y.-T. and Lin, L.-Y. (2013) Rhcg1 and Rhbg mediate ammonia excretion by ionocytes and keratinocytes in the skin of zebrafish larvae: H^+-

ATPase-linked active ammonia excretion by ionocytes. *Am. J. Physiol. Regul. Integr. Comp. Physiol.* 304, R1130–R1138.

Shih, T.-H., Horng, J.-L., Liu, S.-T., Hwang, P.-P. and Lin, L.-Y. (2012) Rhcg1 and NHE3b are involved in ammonium-dependent sodium uptake by zebrafish larvae acclimated to low-sodium water. *Am. J. Physiol. Regul. Integr. Comp. Physiol.* 302, R84–93.

Sinha, A.K., Liew, H.J., Nawata, C.M., Blust, R., Wood, C.M. and De Boeck, G. (2013) Modulation of Rh glycoproteins, ammonia excretion and Na^+ fluxes in three freshwater teleosts when exposed chronically to high environmental ammonia. *J. Exp. Biol.* 216, 2917-2930.

Skov, P.V. and Bennett, M.B. (2004) Structural basis for control of secondary vessels in the long-finned eel *Anguilla reinhardtii*. *J. Exp. Biol.* 207:3339-3348

Skov, P.V. and Steffensen, J.F. (2003) The blood volumes of the primary and secondary circulatory systems in the Atlantic cod *Gadus morhua* L., using plasma bound Evans Blue and compartmental analysis. *J. Exp. Biol.* 206:591-599

Smith, A.A., Zimmer, A.M. and Wood, C.M. (2012) Branchial and extrabranchial ammonia excretion in goldfish (*Carassius auratus*) following thermally induced gill remodelling. *Comp. Biochem. Physiol. A* 162, 185-192.

Smith, H.W (1929) The excretion of ammonia and urea by the gills of fish. *J. Biol. Chem.* 81, 727-742.

Souza-Bastos, L.R., Pascoa, M.I., Freire, C.A. and Wilson, J.M. (2014) Ammonia excretion and expression of transport proteins in the gills and skin of the intertidal fish *Lipophrys pholis*. *Comp. Biochem. Physiol. A* 167, 15-24.

Soyut, H., Beydemir, S. and Hisar, O. (2008) Effects of some metals on carbonic anhydrase from brains of rainbow trout. *Biol. Trace Elem. Res.* 123,179–190.

Steele, S.L., Chadwick, T.D and Wright, P.A. (2001) Ammonia detoxification and localization of urea cycle enzyme activity in embryos of the rainbow trout (*Oncorhynchus mykiss*) in relation to early tolerance to high environmental ammonia levels. *J. Exp. Biol.* 204, 2145-2154.

Steffensen, J.F. and Lomholt, J.P. (1992) The secondary vascular system. In *Fish Physiology* 12A (ed. Hoar WS, Randall DJ, Farrell AP) pp. 185-218. San Diego, CA: Academic Press

Stouthart, X.J.H.X., Haans, J.L.M., Lock, R.A.C. and Wendelaar Bonga, S.E. (1996) Effects of water pH on copper toxicity to early life stages of the common carp (*Cyprinus carpio*). *Environ. Toxicol. Chem.* 15, 376–383.

Tresguerres, M., Parks, S.K. and Goss, G.G. (2006) V-H^+-ATPase, Na^+/K^+-ATPase and NHE2 immunoreactivity in the gill epithelium of the Pacific hagfish (*Eptatretus stoutii*). *Comp. Biochem. Physiol. A* 145, 312-321.

USEPA (2013) Aquatic life ambient water quality criteria for ammonia – freshwater. In:U.S Environmental Protection Agency. Office of Water Regulations and Standards, Washington, DC.

Vitale, A.M., Monserrat, J.M., Castilho, P. and Rodriguez, E.M. (1999) Inhibitory effects of cadmium on carbonic anhydrase activity and ionic regulation of the estuarine crab *Chasmagnathus granulata* (Decapoda, Grapsidae). *Comp. Biochem. Physiol. C* 122, 121-129.

Weihrauch, D., Wilkie, M.P. and Walsh, P.J. (2009) Ammonia and urea transporters in gills of fish and aquatic crustaceans. *J. Exp. Biol.* 212, 1716-1730.

Wells, P.R. and Pinder, A.W. (1996) The respiratory development of Atlantic salmon. II. Partitioning of oxygen uptake among gills, yolk sac and body surfaces. *J. Exp. Biol.* 199, 2737-4274.

Wilkie, M.P. (2002) Ammonia excretion and urea handling by fish gills: present understanding and future research challenges. *J. Exp. Zool.* 293, 284-301.

Wilson, R.W. and Taylor, E.W. (1993) The physiological responses of freshwater rainbow trout, *Oncorhynchus mykiss*, during acutely lethal copper exposure. *J. Comp. Physiol. B* 38–47.

Wilson, R.W., Wright, P.M., Munger, S. and Wood, C.M. (1994) Ammonia excretion in freshwater rainbow trout (*Oncorhynchus mykiss*) and the importance of gill boundary layer acidification: lack of evidence for Na^+/NH_4^+ exchange. *J. Exp. Biol.* 191, 37-58.

Wood, C.M. (1993) Ammonia and urea metabolism and excretion. In *The Physiology of Fishes* (ed. Evans DH), pp 379-425, Boca Raton, FL: CRC Press.

Wood, C.M. and Nawata, C.M. (2011) Nose-to-nose comparison of physiological and molecular responses of trout to high environmental ammonia in seawater versus freshwater. *J. Exp. Biol.* 214, 3557-3569.

Wright, P.A. and Wood, C.M. (1985) An analysis of branchial ammonia excretion in the freshwater rainbow trout: Effects of environmental pH change and sodium uptake blockade. *J. Exp. Biol.* 114, 329-353.

Wright, P.A. and Wood, C.M. (2009) A new paradigm for ammonia excretion in aquatic animals: role of Rhesus (Rh) glycoproteins. *J. Exp. Biol.* 212, 2303–12.

Wright, P.A. and Wood, C.M. (2012) Seven things fish know about ammonia and we don't. *Respir. Physiol. Neurobiol.* 184, 231-240.

Wright, P.A., Felskie, A. and Anderson, P. (1995) Induction of ornithine-urea cycle enzymes and nitrogen metabolism and excretion in rainbow trout (*Oncorhynchus mykiss*) during early life stages. *J. Exp. Biol.* 198, 127–35.

Wu, S.-C., Horng, J.-L., Liu, S.-T., Hwang, P.-P., Wen, Z.-H., Lin, C.-S. and Lin, L.-Y. (2010) Ammonium-dependent sodium uptake in mitochondrion-rich cells of medaka (*Oryzias latipes*) larvae. *Am. J. Physiol. Cell Physiol.* 298, 237-250.

Zhang, L., Nawata, C.M., De Boeck, G. and Wood, C.M. (2015) Rh protein expression in branchial neuroepithelial cells, and the role of ammonia in ventilatory control in fish. *Comp. Biochem. Physiol. A* In Press.

Zhang, L., Nurse, C.A., Jonz, M.G. and Wood, C.M. (2011) Ammonia sensing by neuroepithelial cells and ventilatory responses to ammonia in rainbow trout. *J. Exp. Biol.* 214, 2678-2689.

Zimmer, A.M., Barcarolli, I.F., Wood, C.M. and Bianchini, A. (2012) Waterborne copper exposure inhibits ammonia excretion and branchial carbonic anhydrase activity in euryhaline guppies acclimated to both fresh water and sea water. *Aquat. Toxicol.* 122-123, 172–80.

Zimmer, A.M., Nawata, C.M. and Wood, C.M. (2010) Physiological and molecular analysis of the interactive effects of feeding and high environmental ammonia on branchial ammonia excretion and Na^+ uptake in freshwater rainbow trout. *J. Comp. Physiol. B* 180, 1191-1204.